The Dissertation Committee for David Paul Teague Certifies that this is the approved version of the following dissertation:

Addressing Surface Wave Inversion Non-Uniqueness and the Implications for Seismic Site Response Analyses

Committee:

Brady R. Cox, Supervisor

Ellen M. Rathje

Kenneth H. Stokoe II

Clark R. Wilson

Loukas F. Kallivokas

Addressing Surface Wave Inversion Non-Uniqueness and the Implications for Seismic Site Response Analyses

by

David Paul Teague

Dissertation

Presented to the Faculty of the Graduate School of

The University of Texas at Austin

in Partial Fulfillment

of the Requirements

for the Degree of

Doctor of Philosophy

The University of Texas at Austin

August 2017

Dedication

To my parents, for their unwavering love and support.

Acknowledgements

I would like to thank my supervising professor, Dr. Brady R. Cox, for his guidance and support throughout my graduate studies. I have always been inspired by his passion for his work, his vision, his levelheadedness, and his willingness to pursue new challenges. I am eternally grateful not only for his academic guidance, but also for his role as a mentor and a friend.

I would also like to acknowledge all of the faculty and staff who have helped me to accomplish my research goals. In particular, I would like to thank Dr. Ellen Rathje for her insight and for teaching me many of the core principles of my field of study. Additionally, I would like to thank my dissertation committee members Dr. Kenneth Stokoe, II, Dr. Clark Wilson, and Dr. Loukas Kallivokas for taking an interest in my work and for their valuable insights.

My dissertation would not have been possible without access to a vast collection of technological recourses. I'd like to acknowledge the authors of the open-source Geopsy software, which has played an instrumental role in my research. I'd also like to thank Dr. Alexandros Savvaidis and Ritu Arora for implementing this software on the Stampede supercomputer. Finally, I would be remiss if I did not mention Dr. Clinton M. Wood, who taught me how to use much of the equipment and software used for this research.

The support from the National Science Foundation and the Department of Civil, Architectural and Environmental Engineering is gratefully acknowledged. Furthermore, I learned a great deal while working on consulting projects with Fugro, Inc., S&ME, Inc., and AECOM, Inc.

The friends that I've made at the University of Texas have left a lasting impression on me and have helped me through many personal and professional challenges. In particular, Andrew Stolte and Andrew Keene have been there during my entire journey through graduate school and I am fortunate to have such supportive friends. In addition, I'd like to acknowledge Jeremy Faker, Gavin Power, John Rebuck, Ian McMillan, Sorin Secara, Zachary Bemis, Ivan Garcia, Edward Jaimes, Olivia Deterling, Breanna Peterman, Julia Roberts, Hande Gerkus, Yuta Nakamura, Kaleigh McLaughlin, Jillian Montalvo, Jose Martinez Dauhajre, Michael Little, James Munson, Jakob Walter, Jonas Bauer, Chris Nelsen, Shawn Griffiths, Joseph Vantassel, and all others that made my time at UT so enjoyable.

Most importantly, I'd like to thank my incredible family. My parents Paul and Jeanne, my brother Joe, my sister Michelle, and my yellow lab Maggie, have always inspired me to be caring, honest, hard-working, and humble. They have challenged me to become a better person and I am blessed to have such an incredible family.

Addressing Surface Wave Inversion Non-Uniqueness and the Implications for Seismic Site Response Analyses

David Paul Teague, Ph.D.

The University of Texas at Austin, 2017

Supervisor: Brady R. Cox

Surface ground motions predicted from a seismic site response analysis are strongly dependent on the shear wave velocity (Vs) profile used to represent the small-strain shearing stiffness of subsurface materials as a function of depth. Moreover, uncertainties are present in the input Vs profile and this uncertainty leads to uncertainty in the predicted site response. When Vs profiles are obtained from surface wave inversion, the final derived Vs profiles are non-unique, with many different interpretations of the subsurface shearing stiffness that are consistent with the measured surface wave field data. This non-uniqueness is exacerbated by the ambiguous interpretation of surface wave modes and the subjectivity of defining the inversion parameterization (trial number of layers and ranges in their respective Vs, compression wave velocities, and mass densities). Thus, it is necessary to develop strategies to systematically address these issues in order to develop Vs profiles with realistic estimates of uncertainty for use in site response analyses. First, a-priori information should be sought to aid in interpreting modes and to develop a realistic parameterization to guide the surface wave inversion. In complex geologic settings, it can be extremely challenging or even impossible to obtain geologically-realistic Vs profiles without this a-priori information. However, there are many situations when a-priori information is scarce or

nonexistent. In such cases, alternative mode interpretations and/or parameterizations must be considered.

Even with abundant a-prior information, the non-uniqueness issue generally cannot be eliminated and the variation in seismic site response associated with non-unique Vs profiles derived from the same surface wave dataset is of interest. At the two sites considered in this study, very different Vs profiles derived from surface wave inversion of the same dataset produced very similar site response estimates, provided that the experimental surface wave dispersion data was well-fit. Furthermore, the site response estimates associated with these Vs profiles were more accurate and less variable than those associated with Vs profiles that were developed using common strategies of accounting for Vs uncertainty. Thus, despite the non-uniqueness issue, Vs profiles derived from a rigorous surface wave inversion can yield robust site response estimates.

Table of Contents

List of Tables

List of Figures

Chapter 1: Introduction

1.1 BACKGROUND

Earthquake ground motions experienced at a given location are influenced by a number of factors. These factors include the seismic source (i.e., fault rupture that generates the earthquake), the path taken by seismic waves as they propagate towards the site, and the physical properties of the local soil and rock. The influence of local soil/rock is commonly referred to as "site effects". Site effects are generally predicted using one-dimensional seismic site response analyses. These analyses model the response of an idealized model of the soil/rock at the site to one or more input ground motions. Reference/rock ground motions are applied at the base of the model and the response at the ground surface is computed. A number of approaches may be used to compute the site response, including linear, equivalent-linear, and nonlinear analyses. In all cases, a representative model of the soil/rock at the site is required.

Site response simulations using linear, equivalent linear, and nonlinear analyses are strongly influenced by the shearing stiffness of the various soil/rock layers in the model (Bazurro and Cornell 2004, Rathje et al. 2010, Li and Assimaki 2010, Barani et al. 2013). Specifically, the small-strain shearing stiffness (G_{max}) of these materials significantly impacts the amplitude and frequency content of surface ground motions. Accordingly, reliable site response analyses are dependent upon having robust estimates of G_{max}. Because the velocity at which shear waves propagate through a material (i.e., the shear wave velocity, or Vs) is directly related to G_{max}, it is possible to quantify G_{max} by measuring or inferring Vs. Typically, a profile of Vs as a function of depth is developed and this information is used in the site response analysis.

Uncertainties are inherent in the final Vs profile(s) and these uncertainties lead to uncertainties in the predicted site response. These uncertainties are dependent upon the technique used to obtain the Vs profile. Vs profiles are developed using two main classes of techniques. The first class of techniques, referred to as "direct"/invasive methods, utilize one or more boreholes and involve the direct measurement of Vs. While these techniques vary, they all involve the generation of shear waves by a seismic source and the measurement of these shear waves with one or more receivers at various depths in a borehole. The analysis of data from this type of testing is relatively simplistic and involves the identification of shear wave arrivals in each recorded signal. However, disturbance from drilling, the subjectivity of picking wave arrivals, and assumptions about wave travel paths can lead to significant uncertainty.

The second class of techniques, referred to as "indirect"/non-invasive surface wave methods, do not actually involve the direct measurement of Vs. Rather, surface waves are measured at the ground surface and layered earth models (of which Vs is one property) that are consistent with these surface wave measurements are sought by solving an inverse problem. Surface wave methods vary, but generally consist of the following three steps: (1) measurement of surface waves in the field, (2) computation of experimental dispersion data from the field measurements, and (3) inversion to obtain layered earth models whose theoretical dispersion curves match the field experimental dispersion data. One of the most notable aspects of surface wave methods is the non-uniqueness of the inverse problem. In other words, it is possible to retrieve many, significantly different Vs profiles that are all consistent with the measured surface wave data. This non-uniqueness is exacerbated when the interpretation of surface wave modes is ambiguous and/or the subsurface layering cannot be constrained by a-priori information. This non-uniqueness leads to considerable uncertainty, requiring the analyst

to rigorously consider numerous mode interpretations and/or possible layered earth models.

Clearly, invasive borehole methods and non-invasive surface wave methods are quite different and the uncertainties in the final Vs profile(s) stem from significantly different factors. Nonetheless, these factors are not always considered in a systematic manner and this has significant implications on the predicted seismic site response. Engineering design codes stress the importance of accounting for uncertainty in Vs when performing site response analyses (e.g., ASCE 2010, AASHTO 2011), yet, no firm guidelines are provided. Consequently, many approaches ranging from simplistic to complex are used in practice (Matasovic and Hashash 2012).

When considering uncertainty in the context of Vs profiling, it's important to note that there are two types of uncertainty. The first type, aleatory variability, refers to inherent randomness and is typically deemed to be primarily represented by spatial (horizontal and vertical) variability in Vs across the site. The second type, epistemic uncertainty, stems from data uncertainty or a lack of scientific knowledge. Epistemic uncertainty arises from an inability to perfectly model a process. The distinction between aleatory variability and epistemic uncertainty is not always clear and they are not necessarily perfectly classified and/or decoupled in practice. For example, the spatial variation in Vs at a site is arguably more epistemic in nature because if adequate information were available, then a three-dimensional model could be developed. Moreover, the Vs structure at a site is more-or-less constant (at least on the time scales considered in engineering design) and is not random/aleatory in the same way that rolling a dice is. Nonetheless, spatial variation in Vs is typically considered aleatory in practice.

Despite the ambiguities in the classification of aleatory variability versus epistemic uncertainty, these two types of uncertainty are accounted for in distinctly

separate ways when attempting to account for Vs uncertainty in site response analyses for critical structures such as nuclear facilities (EPRI 2012). However, the approaches prescribed in EPRI (2012) to account for Vs uncertainty do not give significant consideration to the method used to derive the Vs profile(s). Furthermore, recent work by Griffiths et al. (2016a and 2016b) suggests these commonly-used of approaches of accounting for aleatory variability and epistemic uncertainty may lead to inaccurate site response estimates and/or over-estimate the variability in the site response. Thus, the issue of how to consider Vs uncertainty in the seismic site response is an important issue that necessitates further study.

1.2 SCOPE OF RESEARCH

This research considers the several aspects of Vs uncertainty and the associated influence on the seismic site response. First, this research investigates the value of a-priori information when performing surface wave inversion. It is demonstrated that this information can be extremely valuable for both the interpretation of surface wave modes and/or for the development of a realistic inversion parameterization (i.e., trial number of layers and ranges in their respective thicknesses, Vs, Vp, and mass densities). Next, this research discusses a strategy to perform surface wave inversion in the absence of a-priori information. This approach, referred to as the "layering ratio" technique, involves systematically investigating numerous parameterizations, each with a unique number of layers. This approach can greatly aid in developing a realistic ensemble of Vs profiles. However, the non-uniqueness issue generally cannot be eliminated and its influence on the predicted site response must be considered. Thus, this research will subsequently investigate how this uncertainty influences the predicted seismic site response. This question is addressed at both a synthetic and a real-world site. The accuracy and

variability of seismic site response analyses performed using various, non-unique Vs profiles derived from surface wave testing are considered. The accuracy and variability of these site response estimates is then compared to the accuracy and variability of site response estimates performed on Vs profiles developed using common strategies of accounting for Vs uncertainty, both aleatory and epistemic. Finally, improvements are proposed to the current practices of accounting for Vs uncertainty.

1.3 ORGANIZATION OF DISSERTATION

This dissertation contains four main body chapters (Chapters 2 through 5) along with an introduction (Chapter 1) and a conclusion (Chapter 6). Each body chapter is a self-contained journal article that includes a literature review, research findings, and conclusions. (All references are provided at the end of the dissertation). These chapters follow logical progression as detailed below.

Chapter 2 discusses the development of deep (+500 m) Vs profiles in the complex inter-bedded geology of Christchurch, New Zealand. Surface wave testing was performed at a total of 14 sites throughout Christchurch and the inversion of this dataset is discussed. Due to the complex geologic conditions, a-priori information was sought to aid in the interpretation of surface waves modes and in developing the inversion parameterization. This chapter illustrates the value of this a-priori information, demonstrating that it would be nearly impossible to develop geologically-realistic Vs profiles without it.

Despite the value of a-prior information, it is oftentimes not available and a systematic means of investigating the inversion non-uniqueness is needed. Chapter 3 outlines a procedure for investigating this non-uniqueness. This procedure, referred to as the "layering ratio" technique, involves systematically exploring multiple inversion

parameterizations. Each parameterization is defined by a unique layering ratio (Ξ), which defines the number of trial layers and their respective thicknesses. The usefulness of this procedure is demonstrated at a synthetic site, for which a true/solution Vs profile is available, and at real-world site, where there is no such thing as a true/solution Vs profile.

Chapter 4 discusses variability and accuracy of site response predictions performed using Vs profiles derived from non-unique surface wave inversions and other commonly used statistical methods of accounting for epistemic uncertainty and aleatory variability in Vs. The example considered in Chapter 4 is the same synthetic case considered in Chapter 3. Thus, the site response for the true/solution Vs profile was computed and is compared to site response estimates for Vs profiles developed using numerous techniques. These Vs profiles include: (1) 350 Vs profiles developed by performing multiple surface wave inversions, each with a unique set of layering parameters, on a common dispersion dataset, (2) two upper/lower range base-case Vs profiles developed by systematically increasing or decreasing the solution Vs profile by 20%, and (3) 100 Vs profiles developed using the Vs randomization procedure proposed by Toro (1995).

Chapter 5 considers the same topics discussed in Chapter 4. However, the example discussed in Chapter 5 comes from the Garner Valley Downhole Array (GVDA) Site in Southern California. Therefore, this real-world example accounts for additional complexities that are not captured in the synthetic example in Chapter 4. Furthermore, improvements to the current practices of accounting for aleatory variability and epistemic uncertainty are proposed. Finally, Chapter 6 provides concluding remarks and proposes future research topics.

Chapter 2: Development of Deep Shear Wave Velocity Profiles with Estimates of Uncertainty in the Complex Inter-Bedded Geology of Christchurch

David P. Teague, Brady R. Cox, Brendon A. Bradley, and Liam M. Wotherspoon

This chapter contains a journal article that has been submitted to Earthquake Spectra for peer review. The full citation is listed below:

Teague, D. P., Cox, B. R., Bradley, B., Wotherspoon, L. (2017 submitted). "Development of Deep Shear Wave Velocity Profiles with Estimates of Uncertainty in the Complex Inter-Bedded Geology of Christchurch," Earthquake Spectra, in review.

As first author, I was responsible for approximately 33% of the project planning, 20% of the data acquisition, 100% of the data processing, and 50% of the results interpretation.

ABSTRACT

Deep (+500 m) shear wave velocity (Vs) profiles were developed at 14 sites throughout Christchurch, New Zealand, using a combination of active- and passive-source surface wave testing. The geology of Christchurch is quite complex and presents several challenges for surface wave testing. Specifically, the complex inter-layering of relatively stiff gravels with soft sands, silts, and clays makes: (1) the interpretation of experimental dispersion data ambiguous, and (2) complicates the determination of appropriate inversion layering parameterizations. In order to address (1), dispersion data uncertainty was quantified and several mode interpretations were considered during inversion. In order to address (2), 155 geotechnical boreholes and 199 geologic well logs in the vicinity of the test sites were used to guide the choice of layering parameterizations such that geologically-realistic Vs profiles were obtained via surface wave inversion. At each site, suites of 1000 Vs profiles representing the combined effects of epistemic uncertainty and aleatory variability in Vs were obtained. The final Vs profiles from this study are well-constrained to a depth of approximately 500 m. At greater depths, the Vs profiles are less reliable due to limitations of the largest aperture arrays used in passive

surface wave testing. These Vs profiles have been made available and are intended to aid in seismic site response analyses, including back-analyses aimed at better understanding the spatial variability in ground motions experienced during the Canterbury Earthquake Sequence and/or forward-analyses aimed at quantifying the amplitude and frequency content of future design ground motions.

2.1 INTRODUCTION

The 2010-2011 Canterbury Earthquake Sequence (CES) caused significant damage to the city of Christchurch, New Zealand as result of strong ground shaking and soil liquefaction. The most notable event of this sequence was the February 2011 M_W 6.3 Christchurch Earthquake, which caused 185 casualties. Ground motions (GMs) from this event were recorded by a network of 20 seismic recording stations in the greater Christchurch area (Bradley and Cubrinovski 2011). These ground motions were deemed to be quite complex at some locations, with evidence of frequency-dependent amplification caused by overlapping stratigraphic, basin, and directivity effects. In order to fully understand the spatial variability in ground shaking during the CES events, it is necessary to understand both the shallow and deep seismic velocity structure of the Canterbury basin. However, in the immediate aftermath of the CES there was a lack of detailed information on the velocity structure/small-strain shearing stiffness of materials throughout Christchurch, particularly at depths great than 20 - 30 m.

The shearing stiffness of geomaterials is typically quantified using profiles of shear wave velocity (Vs) as a function of depth. Since the small-strain shear modulus (G_{max}) is directly related to Vs, in-situ measurements of Vs are typically used to characterize the small-strain stiffness conditions down to some reference condition (e.g., engineering bedrock or basement bedrock). Numerous site response simulations have

demonstrated the significant influence of the input Vs profile on both the amplitude and frequency content of surface ground motions (e.g., Bazzuro and Cornell 2004, Rathje et al. 2010, Li and Assimaki 2010, Barani et al. 2013, Griffiths et al. 2016b, Chapter 4). Thus, accurate estimates of Vs, including quantification of uncertainty, are of utmost importance for back analyses aimed at replicating recorded GMs and forward analyses aimed at predicting future GMs for seismic design. Vs profiles are typically obtained via invasive borehole measurements (e.g., seismic crosshole, seismic downhole, and PS suspension logging) or non-invasive surface wave measurements (e.g., multi-channel analysis of surface waves, microtremor array measurements, etc.). Invasive borehole methods are relatively costly and time consuming, especially when drilling to significant depths in complex, inter-bedded soil deposits, which are present in many locations beneath Christchurch (Brown et al. 1988). Conversely, surface wave methods offer a non-invasive, cost effective, and efficient means of obtaining Vs profiles to significant depths (Garofalo et al. 2016a), with Vs uncertainty on the order of that obtained from borehole methods when performed by experts (Garofalo et al. 2016b).

Surface wave testing is generally executed in the following three steps: (1) field data acquisition of seismic waveforms, (2) processing of seismic waveforms to extract experimental dispersion data, and (3) inversion of dispersion data to obtain Vs profiles. Data acquisition involves measuring wavefields with strong surface wave content. Wavefields can be actively-generated at the ground surface (e.g., using a hammer, drop weight, or dynamic shaker) or passively-generated from cultural noise/ambient vibrations or seismic microtremors. Processing often involves 2D wavefield transformations (e.g., frequency-wavenumber, slant-stack, etc.) aimed at extracting a site-specific relationship between surface wave phase velocity (typically Rayleigh wave velocity, Vr) and frequency (f) [or, alternatively, wavelength (λ)] from the experimental field

measurements. This relationship between Vr and f [or λ] is often referred to as a field dispersion curve, or, more appropriately, experimental dispersion data. The inversion process consists of finding layered earth models whose theoretical dispersion curves best match the experimental dispersion data. Layered earth models are comprised of a pre-defined number of layers, each characterized by its thickness (H), compression wave velocity (Vp), shear wave velocity (Vs), and mass density (ρ). For seismic site response, the most significant parts of the layered earth model are H and Vs. Fortuitously, the forward problem solved during surface wave inversion is also most sensitive to H and Vs. However, it is important to note that the inverse problem is highly non-unique, meaning that significantly different ground models may yield theoretical dispersion curves that fit the experimental dispersion data equally well (e.g., Foti et al. 2009, DiGiulio et al. 2012, Chapter 3). This inversion non-uniqueness can pose a challenge for developing realistic ground models for site response if proper precautions are not taken to quantify Vs uncertainty in a robust manner.

An analyst must be rigorous in the consideration of inversion non-uniqueness if reliable Vs profiles are to be developed from surface wave testing. A number of studies have demonstrated that the choice of parameterization (i.e., number of layers and ranges in their respective depth/thickness, Vp, Vs, and ρ) significantly influences the final Vs profiles obtained from inversion (DiGiulio et al. 2012, Chapter 3). Thus, it is prudent to consider multiple, unique parameterizations in the absence of a-priori subsurface information to constrain the inversion. However, if supporting data is available, it should be used to constrain the inversion and yield Vs profiles that are more realistic representations of the actual subsurface layering. For example, analysts commonly incorporate additional constraints during inversion, including horizontal-to-vertical spectral ratio (HVSR) curves (e.g., Scherbaum et al. 2003, Arai and Tokimatsu 2005,

Parolai et al. 2005, Piccozi et al. 2005) and/or geotechnical, geophysical, or geologic data, which can aid in reducing the range of possible Vs solutions (e.g., Lai et al. 2005, DiGiulio et al. 2006, DiGiulio et al. 2012, Chapter 2).

In addition to inversion non-uniqueness, the interpretation of experimental dispersion data can introduce significant uncertainty in the derived Vs profiles. For example, certain geologic conditions like shallow stiff layers and low velocity layers sandwiched between layers of greater stiffness (i.e., velocity reversals or inverse layers) are known to cause mode jumps (i.e., higher mode dominance) and/or mode superposition (i.e., effective modes) over certain bandwidths in the experimental dispersion data (Foti et al. 2011, Boaga et al. 2013, Boaga et al. 2014). If these mode issues are not identified and properly accounted for in the inversion, the resulting Vs profiles will not accurately represent the subsurface stiffness conditions. Therefore, it is beneficial to have an understanding of the local geology and general subsurface stratigraphy in order to identify the possibility of higher mode dominance and/or effective modes.

This paper discusses the acquisition and processing of combined active-source and passive-wavefield surface wave data in order to develop deep (+500 m) Vs profiles at 14 sites in Christchurch. Inversion non-uniqueness issues and challenges with accurate mode identification are especially troublesome in the complex, inter-layered geologic conditions that exist beneath Christchurch. Thus, the processing and interpretation of surface wave data at these 14 sites was extremely challenging. Fortunately, an abundance of a-priori information, including geotechnical boreholes and geologic well logs, was available to aid in the inversions (Lee et al. 2015 and 2017). This paper demonstrates how a-priori information was used to help invert challenging datasets and develop geologically-realistic Vs profiles with estimates of uncertainty throughout Christchurch.

The Vs profiles developed from this study are intended to aid in future engineering analyses, such as 3D physics-based ground motion simulations and 1D site response analyses, aimed at better understanding the influence of local soil conditions on the spatial variability in ground motions experienced during the Christchurch Earthquake. Furthermore, the data processing and inversion methodologies discussed herein will be valuable to others in their attempts to develop realistic deep Vs profiles with estimates of uncertainty from surface wave testing in other areas.

2.2 CHRISTCHURCH GEOLOGY AND CHALLENGES FOR SUBSURFACE SITE CHARACTERIZATION

Christchurch is located on the eastern coast of Pegasus Bay on the South Island of New Zealand. The majority of the test sites for this study are located on the deep alluvial soils of the Canterbury Plains and the Pegasus Coast. The Springston and Christchurch Formations make up the near-surface geology (approximately 15 to 40 m), as shown in Figure 2.1. The Springston Formation consists primarily of alluvial sands and gravels. The Christchurch formation is composed of Holocene estuarine, lagoon, dune and coastal swamp deposits of gravel, sand, silt, clay, and peat. Underlying the Christchurch Formation are multiple alternating formations of alluvial gravels and estuarine and marine sands, silts, clays, and peats (Brown et al. 1988). The only borehole in Christchurch that extends to depths in excess of 200 m is Bexley Well 2. This well is located approximately 1.5 km inland from the coast, and ranges from 2 km to 13 km from the 14 sites where deep surface wave testing was conducted for this study (refer to Figure 2.2a). Figure 2.1c shows a simplified representation of the layering in Bexley Well 2. It can be seen that gravels inter-bed with sands, silts, and clays above a depth of roughly 250 m. The well log indicates sand, silt, and clay deposits between 250 and 430 m (Barnes et al. 2011). Miocene-aged volcanics are present throughout much of the

Canterbury Plains and Pegasus Coast. The depth of these materials is relatively shallow close to the Banks Peninsula and becomes quite deep with increasing distance to the north and east (Forsyth et al. 2008). Basement rock, which represents the interface of the Pre-Quaternary and Quaternary geologic units, is quite deep and generally ranges from 1000 to 2000 m in the locations where testing was performed (Lee et al. 2015).

The alternating formations of alluvial gravels and estuarine and marine sands, silts, clays, and peats described in the previous paragraph are present at most sites where deep surface wave testing was conducted. Because gravel is typically much stiffer than clays, silts, and sands at comparable effective stress levels (Kramer 1996, Lin et al. 2014), strong velocity contrasts can be expected at the interfaces of geologic formations. Additionally, velocity reversals occur when sand, silt, or clay layers reside below gravel. As discussed previously, these strong velocity contrasts and velocity reversals are expected to lead to higher and/or effective mode dominance over certain bandwidths of the experimental dispersion data. It is important to recognize these potential mode issues prior to inversion, because if higher modes are incorrectly interpreted as fundamental mode, Vs may be significantly overestimated during inversion.

In addition to the challenges associated with mode interpretations, the complex geology in Christchurch also makes it difficult to adequately constrain the range of possible solutions during the inversion process. As noted earlier, the choice of parameterization significantly influences the Vs profiles derived from inversion. Thus, it is necessary to develop a parameterization that is wide-ranging enough to account for the complex geologic conditions, yet sufficiently constrained to preclude unrealistic ground models. This task is not trivial in complicated geologic settings, such as those in Christchurch. Without a-priori information, it would be extremely difficult, or even

impossible, to develop a set of inversion parameters that accurately capture the subsurface complexity demonstrated in Figure 2.1b and 2.1c.

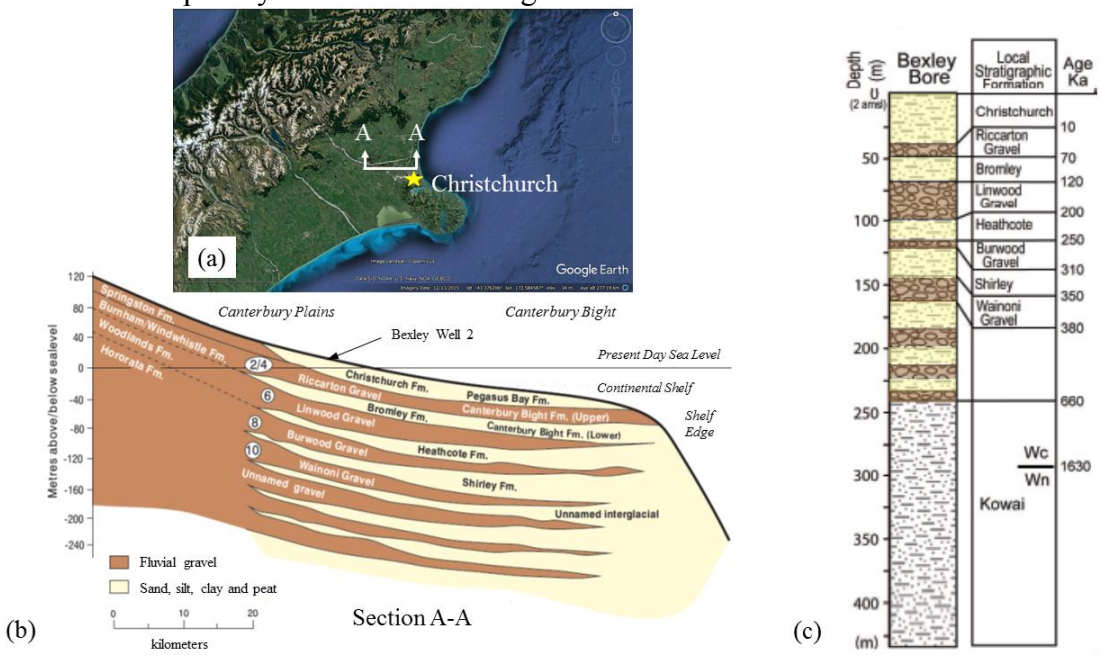

Figure 2.1: (a) Geographical location of Christchurch. (b) Schematic geologic cross-section beneath Christchurch and Pegasus Bay showing a sequence of deep inter-layered gravel and sand formations, and (c) simplified representation of the geologic layering from Bexley Well 2 (modified from Forsyth et al. 2008 and Barnes et al. 2011).

2.3 Surface Wave Testing and Locations

Surface wave testing was conducted at 14 sites throughout Christchurch between January and March 2013. Test site locations are shown in Figure 2.2a. These 14 sites were chosen by balancing the following considerations: adequate spatial coverage across the city of Christchurch, proximity to strong motion seismic recording stations (refer to Figure 2.2a), and sufficient space to conduct testing. Both active- and passive-source surface wave testing were performed. Active-source testing was executed using the Multi-channel Analysis of Surface Waves (MASW) method. Active-sources included both a sledgehammer and the large NHERI@UTexas T-Rex vibroseis truck

(https://utexas.designsafe-ci.org/equipment-portfolio/). Sledgehammer data was obtained using 48, 4.5 Hz vertical geophones with a uniform spacing of 2 m. Vibroseis data was collected using 15 to 24, 1 Hz vertical geophones with a uniform spacing of 10 m. Surface waves were generated at a number of distinct source-offset locations, which are measured relative to the first geophone in the MASW array. Hammer source-offsets were 5, 10, 20, and 40 m and the vibroseis source offsets were 20, 40, and 80 m. The active-source arrays used at the Hagley Park (HP) site are shown as a typical example in Figure 2.2b.

Passive-source measurements (i.e., Microtremor Array Measurments, MAM) were performed using circular arrays with approximate diameters of 60, 200, and 400 m. Ambient noise was measured for approximately a half-hour, one hour, and two hours for each successively larger array, respectively. Circular arrays were generally comprised of ten, three-component Nanometrics Trillium Compact 120s broadband seismometers with a flat response between 100 Hz to 120 seconds. As a typical example, Figure 2.2b shows the ambient circular arrays used at the Hagley Park site. Note that at some sites perfect circular arrays could not be used due to spatial constraints (buildings, roads, etc.). In these situations, some of the receivers in a given array were moved to accommodate site-specific obstacles. While we prefer to use perfectly circular arrays because they provide uniform azimuthal coverage and allow for comparison of multiple array processing techniques when extracting dispersion data, irregular 2D array geometries can be utilized in MAM testing provided the coordinates for each receiver are known.

Raw data collected at all sites are available on the Network for Earthquake Engineering Simulation (NEES) website (https://nees.org/warehouse/project/1173). Data is can also be obtained from the Design Safe website (www.designsafe-ci.org) by searching for the “NEES-2012-1173” group in the data depot. Each site was assigned a

digital object identifier (DOI), as listed in Table 2.1. Detailed metadata describing the array geometries, acquisition parameters, etc. are provided for each site.

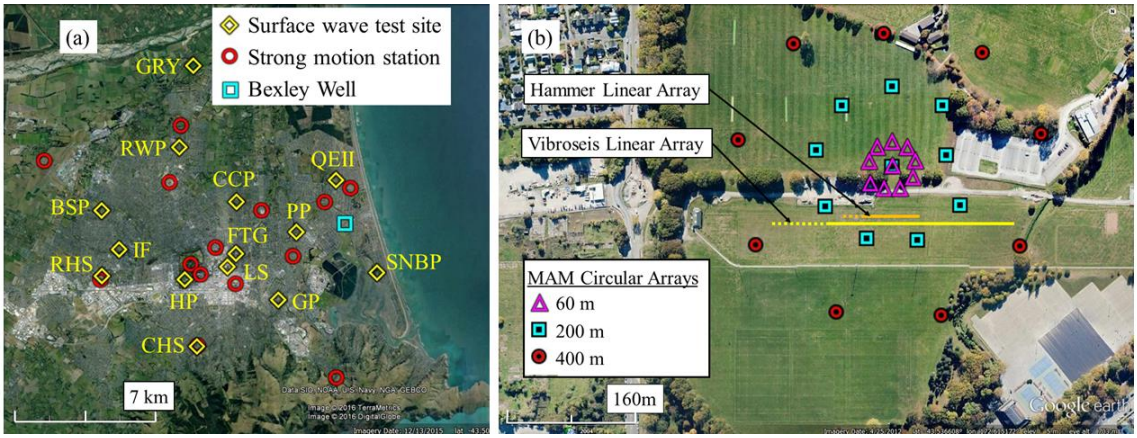

Figure 2.2: (a) Location of all 14 deep surface wave test sites in Christchurch, New Zealand relative to the 20 strong motion stations that recorded the Christchurch Earthquake, and (b) array layouts for a typical site (Hagley Park, HP). Note that some strong motions stations are beyond the extents of (a). Additional details regarding the test sites are provided in Table 1. The extents of the source-offset locations for active arrays are indicated by dashed lines

Table 2.1: Coordinates, Median V_{S30} values with associated variability, and DOI numbers for all surface wave test sites.

Site	Latitude	Longitude	Median V_{S30} (m/s)	$\sigma\ln(V_{S30})$	DOI
Burnside Park (BSP)	-43.50552	172.56591	294	0.04	DOI:10.4231/D3DB7VQ2P
Cashmere High School (CHS)	-43.56667	172.62321	222	0.001	DOI:10.4231/D38K74W89
Christchurch Park (CCP)	-43.50140	172.64795	160	0.05	DOI:10.4231/D34X54G8C
Fitzgerald (FTG)	-43.52482	172.64903	211	0.02	DOI:10.4231/D3154DP4J
Garrick Park (GP)	-43.54658	172.67402	183	0.02	DOI:10.4231/D3WD3Q19Z
Groynes (GRY)	-43.44137	172.62091	223	0.03	DOI:10.4231/D3RN30756
Hagley Park (HP)	-43.53598	172.61637	188	0.04	DOI:10.4231/D3MW28F12
Ilam Fields (IF)	-43.52208	172.57690	297	0.04	DOI:10.4231/D3H41JM7M
Latimere Square (LS)	-43.53039	172.64261	192	0.02	DOI:10.4231/D3CC0TT3G
Porritt Park (PP)	-43.51521	172.68488	186	0.04	DOI:10.4231/D37P8TD2H
QEII Park (QEII)	-43.49214	172.70914	202	0.06	DOI:10.4231/D33X83K84
Redwood Park (RWP)	-43.47638	172.61306	188	0.02	DOI:10.4231/D3057CS49
Riccarton High School (RHS)	-43.53456	172.56578	324	0.03	DOI:10.4231/D3VD6P49Q
South New Brighton Park (SNBP)	-43.53296	172.73389	184	0.04	DOI:10.4231/D3QN5ZB5K

2.4 SURFACE WAVE DISPERSION PROCESSING

Active-source MASW Rayleigh wave data were analyzed using the frequency domain beamformer (FBDF) method (Zywicki 1999) coupled with the multiple source-offset technique for identifying near-field contamination and quantifying dispersion uncertainty (Cox and Wood 2011). Dispersion data influenced by near-field effects and/or significant offline noise were eliminated. A representative mean dispersion curve with corresponding standard deviations was computed using data from all source offsets at each site. This dispersion data was generally in the frequency range of 2 to 50 Hz when sledgehammer and T-Rex data was combined.

Passive-source MAM data were processed using the 2D high resolution frequency-wavenumber (HFK) method (Capon 1969) and the modified spatial autocorrelation (MSPAC) method (Bettig et al. 2001), as implemented in the open-source software Geopsy (www.geopsy.org). For both methods, noise records were divided into 180 s time windows and processed individually, resulting in approximately 10 to 40 time windows per array, depending on the recording time. The choice of a 180 s window length was meant to provide a large number of cycles per window at the lowest frequencies of interest (e.g., 60 cycles at 0.33 Hz), resulting in more robust dispersion estimates per window. Further, the choice of window length still yielded a sufficient number of windows to calculate a robust phase velocity with estimates of uncertainty at each frequency. For HFK processing, a mean phase velocity and standard deviation were computed at each frequency. For MSPAC processing, autocorrelation curves associated with each frequency and spacing were converted to dispersion estimates and plotted on contour plots. "Best" and upper/lower-bound estimates were then manually picked from these contour plots.

Figure 2.3a shows the mean and +/- one standard deviation MASW and MAM dispersion data from the Hagley Park site. The MASW and MAM dispersion data are in satisfactory agreement at overlapping frequencies (roughly 2 to 10 Hz). In the range of 1 to 2 Hz, the MAM experimental dispersion data exhibits a flat/decreasing trend. This flat/decreasing trend could indicate a strong velocity reversal at significant depths. However, in this case, it likely indicates that the dispersion data is transitioning from a higher Rayleigh-wave mode back down to a lower (presumably fundamental) mode. Rather than an abrupt jump from mode-to-mode, the transition is relatively smooth, representing a superposed or effective mode. The higher mode data likely results from the inter-bedding of relatively stiff gravel formations with underlying soft formations comprised of sands, silts, and/or clays (see Figure 2.1). It should be noted that there is no active-source MASW dispersion data below 2 Hz. Thus, if passive-source testing were not performed, the mode transition between 1 and 2 Hz would not be evident and all MASW data may have been erroneously interpreted as fundamental mode. Therefore, the passive-source MAM data greatly aided in the interpretation of the active-source MASW data. Furthermore, knowledge of the geologic conditions can alert an analyst to the possibility of these mode issues and aid in overcoming the ambiguity that is often associated with interpreting the experimental dispersion data.

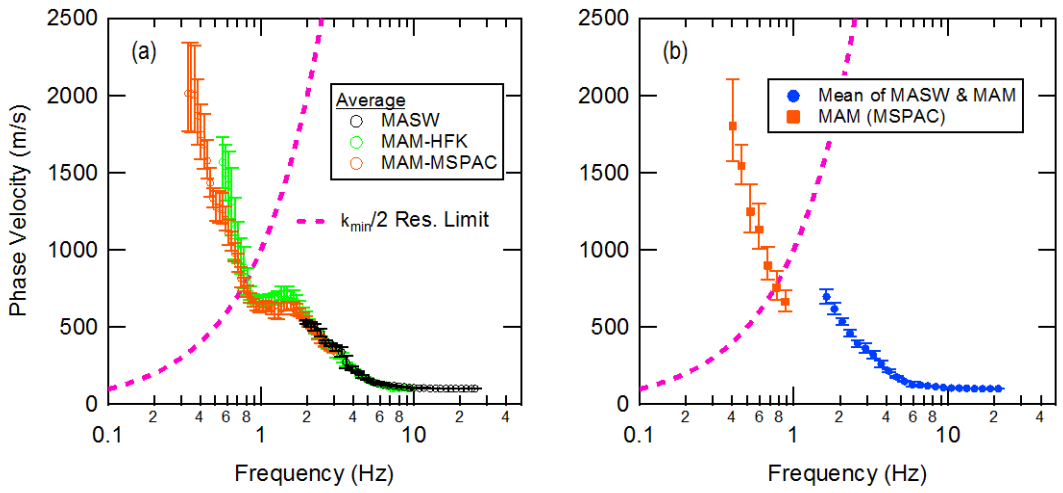

Figure 2.3: (a) Active-source (MASW) and passive-source (MAM) experimental dispersion data from the Hagley Park site. Note that the MAM data was processed using both the HFK and MSPAC methods. (b) Composite dispersion curve developed from experimental dispersion data in (a) and used for inversion. Dispersion data at wavenumbers below the $k_{min}/2$ resolution limit (i.e., at frequencies to the left of the $k_{min}/2$ boundary) are potentially less reliable due to limitations imposed by the maximum array aperture.

Both the MAM-HFK and MAM-MSPAC dispersion estimates exhibit considerable uncertainty (i.e., large standard deviations) at low frequencies (refer to Figure 2.3a). One factor that influences the quality of dispersion data at low frequencies/long wavelengths is the array resolution, which is controlled by the maximum aperture of the largest array. Below 0.8 Hz, the experimental dispersion data exceeds the resolution capabilities of the largest diameter array and is therefore less reliable. During processing, passive-source MAM data at wavenumbers ($k = 2\pi/\lambda$) below the minimum resolvable wavenumber (i.e., the array resolution limit, $k_{min}/2$, determined using the array response function; Wathelet et al. 2008) were removed from the dispersion data obtained using the 60 and 200 m arrays. However, in an effort to profile as deep as possible in the thick soils of the Canterbury Plains, experimental dispersion

data at wavenumbers below $k_{min}/2$ were retained for the 400 m array at each site. Nonetheless, dispersion data at wavenumbers below $k_{min}/2$ may be of lower quality and are significantly more uncertain (Wathelet et al. 2008). Thus, the $k_{min}/2$ limits are clearly marked on the plots of dispersion data for each site.

It is evident that the MAM-HFK dispersion data in Figure 2.3a is biased towards higher phase velocities than the MAM-MSPAC data. As noted by Asten and Boore (2005), low frequency HFK data can exhibit bias towards high surface wave velocities due to azimuthal smearing of wave energy when passive waves are impinging from a wide range of azimuths at the site. However, HFK processing is better suited when passive waves are propagating from a limited range of azimuths. After processing, the HFK and MSPAC dispersion data at each site were compared on a on a frequency-by-frequency basis and the dispersion data that was deemed to be of higher quality was selected based on a number of factors (e.g., smoothness, uncertainty bounds, bias towards high or low phase velocity, noise directionality, etc.). Generally, HFK dispersion data was chosen at higher frequencies (1 to 10 Hz) and MSPAC dispersion data was chosen at lower frequencies (below 1 Hz). At Hagley Park, MSPAC dispersion data was chosen in lieu of the HFK data at frequencies below 1 Hz.

A composite experimental dispersion curve for use in the inversions for each site was developed by combining active- and passive-source dispersion data. At frequencies where active- and passive-source dispersion data overlapped, dispersion data representing the same Rayleigh mode were averaged. Each composite dispersion curve was resampled to a coarser frequency sampling in order to speed up the inversion process. The experimental data was typically resampled to yield approximately 40 logarithmically-spaced dispersion data points. The range in frequencies varied from site-to-site, but was commonly in the range of 0.4 – 30 Hz.

Figure 2.3b shows the resampled, composite dispersion curve that was used for inversion analyses at Hagley Park. Note that MASW and MAM-HFK data were averaged in the frequency bands of overlap (2 and 10 Hz). Furthermore, experimental dispersion data in the range of 1 to 2 Hz was removed after several trial inversions, as it was judged to represent an effective mode that could not be properly accounted for during inversion. As discussed in a later section, a multi-mode forward solution was used to invert the Christchurch dataset. This type of inversion cannot directly account for effectives modes. Thus, effective modes must be identified and removed prior to inversion.

Composite experimental dispersion data for all sites are provided in a later section of this paper. The overall trends in the experimental dispersion data were generally similar to that observed at the Hagley Park site. Detailed figures showing the MASW and MAM dispersion data from each site are available in the Community Data on the Design Safe Website (www.designsafe-ci.org) under the title "Final Results - Deep Shear Wave Velocity Profiling for Seismic Characterization of Christchurch_ NZ".

2.5 HVSR PROCESSING

Horizontal-to-vertical spectral ratio (HVSR) data can aid in constraining a surface wave inversion (e.g., Scherbaum et al. 2003, Arai and Tokimatsu 2005, Parolai et al. 2005, Piccozi et al. 2005). For example, HVSR curves with strong peaks are often used to approximate the fundamental frequency of the shear wave transfer function, f_{0_TF}, (Lermo and Chavez-Garcia 1993, Lachet and Bard 1994) and/or the lowest frequency peak of the fundamental mode Rayleigh wave ellipticity, f_{0_Ell}, (Malischewsky and Scherbaum 2004, Poggi and Fah 2010). If a strong impedance contrast is present, the frequency at which the HVSR curve exhibits a well-defined peak, f_{0_HV}, is approximately equal to f_{0_TF} and f_{0_Ell}. Accordingly, HVSR curves were computed for each broadband

seismometer used in the passive-source circular arrays in an attempt to estimate the fundamental period of the site and constrain the depth to bedrock during inversion.

The squared average of the north and east components (i.e., the square root of the average of the squared north and east components) of the passive data was used to represent a single horizontal component at each seismometer location used in the MAM testing at each site. For each individual station/seismometer, passive noise records were divided into 180 s time windows and the HVSR from all windows were used to calculate a lognormal median and +/- one standard deviation for that location. The total number of windows for each station ranged from 10 to 40, depending on the total record length. Konno and Ohmachi (1998) smoothing with a smoothing constant of 40 was utilized to remove erratic spikes in the Fourier spectra for each time window.

HVSR curves for all 14 sites are shown in Figure 2.4. Solid black lines represent the lognormal median HVSR curve calculated using the individual median curves from all of the stations in the 60, 200, and 400 m diameter arrays and the dashed black lines represent plus/minus one standard deviation. This data was collected using a 0.10 Hz cutoff frequency in the digitizers in order to remove low-frequency drift. However, it can be seen that at some sites (e.g., GRY, LS, IF) the lowest-frequency peak in the HVSR curve is close to this cutoff frequency. Consequently, the digitizer cutoff frequency adversely impacted the data quality in the frequency range of interest at several sites. Therefore, an additional single-station recording with a 0.05 Hz digitizer cutoff frequency was obtained at a later date. These results from the single-station recording are shown in grey in Figure 2.4 and are of better quality at frequencies below 0.20 Hz.

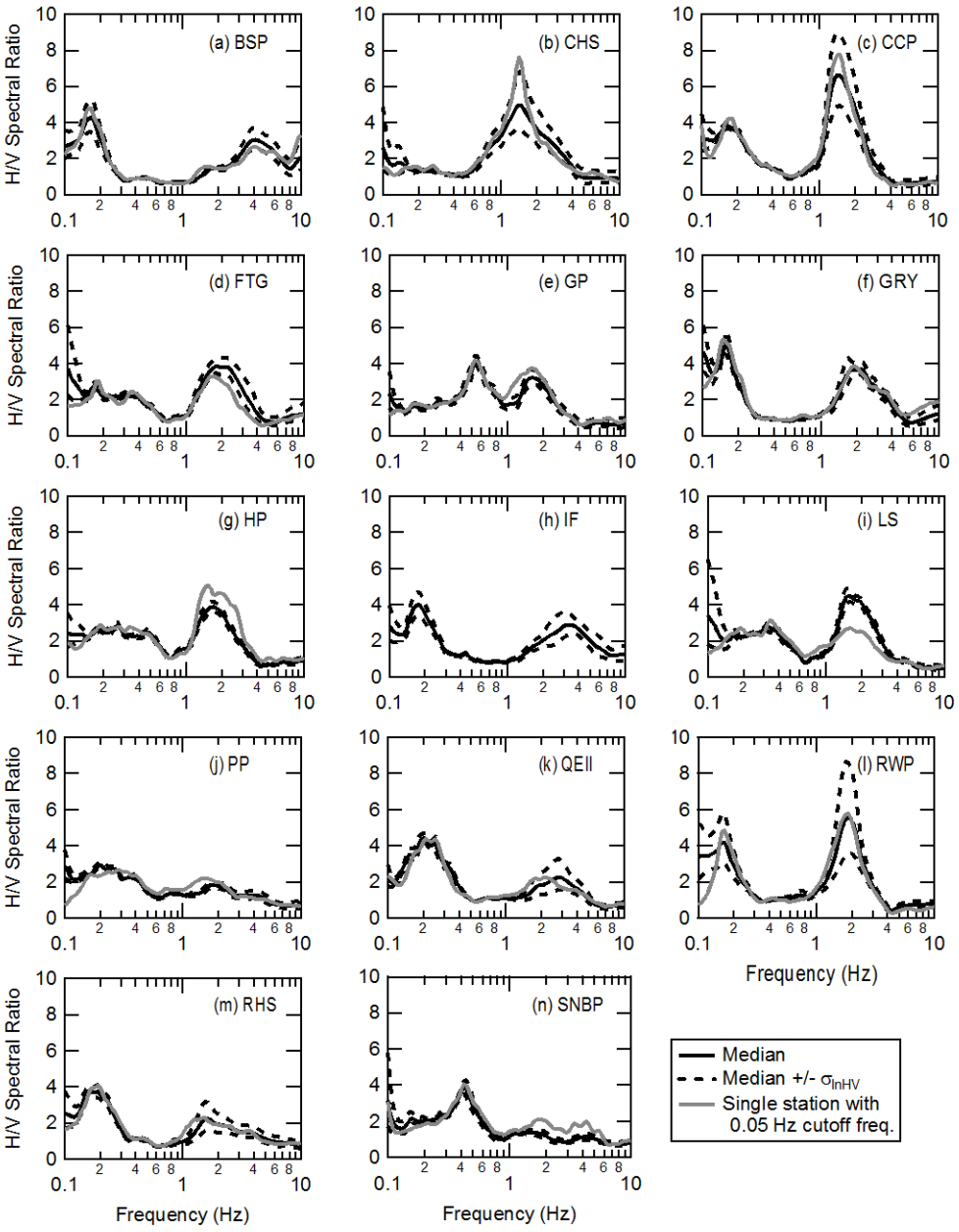

Figure 2.4: Horizontal-to-vertical spectral ratios (HVSR) from all Christchurch test sites. Note that solid and dashed black lines represent the mean and +/- one standard deviation from all stations in the 60, 200 and 400 m MAM arrays, respectively. These recordings were obtained using a digitizer with a 0.10 Hz cutoff frequency. The solid gray line represents a single HVSR measurement taken at a later date using a digitizer with a 0.05 Hz cutoff frequency. Note that an additional HVSR measurement was not obtained at IF.

Well-defined peaks in the HVSR curve are likely caused by large impedance contrasts (SESAME 2004). At sites exhibiting a well-defined peak near 0.2 Hz (BSP, GRY, IF, QEII, RWP, and RHS), this low-frequency peak likely represents the deep interface of the Pre-Quaternary and Quaternary geologic units (i.e., basement rock). At the GP and SNBP sites, which are quite close to the Banks Peninsula, the lowest-frequency peaks (0.54 and 0.43 Hz, respectively) are likely a result of Miocene-aged volcanics, which are expected to be relatively shallow (although still more than 200 m deep). Additionally, a relatively high-frequency peak is also evident at many sites in the range of 1 to 4 Hz (e.g., CHS, CCP, FTG, GP, GRY, HP, LS, RWP). The high-frequency peaks are likely caused by the large impedance contrast at the top of the Riccarton Gravel. Note that the geology at the CHS site is unique and the peak between 1 and 2 Hz is likely a result of very shallow Miocene volcanics.

Some sites exhibit both low- and high-frequency peaks (e.g., GP, GRY and RWP). Other sites exhibit a single well-defined peak and possibly one or more broader, less distinct peaks. The absence of a low- or high-frequency peak suggests smaller impedance contrasts at the top of the Riccarton Gravel, and/or impedance contrasts in the Miocene volanics and Pre-Quaternary geologic units that are too deep to resolve. When identifying peaks in the HVSR spectrum, it is important that the peaks be sufficiently clear (i.e., narrow, stable, and of sufficient amplitude). The SESAME D23.12 Report (2004) provides peak clarity criteria, which was used here to identify stable peaks for use in the inversion.

In an effort to identify volcanics and/or basement rock, the lowest frequency HVSR peak at the BSP, GP, GRY, IF, QEII, RWP, RHS, and SNBP sites was used to constrain the lowest-frequency peak of the fundamental mode Rayleigh wave ellipticity (i.e., f_{0_Ell}) of the theoretical models generated during inversion. These peaks satisfy the

clarity criteria described in SESAME (2004). As noted earlier, peaks in the range of 1-4 Hz are likely caused by the large impedance contrast at the top of the Riccarton Gravel and do not reflect the deep structure of the Canterbury Basin. Because large impedance contrasts are known to exist below the Riccarton Gravel, HVSR peaks in the range of 1-4 Hz were not used to constrain the inversion.

2.6 SURFACE WAVE INVERSION

The inversion of surface wave data involves searching for layered earth models whose theoretical dispersion curves, which are computed via the forward problem, best match the experimentally measured dispersion data. Numerous local and global search algorithms exist. However, global search algorithms are generally preferred because they can keep the inversion from getting trapped in a local minimum, which could lead to erroneous results. Global search algorithms also more elegantly allow for consideration of inversion uncertainty, recognizing that multiple layered earth models commonly result in theoretical dispersion curves that fit the experimental data within its uncertainty bounds. With local and global inversions, the quality of fit between the experimental and theoretical dispersion data is typically quantified using some form of a "misfit" value (e.g., Wathelet 2004, Foti et al. 2009).

All inversions for this study were performed using the open-source software Geopsy. The forward problem in Geopsy is computed using the transfer matrix approach developed by Thomson (1950) and Haskell (1953) and later modified by Dunkin (1965) and Knopoff (1964). Geopsy uses a global search neighborhood algorithm to locate layered earth models within a pre-defined parameterization that yield the lowest possible misfit values between the theoretical and experimental data. Misfit values in this study were computed using Equation 2.1 (modified from Wathelet 2004).

$$m_{d,e} = w_d m_d + w_e m_e = w_d \sqrt{\sum_{i=1}^{n_f} \frac{(x_{di} - x_{ci})^2}{\sigma_i^2 n_f}} + w_e \sqrt{\frac{(f_{0\_Ell,d} - f_{0\_Ell,c})^2}{\sigma_{f0\_Ell}^2}} \qquad (2.1)$$

In Equation 2.1, $m_{d,e}$ is the combined misfit value based on both misfit relative to dispersion data (m_d) and misfit relative to the Rayleigh wave ellipticity peak (m_e). The terms w_d and w_e are user-defined weighting constants for dispersion and ellipticity, respectively, which must sum to 1.0. For the dispersion misfit calculations, x_{di} represents the Rayleigh wave phase velocity of the experimental dispersion data at frequency f_i; x_{ci} is the calculated theoretical Rayleigh wave phase velocity for the trial layered earth model at frequency f_i; σ_i is the standard deviation associated with the experimental dispersion data at frequency f_i; and n_f is the number of frequency samples considered for the misfit calculation. Similarly, for the ellipticity peak misfit calculation, $f_{0\_Ell,d}$ represents the Rayleigh wave ellipticity peak associated with the field data (which is assumed to coincide with the HVSR peak, or f_{0_HV}), $f_{0\_Ell,c}$ represents the calculated theoretical Rayleigh wave ellipticity peak for the trial layered earth model, and σ_{f0_Ell} is the standard deviation associated with the experimental ellipticity peak (which is assumed to be equal to the standard deviation of f_{0_HV}, or σ_{f0_HV}).

At many sites, only dispersion misfit (m_d) was considered during inversion because the HVSR peaks did not exhibit a well-defined, low-frequency peak. In such cases, a misfit value less than 1.0 indicates that, on average (i.e., across the frequency band considered), the theoretical dispersion curve falls within the +/- one standard deviation bounds of the experimental data. Thus, dispersion misfit values in excess of 1.0 suggest a poor fit of the experimental dispersion data. However, it is important to note that misfit values can vary considerably depending on the smoothness and complexity of the experimental dispersion data. Accordingly, dispersion misfit values considered satisfactory at one site may be considered mediocre or poor at another (Chapter 3).

Furthermore, the additional consideration of the ellipticity misfit (m_e) and user-defined weighting makes it difficult to establish universally "good" and "bad" misfit values. Thus, misfit values are most useful for making relative judgements regarding layered earth models derived from the same experimental dispersion and HVSR data at a given site. Meaning, we cannot provide a target misfit value that will indicate a successful inversion across all sites. Rather, the lowest possible misfit values should be sought at each unique site by considering multiple inversion parameterizations and potential mode interpretations. Geopsy allows for multi-mode inversions and, due to the complexity of our datasets, we systematically considered various mode interpretations of our experimental data. Meaning, in our attempts to obtain the lowest misfit values and quantify inversion uncertainty, we considered that the experimental dispersion data could be fit with the fundamental (R0), first higher (R1), second higher (R2), and in some cases the third (R3) and fourth (R4) higher Rayleigh modes.

At those sites where the ellipticity misfit was considered (BSP, GP, GRY, IF, QEII, RWP, RHS, and SNBP), the dispersion misfit was weighted much higher than the ellipticity misfit by setting w_d equal to 0.8 and we equal to 0.2. This decision was made because the ellipticity misfit is computed based on the assumption that the experimental HVSR peak (f_{0_HV}) coincides with the lowest-frequency Rayleigh wave ellipticity peak ($f_{0\_Ell,d}$). Although this assumption is justified when large velocity contrasts are present (Malischewsky and Scherbaum 2004), which is expected to be the case at the interface of Quaternary and Pre-Quaternary units in Christchurch, there is still a possibility that this assumption may be violated. Furthermore, the experimental dispersion data represents a wide range of frequencies, while the ellipticity peak misfit is computed at only one frequency. Thus, the dispersion misfit was chosen to represent 80% of the total misfit.

2.6.1 Inversion Parameters

As demonstrated in several studies (e.g., DiGiulio et al. 2012, Chapter 3), the choice of parameterization (i.e. the number of layers and ranges in their respective thicknesses, Vs, Vp, and mass densities) significantly influences the results of an inversion. It is extremely important to develop a parameterization which is capable of capturing the local site conditions (i.e., not overly restrictive), yet also prohibits the inversion algorithm from pursuing unrealistic solutions. Given the complex interlayered geologic conditions discussed earlier, obtaining realistic inversion parameterizations was not a trivial task for the Christchurch datasets. Fortunately, a multitude of geotechnical boreholes and geologic well logs were available near our test sites. These subsurface logs allowed us to identify the boundaries between different material types/geologic formations at each site and thus develop realistic parameterizations for the near-surface layers. Specifically, for this study, 155 geotechnical boreholes were obtained from the Canterbury Geotechnical Database (now the New Zealand Geotechnical Database; www.nzgd.org.nz) and 199 geologic well logs were obtained from the University of Canterbury (Lee et al. 2017). The majority of boreholes/wells were within or less than 0.5 km from the extents of the largest arrays. Geotechnical boreholes were generally drilled to depths of less than 40 m and allowed for the identification of material types within the Christchurch and Springston Formations. Well logs as deep as 200 m allowed for realistic constraints to be set on the contacts between alternating layers of alluvial gravels and soft, estuarine/marine soils. While still uncertain, due to spatial variations in layer thicknesses and limited data across each site, borehole and well logs generally allowed layer boundaries between major geologic units to be constrained within +/- 3-5 m down to a depth of about 200 m. The boundaries between major geologic units for each site,

including the uncertainty/search boundaries for each formation, are discussed in greater detail and presented later in the paper (see for example Figure 2.6e).

While the overall thicknesses of geologic units beneath each site were fairly well constrained over the top 200 m, many of the thicker geologic formations needed to be subdivide into thinner layers for inversion so that depth-dependent changes in stiffness could be reflected in the inversion results. Note that because the formation thicknesses varied considerably amongst the sites, the same number of layers were not used in each formation at each site. Table 2.2 shows the approximate range of thickness for each geologic formation across all sites in this study. Ranges for the number of layers used in each geologic formation are also summarized in Table 2.2. The Shirley Formation is the last geologic unit whose bottom depth could be ascertained from the geologic well logs. Consequently, the bottom of the Wainoni Gravel and underlying formations could not be constrained by a-priori information. Thus, five to seven layers were incorporated between the bottom of the Shirley Formation and the bottom of the parameterization. These layers became progressively thicker with depth because the resolution of surface wave methods, or the ability to detect thin layers, diminishes with increasing depth (Foti et al. 2014). The bottommost layer in the parameterization was not permitted to extend below a depth of one-half of the maximum wavelength obtained from the dispersion curve, or $\lambda_{max}/2$, which is a long-standing, common assumption in surface wave inversion (e.g., Garafalo et al. 2016a).

Table 2.2: Inversion parameterization summary for geologic formations beneath Christchurch test sites

Geologic Formation	Abbreviation	Approximate Thickness (m)	No. Layers	Velocity Reversals (Analysis 2)
Christchurch & Springston	CH/SP	15 to 40	4 to 6	Yes
Riccarton Gravel	RI	10 to 30	1 to 4	No
Bromley	BR	4 to 20	1 to 2	Yes
Linwood Gravel	LI	25 to 55	2 to 4	No
Heathcote	HE	4 to 20	1	Yes
Burwood Gravel	BU	4 to 20	1	No
Shirley	SH	8 to 22	1	Yes

At many sites, two inversion analyses were performed. While both inversions incorporated the same depth constraints for each layer, Analysis 1 was normally dispersive (i.e., Vs consistently increasing with depth) below the Springston and Christchurch Formations, while Analysis 2 permitted velocity reversals in the Bromley, Heathcote, and Shirley Formations. As mentioned previously, large velocity reversals are likely in the soft, estuarine/marine soils beneath each gravel formation. Thus, Analysis 2 is more consistent with the known geologic setting. However, without a-priori information, examination of the dispersion data alone may not have led one to believe there were multiple velocity reversals present. Thus, the authors sought to investigate whether it was possible to obtain comparable misfit values using both approaches. The Vs parameterization for Analysis 1 was allowed to range broadly between values associated with soft soils (i.e., 100 m/s at shallow depths or low confining pressures) to those associated with dense gravel (i.e., 1000 m/s at significant depths or high confining pressures). The Vs ranges for Analysis 2 were set based on the known material type and effective confining pressure using the relationships provided in Lin et al. (2014) for soft soils, dense sand, and dense gravel. These reference velocity profiles provide reasonable values of Vs as a function of mean effective stress for each soil type, which helps in setting realistic Vs ranges for inversion parameterization. Below the Shirley Formation,

the inversion parameters for Analysis 1 and 2 were equal and normally dispersive since no a-priori information was available to constrain the inversions at greater depths.

2.6.2 Number of Trial Layered Earth Models

The inversion parameterizations described above include many layers and, in the case of Analysis 2, potential velocity reversals. Consequently, each parameterization contained many degrees of freedom and it was necessary to search many trial layered earth models to adequately explore each parameterization and obtain the best solutions. Nonetheless, due to computational limitations, one must strike a balance between full exploration of the parameterization and practical time/data storage constraints. Analyses were originally performed in 2013-2014 that considered approximately 1.5 million trial layered earth models per inversion. These inversions typically took about 3 hours using a desktop computer with an Intel Xeon E5-1650 processor and 32 GB of RAM. However, we recently gained access to the Stampede supercomputer at the Texas Advanced Computing Center (TACC), allowing for much faster inversions involving more trial layered earth models. After some slight modifications to the weighting factors in the misfit calculations (described previously), the inversions were repeated using approximately 5 million trial models per inversion. The goal of repeating these analyses was to achieve lower misfits and to obtain a larger suite of realistic Vs profiles at each site. Results associated with the original analyses have been discussed in several publications (Cox et al. 2014, Wood et al. 2014, Teague et al. 2015, Lee et al. 2015 and 2017, Teague et al. 2017). Although the highest quality results were obtained from the new inversions using the TACC resources (i.e., those presented herein), the results shown in prior publications are still geologically realistic and the discussions are still valid.

It should also be noted that obtaining reasonable/realistic Vs profiles from surface wave inversion is not as simple as setting up a broad parametrization and throwing massive computing power at it. It is generally necessary to explore several parameterizations (possibly many) and investigate alternate mode interpretations. On average, it took 1 to 2 weeks to perform the inversions for each site discussed in this paper.

As discussed earlier, misfit values are subjective and difficult to compare from site-to-site. However, at many sites it is possible to develop a maximum misfit criteria, above which any layered earth models are deemed unacceptable. As stated earlier, a pure dispersion misfit (m_d, see Equation 2.1) less than 1.0 indicates that the theoretical dispersion curve(s) for a given ground model lie within the uncertainty bounds of the experimental data. Conversely, a pure dispersion misfit significantly greater than 1.0 indicates that the theoretical curves fall outside of the experimental uncertainty bounds over wide frequency ranges. Although the misfit values at many sites represented a weighted average of the dispersion and ellipticity misfits (m_d and m_e, respectively), the dispersion misfit was weighted substantially more than the ellipticity misfit term (80% vs 20%, respectively). Thus, we still sought to obtain a large number (10^3 or more) of Vs profiles with misfit values less than or approximately equal to 1.0. Although the number of trial models necessary to accomplish this goal is controlled by the experimental data and model parameterization (i.e., it is site-specific), we found that 5 million trial layered earth models worked well for most sites. At some sites tens- or hundreds-of-thousands of trial earth models achieved misfits below 1.0, while at other sites only about 1000 Vs profiles met this misfit criteria. While it would appear reasonable to extract all Vs profiles with misfit values less than 1.0 as a means to quantify Vs uncertainty, the number of profiles with misfits below 1.0 varies considerably amongst the sites and in

some cases is not computationally manageable. Thus, for consistency, the 1000 lowest misfit Vs profiles were extracted for further analysis at each site. While the decision to extract 1000 profiles is somewhat arbitrary, we found that it provided a suite of Vs profiles that reasonably captured the variability exhibited by those profiles, yet was still manageable from a computational standpoint. It should be noted that far fewer trial models (roughly 800k) were considered at the CHS site because the parameterization was relatively simple due to the unique geology. This is further discussed in the following section.

2.7 SURFACE WAVE INVERSION RESULTS

This section begins by considering the surface wave inversion results from the Hagley Park site as a detailed example. Subsequently, the surface wave inversion results from all sites are provided. Note that detailed inversion summaries and final Vs profiles for all sites are available in the Community Data on the Design Safe Website (www.designsafe-ci.org) under the title "Final Results - Deep Shear Wave Velocity Profiling for Seismic Characterization of Christchurch_ NZ".

2.7.1 Hagley Park

The theoretical dispersion curves associated with the 1000 lowest misfit layered earth models at Hagley Park from Analysis 1 and Analysis 2 are shown in Figure 2.5a and 2.5b, respectively. The fundamental, first-higher, and second-higher theoretical Rayleigh-wave dispersion modes (R0, R1, and R2, respectively) are shown for each model. It is clear that comparable fits of the experimental dispersion data were achieved during both analyses (i.e., using two unique parameterizations). This is underscored by the similar misfit ranges for the best 1000 models, which are shown in brackets. (Note that the values shown are pure dispersion misfits since a clear low frequency peak below

1 Hz was not present in the HVSR data at this site; refer to Figure 2.4g). Both analyses indicate a transition from the fundamental (R0) to the first higher (R1) mode between 2 and 4 Hz. As discussed earlier, after preliminary inversions the experimental dispersion data between 1 and 2 Hz was judged to represent an effective mode that could not be modeled in Geopsy and was removed prior to final inversion. Between 0.70 Hz and 1.0 Hz, both analyses fit the experimental dispersion data with the fundamental mode. Below 0.7 Hz, the mode associated with the experimental data is ambiguous. It can be seen that some Vs profiles fit the experimental dispersion data below 0.7 Hz with the fundamental mode, while others fit this data with the first higher mode. This represents epistemic uncertainty, which could potentially be reduced by using larger arrays and/or obtaining more supporting data regarding the deep velocity structure at the site.

In the absence of a-priori information about the geology of Christchurch, it would be difficult to conclude that one analysis is "better" than another. Indeed, Analyses 1 and 2 yield Vs profiles with very similar minimum dispersion misfit values (m_d = 0.45 and m_d = 0.44, respectively). Since the misfit values are marginally lower for Analysis 1 than for Analysis 2, one may be inclined to state that Analysis 1 is "better". However, it is worth considering the resulting Vs profiles along with the known geotechnical and geologic data.

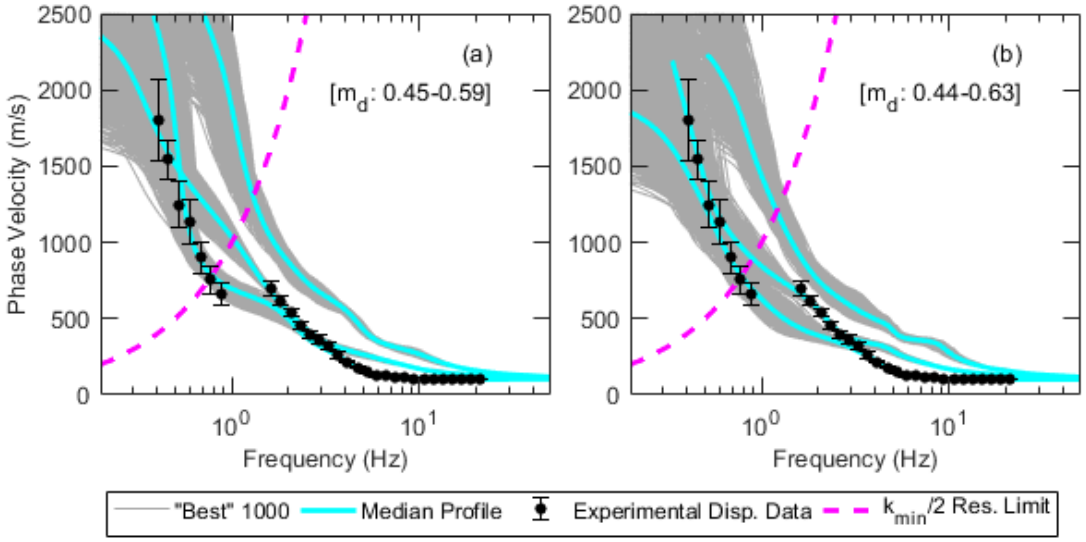

Figure 2.5: Theoretical Rayleigh wave dispersion curves for the "best" (i.e. lowest misfit) 1000 velocity models obtained from the inversion analysis at Hagley Park using: (a) a normally dispersive parameterization (Analysis 1), and (b) a parameterization that permits velocity reversals within the Bromley, Heathcote, and Shirley Formations (Analysis 2). Note that the three distinct bands of curves represent the fundamental (R0), first higher (R1), and second higher (R2) Rayleigh modes. Also highlighted is the theoretical dispersion curve for the median velocity profile obtained from the "best" 1000 profiles. Note that experimental dispersion data with wavenumbers below the array resolution limit ($k_{min}/2$; Wathelet et al. 2008) may be adversely influenced by limitations of the largest (400 m diameter) array.

Vs profiles obtained from Analyses 1 and 2 are shown on depth scales of 150 m (Figure 2.6a and 2.6c) and 2000 m (Figure 2.6b and 2.6d) in Figure 2.6. The standard deviation of the natural logarithm of Vs (σ_{lnVs}), which is commonly used to quantify variability in Vs (e.g., Toro 1995, EPRI 2012, Griffiths et al. 2016a), is shown in Figures 2.6e and 2.6f. The geologic stratigraphy is superimposed on Figure 2.6e. Vs profiles from Analysis 2 (Figure 2.6c and 2.6d) better capture the complex geology of Christchurch than those from Analysis 1 (Figure 2.6a and 2.6b) due to the a-priori geologic layering information used to constrain the Analysis 2 inversions. The contacts between the alluvial

gravels and the estuarine and marine sands, silts, and clays are shown in Figure 2.6e along with uncertainty bounds for the locations of these contacts that were used during inversion. Vs profiles from Analysis 2 exhibit strong velocity contrasts and velocity reversals at these boundaries. Conversely, Analysis 1 does not include velocity reversals in formations where they are highly probable. It is also clear from the Lin et al. (2014) material reference curves for soft soil, dense sand, and dense gravel shown in Figures 2.6a and 2.6c that the velocities within each layer in Analysis 2 are more consistent with the known material types. For example, in the Riccarton (RI), Linwood (LI), and Burwood (BU) Gravel formations, Vs is consistent with the reference curve for dense gravel, while in the Bromley (BR), Heathcote (HE), and Shirley (SH) formations Vs is more consistent with the dense sand reference curve. Conversely, the Vs profiles from Analysis 1 essentially average the Vs across material types and are less consistent with the known geology.

It is important to note that the Heathcote, Burwood, and Shirley formations are relatively thin formations (refer to Table 2.2). At long wavelengths (i.e., lower frequencies), the experimental dispersion data is less sensitive to these thin layers. Thus, it would be essentially impossible to obtain the results from Analysis 2 without a-priori information regarding the subsurface layering, while Vs profiles similar to those shown in Analysis 1 could be more readily obtained in a blind inversion. Moreover, given the relative insensitivity of the dispersion data to these thin layers at depth, one may argue that the inclusion of these thin velocity reversals may be unnecessary/unimportant to seismic site response (Teague et al. 2017). However, given the strong geotechnical and geologic evidence that these layers are present, the authors believe it is important to include them in the analyses.

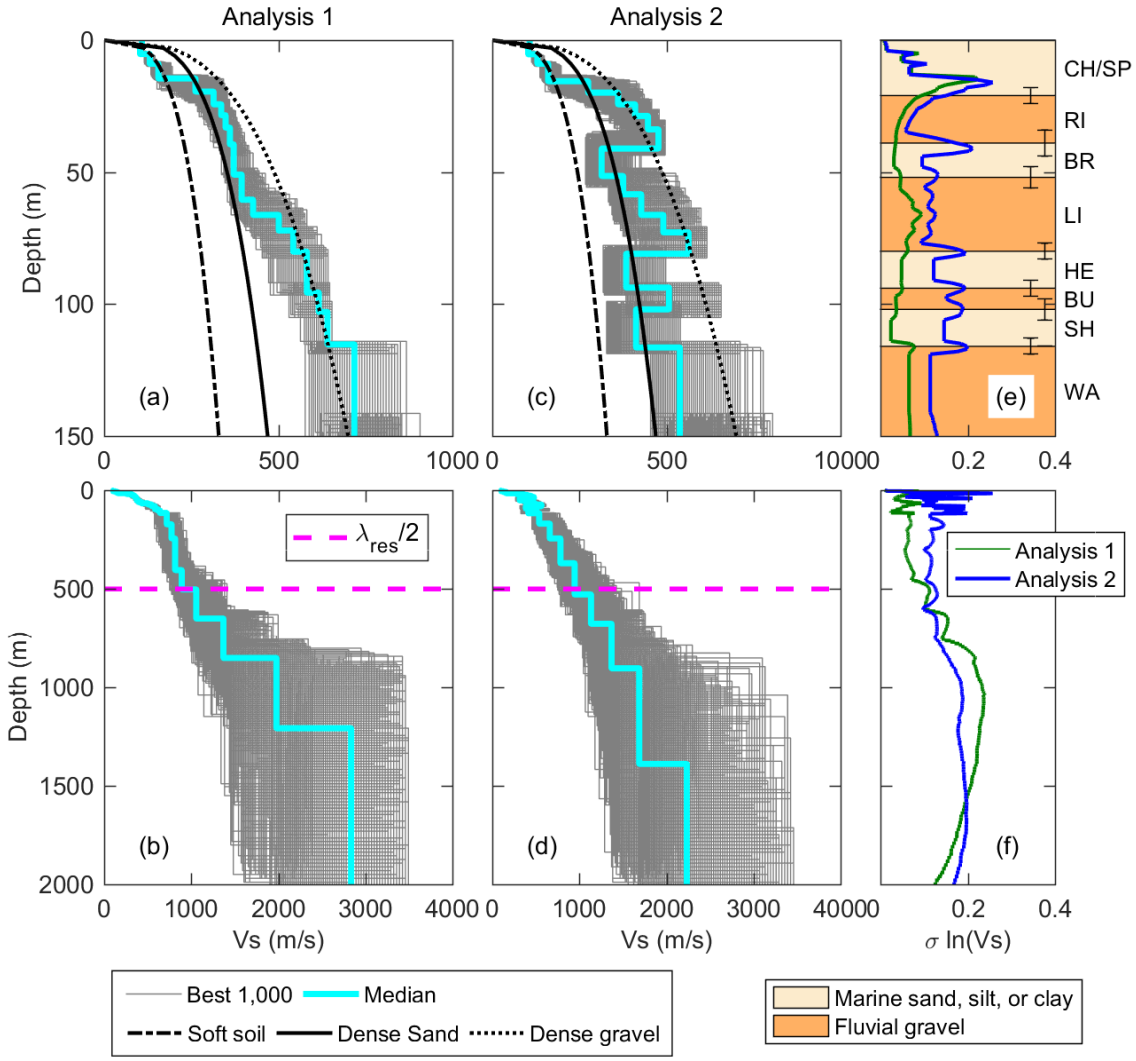

Figure 2.6: The 1000 "best" (i.e., lowest misfit) shear wave velocity (Vs) profiles obtained from over 5 million models searched during inversion Analysis 1 (a, b) and Analysis 2 (c, d) at Hagley Park. Also shown in (a) and (c) are the soil-type Vs reference curves from Lin et al. (2014). Note that the $\lambda_{res}/2$ line in (b) and (d) identifies the approximate depth where the Vs profiles are best constrained by the resolution limits of the largest circular array. All Vs profiles were cutoff at a depth of 2000 m, which is roughly one-half of the maximum resolved wavelength ($\lambda_{max}/2$). The standard deviation of the natural logarithm of Vs (σ_{lnVs}) for the "best" 1000 models from each analysis are shown in (e) and (f). The geologic stratigraphy obtained from geologic well logs is superimposed on the σ_{lnVs} profile in (e), with error bars representing uncertainties in the depth to each interface.

The median of the 1000 lowest misfit Vs profiles is shown in Figure 2.6 for each analysis. Note that these median Vs profiles were not derived directly from inversion. Rather, since all Vs profiles from a given parameterization incorporated an equal number of layers, a median bottom depth and median Vs could be readily computed for each layer. The theoretical dispersion curves associated with the median Vs profile are shown for each analysis in Figure 2.5. Note that the computation of theoretical dispersion curves requires values of Vp and mass density for each layer in addition to depth/thickness and Vs. Thus, the median Vp and mass density of the 1000 lowest misfit ground models were also used calculated and used to compute the theoretical dispersion curves shown in Figure 2.5. It is clear that the theoretical dispersion curves associated with the median Vs profile satisfactorily fit the experimental dispersion data. Thus, the median Vs profiles are both statistically representative of the "best" Vs profiles from each analysis and consistent with the experimental dispersion data. In addition to the median, it is also useful to consider the variability (i.e., σ_{lnVs}) in the suite of Vs profiles from each analysis.

It is clear from Figure 2.6e and 2.6f that both Analyses 1 and 2 exhibit significant variability in Vs. This underscores the non-uniqueness associated with the surface wave inverse problem. It is worth noting that the Vs profiles from Analysis 1 exhibit less variability than those associated with Analysis 2. This is partly because the inclusion of potential velocity reversals in the parameterization for Analysis 2 exacerbates the non-uniqueness of the inversion (i.e., allows for more possible Vs profiles when fitting the data). However, given the a-priori information, the inclusion of these velocity reversals is warranted. Over the top 500 m, Analysis 2 exhibits a σ_{lnVs} around 0.10 within each layer and "spikes" at layer interfaces. These "spikes" do not represent uncertainties in Vs within a given layer, rather, they represent uncertainties in the depth to layer interfaces.

Below 500 m (i.e., the approximate resolution limit of the largest array, as discussed subsequently), σ_{lnVs} increases to approximately 0.20.

During the inversion process, we generally used two wavelengths obtained from the experimental dispersion data to guide the approximate depth ranges reported in our Vs profiles. The first guiding wavelength is referred to as λ_{res}, which is the wavelength corresponding to the array resolution limit (i.e., $\lambda_{res} = 2\pi/[k_{min}/2]=4\pi/k_{min}$). The second guiding wavelength is referred to as λ_{max}, which is the maximum wavelength (corresponding to the lowest frequency and highest Vr value) in the experimental dispersion data. Fundamental mode Rayleigh waves at a given wavelength are generally capable of profiling to a maximum depth of approximately 1/3 to 1/2 of their wavelength (Foti et al. 2014). While much of the experimental dispersion data in this study represented higher modes and thus could theoretically profile deeper, it is often difficult to definitively identify higher modes. Thus, this conservative assumption was still utilized and Vs profiles obtained from inversion are considered most reliable at depths less than approximately $\lambda_{res}/2$. The $\lambda_{res}/2$ depth limits, which range from 450 m to 550 m based on the arrays used at the 14 sites in this study, are clearly indicated in all Vs profiles presented below. At greater depths (i.e., at depths exceeding $\lambda_{res}/2$), the Vs profiles are constrained by less reliable dispersion data. Hence, the Vs profiles below $\lambda_{res}/2$ should also be considered less reliable and used with caution. Vs profiles were not extended below a depth of $\lambda_{max}/2$ because there were no dispersion data to constrain them at greater depths. Additionally, no Vs profiles were extended below a depth of 2000 m, even if $\lambda_{max}/2$ was more than 2,000 m. Accordingly, all Vs profiles at Hagley Park were cutoff at a depth of 2000 m.

For the reasons outlined in the previous paragraphs, inversions informed by a-priori geotechnical and geologic information at each site (i.e., Analysis 2 inversions)

were deemed to be most realistic. All subsequent results shown in this paper were derived using inversion parameterizations that incorporated information about site-specific layering and permitted velocity reversals beneath each gravel formation. Although the resulting Vs profiles are not simple/smooth, they are consistent with the local geology and yield satisfactory fits to the experimental dispersion data. It should be noted that a common approach to an inverse problem is to seek the most simple/smooth solution that explains the observed data (Constable et al. 1987). While this approach is certainly warranted in many geologic settings (e.g., gradual increases in Vs with increasing depth), it is clear that such an approach could not have produced geologically-realistic Vs profiles in Christchurch. Nonetheless, it would be extremely difficult and potentially impossible to develop geologically-realistic Vs profiles at these sites without the aid of a-priori information.

2.7.2 All Sites

The 1000 lowest misfit Vs profiles from all sites have been made available as text files on the Design Safe website. Also available are PDF files for each site detailing the array locations, the experimental dispersion and HVSR data from all arrays, and the 1000 lowest misfit Vs profiles and their associated dispersion curves.

The theoretical dispersion curves (fundamental and higher mode) associated with the 1000 lowest misfit ground models are shown with the experimental data for all 14 sites site in Figure 2.7. The dispersion curves at most sites exhibit similar characteristics as those from Hagley Park. The experimental dispersion data was generally fit with the fundamental mode at high frequencies. However, as frequency decreased, the experimental dispersion data generally transitioned to higher Rayleigh-wave modes and then eventually back to the fundamental mode between 1 and 2 Hz. Low-frequency

experimental dispersion data below 1 Hz were fit solely with the fundamental mode at some sites (BSP, GRY, RWP, RHS). At other sites, some theoretical dispersion curves fit the experimental data with the fundamental mode, while others fit the same experimental dispersion data with the fist higher mode. As noted earlier, these two mode interpretations represent epistemic uncertainty in the inversion results and both are reasonable within the bounds of existing knowledge.

Figures 2.8 and 2.9 show the 1000 lowest misfit Vs profiles for all 14 sites to depth scales of 150 and 2000 m, respectively. Table 2.3 provides the median Vs profile of the 1000 lowest misfit profiles for all 14 sites. Similar to Hagley Park, Vs profiles at all sites generally exhibit velocity reversals beneath each gravel formation (RI, LI, and BU). These velocity reversals are consistent with the geologic layering that was determined from geotechnical boreholes and geologic well logs. It should be noted that the CHS site is located on the Banks Peninsula and the geologic conditions at this site are quite different from all other test sites. Beneath the Christchurch formation, the CHS site is characterized by Pliocene-aged materials underlain by Miocene volcanic rock. Thus, the complex inter-layering of gravel formations with sands, silts, and/or clays was not present at this site. Given the lack of inter-layering and relatively shallow structure, less than 1 million trial earth models were necessary for the inversion at this site.

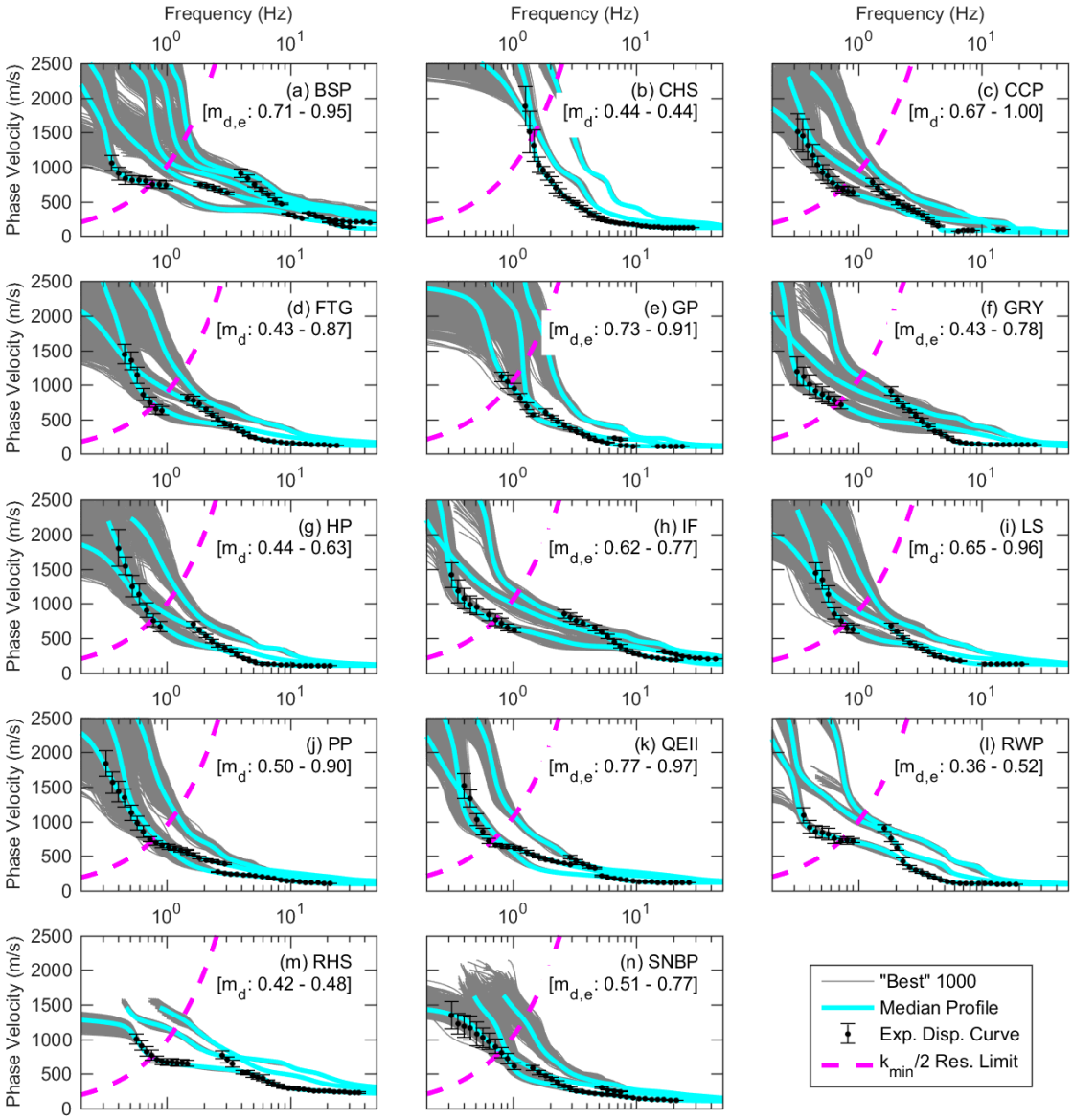

Figure 2.7: Experimental dispersion data shown along with the theoretical dispersion curves for the 1000 "best" (i.e., lowest misfit) ground models at all 14 test sites. (Test site locations are provided in Figure 2.2 and Table 1.1). Also shown are the theoretical dispersion curves for the median ground model. The R0, R1 and R2 modes are shown for all ground models. Additionally, the R3 and R4 modes are shown for all models at Burnside Park (BSP). Note that experimental dispersion data with wavenumbers below the array resolution limit ($k_{min}/2$, Wathelet et al. 2008) may be adversely influenced by limitations of the largest (400 m diameter) array.

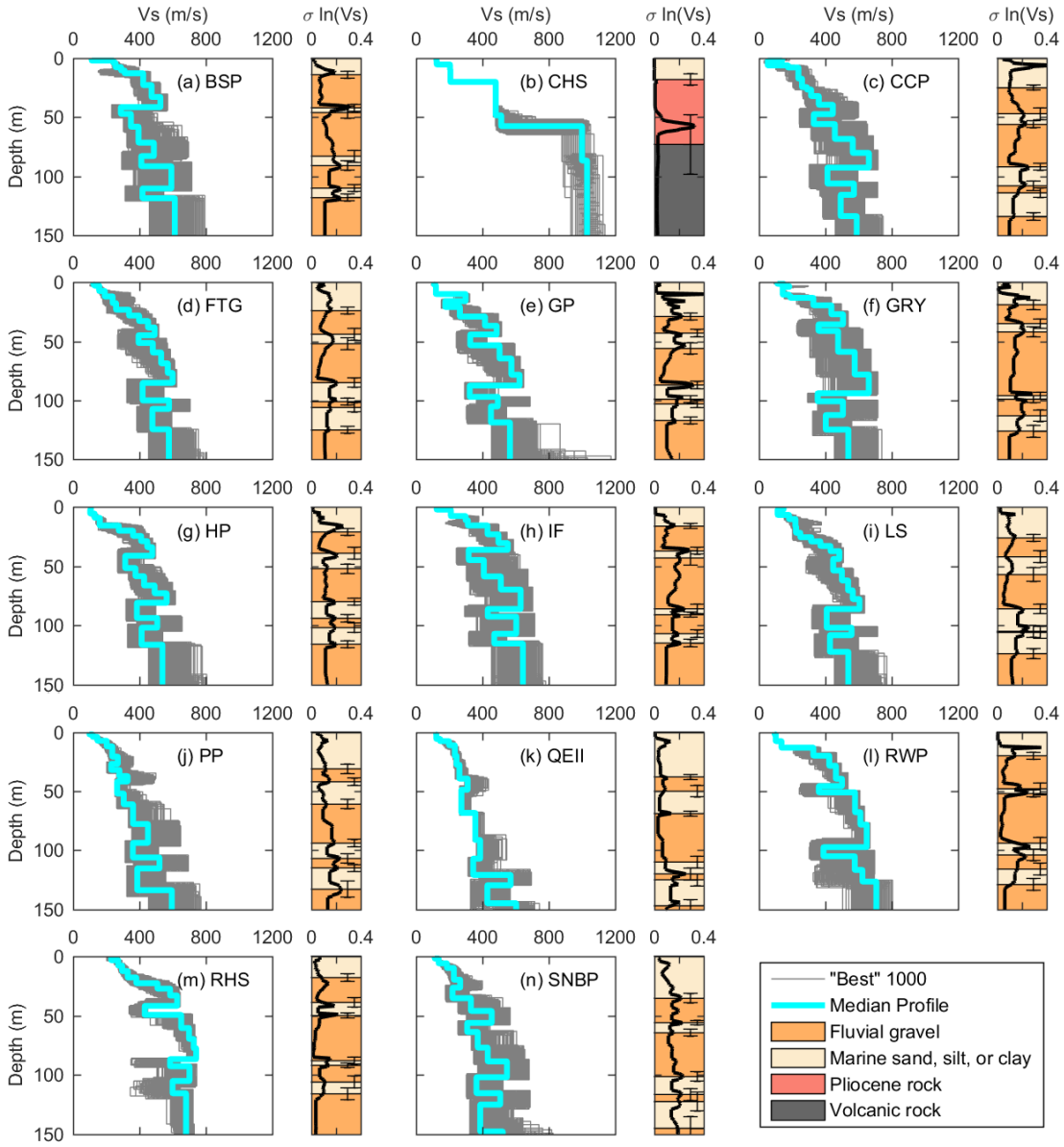

Figure 2.8: The 1000 "best" (i.e., lowest misfit) shear wave velocity (Vs) profiles obtained during the inversion analyses performed at all 14 sites, *shown to a depth scale of 150 m*. Also shown is the median Vs profile of the best 1000. Shown to the right of each suite of Vs profiles is the standard deviation of the natural logarithm of Vs (σ_{lnVs}) as a function of depth. The geologic stratigraphy is superimposed on the σ_{lnVs} profile, with error bars representing uncertainties in the depth to each interface.

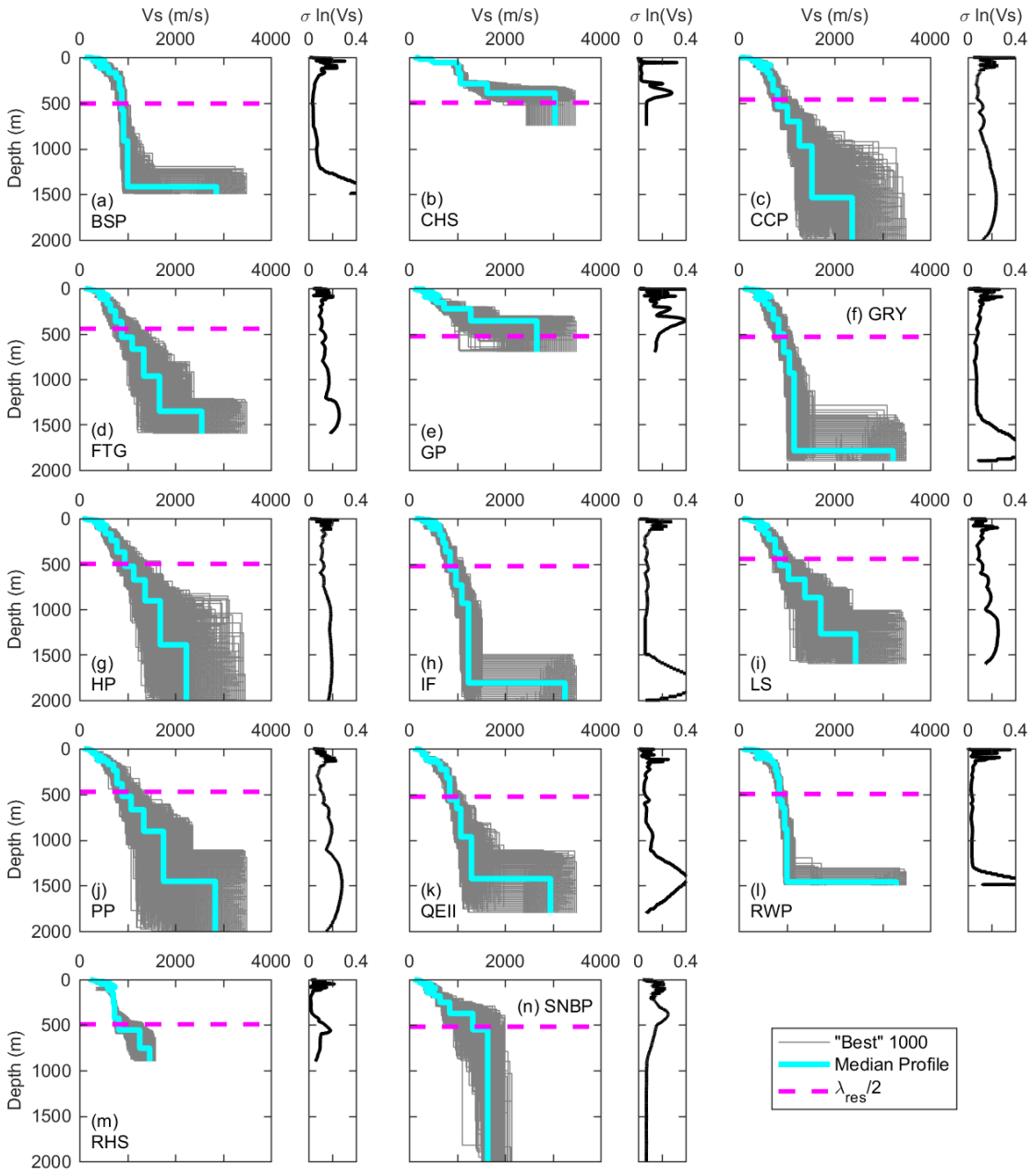

Figure 2.9: The 1000 "best" (i.e., lowest misfit) shear wave velocity (Vs) profiles obtained during the inversion analyses performed at all 14 sites, shown to a depth scale of 2000 m. Note that the Vs profiles are most reliable at depths less than $\lambda_{res}/2$. All Vs profiles were cutoff at a depth of one-half of the maximum resolved wavelength ($\lambda_{max}/2$) or 2000 m, whichever was shallower.

Table 2.3: Median Vs Profiles for all surface wave test sites. Note that the all layers below the vertical dashed line exceed $\lambda_{res}/2$, or the approximate depth where the Vs profiles are best constrained by the resolution limits of the largest circular array. All Vs profiles were cutoff at a depth of one-half of the maximum resolved wavelength ($\lambda_{max}/2$) or 2000 m, whichever was shallower.

Burnside Park		Cashmere High School		Christchurch Park		Fitzgerald		Garrick Park		Groynes	
Depth [m]	Vs [m/s]	Depth [m]	Vs [m/s]	Depth [m]	Vs [m/s]	Depth [m]	Vs [m/s]	Depth [m]	Vs [m/s]	Depth [m]	Vs [m/s]
2.0	112	2.5	123	2.0	140	2.0	123	2.0	109	1.3	111
4.0	243	5.3	124	6.1	53	2.9	130	2.7	115	3.3	150
7.6	256	9.7	205	7.8	175	7.3	157	9.9	120	3.9	182
10.3	289	20	207	17	237	12	190	16	298	10	143
13	310	48	480	24	259	18	238	21	176	12	181
23	422	57	513	27	289	23	259	29	264	13	190
33	473	87	1000	32	314	28	337	37	415	19	328
41	526	172	1030	39	360	33	398	44	486	27	436
47	288	289	1072	47	445	38	451	53	327	36	506
58	348	392	1628	56	330	45	491	65	503	41	359
71	394	750	3048	68	457	51	395	78	574	59	477
83	486			80	565	59	480	87	624	78	576
91	411			93	662	69	531	97	324	94	662
110	592			106	412	77	570	105	493	101	354
118	418			116	572	85	600	119	451	112	506
169	613			134	492	100	419	156	566	125	402
224	766			171	589	107	578	225	729	173	538
352	839			237	653	124	478	359	1287	230	634
580	882			362	715	171	577	700	2667	341	723
915	920			538	814	249	647			502	831
1417	1006			704	1016	366	752			704	938
1500	2859			971	1264	538	882			934	1057
				1536	1527	669	1100			1787	1156
				2000	2369	966	1342			1900	3224
						1352	1671				
						1600	2554				

Table 2.3 (continued): Median Vs Profiles for all surface wave test sites. Note that the all layers below the vertical dashed line exceed $\lambda_{res}/2$, or the approximate depth where the Vs profiles are best constrained by the resolution limits of the largest circular array. All Vs profiles were cutoff at a depth of one-half of the maximum resolved wavelength ($\lambda_{max}/2$) or 2000 m, whichever was shallower.

Hagley Park		Ilam Fields		Latimere Square		Porritt Park		QEII Park		Redwood Park	
Depth [m]	Vs [m/s]	Depth [m]	Vs [m/s]	Depth [m]	Vs [m/s]	Depth [m]	Vs [m/s]	Depth [m]	Vs [m/s]	Depth [m]	Vs [m/s]
2.0	107	2.0	124	2.0	148	2.0	98	2.0	121	2.0	95
5.3	103	7.5	210	6.5	112	4.0	118	5.7	122	7.7	101
8.9	130	11	298	10	181	7.3	146	7.6	145	13	135
16	160	15	312	16	220	12	202	11	199	20	328
20	275	23	431	22	223	21	236	20	234	28	423
24	361	30	497	25	249	27	270	28	244	39	463
29	410	36	553	29	314	32	230	39	261	46	500
34	447	45	317	33	370	37	279	49	311	51	361
41	477	59	408	37	431	42	328	68	273	68	579
51	314	70	511	44	484	52	265	91	357	78	611
58	376	86	630	54	447	61	305	107	386	97	649
66	427	93	432	62	500	78	361	121	344	105	389
73	491	107	604	70	537	94	451	130	570	117	577
81	563	115	471	78	565	106	360	145	429	126	623
94	384	181	644	86	606	115	520	168	603	164	707
102	507	270	707	102	408	134	387	228	654	242	767
116	413	366	759	108	558	174	595	322	782	322	806
169	538	560	856	122	427	239	707	560	847	566	847
244	660	732	976	164	538	385	782	656	996	650	901
370	782	934	1100	232	628	522	890	966	1078	879	957
528	945	1809	1239	373	759	669	1078	1425	1303	1460	1006
676	1133	2000	3257	517	859	906	1342	1800	2951	1500	3292
906	1369			669	1036	1453	1756				
1390	1687			871	1381	2000	2836				
2000	2233			1270	1711						
				1600	2440						

Table 2.3 (continued): Median Vs Profiles for all surface wave test sites. Note that the all layers below the vertical dashed line exceed $\lambda_{res}/2$, or the approximate depth where the Vs profiles are best constrained by the resolution limits of the largest circular array. All Vs profiles were cutoff at a depth of one-half of the maximum resolved wavelength ($\lambda_{max}/2$) or 2000 m, whichever was shallower.

Riccarton High School		South New Brighton Park	
Depth [m]	Vs [m/s]	Depth [m]	Vs [m/s]
2.0	230	2.0	113
3.4	230	6.0	136
7.9	272	10.0	186
13	295	20	228
18	329	27	266
23	381	35	220
27	508	46	330
33	584	56	456
42	626	64	308
49	432	77	372
61	651	89	432
70	698	102	548
78	727	115	364
87	741	125	507
93	584	148	387
105	701	180	522
116	599	251	647
155	681	373	847
262	708	552	1329
425	730	2000	1641
555	822		
754	1259		
900	1466		

Shear wave velocities in Christchurch exhibit some general geographic trends. In the top 200 m, Vs is generally highest in the west, where the Springston gravel formation is at or near the surface, and lowest along the coast, where the Christchurch formation is thickest. This observation is clear from the time averaged shear wave velocity over the top 30 m (V_{S30}). V_{S30} was computed for each of the 1000 lowest misfit Vs profiles at each site. A lognormal median and standard deviation (σ_{lnVs30}) were then computed, as

summarized in Table 2.1. It can be seen that the QEII, PP and SNBP sites have significantly lower V_{S30} values than the BSP, IF, and RHS sites (refer to Table 2.1 and Figure 2.2a). With the exception of RWP, V_{S30} is significantly higher at sites located in the west. It is worth noting that, despite significant variations in the Vs profiles from each site, V_{S30} exhibits minimal variability, with σ_{lnVs30} below 0.06 at all sites. Thus, while the Vs profiles derived from surface wave inversion visually appear to be quite variable, they are well-constrained in the near-surface. As discussed previously, many sites exhibited a well-defined, low-frequency (i.e., less than 1 Hz) peak in their respective HVSR curves (refer to Figure 2.4). At these sites, this lowest-frequency HVSR peak was used to constrain the depth to a strong impedance contrast during inversion. Based on the available geologic data, the low-frequency peak in the HVSR curves from the GP and SNBP sites are presumed to be a result of the impedance contrast at the top of the Miocene volcanics. These sites are located close to the Banks Peninsula, where Miocene volcanics are relatively shallow. Thus, the HVSR peaks at these sites were used in the inversion to aid in characterizing the depths to these volcanic materials. Because the depth of these materials is less than $\lambda_{res}/2$, they are also well-constrained by the experimental dispersion data. The Miocene volcanics do not appear to strongly influence the HVSR curves at other sites, where the low-frequency HVSR peaks at approximately 0.2 Hz are presumed to be a result of the velocity contrast at the top of the basement rock. This suggests that the velocity contrast at the top of the Miocene volcanics is not present or less pronounced at these other sites.

The depth of the interface of Pre-Quaternary and Quaternary units (i.e., basement rock) is expected to be on the order of 1000 to 2000 m at most sites (Lee et al. 2015), which is well below the resolution depth ($\lambda_{res}/2$, discussed previously) of 450 to 550 m (denoted by horizontal dashed lines in Table 2.3 and Figure 2.9). Thus, basement rock

generally could not be estimated with a great deal of confidence. While the estimates presented in our Vs profiles are deemed to be better than what one would assume with no data at all, the authors recommend that other sources of information be considered when estimating the depth to basement rock (e.g., Lee et al. 2015). Additionally, the depth to basement rock was far in excess of $\lambda_{max}/2$ and therefore cannot be estimated at the RHS site. Thus, while the HVSR peak was initially considered at this site, the ellipticity peak was ultimately not used to constrain the inversion.

2.8 DISCUSSION

Vs profiles discussed in the previous section are intended to aid in seismic site response analyses. These analyses may include back-analyses aimed at better understanding the spatial variability in ground motions experienced during the CES or forward-analyses aimed at quantifying the amplitude and frequency content of future design ground motions. This section is intended to provide guidance regarding the use of results from this study in subsequent site response analyses. First, velocities within the Riccarton Gravel are considered in detail, as this layer is expected to play a significant role in seismic site response. Next additional considerations are discussed. These topics include the influence (or lack thereof) of velocity reversals in site response analyses, the selection of an appropriate stratum for the application of input GMs, and consideration of Vs uncertainty.

2.8.1 Riccarton Gravel Velocity Model

The first major velocity contrast at many sites in Christchurch occurs at the top of the Riccarton Gravel (RI), which is often found at a depth of approximately 15 to 40 m. This formation can be expected to play a significant role in seismic site response. For example, Markham et al. (2016) recently used this layer as the half-space when

deconvolving surface ground motions for their one-dimensional, nonlinear, effective stress site response analyses aimed at modelling the response of potentially liquefiable soils during strong shaking. Therefore, an estimation of the shearing stiffness (i.e., Vs) of the RI is necessary for accurate seismic analyses.

In order to characterize the Riccarton Gravel, the median Vs value for each layer within this formation was plotted against the mean effective stress at the middle of the layer for all sites, as shown in Figure 2.10. As noted earlier, the RI was often subdivided into multiple layers at each site. Thus, more than 13 data points (i.e., the number of test sites minus the CHS site, where the RI is absent) are shown in Figure 2.10. Mean effective stress calculations were based the following assumptions: hydrostatic pore pressures with a ground water level 2 m below the surface, a unit weight of 19 kN/m3 in the Springston and Christchurch Formations and 21 kN/m3 within the Riccarton Gravel, and an at-rest earth pressure coefficient of 0.5. It is clear that the Vs of the RI is highest at sites located in the west and north (BSP, GRY, IF, RWP and RHS), lowest in the east (GP, PP, QEII and SNBP), and moderate in central Christchurch (CCP, FTG, HP and LS).

All data were fit with a power-law function relating Vs to mean effective stress in the same form as Lin et al. (2014). This equation is shown in Figure 10. Originally, the authors attempted to fit the data from the east, central, and west/north locations individually. However, these sample sizes were insufficient to develop reasonable parameters relating Vs to mean effective stress. Accordingly, a single equation was developed for all sites. Therefore, one should not use this equation without careful consideration. This equation may overestimate Vs in the east and underestimate Vs in the west and north. It is crucial that the possible over- or underestimation due to geographic location be considered when using this equation. Note that the authors attempted to

develop similar power-law functions for the underlying geologic formations (i.e, the Bromley Formation, Linwood Gravel, Heathcote Formation, and the Burwood Gravel). However, the results were either too variable and/or the formations were too thin to develop power-law relationships with reasonable parameters in the same form as the equation shown in Figure 2.10.

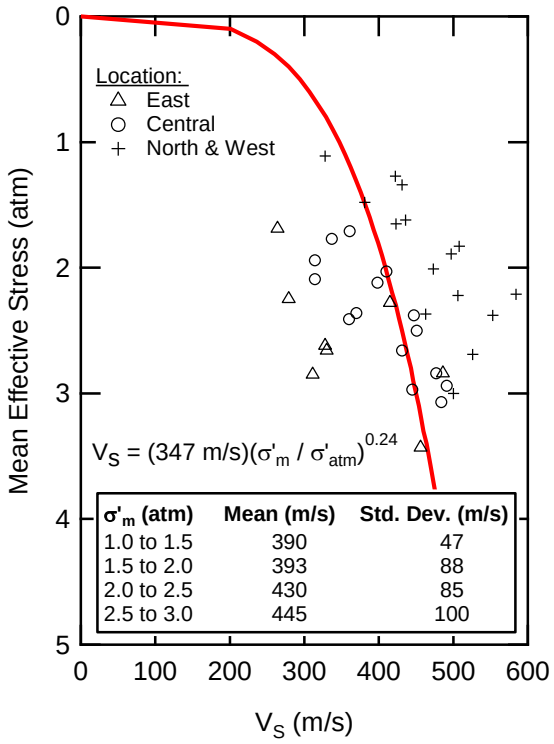

σ'_m (atm)	Mean (m/s)	Std. Dev. (m/s)
1.0 to 1.5	390	47
1.5 to 2.0	393	88
2.0 to 2.5	430	85
2.5 to 3.0	445	100

Figure 2.10: Median Vs (of the 1000 lowest misfit Vs profiles) as a function of the estimated mean effective stress (σ'_m) in the Riccarton Gravel (RI) at all sites. Note that because the RI was generally subdivided into multiple layers, more than one data point is shown per site. Sites are differentiated by geography, with sites in eastern (GP, PP, QEII and SNBP), central (CCP, FTG, HP and LS) and northern/western (BSP, GRY, IF, RWP and RHS) Christchurch denoted by different marker types. All data were fit with a power law relationship similar to those detailed in Lin et al. (2014). Note that this relationship should be used with caution and potential over- or underestimation resulting from geographic location should be considered.

2.8.2 Considerations for Seismic Site Response

As discussed previously, Vs profiles which include sharp velocity reversals and account for the complex inter-layered geology (i.e., Analysis 2) yield comparable fits of the experimental dispersion data as overly-simplistic Vs profiles that fail to account for this inter-layered geology (i.e., Analysis 1; refer to Figures 5 and 6). Ultimately, the influence of these velocity reversals (or lack thereof) on the predicted seismic site response is of interest. While a detailed discussion is beyond the scope of this paper, site response estimates with and without velocity reversals was explored at the Hagley Park site in Teague et al. (2017). Interestingly, Vs profiles from Analysis 1 and Analysis 2, as developed in our original study (using an inversion that considered 1.5 million trial models rather than 5 million), exhibited similar seismic site response at the ground surface. These results suggest that Vs profiles that yield similar fits of the experimental dispersion data yield similar seismic site response, even though the exact subsurface layering between models may vary substantially. This is consistent with previous studies considering the influence of surface wave inversion non-uniqueness on the predicted site response (e.g., Foti et al. 2009, Griffiths et al. 2016b, Chapters 4 and 5). However, further research is needed on this topic. In the meantime, one should attempt to model the Vs profile as accurately as possible for use in site response calculations.

Another important consideration in seismic site response is the selection of an appropriate stratum to apply input ground motions. Hard-rock (IBC Site Class A, or Vs > 1500 m/s) in Christchurch is generally encountered below 500 m, where the Vs profiles are not well-constrained by the resolution capabilities of the largest array used in this study (refer to Figure 2.9). Thus, extreme caution should be exercised when applying input ground motions at a hard-rock stratum below 500 m based on the results of this study. The substantial uncertainties in depth and Vs of the basement rock should be

considered. Further, additional data regarding reasonable depths to basement rock in Christchurch may be sought. For example, contours showing the interface of Quaternary and Pre-Quaternary geologic units (i.e., basement rock) are provided in Lee et al. (2015). These contours were developed using large reflection surveys, which are better-suited to resolve the depth of this interface. It is important to note that most Vs profiles encounter engineering rock (IBC Site Class B, or Vs > 760 m/s) above 500 m. Thus, these materials can be more accurately resolved by our testing. In some instances it may be sufficient to apply input rock ground motions (GMs) at the first layer exceeding 760 m/s, where the Vs profiles are still well-constrained by the experimental dispersion data. However, if the long-period site response is of interest (e.g., for tall structures), then it would be judicious to consider the influence of the deeper hard-rock layers.

The 1000 lowest misfit Vs profiles for each site are available on the Design Safe website. The authors believe that a reasonable approach to consider Vs uncertainty would be to randomly sample any desired number of Vs profiles from these 1000 lowest misfit profiles and perform site response on the profiles within this sample. It is recommended that users ensure the sample be representative of the population of 1000 profiles (i.e., that the sample and population have similar median and σ_{lnVs} profiles).

As illustrated by the σ_{lnVs} profiles in Figure 2.8, there are significant uncertainties in Vs over certain depth intervals at all sites. However, this site-specific Vs uncertainty is still lower than what most analysts would assume for use in site response analyses. The Vs uncertainties derived from surface wave inversion include both aleatory variability and epistemic uncertainty, which are extremely difficult to decouple in surface wave testing (Griffiths et al. 2016a). In practice, epistemic uncertainty is commonly accounted for via the development of alternate base-case Vs profiles and aleatory variability is accounted for using a randomization model (Toro 1995, EPRI 2012). The authors urge

any users of the Vs profiles provided in this study to exercise caution when developing base-case profiles and performing Vs randomization (Chapter 4). We suggest that theoretical dispersion curves be computed for any base-case or randomized Vs profiles and compared to the experimental dispersion data. These dispersion data were developed using arrays that sample over a large footprint (hundreds of meters). Thus, epistemic uncertainty and aleatory variability are inherent in the experimental dispersion data. We do not claim that these Vs profiles developed from inversion of the dispersion data fully encompass all Vs uncertainties. However, we encourage users to question the validity of Vs profiles whose theoretical dispersion curves are extremely inconsistent with the measured experimental dispersion data at a given site.

2.9 CONCLUSIONS

Deep (+500 m) shear wave velocity profiles have been developed using surface wave testing at 14 sites located throughout Christchurch. The geology of Christchurch presented several challenges for surface wave testing. Specifically, the complex inter-layering of relatively stiff gravels with relatively soft sands, silts, and clays complicated both the interpretation of the experimental dispersion data and the setup of the inversion parameterizations. For these reasons, a-priori information, including hundreds of geotechnical boreholes and geologic well logs, were obtained to assist in developing Vs profiles. This information proved to be invaluable for developing geologically-realistic Vs profiles from surface wave inversion. The results of this study provide well-constrained Vs profiles with estimates of uncertainty to a depth of approximately 500 m, which far exceeds currently available Vs models. While Vs profiles may be deemed less reliable at greater depths due to the limited aperture of the largest arrays used in surface wave testing, they still provide Vs data at depths where it is currently nonexistent. The Vs

profiles provided in this study will also be useful for estimating Vs uncertainty for seismic site response analyses, including back-analyses aimed at better understanding the spatial variability of ground motions experienced during the Christchurch Earthquake and forward-estimates of the amplitude and frequency content of future ground motions.

Chapter 3: Layering Ratios: A Systematic Approach to the Inversion of Surface Wave Data in the Absence of A-priori Information

Brady R. Cox and David P. Teague

This chapter is a pre-copyedited, author-produced version of an article accepted for publication in Geophysical Journal International following peer review. The version of record is cited below:

Cox, B. R. and Teague, D. P. (2016). "Layering Ratios: A Systematic Approach to the Inversion of Surface Wave Data in the Absence of A-priori Information." Geophysical Journal International, Vol. 207, pp. 422–438, https://doi.org/10.1093/gji/ggw282.

As second author, I was responsible for approximately 33% of the concept development, 100% of the data processing, 50% of the data interpretation/synthesis, and 50% of the concept modification/refinement.

ABSTRACT

Surface wave methods provide a cost effective means of developing shear wave velocity (Vs) profiles for applications such as dynamic site characterization and seismic site response analyses. However, the inverse problem involved in obtaining a realistic layered earth model from surface wave dispersion data is inherently ill-posed, nonlinear, and mix-determined, without a unique solution. When available, a-priori information such as geotechnical boreholes or geologic well logs should be used to aid in constraining site-specific inversion parameters. Unfortunately, a-priori information is often unavailable, particularly at significant depths, and a "blind analysis" must be performed. In these situations, the analyst must decide on an appropriate number of layers and ranges for their corresponding inversion parameters (i.e., trial number of layers and ranges in their respective thicknesses, shear wave velocities, compression wave velocities, and mass densities). Selection of these parameters has been shown to significantly impact the results of an inversion. This paper presents a method for conducting multiple inversions utilizing systematically-varied inversion layering parameterizations in order to identify

and encompass the most reasonable layered earth models for a site. Each parameterization is defined by a unique layering ratio, which represents a multiplier that systemically increases the potential thickness of each layer in the inversion parameterization based on the potential thickness of the layer directly above it. The layering ratio method is demonstrated at two sites associated with the InterPacific Project, wherein it is shown to significantly aid in selecting reasonable Vs profiles that are close representations of the subsurface. While the goal of the layering ratio inversion methodology is not necessarily to find the "optimal" or "best" Vs profile for a site, it may be successful at doing so for certain sites/datasets. However, the primary reason for using the layering ratio method is to find Vs profiles that realistically represent the uncertainty in Vs resulting from surface wave inversion, and to avoid selection of Vs profiles that are unrealistic and adversely influenced by the choice of inversion parameterization.

3.1 INTRODUCTION

Surface wave methods provide a cost effective means of developing shear wave velocity (Vs) profiles for applications such as dynamic site characterization and seismic site response analyses. While numerous techniques are available for collecting and analyzing surface wave data, all generally consist of the following three steps: (1) field data acquisition, (2) dispersion processing, and (3) inversion to obtain a layered earth model, from which the Vs profile is extracted (Foti et al. 2014). Data acquisition involves measuring wavefields, either actively-generated or passively-monitored, with strong surface wave content. Dispersion processing involves deriving a relationship between Rayleigh wave phase velocity (Vr) and frequency (f), or wavelength (λ), from the experimentally-measured wavefields. The inversion process involves finding one or more layered earth models whose theoretical dispersion curve(s) fit the experimentally-

determined dispersion data, as shown in Figure 3.1. Layered earth models comprise a system of stacked, linear elastic, horizontal layers over a half-space. Each layer is defined by its inversion parameters: thickness (t), shear wave velocity, compression wave velocity (Vp) or Poisson's ratio (ν), and mass density (ρ). The total number of layers is generally unknown and specified/assumed by the analyst prior to inversion. The layer parameters are then varied during the inversion until an acceptable match is made between the theoretical dispersion curve and the experimental dispersion data. However, the inverse problem involved in obtaining a realistic layered earth model from surface wave dispersion data is inherently ill-posed, nonlinear, and mix-determined, without a unique solution. The ill-posed nature of the problem results from trying to recover four parameters (t, Vs, Vp, ρ) for each layer in the model indirectly from the two measured data parameters of Rayleigh wave phase-velocity and frequency /wavelength. The problem is further complicated by the nonlinear relationship between the data parameters, which vary as a function of frequency/wavelength, and the desired model space parameters, which vary as a function of depth. Additionally, the model solution for deeper layers is dependent on the model solution for shallow layers, resulting in a mix-determined problem. As a result, a number of significantly different layered earth models may possess theoretical dispersion curves that fit the experimental data within its uncertainty bounds.

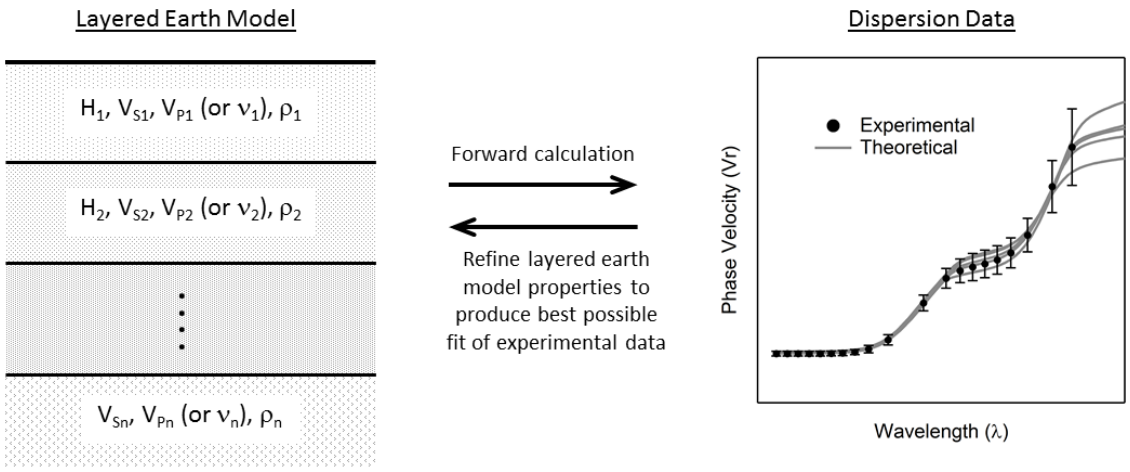

Figure 3.1: General surface wave inversion procedure used to obtain a layered earth model that matches experimental dispersion data within its uncertainty bounds.

Most inversion programs use an optimization algorithm to search the parameter space for layered earth models whose forward-calculated theoretical dispersion curves match the measured experimental dispersion data. Local search algorithms search in the vicinity of a starting model, often using linearized least-squares to optimize the fit between theoretical and experimental dispersion data. These search algorithms are effective for optimizing the layered earth model to fit the experimental data. However, they are heavily influenced by the starting model and can get stuck in local minima without obtaining the "best"/lowest misfit model(s) (Socco et al. 2010).

Global search methods such as Monte-Carlo, genetic algorithm, simulated annealing, and the neighbourhood algorithm (e.g., Foti et al. 2009, Yamanaka and Ishida 1996, Wathelet et al. 2004) are commonly utilized to search a broad parameter space, thus avoiding the problem of getting stuck in a local minima. These algorithms typically use some form of a misfit function to quantify the goodness of fit between each trial model and the experimental data. While the exact forms of these misfit functions vary

(e.g., Maraschini and Foti 2010 and Wathelet 2004), they are generally proportional to the sum of squared residuals between the theoretical and experimental dispersion curves at discrete frequencies. Global search algorithms are designed to search for theoretical layered earth models within a predefined inversion parameter space. Therefore, the entire space of possible layered earth models must be defined by the analyst prior to performing the inversion. This task is not trivial, as the parametrization must be sufficiently broad to include all realistic layered earth models, yet sufficiently constrained to prevent the inversion from pursuing unrealistic models. When available, a-priori information such as geotechnical boreholes or geologic well logs should be used to aid in developing site-specific inversion parameters. This can greatly reduce the range of possible solutions and is particularly useful when complex geologic conditions are encountered (Chapter 2). Unfortunately, a-priori information is often unavailable, particularly at significant depths, and a "blind analysis" must be performed. In these situations, the analyst must decide on an appropriate number of layers and ranges for their corresponding inversion parameters. Selection of these parameters has been shown to significantly impact the results of an inversion (DiGiulio et al. 2012). If an inappropriate number of layers or property ranges are incorporated in the inversion parameterization, then the resulting layered earth models may be excessively complicated (i.e., too many layers/under-constrained) or overly simplistic (i.e., too few layers/over-constrained). In either case, models with low dispersion misfit values (i.e., apparently good solutions) will not well-represent actual site conditions.

It is fairly common for those inverting massive amounts of surface wave data to assume a constant distribution of many relatively thin layers in the hopes of being able to resolve subtle changes in stratigraphy/stiffness during inversion. However, there is no single set of inversion parameters that will work in every situation. Even the most robust

of global search methods cannot produce acceptable results when the parameter space is poorly or excessively constrained. Thus, it would be ill-advised to propose a layered earth model solution after considering only a single set of inversion parameters. Several researchers have addressed the issue of qualitatively and quantitatively evaluating results from different inversion parameterizations. For example, DiGiulio et al. (2012) evaluated four distinct classes of inversion parameterizations at 14 European strong-motion sites using the Akaike information criterion. However, no study we are aware of has proposed a technique for rigorously and systematically developing and evaluating various inversion layering parameterizations. This paper presents a new method called the "layering ratio procedure" for conducting multiple inversions utilizing systematically-varied inversion parameters in order to identify and encompass the most reasonable layered earth models. The method is first described in detail, and then demonstrated by presenting its application for two blind analysis sites associated with the InterPacific (Intercomparison of methods for site parameter and velocity profile characterization) project (Garafalo et al. 2016a, 2016b).

3.2 LAYERING RATIO PROCEDURE

Surface wave methods provide better resolution at shallow depths than significant depths, allowing for thinner layers and smaller variations in velocity to be detected near the surface when small sensor spacings and high frequency active sources are used. Conversely, as depth increases, resolution decreases and only significant changes in layering can be distinguished (Foti et al. 2014). Therefore, a rational approach is to incorporate more/thinner layers in the inversion parameterization close to the ground surface where subtle changes in velocity may be resolved, and few/thicker layers at depth where thin layers and minor changes in velocity cannot be detected. The layering ratio

(Ξ) represents a multiplier that systemically increases the potential thickness of each layer in the inversion parameterization based on the potential thickness of the layer directly above it. By considering multiple layering ratios, it is possible to systematically investigate non-unique Vs profiles that could be adversely influenced by either too many or too few layers in the inversion parameterization, resulting in unrealistic representations of the subsurface. Small layering ratios yield many trial layers, while large layering ratios yield only a few trial layers. Note that the layering ratio methodology requires an inversion algorithm that allows for a range in the thickness/bottom depth of each layer to be explored. Meaning, the exact layer thicknesses are not constrained prior to the inversion. Rather, the inversion algorithm is allowed the flexibility of searching for the best combinations of layer thicknesses within the boundaries specified by the analyst. The program Geopsy (http://www.geopsy.org/) is a multifaceted, open-source software package that can be used for this purpose.

3.2.1 Number of Layers and Corresponding Depth Ranges

First, constraints are applied to the top layer in the inversion parameterization. Specifically, the minimum and maximum potential depth to the bottom of the first layer ($d_{min,1}$ and $d_{max,1}$, respectively) are selected. These values should be chosen based on the experimental Rayleigh wave dispersion data, as shown in Figure 3.2. The authors typically set dmin,1 and dmax,1 equal to approximately one-third and one-half of the minimum resolved wavelength (λ_{min}), respectively. The surface layer should not be much thinner than λ_{min} /3 because the experimental dispersion data does not allow for better resolution (Garafalo et al. 2016a). While the authors have chosen to set $d_{min,1}$ equal to approximately $\lambda_{min}/2$, this parameter can be set to a larger value, such as λ_{min}. However, excessively thick, uniform, near-surface layers are rare in nature and should not be

incorporated in the inversion parameters if a realistic layered earth model is needed for engineering purposes like site response analyses.

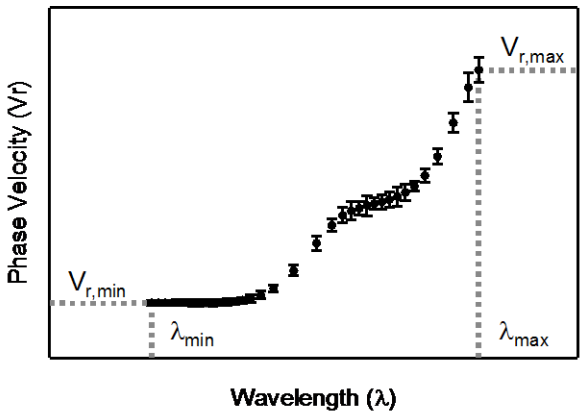

Figure 3.2: Experimental Rayleigh wave dispersion data values used to guide the selection of $d_{min,1}$, $d_{max,1}$, and d_{res} for the layering ratio (Ξ) procedure.

After constraining the bottom depth of the surface layer, the approximate maximum depth that the soil profile can be characterized to, or the resolution depth (d_{res}), should be estimated. This depth can be set equal to approximately one-third to one-half of the maximum resolved wavelength (λ_{max}) from the experimental dispersion data. This is a common assumption for the maximum depth of resolution, as the fundamental mode Rayleigh wave dispersion curve is not very sensitive to material properties at depths greater than approximately $\lambda_{max}/3$ to $\lambda_{max}/2$ (Richart et al. 1970, Garofalo et al. 2016a). Note that if low frequency experimental dispersion data is deemed to represent a higher mode, then the resolution depth may actually be greater because higher modes have a greater penetration depth than lower modes (Foti et al. 2014). Nonetheless, mode interpretations are often uncertain and we prefer not to extend the inversion parameterizations below this criteria in most cases.

Once $d_{min,1}$, $d_{max,1}$, and d_{res} have been selected, a layering ratio (Ξ) is chosen. While there are no absolute rules, the following layering ratio values are commonly used by the authors to systematically investigate potential subsurface models with significantly different numbers and thicknesses of layers: 1.2, 1.5, 2.0, 3.0, 5.0, and 7.0. Depending on the inversion results, other intermediate values (e.g., 2.5, 3.5, 4.0) may need to be investigated, as discussed later in the paper. Note that these are layering ratios are based on the authors' experience. The choice of appropriate layering ratios is site-specific and these may not be sufficient/appropriate for all sites. As discussed above, the layering ratio represents a multiplier that systemically increases the potential thickness of each layer in the inversion parameterization based on the potential thickness of the layer directly above it. This concept is illustrated in Figure 3.3 and detailed in Equation 3.1. The minimum potential bottom depth for each non-surface layer (i.e., all layers except Layer 1) is equal to the maximum potential bottom depth of the layer directly above it (Equation 3.1a). The maximum potential bottom depth for each non-surface layer is determined by adding the product of the layering ratio and the difference between the maximum and minimum potential bottom depths of the overlying layer to the minimum potential bottom depth of the current layer (Equation 3.1b). The only exception to this rule is for Layer 2, where the maximum potential bottom depth is determined by adding the product of the layering ratio and $d_{max,1}$ (i.e., $\lambda_{min}/2$) to $d_{min,2}$.

$$d_{min,i} \approx \begin{cases} \lambda_{min}/3 & for\ i = 1 \\ d_{max,i-1} & for\ i > 1 \end{cases} \tag{3.1a}$$

$$d_{max,i} \approx \begin{cases} \lambda_{min}/2 & for\ i = 1 \\ d_{min,i} + \Xi(\lambda_{min}/2) & for\ i = 2 \\ d_{min,i} + \Xi\left(d_{max,i-1} - d_{min,i-1}\right) & for\ i > 2 \end{cases} \tag{3.1b}$$

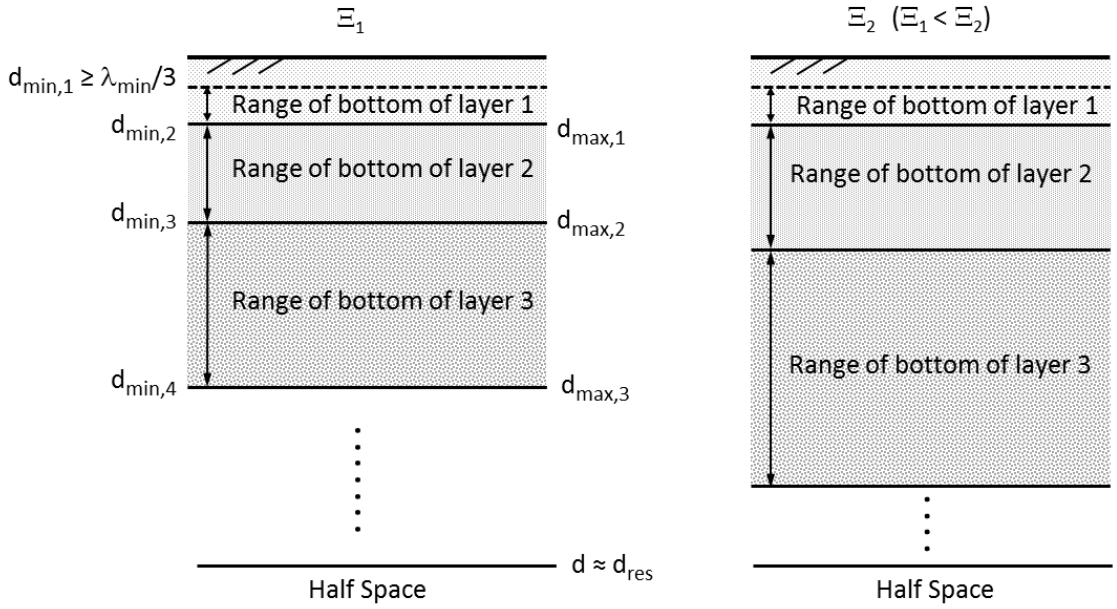

Figure 3.3: Schematic illustration of the layering ratio (Ξ) inversion parameterization.

The depth to the top of the half-space (i.e., the bottom-most layer) should not exceed the resolution depth. Therefore, layers should be added to the inversion parameterization until the resolution depth is reached. Since it is rare that the bottom of a layer will exactly coincide with the resolution limit for a given set of experimental dispersion data, the maximum bottom depth of the layer directly above the half-space may need to be increased or decreased slightly to match dres. A maximum depth/thickness is not specified for the half-space.

A simple example of how to establish depth boundaries using the layering ratio procedure is shown in Table 3.1. In this example, the minimum and maximum resolved wavelengths of the hypothetical experimental dispersion data are 6 m and 100 m, respectively, and a layering ratio of 2.0 is utilized. The minimum and maximum potential bottom depth of Layer 1 are assigned based on the minimum resolved wavelength. The approximate resolution depth is estimated to be one-half of the maximum wavelength, or

50 m. Potential bottom depth boundaries for Layers 1, 2, 3, and 4 are computed using Equation 1. The maximum potential bottom depth of Layer 4 (45 m) is quite close to the approximate resolution limit (50 m). Therefore, Layer 4 should be the final layer above the half space and dmax,4 can be increased slightly to 50 m. Conversely, if dmax,4 where calculated to be slightly greater than the resolution depth, it could be decreased to 50 m.

The layering ratio approach produces layered earth models in which layer thicknesses generally tend to increase with depth. However, it is important to note that each layer is not required to be thicker than the overlying layer. This is because the layering ratio technique involves specifying bottom depth ranges for each layer, not layer thicknesses. For example, consider Layers 1, 2, 3 and 4 in Table 3.1. The parameters allow the bottom depths in these layers to lie between 2–3, 3–9, 9–21 and 21–50 m, respectively. If the inversion process found the bottom of Layers 1, 2, 3 and 4 to optimally be located at 2, 8, 11 and 23 m, then the corresponding layer thicknesses would be 2, 6, 3 and 12 m, respectively. In other words, Layer 3 is permitted to be significantly thinner than Layer 2 if required to fit the experimental dispersion data. This is important, because although surface wave resolution generally diminishes with depth, there are many subsurface profiles that contain thinner layers overlain by thicker layers. Thus, it is important that the parameterization does not force the solution space to use a series of layers that monotonically increase in thickness with depth if an alternate solution yields a better fit to the experimental data.

Table 3.1: Layering ratio example wherein the minimum ($d_{min,i}$) and maximum ($d_{max,i}$) potential bottom depths for each layer are based on minimum (λ_{min}) and maximum (λ_{max}) experimental dispersion wavelengths of 6 and 100 m, respectively, a depth of resolution (d_{res}) equal to 50 m (i.e, λ_{max} /2), and a layering ratio (Ξ) of 2.0.

Layer	$d_{min,i}$ (m)	$d_{max,i}$ (m)
1	6/3 = 2	6/2 = 3
2	3	3+(2)(3) = 9
3	9	9+(2)(9-3) = 21
4	21	21+(2)(21-9) = 45 ≈ d_{res} → set to d_{res} = 50
Half Space	NA	NA

3.2.2 Ranges in Vs, Vp (or Poisson's Ratio), and Density

In addition to depth ranges for each layer, ranges in Vs, Vp or Poisson's ratio, and mass density must be selected for each layer. Mass density has little impact on the dispersion curve and reasonable values may be assigned to each layer if something is known of the material types/geology. If not, mass density may be fixed at a constant value in each layer (Wathelet 2004). For the purpose of assigning Vs ranges, the experimental dispersion data can once again be utilized. The ratio of shear wave to Rayleigh wave velocity (Vs/V_R) ranges from 1.04 to 1.16, depending on Poisson's ratio (Richart et al. 1970). Thus, if the experimental dispersion data represents the fundamental Rayleigh mode, then the minimum shear wave velocity for any layer should not be less than the minimum Rayleigh wave velocity ($V_{R,min}$) in the experimental dispersion data (Figure 3.2). If a low velocity layer (i.e., inverse layer) is present in the subsurface, the minimum Rayleigh wave velocity may not coincide with the minimum wavelength. Rather, it may occur at a greater wavelength, resulting in a downward kink/bend in the dispersion data. In these cases, the minimum Vs should be set slightly lower than $V_{R,min}$. In some instances, the maximum Rayleigh wave velocity ($V_{R,max}$) may be used to set an upper limit on Vs. Consider the two hypothetical dispersion curves in Figure 3.4.

Dispersion curve A levels off at long wavelengths (i.e., low frequencies). This part of the dispersion curve represents the Rayleigh wave velocity of the half-space, which has a higher velocity than overlying layers. Thus, the maximum Vs for all layers may be set to approximately $1.16 \cdot V_{R,max,A}$. On the other hand, it is not possible to infer a reasonable upper limit from experimental dispersion curve B because it does not appear to resolve the half space velocity (i.e., it does not level off or flatten at low frequencies). Moreover, even in situations when the dispersion data appears to resolve the half space velocity, this may be an artefact of near-field effects or poor data quality. Thus, engineering judgement should be exercised when setting parameterization limits on Vs. If the inversion results tend to cluster around the upper/lower parameterization limit for a particular layer, then the limits for this layer may need to be broadened and the inversion repeated. Moreover, even a crude understanding of the geology (e.g., soft soil, stiff soil, soft rock, or hard rock) can aid in setting reasonable upper and lower Vs boundaries if an analyst possess an understanding of realistic Vs ranges for various soil and rock types. If general material types can be identified on the basis of a-priori information, then confining pressure-dependent reference curves, such as those discussed in Lin et al. (2014), may be used to develop realistic Vs constraints for each layer in the parameterization (e.g., Chapter 2).

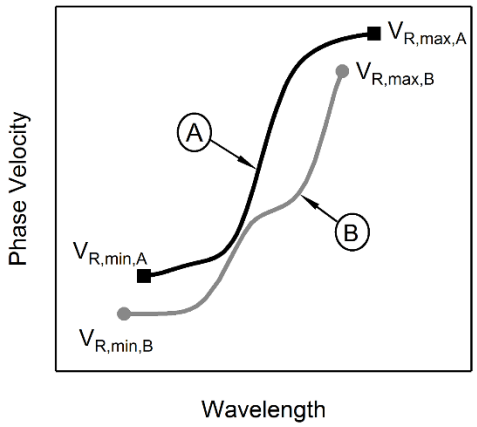

Figure 3.4: Hypothetical dispersion curves which (A) flatten at long wavelengths, thereby helping to resolve the half space velocity, and (B) remain steep at long wavelengths, limiting the ability to estimate the half space velocity.

For saturated, soft soil layers, Vp can be set equal to the compression wave velocity of water (approximately 1,500 m/s), which will result in a Poisson's ratio near 0.5. Thus, knowledge of an approximate location of the water table is important and can help to constrain the inversion parameters. For all unsaturated soil layers, and very stiff soil or rock layers below the water table where Vs exceeds about 700 m/s, the compression wave velocity is no longer exclusively governed by the pore fluid. In these cases it is common to estimate Poisson's ratio between 0.25 and 0.35. Since Vs, Vp, and Poisson's ratio (ν) are related by Equation 2, it is possible to develop ranges in Vp using limiting values of Vs and Poisson's ratio. Alternatively, some inversion software packages enable the user to specify Poisson's ratio instead of Vp.

$$\frac{V_P}{V_S} = \sqrt{\frac{2(1-\nu)}{(1-2\nu)}} \qquad (3.2)$$

It is recommended that the initial inversion parameterization be normally dispersive (i.e., Vs increasing with depth) unless the geologic conditions or shape of the

experimental dispersion curve dictate otherwise (e.g., portions of the dispersion data decrease with decreasing frequency/increasing wavelength). Permitting velocity reversals (i.e., layers in which Vs is lower than the overlying layer) greatly increases the range of possible solutions and may allow the inversion to pursue unrealistic layered earth models if not carefully constrained. Nonetheless, there are many geologic conditions in which velocity reversals are present (e.g., DiGiulio et al. 2012, Dou and Ajo-Franklin 2014, Chapter 2). In these situations, the inversion parameters may include one or more velocity reversals. However, the analyst should carefully inspect the inversion results to ensure that the resulting layered earth models are realistic. For example, thin layers with either extremely high or low Vs relative to layers above or below may simply be a result of overly-broad inversion parameters and not actual geologic conditions at the site. When complex geologic conditions are encountered, it is recommended that a-priori information be sought to help constrain the inversion parameterization. Under these conditions, there may not be a simple strategy for exploring various sets of inversion parameters and there is no substitute for knowledge of the subsurface geology and sound engineering judgement.

A schematic summary of the layering ratio inversion procedure is shown in Figure 3.5. Various layering ratios (i.e., sets of inversion parameters) should be investigated in an attempt to find the layered earth models with the lowest dispersion misfit values. We typically search 100K – 2M models during each layering ratio inversion. After each layering ratio inversion, a certain number of acceptable models whose theoretical dispersion curves fit the experimental dispersion data are retained for further scrutiny. This process is demonstrated in detail for the case study sites discussed below.

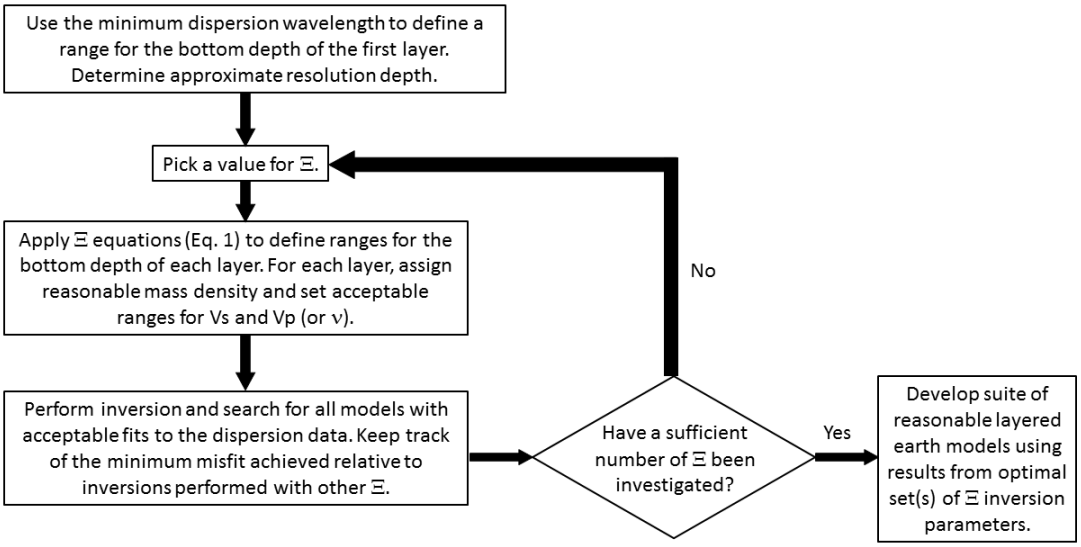

Figure 3.5: Schematic representation of the general layering ratio (Ξ) inversion procedure.

3.3 LAYERING RATIO INVERSION PROCEDURES FOR TWO EXAMPLE SITES

Both of the examples discussed below are associated with the InterPacific (Intercomparison of methods for site parameter and velocity profile characterization) project. The objective of the InterPacific project was to assess the reliability of invasive and non-invasive seismic site characterization methods in various geologic conditions using blind-analysis comparative studies. While the InterPacific project included a number of researchers and practitioners from around the world, the results discussed herein only reflect the work of the present authors. For additional information about the InterPacific project, the reader is referred to Garafalo et al. (2016a and 2016b).

At both sites discussed below, individual inversions were conducted for various layering ratios using the Geopsy software. In Geopsy, the theoretical dispersion forward computations for each trial earth model are based on the work originally developed by

Thomson (1950) and Haskell (1953) and later modified by Dunkin (1965) and Knopoff (1964). For each trial model, a dispersion misfit value was computed as shown in Equation 3.3 (Wathelet 2004).

$$\text{misfit} = \sqrt{\sum_{i=1}^{n_f} \frac{(x_{di} - x_{ci})^2}{\sigma_i^2 n_f}} \qquad (3.3)$$

In the above equation, x_{di} represents the Rayleigh wave phase velocity of the experimental dispersion data at frequency f_i; x_{ci} is the theoretical Rayleigh wave phase velocity computed for the trial layered earth model at frequency f_i; σ_i is the standard deviation associated with the experimental dispersion data at frequency f_i; and n_f is the number of frequency samples considered for the misfit calculation. Geopsy utilizes a neighborhood algorithm to find layered earth models within the inversion parameters that result in the lowest possible dispersion misfit values. According to the definition of dispersion misfit presented in Equation 3.3, a misfit value less than 1.0 essentially means that on average (i.e., across the frequency band considered) the theoretical dispersion curve falls within the +/- one standard deviation bounds of the experimental data. Thus, dispersion misfit values far in excess of 1.0 suggest a poor fit of the experimental dispersion data. However, it is important to recognize that there is currently no universally-accepted way of calculating the dispersion misfit. Further, dispersion misfits deemed to be satisfactory at one site may be considered mediocre or poor at another. For example, consider the dispersion curves and misfit values shown in Figure 3.6a and 3.6b for sites in Christchurch, New Zealand and White River, Arkansas, respectively. Both dispersion misfit values are essentially equal. At the Christchurch site (Figure 3.6a), the experimental dispersion data is influenced by higher and effective modes and is quite complex. This experimental data was fit with a multi-mode inversion and the theoretical

curves shown represent the best possible fit to this challenging dataset after considering many inversion parameterizations. Conversely, the experimental dispersion data at the White River site (Figure 3.6b) represents the fundamental mode and is fairly simple. However, the theoretical dispersion curve shown for this site does not match the mean trend of the experimental dispersion data at many wavelengths, although it still falls within the uncertainty bounds. While one might potentially deem this fit to be acceptable, substantially better fits of the experimental dispersion data (i.e., lower misfit values) were achieved through the use of alternate inversion parameterizations. Thus, misfit values from different sites generally cannot be compared directly with one another for a measure of the overall inversion quality from site-to-site. Rather, the misfit values can simply be used to guide relative judgements about the quality of certain layered earth models relative to others at the same site (Griffiths et al. 2016a).

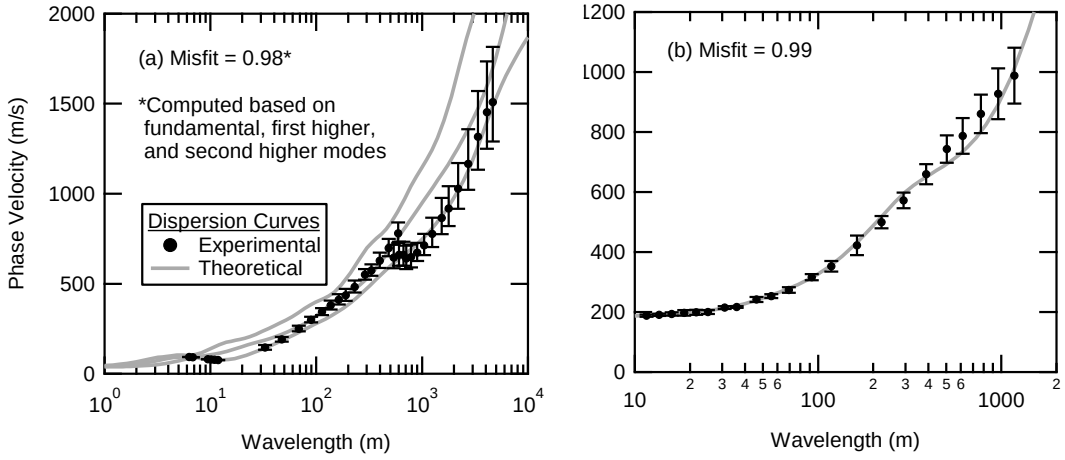

Figure 3.6: Theoretical dispersion curves for a single layered earth model along with the experimental dispersion data at sites in (a) Christchurch, New Zealand and (b) White River, Arkansas. Note that the dispersion misfit values in (a) and (b) are approximately equal.

Computational expense imposes a practical limitation on the extent to which global search methods like the neighborhood algorithm implemented in Geopsy can investigate the parameter space for any given inversion. In the authors' experience, a total of 10^5 to 10^6 layered earth models for a single layering ratio inversion usually provides an acceptable balance between full exploration of the parameter space and practical time constraints. Note that the computation time is very dependent upon the complexity of the experimental dispersion data (e.g., number of frequency samples, whether or not higher modes must be computed, etc.), the number of layers in the inversion parameterization, and the hardware used by the analyst. In our experience (using a desktop computer with an Intel Xeon E5-1650 processor and 32 GB of RAM), computations may take 10 minutes or less for simple datasets and relatively few trial layered earth models comprised of relatively few layers. Conversely, complicated datasets requiring a large number of trial layered earth models, especially when these earth models are comprised of many layers, can take several hours and in extreme cases up to a day.

At the example sites discussed herein, approximately 200,000-500,000 layered earth models were explored during each inversion (i.e., for each layering ratio). Ensembles of the 1,000 lowest misfit layered earth models were then partitioned from the results of each inversion for further processing and comparison. Selecting the 1,000 lowest misfit models for further inspection is, again, a bit arbitrary, representing another necessary compromise between robustness and practicality. We are not suggesting that the 1,000 lowest misfit models from an inversion are always "acceptable", nor are we suggesting that models with slightly greater misfits than the top 1,000 are "unacceptable". The goal of this paper is not to establish a robust misfit criteria regarding which Vs profiles from a given parameterization may be considered acceptable or unacceptable. As stated earlier, this determination is quite subjective and, in our opinion, site specific. The

goal here is to demonstrate the influence of the parameterization on the range of derived Vs profiles. Also note that for each example site described herein, the same number of trial layered earth models were considered for each layering ratio. Thus, by considering the same number of Vs profiles per layering ratio, we were able to assess whether or not the inversion converged to a narrow region of the parameter space or whether the inversion required more iterations to achieve convergence.

3.4 BLIND-STUDY SITE 4

The dataset considered here was originally provided to participants in the InterPacific project. While Garafalo et al. (2016a and 2016b) document the results obtained from three blind-study sites in Europe, the results from blind-study Site 4 have not yet been published. Thus, we refer only to our own results and methodologies herein. The experimental data for Site 4 was provided by Dr. Cecile Cornou, from ISTerre (Institut des Sciences de la Terre), Grenoble, France. According to Dr. Cornou, the dispersion data was based partially on experimental data and partially on a theoretical dispersion curve. In order to develop the dispersion data Dr. Cornou first performed a surface wave inversion on experimentally measured Rayleigh wave dispersion data from an actual field site. The minimum misfit ground model from this inversion was then chosen by Dr. Cornou as the "true" solution profile for the semi-synthetic Site 4. The uncertainty associated with the original experimental dispersion data was then applied on a frequency-by-frequency basis to the theoretical Rayleigh wave dispersion curve associated with the true solution profile in order to produce an "experimental" dispersion curve which reflects realistic uncertainty. Although this curve was not measured directly in the field, it was derived directly from field data and will be referred to as the "experimental dispersion curve" for the remainder of the paper. All participants in the

InterPacific project were provided with this same experimental dispersion curve for Site 4 and asked to perform a blind inversion (i.e., no a-priori information about the site was made available). The mean experimental dispersion data provided to the blind-study participants, including +/- one standard deviation bounds, are shown in Figure 3.7a. Analysts were informed that the data represented the fundamental Rayleigh mode, eliminating the need to consider higher modes during inversion. Each analyst was asked to submit a single "best" Vs profile obtained from inverting the data, and were allowed to also submit a range of Vs profiles that accounted for uncertainty if they so desired. After submissions were completed, the true solution Vs (Figure 3.7b) and Vp (Figure 3.7c) profiles for Site 4 were made known to the participants by Dr. Cornou.

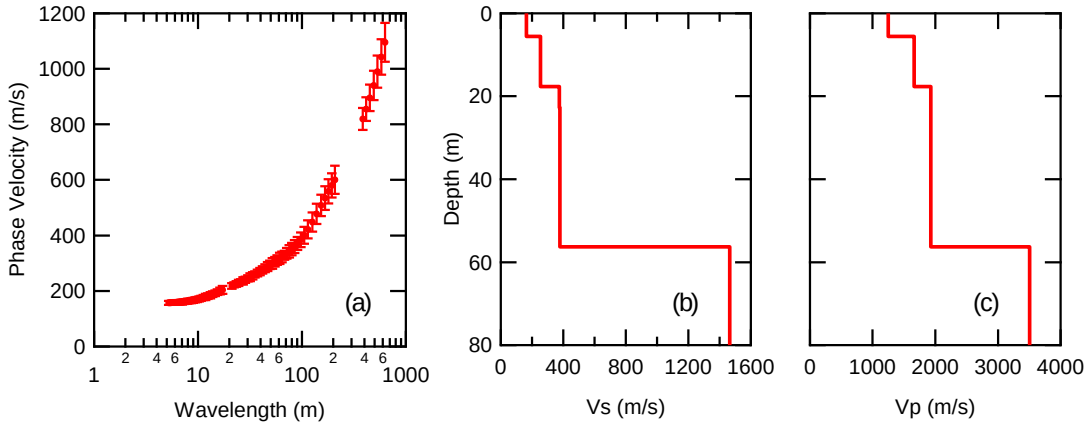

Figure 3.7: InterPacific project semi-synthetic blind-study Site 4 (a) experimental Rayleigh wave dispersion data, (b) true solution Vs profile, and (c) true solution Vp profile.

During our blind analyses, we considered six different layering ratios (1.2, 1.5, 2.0, 3.0, 3.5 and 5.0) for inverting the dispersion data at Site 4. Based on the characteristics of the experimental dispersion data, the following constraints were made on the parameterization: (a) The minimum Vs for all layers was set to approximately 150

m/s based on the minimum phase velocity at short wavelengths; (b) While the half-space Vs was clearly greater than 1,100 m/s, a tight upper bound Vs could not be inferred from the dispersion data because there was no flattening of the curve at long wavelengths. Thus, in the absence of other a-priori information, the maximum Vs was set to 3,500 m/s, which corresponds to the approximate maximum value possible for very hard rock; and (c) The resolution depth was estimated to be 300 m, or roughly half of the maximum experimental wavelength.

The Vs profiles corresponding to the 1,000 lowest misfit models out of approximately 200,000 trial models are shown for each layering ratio in Figure 3.8. Also shown are their corresponding theoretical dispersion curves relative to the experimental dispersion data. The range of misfit values for the "best" 1,000 theoretical dispersion curves associated with each layering ratio inversion are shown in brackets within the dispersion curve subfigures (i.e., Figures 3.8a, 3.8c, 8e, 3.8g, 3.8i, and 3.8k). Upon inspection, it is clear that the 1,000 best theoretical dispersion curves visually fit the experimental data extremely well for all layering ratios, making it difficult to distinguish individual curves. Furthermore, even the maximum misfit values for each inversion are all less than 0.5, and closer to 0.25 or less on average, indicating good fits to the experimental data. Thus, if only a single one of these inversions had been performed for the site, then we may have been inclined to believe that the resulting Vs profiles were a reasonable representation of the subsurface. However, when comparing the results across analyses, it is clear that the Vs profiles resulting from different inversion parameterizations are very different. Indeed, upon inspection of the best 1,000 Vs profiles obtained from each layering ratio inversion (i.e., Figures 3.8b, 3.8d, 3.8f, 3.8h, 3.8j, and 3.8l), one can clearly see that many of the Vs profiles do not well-represent the true solution for the subsurface stiffness profile (keeping in mind that the true Vs profile was

not known to us at the time of performing these inversions). It is clear that the closest Vs profile representations were obtained using a layering ratio of 3.5 (Figure 3.8j), and the dispersion misfit values associated with this layering ratio (Figure 3.8i) were also the lowest.

The following general observations are made regarding the Vs profiles obtained from the layering ratio inversions: (a) When too many layers were utilized in the inversion parameterization (i.e., $\Xi = 1.2$) significant velocity contrasts were not resolved and there was substantial variability in the 1,000 best Vs profiles; (b) When an inversion was performed with a number of layers similar to the true subsurface profile (i.e., $\Xi = 3.5$) the variability in the 1,000 best Vs profiles was reduced, particularly above the half-space, and velocity contrasts were more correctly identified; and (c) When too few of layers were used in the inversion parameterization (i.e., $\Xi = 5$) there was also very little variability in the 1,000 best Vs profiles, but significant velocity contrasts were placed in the wrong locations. Thus, it is valuable to consider both variability in Vs (i.e., precision) as well as bias in Vs (i.e., accuracy), and the results from this study allow us to reflect on both, since the true solution for the semi-synthetic site was ultimately made known to us. The Vs profiles associated with layering ratios of 1.2, 3.5 and 5.0 are examined in more detail below because the inversion parameterizations for these layering ratios were judged to be under-constrained, near-optimal, and over-constrained, respectively, based on consideration of both the dispersion misfit values and the extreme variability (or lack thereof) in the Vs profiles.

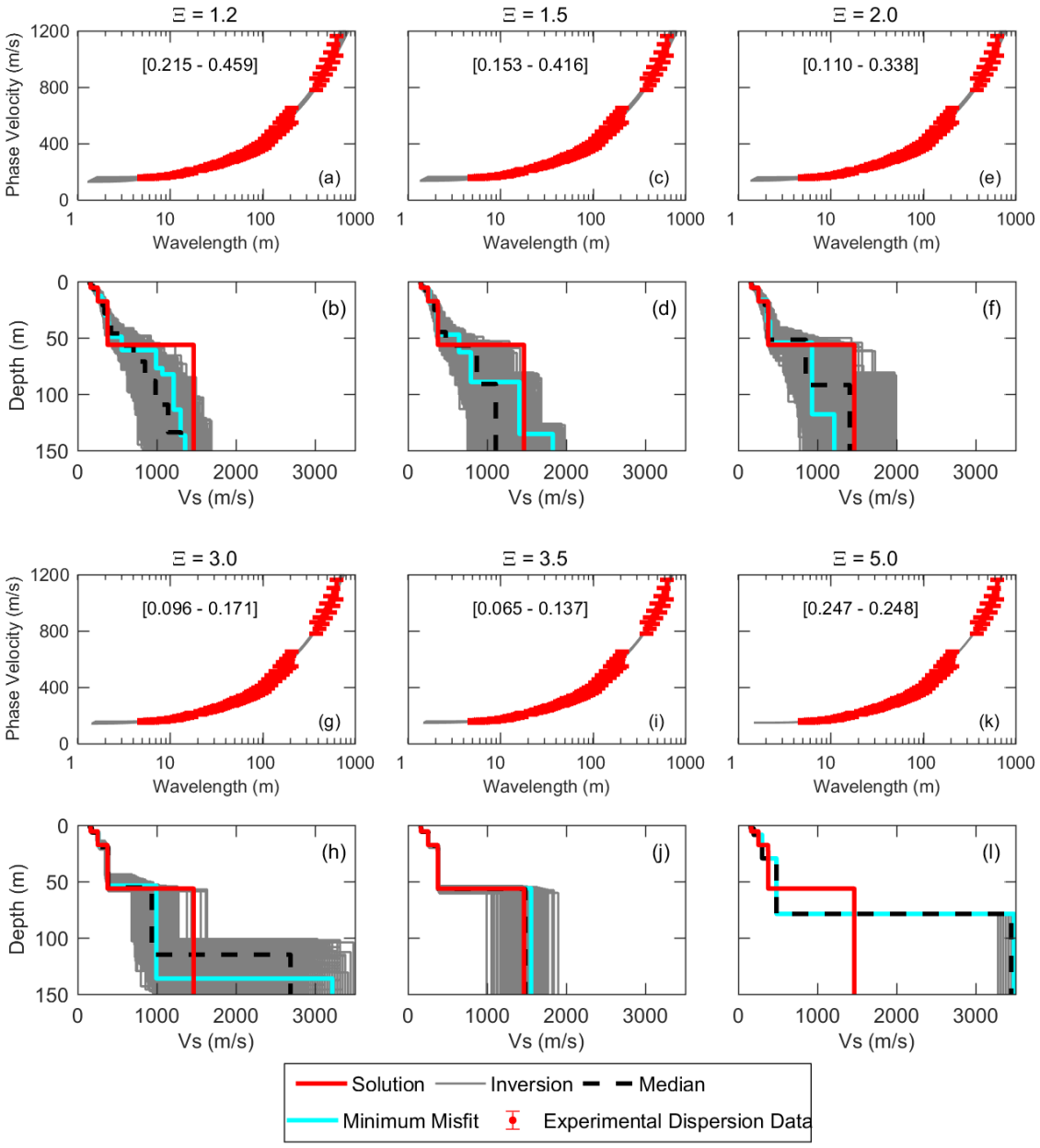

Figure 3.8: The one thousand lowest misfit theoretical dispersion curves and 1,000 corresponding Vs profiles, respectively, obtained from surface wave inversions at blind-study Site 4 based on the following layering ratios: (a, b) 1.2, (c, d) 1.5, (e, f) 2.0, (g, h) 3.0, (i, j) 3.5, and (k, l) 5.0. Note that the numbers in brackets represent the ranges of dispersion misfit values for the 1,000 best (i.e., lowest misfit) models resulting from each inversion. Also shown are the median and minimum misfit profiles for each inversion.

As noted earlier, the choice to examine the 1,000 lowest misfit Vs profiles for each inversion is somewhat arbitrary and based on the need for a consistent means of comparing layering ratios. The authors considered using a maximum misfit criteria, where all profiles below a particular misfit are considered for each layering ratio. Another possibility would be to consider profiles from each inversion whose misfits are within a particular percentage of the minimum misfit for that particular inversion. However, the selection of a maximum acceptable misfit or a percentage of the minimum misfit value is also a bit arbitrary. Moreover, given the broad range in misfit values across layering ratios, this would result in vastly different numbers of profiles being considered for each analysis. Thus, the authors chose to quantify the results from each analysis using the 1,000 lowest misfit profiles, keeping in mind that there is no perfect means of comparing results from each inversion. We understand that differences in the 1,000 best Vs profiles are quite significant for some layering ratios and less significant for other layering ratios. This is largely due to the fact that inversions that incorporate a large number of layers (i.e., free parameters) require substantially more iterations to converge than those inversions with fewer layers. For example, the differences between the 1,000 best Vs profiles for a layering ratio of 5.0 are very minor, as the inversion essentially converged to a single solution after only a few iterations.

A more detailed view of the profiles associated with a layering ratio of 1.2 is shown in Figure 3.9. Figure 3.9a shows the layering parameterization and depth constraints for each layer utilized in the inversion. The top and bottom of each rectangle (shown with alternating white and gray in-fill for clarity) represent the potential top and bottom depth for each layer in the parameterization. The parameterization is comprised of 18 layers down to the depth of resolution. Figure 3.9b shows the 1,000 best (i.e., lowest misfit) Vs profiles obtained from the inversion along with their median Vs profile and the

Vs profile associated with the minimum misfit model. These are all shown relative to the true solution Vs profile. Note that since all Vs profiles within a layering ratio have the same number of layers, the median Vs profile was computed simply by sorting the depth and Vs values for each layer and taking the 50th percentile value. The median Vs profile is considered herein as a means to statistically represent the "average" trend of the 1,000 lowest misfit profiles. Moreover, if the theoretical dispersion curves for the 1,000 lowest misfit profiles match the experimental dispersion data, then the theoretical dispersion curve computed for the median profile tends to fit the experimental dispersion data equally well, despite the fact that it did not directly result from the inversion process (Griffiths et al. 2016a). It is clear from Figure 3.9b that the median profile is comprised of thin layers whose velocity and thickness gradually increase with depth, which is in stark disagreement with the true solution profile. Thus, on average, the Vs profiles fail to detect any of the significant impedance contrasts, and do a particularly poor job at capturing the half-space contrast at approximately 56 m. While the minimum misfit profile does incorporate a strong velocity contrast near the top of the half-space, it still smooths across it and fails to capture its true magnitude. Moreover, many profiles, including those with misfits only marginally higher than the minimum, completely failed to detect this contrast.

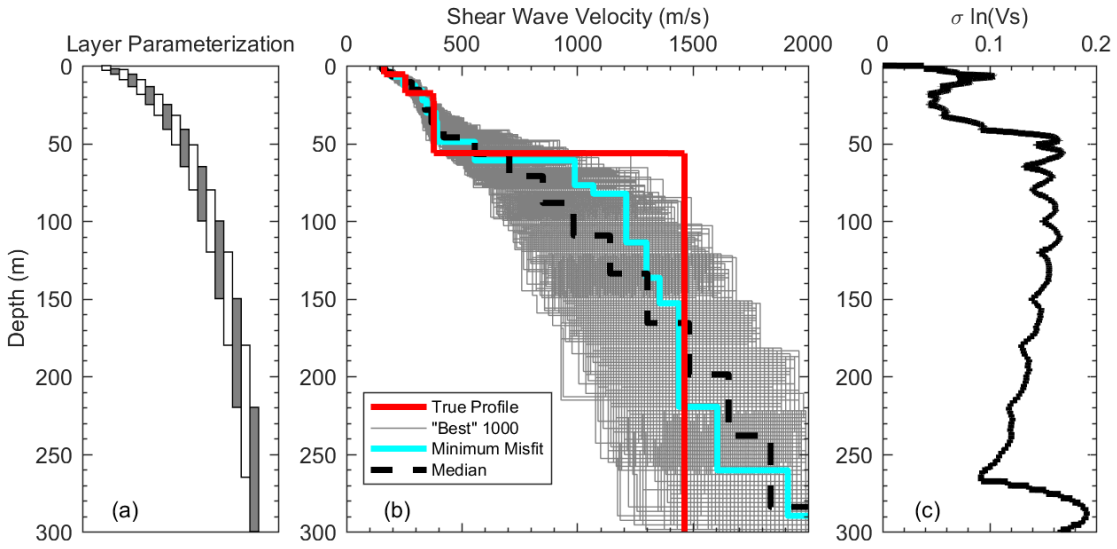

Figure 3.9: (a) Depth ranges permitted in each layer by the inversion parameterization, (b) true solution Vs profile in comparison to the best 1,000, minimum misfit, and median Vs profiles obtained from inversion, and (c) σ_{lnVs} for a layering ratio of 1.2.

In environments where large velocity contrasts are not expected, the smooth nature of the Vs profiles for this layering ratio may be desirable. Hence, one should not assume that using small layering ratios (i.e., many thin layers) is never appropriate. However, at sites with abrupt changes in Vs at depth, the use of too many layers during inversion may result in Vs profiles lacking strong velocity contrasts. Horizontal-to-vertical (H/V) spectral ratios (i.e., the ratio of the horizontal and vertical Fourier amplitude spectra of ambient noise measurements) can be used to indicate the presence or lack of strong velocity contrasts. Moreover, these H/V noise measurements can be incorporated into many inversion routines, thereby adding additional constraints to the inversion. The ability/inability to detect major velocity contrasts at the proper depth has a significant impact on seismic site response estimates. While variability in site response due to uncertain/non-unique Vs inversion is beyond the scope of work discussed in this

paper, Chapter 4 investigates site response estimates using 50 Vs profiles obtained from each layering ratio inversion shown in Figure 3.8.

The inclusion of many thin layers during inversion parameterization is a quite common and tempting strategy to employ because many analysts believe it will allow complicated layering and/or velocity contrasts to be detected more accurately. We have found this generally not to be the case based on our analyses of several synthetic and real sites for which borehole or other a-priori information about the layering was available. Rather, the Vs profiles shown in Figure 3.9b demonstrate that incorporating an excessive number of layers in the inversion parameterization inhibits the ability of the inversion to find the true solution and strong velocity contrasts are, on average, smoothed out. The parameters associated with a layering ratio of 1.2 are too permissive for Site 4, based on the fact that significantly better fits of the experimental dispersion data were achieved using far fewer layers (i.e., higher layering ratios) given the same number of trial models searched. Moreover, the high variability in the Vs profiles using a layering ratio of 1.2 indicates that the inversion algorithm may not have been able to find the most promising regions of such a broad parameter space and/or that the parameterization included too many degrees of freedom (DOF). When too many DOF are incorporated into the parameterization, the experimental data may be insufficient to constrain them. Additionally, even if all DOF may be constrained by the experimental data, the analyst may not possess the computational ability/time to investigate the number of ground models required to find an acceptable solution, as more DOF require more trial layered earth models to be searched (DiGiulio et al. 2012).

Even if it is possible to achieve convergence by exploring more trial layered earth models for a given layering ratio with many DOF, it may not necessarily be useful to do so. For example, we performed this same layering ratio analysis (Ξ = 1.2) using 20

million layered earth models (as opposed to 200,000) using the Stampede supercomputer at the Texas Advanced Computing Center. We re-ran the analysis four different times (i.e., 80 million total inversion models searched) with a unique seed in the pseudo-random number generator for each inversion. Figure 3.10 shows the 1,000 lowest misfit Vs profiles and corresponding misfit values obtained from each random seed (simply labeled as seeds 1, 2, 3, and 4). It is quite clear that the 1,000 lowest misfit Vs profiles associated with each inversion/random seed are essentially on top of one another and exhibit minimal variability. However, it is also clear that the final Vs profiles are influenced by the random seed. In other words, since the parameter space is so broad, the starting point strongly influences where the Neighborhood algorithm converges to. However, what is most important is the fact that all Vs profiles are in poor agreement with the solution. Thus, little was gained from the considerable computational effort required to perform these analyses.

In order to quantify the variability in the 1,000 best Vs profiles obtained with a layering ratio of 1.2 (for the original inversion using 200,000 trial earth models), the standard deviation of the natural logarithm of Vs (σ_{lnVs}) was computed as a function of depth, as shown in Figure 3.9c. This parameter (i.e., σ_{lnVs}) is commonly utilized to quantify variability in Vs randomization models (e.g., Toro 1995, Griffiths et al. 2016b, Chapters 4 and 5). It can be seen that the variability below 50 m is roughly double the variability at shallower depths. This trend is generally observed for profiles developed at sites consisting of soft-to-stiff soil overlying bedrock when utilizing surface wave methods (Garofalo et al. 2016a).

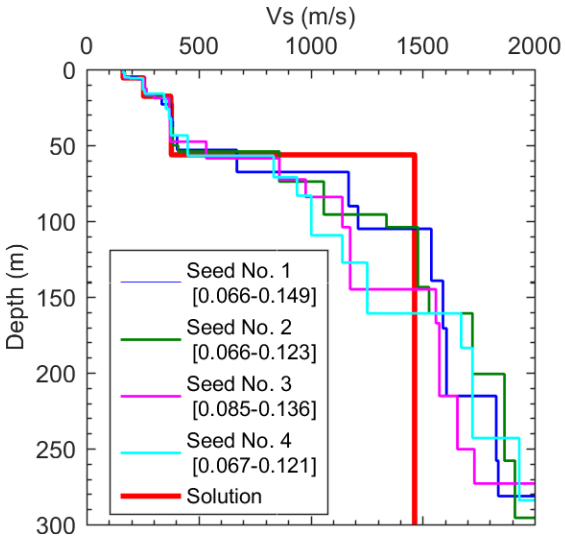

Figure 3.10: Inversion results corresponding to a layering ratio of 1.2 and 20 million trial layered earth models. Note that the inversion was run four times (for a total of 80 million models searched), each with a unique seed in the pseudo-random number generator. The 1,000 lowest misfit profiles for each seed are plotted (essentially on top of one another) with the numbers in brackets representing the range in misfit values.

As shown in Figure 3.11a, the layering parameterization for a layering ratio of 3.5 incorporates five layers down to the depth of resolution. This is less than one-third the number of layers used in the parameterization for a layering ratio of 1.2. However, it is still slightly more than the number of layers in the true solution profile (i.e., 3 layers above the half-space). Nevertheless, it is clear from Figure 3.11b that the 1,000 lowest misfit Vs profiles associated with a layering ratio of 3.5 match the true solution Vs profile quite well. Above the half-space, all Vs profiles, including the median and minimum misfit, are essentially identical to the true solution. With the exception of the "spikes" at each layer interface, the σ_{lnVs} values over the top 56 m for a layering ratio of 3.5 (Figure 3.11c) are up to an order of magnitude lower than those for a layering ratio of 1.2 (Figure 3.9c). These spikes represent small variations in the depth of a significant velocity

contrast in the 1,000 Vs profiles. In the narrow depth range where these spikes occur, standard deviations are computed using velocities corresponding to two layers with significantly different Vs. Thus, they do not represent the actual variability in Vs within a layer. The relatively low variability within each layer is the result of a well constrained parameterization, wherein the global search algorithm was able to quickly narrow in on the most promising areas.

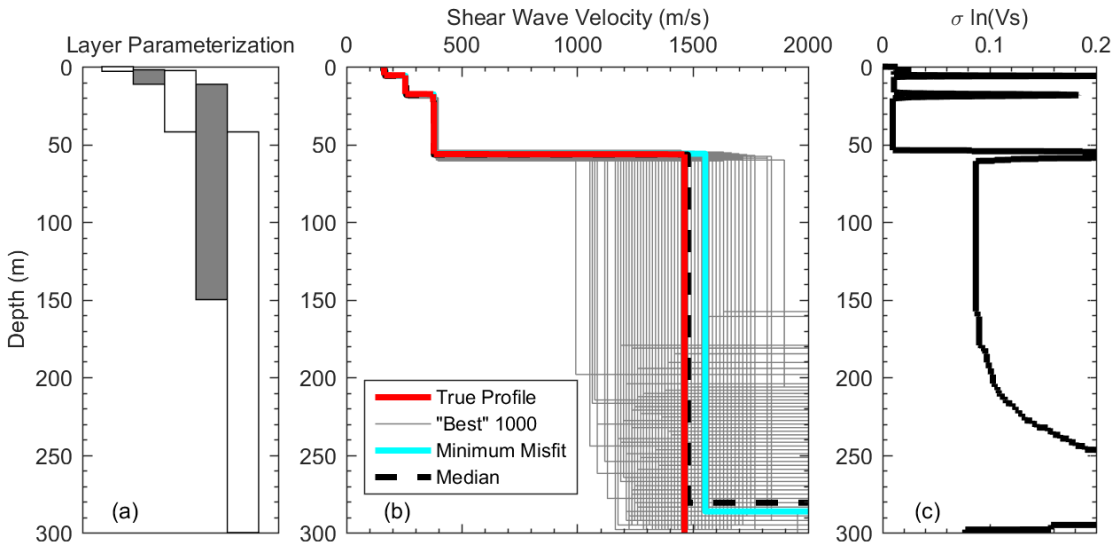

Figure 3.11: (a) Depth ranges permitted in each layer by the inversion parameterization, (b) true solution profile in comparison to the best 1,000, minimum misfit, and median Vs profiles obtained from inversion, and (c) σ_{lnVs} for a layering ratio of 3.5.

Below the true solution half-space, the 1,000 lowest misfit Vs profiles exhibit more variability, with σ_{lnVs} ranging from 0.08 to greater than 0.2. This is due to the fact that the calculation of theoretical dispersion curves is more sensitive to shallow layers than deeper layers. Moreover, the experimental dispersion data does not level-off at long wavelengths, making it more difficult to constrain the Vs of the deepest layers.

Nonetheless, the median Vs profile for this layering ratio matches the true solution profile quite well, and does an even better job than the minimum misfit Vs profile. These results show that Vs profiles derived from inversion can indeed be very realistic representations of the subsurface if reasonable inversion parameterizations are used in conjunction with high-quality dispersion data.

It can be seen that most Vs profiles incorporate an additional stiff layer that is inconsistent with the true solution profile between 160 and 300 m. Because the top of this layer was near the resolution limit in many instances, the authors tested its validity by performing an addition inversion using a parameterization that omitted the bottommost layer. The results from this analysis are shown in Figure 3.12, and it is hereafter referred to as 3.5*, where the * designation refers to a slight manual modification to a layering ratio of 3.5 based on engineering judgement. It can be seen that all 1,000 lowest misfit profiles from this analysis match the true solution profile remarkably well, even below 56 m. Moreover, the profiles exhibit minimal variability at all depths, with σ_{lnVs} values an order of magnitude lower than for the original layering ratio of 3.5 (Figure 3.12c, versus Figure 3.11c, respectively). This is underscored by the fact that the median Vs profile is essentially identical to all other Vs profiles, including the minimum misfit profile.

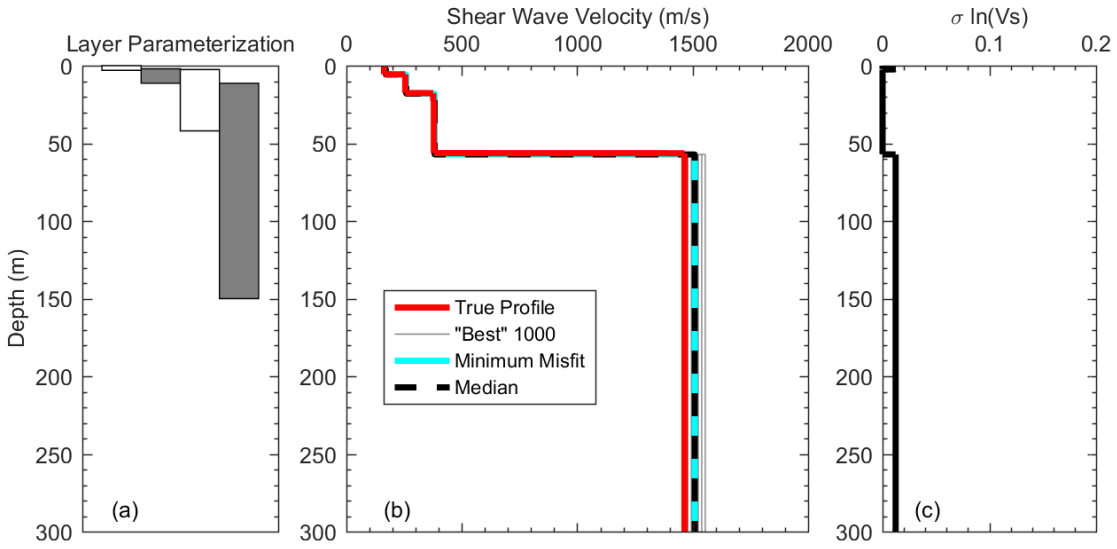

Figure 3.12: (a) Depth ranges permitted in each layer by the inversion parameterization, (b) true solution profile in comparison to the best 1,000, minimum misfit, and median Vs profiles obtained from inversion, and (c) σ_{lnVs} for a layering ratio of 3.5*.

The layering parameterization for a layering ratio of 5.0 is shown in Figure 3.13a. It incorporates a total of four layers, which is the exact same number of layers contained in the parameterization for the Ξ = 3.5* case, and only one less than the number of layers for the Ξ = 3.5 case. However, close scrutiny of Figure 3.12a relative to Figure 3.13a reveals differences in the potential depth ranges for these four layers, which are set by the layering ratio equations. Indeed, the potential depth ranges for the layers in the Ξ = 5.0 case are incompatible with the locations of the layer boundaries in the true solution profile. As a result, the Vs profiles associated with a layering ratio of 5.0 (Figure 3.13b) poorly match the true solution profile, while those associated with a layering ratio of 3.5* match the true solution profile remarkably well (Figure 3.12b). Therefore, even if an appropriate number of layers are included in the inversion parameterization, the inversion

may still fail to find an acceptable solution if the depth ranges are incompatible with the actual subsurface layering.

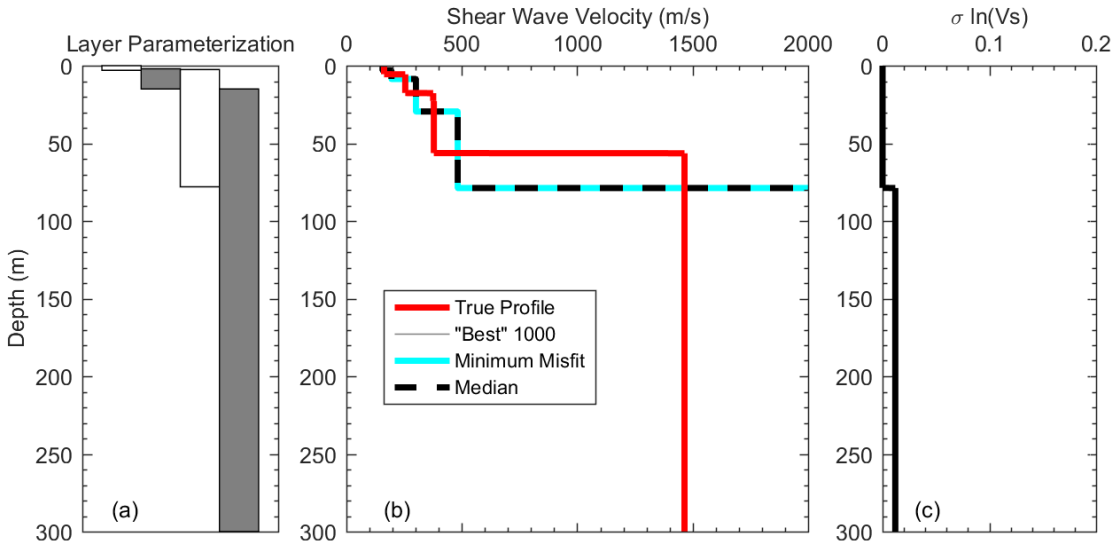

Figure 3.13: (a) Depth ranges permitted in each layer by the inversion parameterization, (b) true solution profile in comparison with the best 1,000, minimum misfit, and median Vs profiles obtained from inversion, and (c) σ_{lnVs} for a layering ratio of 5.0.

The 1,000 lowest misfit Vs profiles associated with a layering ratio of 5.0 exhibit essentially no variability (Figure 3.13c). Similar to a layering ratio of 3.5* (Figure 3.12c), the median and minimum misfit Vs profiles are essentially identical to all other profiles. While the minimal variability for these two layering ratios may be quite similar, the causes are very different. Both layering ratios result in a relatively small parameter space (i.e., few degrees of freedom), which limits the possible layered earth models that can be explored. For the layering ratio of 3.5*, the true solution fell within the layering parameterization and the inversion was able to efficiently find it, thus, other areas of the parameterization could be quickly disregarded because they yielded relatively higher misfit values. Conversely, the layer parameters associated with a layering ratio of 5.0

failed to encompass the true profile. Consequently, the inversion settled for the best possible solution within these overly-restrictive parameters, and the best possible solution did not well-match the true Vs profile. If only a single inversion had been considered using a layering ratio of 5.0, it would have been impossible to know whether the lack of variability in the ensemble of the best 1,000 Vs profiles was low because Vs profiles matching the "true" subsurface profile were found or because the parameters were too restrictive to find the "true" solution.

The ranges in dispersion misfit values for the best 1,000 models resulting from all layering ratio inversions are shown in Figure 3.14. It can be seen that the misfit values are lowest, with essentially no variability, for a layering ratio of 3.5*. Profiles from this inversion are also essentially identical to the true solution Vs profile (Figure 3.12b). It is clear that that as the layering parameterizations approach the optimum condition, their dispersion misfit values decrease. Furthermore, the ranges of misfit values for the best 1,000 models also narrow. Above the optimal layering ratio, dispersion misfit values increase, yet still exhibit minimal variability within the best 1,000 models. Hence, multiple parameterizations need to be considered if realistic representations of the subsurface are desired. Both the dispersion misfit values and the range/variability in Vs among a population of lowest misfit models should be assessed in order to judge which parametrization(s) are most appropriate.

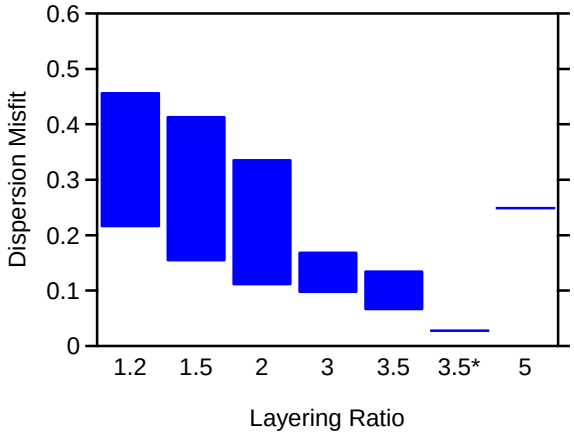

Figure 3.14: Ranges in dispersion misfit values for the 1,000 best (i.e., lowest misfit) subsurface models obtained for each layering ratio inversion performed for blind-study Site 4.

Participants in the InterPacific study were asked to submit a single "best" profile from their blind inversion of Site 4. Based on the dispersion misfits shown in Figure 3.14, and the previous discussions regarding potential causes of variability in Vs among a population of lowest misfit profiles, the median Vs profile from the layering ratio of 3.5* was chosen and submitted. We later discovered that this Vs profile matched the true solution remarkably well, validating the usefulness of the layering ratio methodology when applied in conjunction with experience and sound judgement. Nevertheless, a true solution profile is rarely available for validation at real sites in practice. Thus, it can be difficult to conclude if an inversion parameterization has been too restrictive or too permissive without significant a-priori information about layering beneath the site, especially when the misfit values for profiles derived from different inversion parameterizations are similar. In the case of blind-study Site 4, the trend in dispersion misfit values and the variability, or lack thereof, in Vs profiles allowed us to determine a single solution that was quite obvious after exploring various layering ratio inversions.

As this is not always possible, another case history site is discussed below to demonstrate what can be done when trends are not as obvious.

3.5 MIRANDOLA, ITALY SITE

Active- and passive-source surface wave testing were performed at the Mirandola, Italy site as part of the InterPacific Project. All participants were given the raw field data and asked to develop Vs profiles for the site. A detailed description of the surface wave data acquisition at Mirandola and comparisons of the dispersion and inversion results obtained from all InterPacific project participants are provided in Garafalo et al (2016a). A brief overview of the surface wave data and dispersion processing methodologies that we used to develop a Rayleigh wave dispersion curve for the site is included below.

3.5.1 Site Information and Dispersion Processing

Active-source data were acquired by the InterPacific organizing team using two 48-channel linear arrays with spacings of 1 and 2 m, respectively, between successive 4.5-Hz vertical geophones. Passive-source (i.e., ambient vibration) data were acquired using 3-component, intermediate-period seismometers. Multiple passive-source arrays were used, including circular (5 m to 405 m radius), triangular (sides ranging from 12.5 m to 300 m), and L-shaped arrays (sides 150 m long).

We processed the active-source data from each linear array and shot location using the Frequency Domain Beamformer (FDBF) method (Zywicki 1999) and combined the dispersion data from all shot locations using the methods described in Wood and Cox (2012) to develop a mean active-source Rayleigh wave dispersion curve with uncertainty estimates. Active-source dispersion data ranged from 5 to 25 Hz. Passive-source data was processed using both the High Resolution Frequency-Wavenumber Transformation (HFK) and the Modified Spatial Autocorrelation (MSPAC) methods (Capon 1969, Bettig

et al. 2001). Ambient vibration HFK data was used between frequencies of 4 to 25 Hz and 0.7 to 1.3 Hz, while MSPAC data was used at frequencies ranging from 1.5 to 3.5 Hz. The choice between HFK and/or MSPAC data was made after visually inspecting the dispersion data and judging which was of higher quality based on a number of factors (e.g., smoothness, uncertainty bounds, bias towards high or low phase velocity, noise directionality, etc.). Active- and passive-source Rayleigh wave dispersion data were then combined to develop a composite experimental dispersion curve, as shown in Figure 3.15a. Errors bars represent +/- one standard deviation in phase velocity.

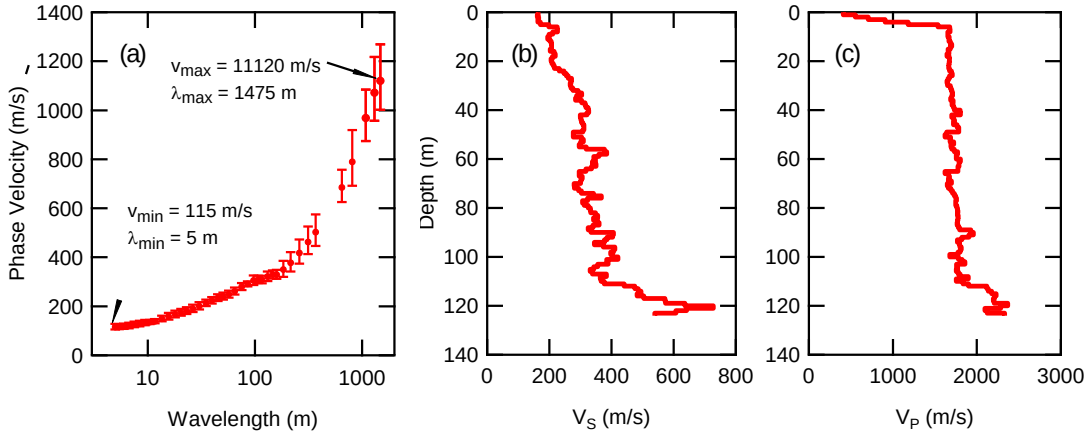

Figure 3.15: Mirandola, Italy (a) active- and passive-source experimental dispersion data, and (b) and (c) crosshole Vs and Vp profiles, respectively.

Seismic crosshole testing was performed independently at the Mirandola site by several teams in order to directly measure Vs and Vp (Garafalo et al. 2016b). The crosshole Vs and Vp profiles that are deemed to be of the highest quality are shown in Figure 3.15b and 3.15c, respectively. In contrast to the previous semi-synthetic Site 4 case study, there is no "true solution profile" available for this site. Thus, the crosshole profiles are provided as a reference. However, it is important to note that invasive

crosshole testing samples over a relatively small area when compared to surface wave methods, particularly when large-aperture passive arrays are used to profile to significant depths. Thus, differences can be expected between Vs profiles obtained using borehole and surface wave methods. Nonetheless, unless extreme heterogeneity is present at a site, Vs profiles obtained from these two methods should agree reasonably well. The crosshole Vs profile is quite smooth with no abrupt velocity contrasts until soft rock is reached at a depth between 110 -120 m. There is a decrease in Vs below 120 m, possibly as a result of variable weathering patterns within the top several meters of the soft rock layer. It should be noted that this decrease was observed by multiple teams that performed seismic crosshole testing, but the boreholes did not go deep enough into the rock to determine the thickness of this presumed zone of weathering.

During inversion of the dispersion data shown in Figure 3.15a, the authors noted that the experimental dispersion data at wavelengths greater than approximately 1,000 m could be fit with either a fundamental or first-higher Rayleigh wave mode. The former interpretation results in a higher Vs in the rock material encountered at 110 to 120 m. The authors had developed and submitted Vs profiles for the site to the InterPacific blind-study prior to developing the layering ratio technique and prior to knowing the crosshole results. At the time, we chose to fit all dispersion data with the fundamental mode. These results are detailed in Griffiths et al. (2016) and Garafalo et al. (2016a). However, for the present study, the authors re-analyzed the data using the layering ratio approach and chose to fit the long-wavelength experimental data with the first-higher Rayleigh wave mode. This resulted in Vs values in the rock that more closely matched the crosshole data (Figure 3.15b). Nonetheless, as discussed above, the crosshole data may have only penetrated the uppermost/weathered portion of the rock, while the surface wave data sampled material at much larger depths, which would be expected to have higher seismic

velocities. Thus, both interpretations are reasonable within the bounds of knowledge that currently exists for the site. While a detailed discussion of mode-interpretations and Vs uncertainty is beyond the scope of this paper, it is in the opinion of the authors that both possibilities should be considered in subsequent engineering analyses, such as seismic site response.

3.5.2 Layering Ratio Analyses

Layering ratios of 1.2, 2.0, 3.5, 5.0, and 7.0 were considered during inversion analyses for the Mirandola Site. Figure 3.16 shows the 1,000 lowest misfit theoretical dispersion curves and corresponding Vs profiles for all layering ratios considered. Note that both the fundamental and first-higher theoretical Rayleigh wave modes are shown in Figure 3.16a, 3.16c, 3.16e, 3.16g, and 3.16i, as experimental data with wavelengths greater than 1,000 m were fit with the first higher mode. Similar to blind-study Site 4, all theoretical dispersion curves match the experimental data quite well by visual inspection. However, the dispersion misfit values associated with a layering ratio of 7.0 are generally more than double the misfit values associated with all other layering ratios. However, since the dispersion misfit values for the $\Xi = 7.0$ case are less than 1.0 (i.e., on average fall within the uncertainty bounds of the data) and visually appear to fit the data quite well, an analyst may have concluded that the resulting Vs profiles were acceptable representations of the subsurface if only a single parameterization were performed. Nonetheless, it is clear that much lower misfit values and more accurate representations of the subsurface are possible when other parameterization are considered.

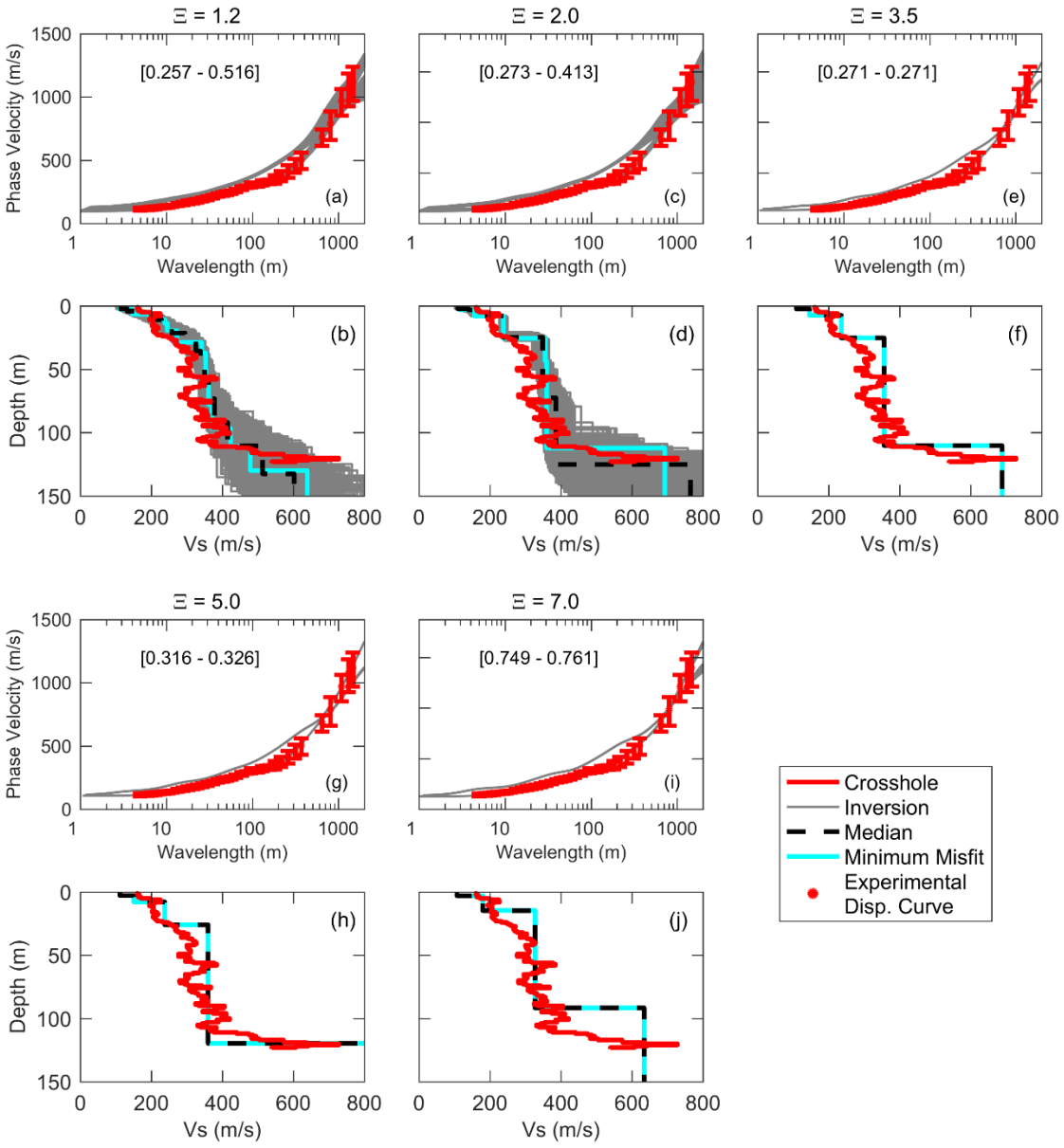

Figure 3.16: The one thousand lowest misfit theoretical dispersion curves and 1,000 corresponding Vs profiles, respectively, obtained from surface wave inversions at Mirandola based on the following layering ratios: (a, b) 1.2, (c, d) 2.0, (e, f) 3.5, (g, h) 5.0, (i, j) and 7.0. Note that the numbers in brackets represent the ranges of dispersion misfit values for the 1,000 best (i.e., lowest misfit) models resulting from each inversion. Also shown are the median and minimum misfit profiles for each inversion.

Vs profiles associated with each layering ratio are shown relative to the crosshole Vs profile in in Figure 3.16b, 3.16d, 3.16f, 3.16h, and 3.16j. It is clear that the 1,000 best Vs profiles derived from layering ratios of 1.2 and 2.0 exhibit significantly more variability than those derived using higher layering ratios. Vs profiles derived from layering ratios of 2.0, 3.5 and 5.0 yield better estimates than the other layering ratios of the rock velocity contrast indicated in the crosshole Vs profile between 110-120 m. Furthermore, the Vs profiles obtained from these three layering ratios all indicate an increase in velocity near 25 m, which is also present in the crosshole Vs profile, albeit much more subdued. While a layering ratio of 1.2 yielded smoother Vs profiles that visually seem to agree better with the crosshole Vs over the top 100 m, these Vs profiles generally did a poor job resolving the rock velocity contrast. However, it should be noted that the decrease in Vs in the crosshole profile below 120 m adds ambiguity to the velocity of rock at this site and gives credibility to an interpretation where a weathered zone is reflected in the Vs profiles derived from a layering ratio of 1.2. Moreover, the lowest dispersion misfit value (0.257) was achieved using a layering ratio of 1.2, albeit marginally lower than those associated with layering ratios of 2.0, 3.5, and 5.0. These points make it difficult to discount the results from a layering ratio of 1.2. This would particularly be true if the crosshole Vs was not available for a reference and no other data were available to constrain the depth to rock. Conversely, the best 1,000 Vs profiles associated with a layering ratio of 7.0 exhibit essentially no variability and incorporate several significant velocity contrasts at the wrong locations. In particular, the rock velocity contrast at 92 m is located more than 20 m shallower than indicated by the other layering ratio inversions and the crosshole data. Based on the relatively high misfit values and the minimal variability, it can be concluded that the inversion parameterization for the $\Xi = 7.0$ case was too restrictive.

Figure 3.17a shows the misfit ranges for the best 1,000 models obtained from each layering ratio inversion considered at the Mirandola Site, while Figure 3.17b compares the median Vs profiles derived from the best 1,000 Vs profiles obtained from each layering ratio. In contrast to Site 4 (refer to Figure 3.14), the minimum misfit is quite similar for all layering ratios less than 7.0. Thus, careful consideration is required in order to decide whether one layering ratio is "better" than another. While the Vs profiles derived using a layering ratio of 7.0 can be discounted as unrealistic for reasons discussed previously (i.e., minimal Vs uncertainty within the best 1,000 Vs profiles in conjunction with dispersion misfit values that are significantly higher than those achieved with smaller layering ratios), it is difficult to discount Vs profiles derived from any of the other layering ratios. The median Vs profiles associated with layering ratios of 2.0, 3.5, and 5.0 all incorporate a significant impedance contrast between 110 and 120 m, which are in good agreement with the crosshole Vs profile. While the median profile for a layering ratio of 1.2 does not incorporate as stiff of a rock impedance contrast, it still represents a reasonable interpretation for reasons discussed previously. Borehole Vs profiles are rarely available, especially to depths exceeding 100 m, and thus cannot be relied upon to aid in interpretation of the "best" inversion results at most real sites. Indeed, a "true solution" profile does not exist in real situations where vertical and spatial heterogeneity are present, and the velocity profiles from layering ratios of 1.2, 2.0, 3.5, and 5.0 could all be deemed reasonable within the bounds of the 405-m diameter passive array used to collect passive surface wave data. Thus, it is critical that multiple inversion parameterizations be considered in order to quantify reasonable Vs uncertainty for subsequent engineering analyses. If only a single Vs profile is provided, or if estimates of Vs uncertainty are restricted to a single parameterization, it becomes more difficult to meaningfully quantify the Vs uncertainty (both aleatory variability and epistemic

uncertainty) and its influence on subsequent site response analyses (e.g., Griffiths et al. 2016a, Griffiths et al. 2016b, Chapters 4 and 5).

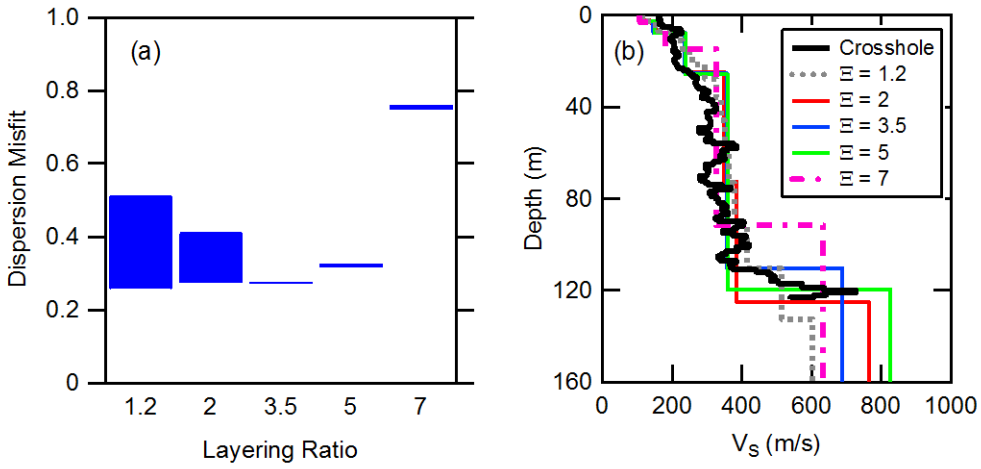

Figure 3.17: (a) Ranges in dispersion misfit values and (b) median Vs profile for the 1,000 best (i.e., lowest misfit) subsurface models obtained for each layering ratio inversion at Mirandola.

3.6 CONCLUSIONS

The inverse problem involved in obtaining a realistic layered earth model from surface wave dispersion data is inherently ill-posed, nonlinear, mix-determined, and without a unique solution. When performing an inversion with limited a-priori information, analysts must decide on an appropriate number of layers to represent the subsurface. The choice of layering parameterization has been shown to significantly impact Vs profiles resulting from inversion. This paper presents a method for conducting multiple inversions utilizing systematically-varied inversion layering parameterizations in order to identify and fully encompass the most reasonable layered earth models for a site. Each parameterization is defined by a unique layering ratio, which represents a multiplier

that systemically increases the potential thickness of each layer in the inversion parameterization based on the potential thickness of the layer directly above it.

The layering ratio method has been demonstrated at two case history sites associated with the InterPacific Project. At blind-study Site 4, the layering ratio methodology was used to almost perfectly recover the true Vs profile for a semi-synthetic site. At the Mirandola site, a single "best" model could not be extracted. However, results from several layering ratios were found to realistically bound/bracket the subsurface conditions indicated by crosshole results in a 120-m deep borehole. While the goal of the layering ratio inversion methodology is not necessarily to find the "optimal" or "best" Vs profile for a site, it may be successful at doing so for certain sites/datasets. However, the primary reason for using the layering ratio method is to avoid selection of Vs profiles that are adversely influenced by the choice of inversion parameterization, and realistically represent the uncertainty in Vs resulting from surface wave inversion.

At both study sites, layering parameterizations that incorporated a lot of layers were found to yield Vs profiles with relatively high variability for the given number of trial models searched. Additionally, Vs in these many-layered profiles gradually increased with depth and many profiles failed to detect the location and magnitude of significant impedance contrasts. While this variability can be reduced and lower misfit values may be achieved by running additional iterations/trial models in the inversion, results presented herein have shown that even after many millions of trial models the "true" Vs profile may not be recovered. This occurs because when too many layers (i.e., degrees of freedom) are included in the inversion parameterization the experimental dispersion data may be insufficient to constrain them. Moreover, practical time constraints often preclude the full exploration of such a broad parameterization. In spite of these observations, the theoretical dispersion curves associated with layered earth

models from under-constrained inversions generally fit the experimental dispersion data quite well, so caution should be exercised when using many trial inversion layers for sites where strong impedance contrasts are expected.

At both study sites, parameterizations that incorporated too few layers were found to yield Vs profiles with minimal variability and strong velocity contrasts at incorrect locations. When observed together, these two phenomena indicate that the inversion was forced to settle for the best possible solution within an over-constrained parameter space after considering a relatively low number of trial models. While the misfit values associated with these overly-restrictive inversion parameters were generally higher than those that incorporated more layers, the theoretical dispersion curves still fit the experimental dispersion data reasonably well.

Without considering multiple inversion parameterizations it is generally not possible to know whether the results of an inversion are adversely influenced by the inversion parameterization, and the full non-uniqueness associated with the surface wave inverse problem cannot be investigated. The layering ratio technique described in this paper provides a systematic means of investigating the impact of layering parameterization. Furthermore, it has been shown to significantly aid in selecting Vs profiles that are close representations of the subsurface. This goal cannot be achieved if only a single parameterization is considered. Further studies are needed to determine if the layering ratio methodology will work well for more complicated sites that contain, for example, low velocity layers beneath stiffer overlying layers. Even if it does not, and even if readers choose not to implement the layering ratio methodology, we cannot stress enough the importance of investigating multiple parameterizations during surface wave inversion if realistic models of the subsurface, and uncertainty associated with those

models, are to be developed. These types of investigations are particularly needed in order to quantify the influence of Vs uncertainty on subsequent engineering analyses.

Chapter 4: Site Response Implications Associated with using Non-Unique Vs Profiles from Surface Wave Inversion in Comparison with Other Commonly Used Methods of Accounting for Vs Uncertainty

David P. Teague and Brady R. Cox

This chapter is a pre-copyedited, author-produced version of an article accepted for publication in Soil Dynamics and Earthquake Engineering following peer review. The version of record is cited below:

Teague, D. P. and Cox, B. R. (2016). "Site Response Implications Associated with using Non-Unique Vs Profiles from Surface Wave Inversion in Comparison with Other Commonly Used Methods of Accounting for Vs Uncertainty." Soil Dynamics and Earthquake Engineering, Vol. 91, pp. 87–103, https://doi.org/10.1016/j.soildyn.2016.07.028.

As first author, I was responsible for approximately 75% of the data processing and 50% of the results interpretation.

ABSTRACT

This paper discusses variability and accuracy of site response predictions performed using shear wave velocity (Vs) profiles derived from non-unique surface wave inversions and other commonly used statistical methods of accounting for epistemic uncertainty and aleatory variability in Vs. Specifically, linear and equivalent linear site response analyses were performed on the following three classes of Vs profiles: (1) 350 Vs profiles developed by performing multiple surface wave inversions, each with a unique set of layering parameters, on a common dispersion dataset, (2) two upper/lower range base-case Vs profiles developed by systematically increasing or decreasing the solution Vs profile by 20%, and (3) 100 Vs profiles developed using the Vs randomization procedure proposed by Toro (1995). Vs profiles derived from surface wave inversions generally yielded accurate site response estimates with minimal variability, so long as their theoretical dispersion data fit the experimental dispersion data

well. On the other hand, the upper/lower range and randomized Vs profiles generally produced inaccurate and highly variable site response predictions, although the inclusion of site-specific parameters in the randomization model improved the results. At real sites where substantial aleatory variability is anticipated and/or the epistemic uncertainty is quite high, the site response estimates associated with the randomized and/or upper/lower range Vs profiles may be deemed acceptable. However, if the experimental dispersion data and horizontal-to-vertical spectral ratios are shown to be consistent over the footprint of a site, it may be possible to significantly reduce the uncertainty associated with the input Vs profile and the resulting uncertainty in the site response.

4.1 INTRODUCTION

Site response simulations using equivalent linear and nonlinear analyses have shown that the shear wave velocity (Vs) profile selected to anchor small-strain subsurface stiffness conditions has a large influence on the amplitude and frequency content of predicted surface ground motions (e.g., Bazurro and Cornell 2004, Rathje et al. 2010, Li and Assimaki 2010, Barani et al. 2013). Hence, the development of appropriate Vs profiles for use in site response analyses is of paramount importance. Engineering design codes stress the importance of accounting for uncertainty in Vs when performing site response analyses (e.g., ASCE 2010, AASHTO 2011), yet, no firm guidelines are provided regarding how to appropriately/realistically account for these uncertainties.

Both epistemic uncertainty and aleatory variability in Vs are typically accounted for in probabilistic site response analyses for critical projects such as nuclear facilities (EPRI 2012). Epistemic uncertainty is accounted for by considering multiple base-case Vs profiles. Typically, a “mean” and upper/lower range base-cases are developed. When multiple Vs profiles are available for a given site, the “mean” base-case may be

computed as the average (or median) of the available Vs profiles. However, oftentimes only a single Vs profile is available and assumed to represent the mean. The upper/lower range base-cases are developed by applying an estimated level of epistemic uncertainty to the "mean" base-case Vs profile. Oftentimes, upper/lower range base-cases are generated by arbitrarily increasing and decreasing the reference Vs profile by a constant factor such as +/- 20% to 30%. Aleatory variability in Vs is accounted for in site response analyses via a randomization process about the base-case Vs profiles. This is most commonly performed using the Toro (1995) Vs randomization model. If abundant Vs data is available at a site, the statistical parameters needed to constrain epistemic uncertainty and aleatory variability can be obtained. Otherwise, conservative estimates must be made (Griffiths et al. 2016a).

Vs profiles can be measured in-situ using invasive or non-invasive techniques. In either case, there is uncertainty associated with the final Vs profiles, which may or may not be openly acknowledged to the end-user. While it is commonly assumed that there is less uncertainty associated with invasive/borehole methods, a recent, comprehensive, blind-analysis study at three geologically-distinct sites in Europe revealed that Vs profiles derived from surface wave testing had coefficients of variation that were similar to, and at times lower than, those derived from a combination of crosshole, downhole and suspension logging (Garafalo et al. 2016a, Garafalo et al. 2016b). Nonetheless, when Vs profiles are derived from an inversion of surface wave data, one must acknowledge that the solution is non-unique (Lai et al. 2005, Cornou et al. 2009, Cox et al. 2014, Garafalo et al. 2016a), and the uncertainties may be significant, particularly if results are reported without performing a systematic, rigorous investigation of different trial subsurface layering models (DiGiulio et al. 2012, Chapter 3).

The surface wave inversion process involves finding one or more layered earth models whose theoretical dispersion curve(s) fit the experimentally-measured dispersion data. While in the past it was common to simply seek a solution that yielded a "reasonable" fit by-eye, it is presently common to quantify the quality of fit using some sort of a least-squares misfit value, with lower misfit values indicating a better fit. Layered earth models are comprised of a system of stacked, linear elastic, horizontal layers over a half-space. Each layer is defined by its inversion parameters: thickness (t), shear wave velocity (Vs), compression wave velocity (Vp) or Poisson's ratio (ν), and mass density (ρ). The total number of layers is generally unknown and specified/assumed by the analyst. The layer parameters are then varied by a search-algorithm until an acceptable match is made between the theoretical dispersion curve and the experimental dispersion data. However, the inverse problem involved in obtaining a realistic layered earth model from surface wave dispersion data is inherently ill-posed, nonlinear, and mix-determined, without a unique solution. The ill-posed nature of the problem results from trying to recover four parameters (t, Vs, Vp, and ρ) for each layer in the model indirectly from the two measured data parameters of Rayleigh phase velocity (Vr) and frequency (f). The problem is further complicated by the nonlinear relationship between the data parameters, which vary as a function of frequency/wavelength, and the desired model space parameters, which vary as a function of depth. Additionally, the model solution for deeper layers is dependent on the model solution for shallow layers, resulting in a mix-determined problem. As a result, a number of significantly different layered earth models may possess theoretical dispersion curves that fit the experimental data equally well (Foti et al. 2009, Chapters 2 and 3).

Multiple studies have considered the variability in site response estimates derived from non-unique Vs profiles obtained from surface wave testing (e.g., Foti et al. 2009,

Boaga et al. 2011, Jakka et al. 2014a, Griffiths et al. 2016b). Conclusions drawn from these studies have been somewhat conflicting. For example, Foti et al. (2009) used Monte Carlo inversions of synthetic and real datasets to conclude that Vs profiles with equivalent dispersion misfit values are essentially equivalent with regards to site response. On the other hand, Boaga et al. (2011) argued that profiles with comparable dispersion misfit values may potentially exhibit significant variability with regards to site amplification if a sharp velocity contrast is not present beneath the site. Similarly, Jakka et al. (2014a) argue that profiles with comparable misfit values exhibit significant variability with regards to site response. However, as pointed out by Comina and Foti (2014), the theoretical dispersion curves associated with many of the Vs profiles in the Jakka et al. (2014a) study fall outside of the uncertainty bounds of the experimental data at high frequencies, and do not follow the general trend/shape of the experimental data at low frequencies. Several follow up discussions have ensued between these differing schools of thought (e.g., Comina and Foti 2014, Jakka et al. 2014b, Boaga et al. 2012, Socco et al. 2012). One particular point of debate is focused on what constitutes "equivalence" in terms of dispersion misfit when attempting to select appropriate candidate Vs profiles for use in site response.

A companion study documented by Griffiths et al. (2016a and 2016b) investigated site response variability at two sites (one with a strong impedance contrast and one without) using many Vs profiles derived directly from a single surface wave inversion and from several statistically-based methods commonly used to account for epistemic uncertainty and aleatory variability. In the initial study, Griffiths et al. (2016a) argued that the experimentally-measured dispersion data represents the "site signature", which reveals important information about wave propagation across the site, and any Vs profiles that fail to capture the site signature (i.e., fail to match the experimental dispersion data)

may not be appropriate for trying to quantify the variability in site response. Inherent in this argument is the assumption that a broadband, high-quality experimental dispersion curve has been obtained and demonstrated to be representative of the site. The quality of fit in their study was quantified using the dispersion misfit equation of Wathelet et al. (2004):

$$\text{misfit} = \sqrt{\frac{1}{n_f}\sum_{\mathrm{i=1}}^{\mathrm{n_f}}\frac{(\mathrm{x_{di}} - \mathrm{x_{ci}})^2}{\sigma_{\mathrm{i}}^2}} \qquad (4.1)$$

Where, x_{di} represents the Rayleigh wave phase velocity of the experimental dispersion data at frequency f_i; xci is the theoretical Rayleigh wave phase velocity computed for the trial layered earth model at frequency f_i; σ_i is the standard deviation associated with the experimental dispersion data at frequency f_i; and n_f is the number of frequency samples considered for the misfit calculation. The misfit value is essentially a root-mean-squared-error (RMSE) between the experimental and theoretical dispersion curves with a normalization factor equal to the inverse of the experimental standard deviation at a given frequency. According to this definition of misfit, a value less than 1.0 essentially means that on average (i.e., across the frequency band considered) the theoretical dispersion curve falls within the +/- one standard deviation bounds of the experimental data. Thus, misfit values far in excess of 1.0 suggest a poor fit of the experimental dispersion data. Misfit values approaching zero represent better fits to the mean trend of the experimental data, and for a given set of data, dispersion misfit values can be used to make relative judgements regarding the quality of trial layered earth models. However, the authors acknowledge that misfit values deemed to be acceptable at one site may be considered unacceptable at another. For example, a misfit value of 0.9 might be “good” at one site because the theoretical dispersion curve visually fits a

complicated dataset. However, a misfit value of 0.3 might be "bad" at another site because the theoretical dispersion curve does not agree well at all frequencies for a simple dispersion dataset. Thus, misfit values from different sites generally cannot be compared directly with one another for a measure of the overall inversion quality from site-to-site. Rather, the misfit values can simply be used to guide relative judgements about the quality of certain trial layered earth models relative to other potential models at the same site.

Griffiths et al (2016a) found that theoretical dispersion curves associated with upper/lower range Vs profiles (e.g., median +/- 20%) commonly used to account for epistemic uncertainty (e.g. Matasovic and Hashash 2012, EPRI 2012) yielded a poor fit to the experimental dispersion data (i.e., relatively high misfit values) measured at their study sites. They also found that Vs randomization (Toro 1995) commonly utilized to account for aleatory variability resulted in only a few acceptable, and many unacceptable, Vs profiles based on dispersion misfit. However, Vs profiles derived directly from a surface wave inversion resulted in a satisfactory fit of the experimental dispersion data because the inversion algorithm seeks to achieve the best possible fit to the data and thus seeks profiles that best capture the experimentally-measured "site signature."

The follow-up study by Griffiths et al. (2016b) documented linear and equivalent linear site response analyses performed using Vs profiles derived in their previous study. A total of 50 Vs profiles with comparable misfit values derived from surface wave inversion were considered for each site. The response spectra (RS) and amplification factors (AF) associated with these profiles resulted in minimal variability, which supports the conclusions of Foti et al. (2009). On the other hand, the upper/lower range Vs profiles and the randomly-generated Vs profiles exhibited substantial variability in terms of RS and AF. The authors argue that since these statistically-generated profiles do not capture

the “site signature”, the variability that they exhibit may not be realistic, and may potentially result in underestimation of site response due to flattening-out of resonant frequencies. Overall, the results presented in Griffiths et al. (2016b) show a strong, albeit not perfect, trend of increasing variability in equivalent linear site response estimates with increasing surface wave dispersion misfit values at their study sites.

It is important to briefly raise a few points regarding the experimental dispersion data obtained at real sites and the so-called “site signature”. An experimental dispersion curve represents a spatial average of material properties over the length/area of the array used to measure surface waves (with the degree of averaging changing with frequency). Thus, if a single active-source survey (i.e., MASW or SASW) is conducted using an array that is relatively small in comparison to the area of interest, the resulting data cannot be deemed a “signature” of the site. Indeed, experimentally measured dispersion data measured using relatively small arrays at geologically-complex sites may vary considerably over short distances. For example, Thompson et al. (2012) present dispersion data collected at two Kiknet sites in Japan, at which four independent spectral analysis of surface wave (SASW) surveys were conducted within a few hundred meters of one another. The experimental dispersion data at the first site was in excellent agreement over the frequency ranges that were resolved by the individual surveys. Thus, it can be argued that this site had a narrowly-defined site signature. Conversely, the experimental dispersion data derived from the four SASW surveys at the second site showed extreme variability. At such a geologically-complex site it may not be possible to establish a single dispersion curve with relatively narrow uncertainty bounds. Rather, the site signature may need to be characterized by a broad range of experimental dispersion data compiled from either a number of smaller arrays spread across the site and/or a

combination of smaller active-source arrays and larger two-dimensional passive-source arrays that span the footprint of the site.

While many of the aforementioned studies examined the variability in site response estimates obtained using non-unique Vs profiles derived from surface wave inversion, each example considered only a single set of non-unique Vs profiles developed using the same set of inversion parameters (i.e., a single parameterization). In each case, the inversion algorithm was restricted to a single, predefined number of layers and ranges in their respective properties. As mentioned above, the inversion parameterization has been shown to significantly impact the results of a surface wave inversion (DiGiulio et al. 2012, Chapter 3). This is because the number of unknowns, which is controlled by the number of layers in the parameterization, is itself an unknown. While Vs profiles developed from within a single set of parameters may exhibit significant differences, the differences between profiles derived from different sets of parameters has been shown to be even more significant. Indeed, it is possible to obtain comparable dispersion misfit values from profiles comprised of many layers with gradual increases in Vs and profiles with fewer layers and significant velocity contrasts. Without exploring different parameterizations comprised of different numbers of layers, it is not possible to fully capture the non-uniqueness associated with the inverse problem and the resulting variability in site response estimates.

Chapter 3 outlined a systematic procedure to investigate potential inversion parameterizations, each with a unique number of layers defined by a specific layering ratio. This procedure aids in avoiding blatantly under- and over-constrained parameterizations. However, even when this procedure is used, it is possible to have multiple inversion parameterizations that are adequately constrained, yet produce significantly different Vs profiles. In such cases, it may be difficult to decide which Vs

profiles best represent the "true" subsurface layering without a-priori information, and the overall influence of this non-uniqueness on site response is of interest.

The present study expands on the results presented in Chapter 3. Specifically, linear-elastic and equivalent-linear site response analyses using both low- and high-intensity input ground motions have been performed on Vs profiles from the semi-synthetic blind-study site inverted in Chapter 3. Vs profiles considered include those that were developed from under-, over-, and adequately-constrained inversion parameterizations. Additionally, commonly-used strategies of accounting for Vs profile uncertainty and its influence on the predicted site response are considered. These commonly-used strategies of accounting for Vs uncertainty include upper/lower range base-case Vs profiles meant to account for epistemic uncertainty and statistically-based, randomly generated Vs profiles meant to account for aleatory variability.

With regards to surface wave testing, epistemic uncertainty represents data uncertainty and/or lack of scientific knowledge regarding mode interpretations and which processing and inversion algorithms are "best", while aleatory variability reflects the vertical and horizontal spatial variability of Vs across the site, which also contributes to data uncertainty. While the uncertainty associated with the inversion itself is purely epistemic, the data used as input into the inversion (i.e., the experimental dispersion data) is influenced by both aleatory variability and epistemic uncertainty. Therefore, the final Vs profiles derived directly from surface wave testing are influenced by both sources of uncertainty and it would be very difficult to decouple them (Griffiths et al. 2016a). In this study, no attempt was made to do so. Consequently, any uncertainty/variability in site response performed on these Vs profiles also reflects both sources of uncertainty/variability. However, we do not claim that the surface wave dispersion approach of accounting for Vs uncertainty will encompass all sources/forms of aleatory

variability and epistemic uncertainty associated with non-unique Vs profiles used in site response. For example, if a surface wave survey is conducted over an area that is relatively small compared to the area of interest, then it cannot capture the full aleatory variability. Moreover, if an experimental dispersion curve does not extend to low enough frequencies to constrain the depth to bedrock, then the epistemic uncertainty regarding the depth to bedrock cannot be reduced and multiple base-case Vs profiles accounting for this uncertainty may be required. Nonetheless, if high quality surface wave surveys are conducted over the area of interest, it may be possible to substantially reduce site response uncertainty by only considering Vs profiles that realistically fit the site signature.

4.2 INTERPACIFIC BLIND-STUDY SITE 4

The dataset considered in this paper was originally provided to participants in the InterPACIFIC (Intercomparison of methods for site parameter and velocity profile characterization) project. While Garafalo et al. (2016a) and (2016b) document the results obtained from three InterPACIFIC blind-study sites in Europe, the results from blind-study Site 4 have not yet been published. Thus, we refer only to our own results and methodologies herein.

The experimental data for Site 4 was provided by Cecile Cornou, from ISTerre (Institut des Sciences de la Terre), Grenoble, France. The semi-synthetic experimental data was developed by first performing a surface wave inversion on experimentally-measured Rayleigh wave dispersion data from a real site. The minimum misfit ground model from this analysis was then chosen as the "true" solution profile for Site 4. The theoretical dispersion curve for this true solution profile was discretized at the frequencies corresponding to the experimentally-measured dispersion data from the real

site. Additionally, the frequency-dependent uncertainty bounds associated with the original experimentally-measured dispersion data were applied to this discretized theoretical dispersion curve. This produced a pseudo-experimental dispersion curve, with the mean value at each frequency corresponding to the theoretical Rayleigh phase velocity of the true solution Vs profile and the uncertainty bounds reflecting realistic uncertainty from actual surface wave testing. Although this curve was not measured directly, it will be referred to as the "experimental dispersion curve" for the remainder of the paper.

All participants in the project were provided with the experimental dispersion curve for Site 4 and asked to invert the data in a blind manner (i.e., no a-priori information about the site was made available). The mean experimental dispersion data provided to the blind-study participants, including +/- one standard deviation bounds, are shown in Figure 4.1a. Analysts were informed that the data represented the fundamental Rayleigh mode, eliminating the need to consider the possibility of effective or higher modes in their inversions. Each analyst was asked to submit a single "best" Vs profile, and were allowed to also submit a range of Vs profiles that accounted for Vs uncertainty if they so desired. After final submissions, a mean and +/- one standard deviation horizontal-to-vertical (H/V) spectral ratio curve (i.e. the ratio between the Fourier amplitude spectra of the horizontal and vertical components of ambient vibrations) measured at the real site and the true solution Vs profile for Site 4 were made known to the participants. The H/V curves and true solution Vs profile are shown in Figure 4.1b and Figure 4.1c, respectively. The true solution Vs profile is defined by a large velocity contrast at 56 m, which is the cause of the sharp peak in the H/V curve at 1.6 Hz.

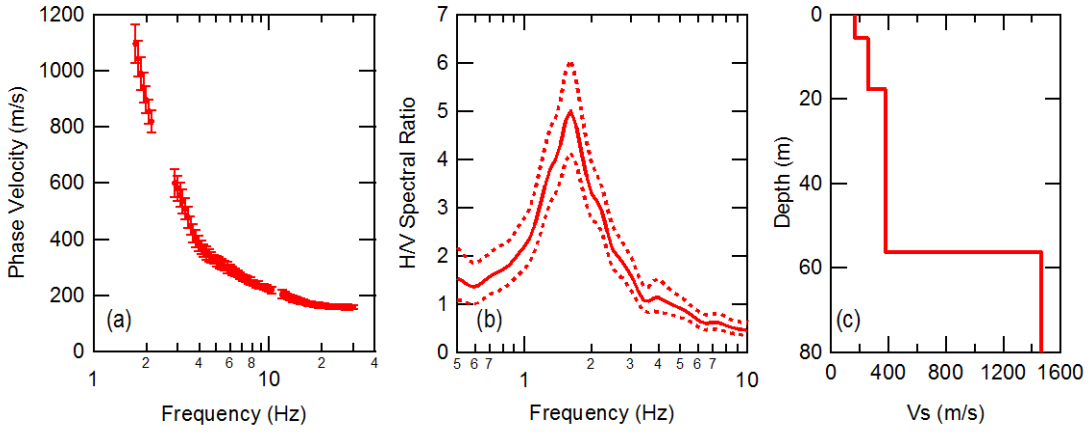

Figure 4.1: InterPacific blind-study Site 4: (a) dispersion data, (b) mean (solid line) and +/- one standard deviation (dotted lines) H/V spectral ratio curves, and (c) true solution Vs profile.

4.3 Vs Profiles Used in Site Response

Vs profiles considered in this study include: (1) 350 Vs profiles developed by performing multiple inversions, each with a unique set of layering parameters, on the blind-study Site 4 dispersion data shown in Figure 4.1a; (2) two upper/lower range Vs profiles developed by systematically increasing or decreasing the Site 4 true solution Vs profile by 20%; and (3) 100 profiles developed using the Vs randomization procedure proposed by Toro (1995). Before discussing the results of the site response analyses, it is important to provide background information on how the Vs profiles used in this study were developed. This discussion will serve as a basis for considering which Vs profiles can be considered useful for quantifying the variability in site response estimates.

4.3.1 Vs Profiles Derived from the Layering Ratio Surface Wave Inversion Technique

After receiving the experimental dispersion data for blind-study Site 4, we performed multiple inversions on the data using the layering ratio approach detailed in Chapter 3 and described briefly in the following paragraphs. Inversions were performed

using the Geopsy software (www.geopsy.org). Geopsy utilizes a neighbourhood algorithm and the misfit function detailed in Equation 1 to search for the "best" layered earth models within a predefined inversion parameter space (Wathelet et al. 2004). The theoretical dispersion forward computations for each trial earth model are based on the work originally developed by Thomson (1950) and Haskell (1953) and later modified by Dunkin (1965) and Knopoff (1964).

Seven distinct inversions were performed on the experimental dispersion data from Site 4. Each inversion utilized a unique set of parameters, where the number of trial layers was defined by a unique layering ratio (Ξ). The layering ratio represents a multiplier that systemically increases the range of possible depths to the bottom of each layer in the parameterization based on the range of possible depths to the bottom of the layer directly above it. By considering multiple layering ratios, it is possible to systematically investigate non-unique Vs profiles that could be adversely influenced by either too many or too few layers. Small layering ratios yield many thin trial layers in an inversion, while large layering ratios yield only a few thick trial layers in an inversion. Initially, six inversions were performed using layering ratios of 1.2, 1.5, 2.0, 3.0, 3.5 and 5.0. Subsequently, the inversion parameters corresponding to a layering ratio of 3.5 were deemed to be most representative of subsurface conditions and were slightly modified using engineering judgement in order to achieve an even better fit of the experimental data. This inversion is referred to as 3.5*. Approximately 200,000 layered earth models were explored during each layering ratio inversion. An ensemble of the 1,000 lowest misfit profiles was selected to represent each analysis. Of these 1,000 Vs profiles, 50 were randomly selected for use in subsequent site response analyses. The number 50 was chosen because it is manageable, from a computational standpoint, and because 50 Vs profiles chosen randomly from the population of the best 1,000 Vs profiles was found to

statistically reproduce the same median and standard deviation as the population of 1,000. The same conclusions were reached at the two sites discussed in Griffiths et al. (2016a). Thus, 350 total Vs profiles resulting from surface wave inversion were selected for site response (i.e., 50 Vs profiles from 7 unique inversions of the same dataset).

The 50 Vs profiles selected from each layering ratio inversion are shown along with their corresponding theoretical dispersion curves relative to the experimental dispersion data in Figure 4.2. The range of misfit values for the 50 theoretical dispersion curves associated with each layering ratio inversion are shown in brackets within the dispersion curve subfigures (i.e., Figures 4.2a, 4.2c, 4.2e, 4.2g, 4.2i, and 4.2k). Upon inspection, it is clear that the theoretical dispersion curves visually fit the experimental data extremely well for all layering ratios, making it difficult to distinguish individual curves. Furthermore, the maximum misfit values for each inversion are all less than 0.5, and closer to 0.25 or less on average. Thus, if only a single one of these inversions had been performed for the site, an analyst may have been inclined to believe that the resulting Vs profiles were a reasonable representation of the subsurface. However, upon inspection of the 50 Vs profiles obtained from each layering ratio inversion (i.e., Figures 4.2b, 4.2d, 4.2f, 4.2h, 4.2j, and 4.2l), one can clearly see that many of the Vs profiles do not well-represent the true solution for the subsurface stiffness profile. The closest representations were obtained using layering ratios of 3.5 and 3.5* (Figure 4.2j), and the dispersion misfit values associated with these layering ratios (Figure 4.2i) are in some cases an order of magnitude lower than those associated with higher or lower layering ratios. In the original InterPACIFIC project blind study, the profiles associated with a layering ratio of 3.5* were deemed by the authors to be the "best" representation of the subsurface (keeping in mind that we did not have the true solution profile at the time) and the median Vs profile of this ensemble was submitted as our single best Vs profile.

However, for a real site, where the true answer is unknown, and in the typical case of sparse borehole data horizontally and vertically, one may struggle to know what the "best" answer is and how to realistically account for Vs uncertainty. Thus, these results underscore some of the challenges associated with the non-unique nature of surface wave inversion. For example, Vs profiles associated with a layering ratio of 1.2 (i.e., many thin layers) show gradual increases in Vs with depth, while Vs profiles associated with a layering ratio of 5.0 (i.e., fewer thick layers) exhibit significant velocity contrasts at the wrong depths. These strong velocity contrasts (or lack thereof) are of particular interest in site response analyses. Moreover, they also play a significant role in probabilistic seismic hazard analyses (PSHA) because many ground motion prediction equations incorporate velocity horizons (e.g. depth to 1.0 and 2.5 km/s shear-wave velocity horizons, or $Z_{1.0}$ and $Z_{2.5}$, respectively). Thus, these velocity contrasts also influence the selection of input ground motions prior to the site response analyses.

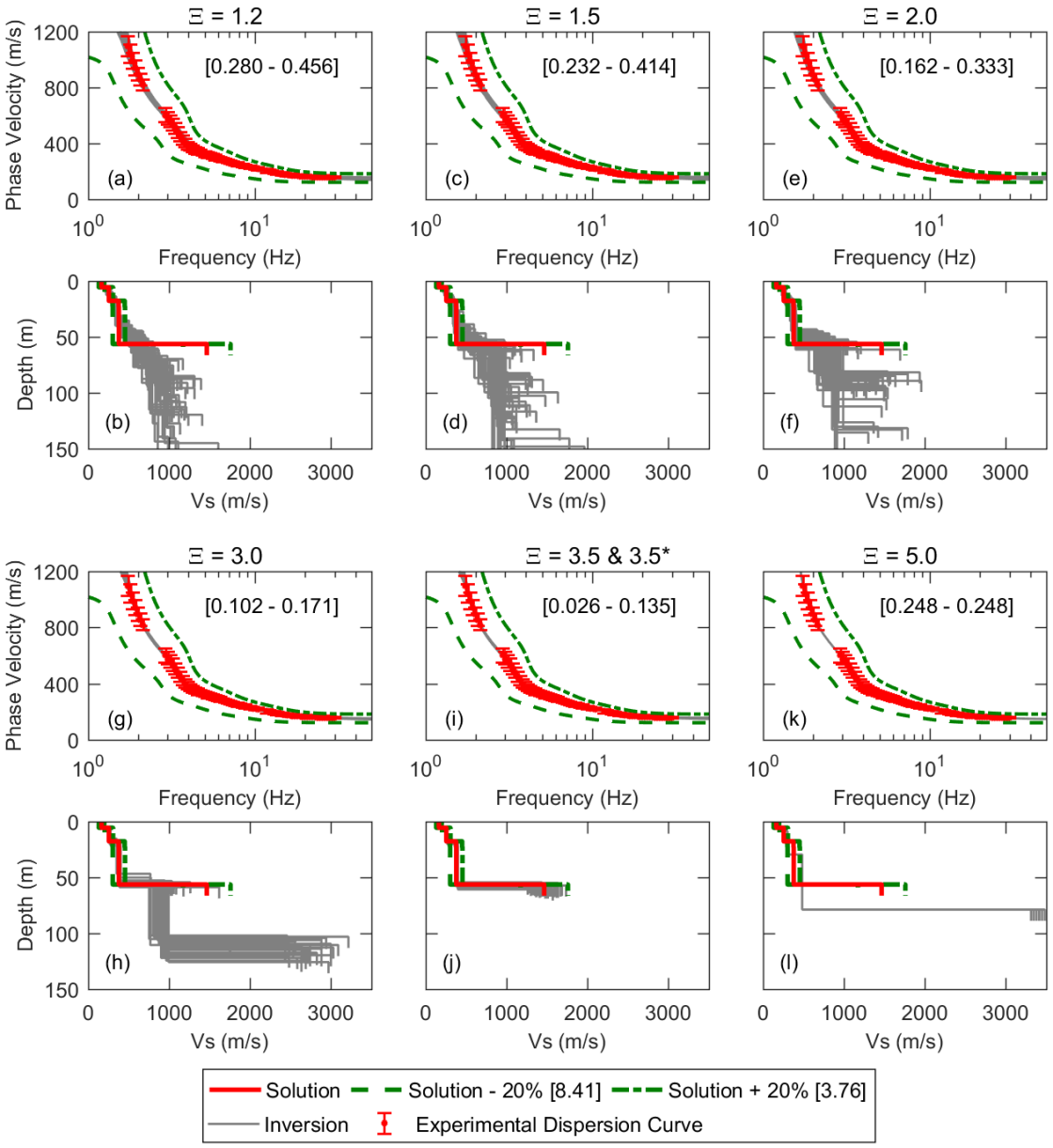

Figure 4.2: Fifty theoretical dispersion curves and 50 corresponding Vs profiles, respectively, obtained from surface wave inversions based on the following layering ratios: (a, b) 1.2, (c, d) 1.5, (e, f) 2.0, (g, h) 3.0, (i, j) 3.5 and 3.5*, and (k, l) 5.0. Note that the numbers in brackets represent dispersion misfit values. Each set of 50 Vs profiles were randomly sampled from a suite of the 1,000 lowest misfit profiles obtained from each layering ratio inversion. Also shown are the theoretical dispersion curves and the Vs profiles corresponding to the solution profile +/- 20%.

Interestingly, Chapter 3 argued that they would have discarded the results from layering ratios of 1.2 and 5.0 as not likely representative of the true subsurface profile, even without a-priori information about the site layering. This argument was based on consideration of both the dispersion misfit values and the extreme variability (or lack thereof) in the best 1,000 Vs profiles. For example, the relatively high misfit values associated with a layering ratio of 5.0 (in comparison to those achieved with a layering ratio of 3.5), the narrow range of misfit values, and the minimal variability of the Vs profiles suggest that the inversion parameterization is overly-restrictive and incorporates too few layers. Essentially, the inversion algorithm found, and settled for, the best possible solution within an overly-restrictive parameterization. Additionally, they claim that the parameters associated with a layering ratio of 1.2 are too permissive. This claim is made based on the fact that significantly better fits of the experimental dispersion data were achieved using far fewer layers (i.e., higher layering ratios) given the same number of searched trial models. Moreover, the high variability in the Vs profiles using a layering ratio of 1.2 suggests that the inversion algorithm may not have been able to find the most promising regions of such a broad parameter space and/or that too many degrees of freedom result in highly variable solutions. Thus, in some of the discussions presented below, Vs profiles derived from layering ratios of 1.2 and 5.0 will not be included when trying to realistically quantify Vs uncertainty at the site. These cases will be clearly noted. Nonetheless, in practice, it can be difficult to conclude if a parameterization is too restrictive or too broad without significant experience and/or a wealth of other subsurface data. Thus, Vs profiles from layering ratios of 1.2 and 5.0 will still be included in subsequent site response analyses as a means to determine the impact of unintentionally using poorly-parametrized models.

In order to conduct site response analyses, all profiles shown in Figure 4.2 were truncated at the first layer with a Vs exceeding 1,000 m/s. This layer, whatever the absolute velocity was, so long as it exceeded 1,000 m/s, was chosen as the half-space layer for input of ground motions (GMs). A cut-off value of 1,000 m/s whose chosen, somewhat arbitrarily but after thoughtful consideration, because it was within the bounds of NHERP Site Class B rock site conditions (i.e., 760–1500 m/s), and it would yield Vs profiles with a range of half-space velocities that encompassed the velocity of the half-space in the solution profile (i.e., about 1,500 m/s). As a result, half-space velocities for the 350 Vs profiles determined via surface wave inversion ranged from just over 1,000 m/s to greater than 3,000 m/s. Furthermore, the depths for the half-space layers ranged from less than 50 m to over 150 m.

4.3.2 Upper/Lower Range and Statistically-Based, Randomly Generated Vs Profiles

In addition to performing site response analyses on Vs profiles derived directly from a surface wave inversion, additional techniques of accounting for Vs uncertainty were considered. These techniques included the use of upper/lower range profiles to account for epistemic uncertainty and the use of statistically-based, randomly generated Vs profiles to account for aleatory variability. The development of these Vs profiles is discussed below.

For this study, the true solution was chosen as the "mean" base-case Vs profile. The "mean" base-case Vs profile was then increased and decreased by 20% to develop upper/lower range base-case profiles for use in site-response analyses. The upper/lower range profiles are shown relative to the solution Vs profile and the inversion Vs profiles in Figure 4.2. These profiles look very reasonable when considering the variability among the Vs profiles derived from the various surface wave inversion

parameterizations. In fact, one could argue that they significantly underestimate the uncertainty in Vs resulting from surface wave inversion. However, as discussed in Griffiths et al. (2016a), it is useful to compute theoretical dispersion curves for these Vs profiles and assess whether or not they match the experimental dispersion data. As shown in Figure 4.2, theoretical dispersion curves for the +/-20% profiles fall well above and well below the experimental dispersion data, with misfit values for the +/-20% profiles of 3.76 and 8.41, respectively. Thus, while the upper/lower range Vs profiles visually appear to be a much better representation of the true solution Vs profile than many of the profiles derived from surface wave inversion, their theoretical dispersion curves do not fit the experimental data nearly as well. It should be noted that in order to compute theoretical dispersion curves for these upper/lower range profiles, assumptions were made regarding Vp and mass density. In order to be consistent, we used the same assumptions utilized during inversion of the surface wave data. Namely, Vp was constrained using reasonable values for Poisson's ratio above the water table (i.e., 0.25-0.33) and by assuming a value of 1,500 m/s below the water table, unless Vs exceeded 750 m/s, at which point Poisson's ratio was again utilized to estimate Vp. While, the mass density has minimal influence on the theoretical dispersion curve (Wathelet 2004), reasonable ranges for geomaterials of various stiffness are well-established.

The Vs randomization model proposed by Toro (1995) was used in this study to investigate common methods of accounting for aleatory variability. Once again, the true solution was chosen as the baseline Vs profile about which Vs randomization would occur. The Toro (1995) model has been implemented in the software STRATA (Kottke and Rathje 2009) and operates on the following three categories of parameters: (1) the Vs statistical parameters, (2) the layering parameters, and (3) the depth to bedrock parameters. Two distinct sets of randomized Vs profiles were developed using the Toro

model in order to investigate the impact of using different sets of model parameters. Where possible, site-specific parameters were used to develop the first set of randomized Vs profiles, while default/recommended parameters corresponding to sites with a V_{S30} ranging from 180 to 360 m/s (USGS C in Table 5 of Toro (1995)) were used to develop the second set. These randomized Vs profiles are referred to for the remainder of the paper as the "site-specific Toro profiles" and the "default Toro profiles", respectively. The parameters used to generate each set are discussed below and summarized in Table 4.1.

Table 4.1: Default and site-specific Toro (1995) randomization parameters used in this study

Vs statistical parameters			Layering parameters			Depth to bedrock parameters		
	Default[A]	Site-specific		Default	Site-specific		Default[B]	Site-specific
σ_{lnVs}	0.31	0.04 to 0.22	a	1.98	2.4	base-case [m]	56	56
Δ	3.9	default	b	10.86	4.0	$\sigma_{lnZrock}$	0.33	0.33
d_0	0	default	c	-0.89	-1.15			
b	0.344	default						
ρ_0	0.99	default						
ρ_{200}	0.98	default						

A. Default for sites with a V_{S30} ranging from 180 to 360 m/s

B. No default/recommended values provided in Toro (1995). Site-specific values were used.

In order to compute site-specific Toro model parameters, a population of 250 Vs profiles was created by combining each of the sets of 50 Vs profiles developed from surface wave inversion using layering ratios of 1.5, 2.0, 3.0, 3.5 and 3.5*. As noted above, the Vs profiles derived from layering ratios of 1.2 and 5.0 were not used to develop site-specific Toro parameters because they were obtained from inversions judged to be poorly-parameterized by Chapter 3. The population of 250 Vs profiles is shown in Figure 4.3a relative to the solution profile. As noted earlier, both aleatory variability and epistemic uncertainty are inherent in this population of Vs profiles. However, the Toro

(1995) model is theoretically used solely to account for aleatory variability (EPRI 2012). Thus, one could argue that this approach improperly mixes the two types of uncertainty. However, there is certainly epistemic uncertainty associated with the Vs profiles used to develop the Toro (1995) model because epistemic uncertainty is inherent in all techniques used to measure Vs. For example, wave travel paths are often assumed to be straight lines between the source and receiver in crosshole and downhole seismic testing, yet in reality the travel paths and arrival time picks are uncertain and may be quite complex. This underscores the difficulty in perfectly decoupling aleatory variability and epistemic uncertainty. In any case, we acknowledge that in an effort to decouple some of the epistemic uncertainty, a representative base-case Vs profile could be developed for each unique layering ratio, with randomization parameters developed using only Vs profiles from that single layering ratio. This approach may be warranted and requires further study. However, given the large number of base-cases, this approach may not be palatable to many practitioners.

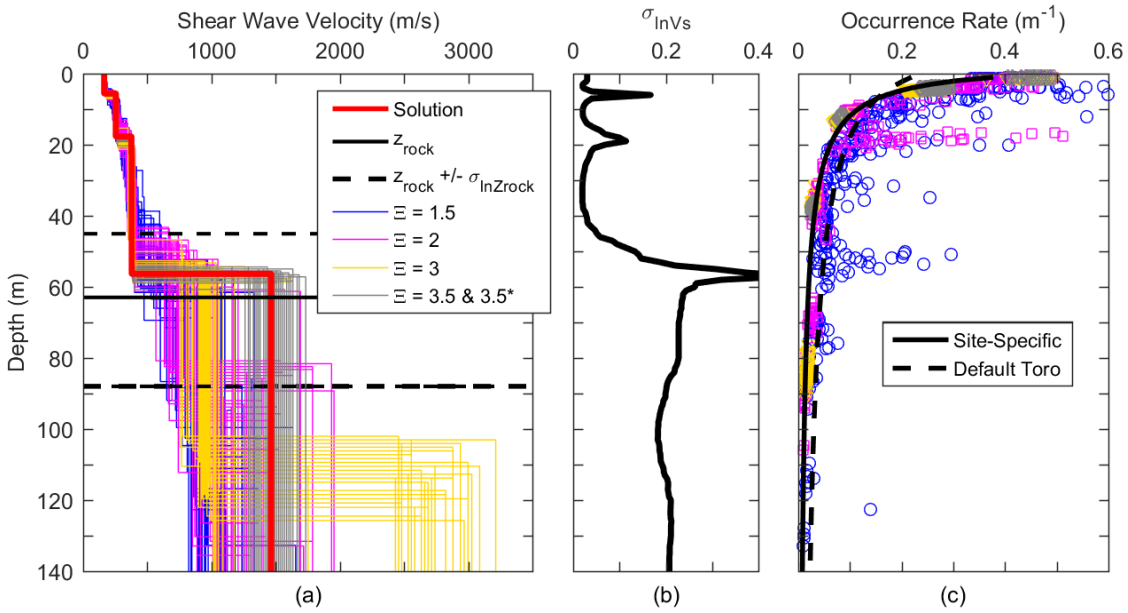

Figure 4.3: (a) Population of 250 Vs profiles derived from layering ratio surface wave inversions used to develop site-specific Toro (1995) randomization parameters. Site-specific parameters used in Toro randomization include: (a) standard deviation of the natural logarithm of the depth to bedrock, (b) standard deviation of natural logarithm of Vs as a function of depth, and (c) transition rate relationship.

The depth to bedrock in the solution profile, which corresponds to the base-case (z_{rock}), is indicated by a Vs jump from approximately 400 to 1,500 m/s at a depth of 56 m. In order to quantify the uncertainty associated with this depth, as required by the Toro (1995) model, the variable depths to bedrock associated with the Vs profiles derived from surface wave inversion were used. As mentioned above, the depth to bedrock for each Vs profile derived from surface wave inversion was determined to coincide with the first layer to exceed 1,000 m/s. These depths to bedrock were weighted by the inverse of their dispersion misfit values (i.e. the inverse of Eq. 4.1) prior to calculating the lognormal standard deviation ($\sigma_{lnZrock}$). Meaning, Vs profiles with lower dispersion misfit values were given higher weights since they were believed to more accurately represent

subsurface conditions. Note that the lognormal distribution does not perfectly match the depth to bedrock data. However, the Toro (1995) model as implemented in STRATA requires that the depth to rock be modelled with either a uniform, normal, or lognormal distribution (Kottke and Rathje 2009) and the lognormal distribution was found to be most representative with $\sigma_{lnZrock}$ = 0.33. The +/- one standard deviation values for the depth to bedrock are shown relative to the Vs profiles in Figure 4.3a. Note that there is no default/recommended depth to rock or standard deviation for depth to rock in the Toro (1995) model. Thus, these site-specific values were also used to generate the default Toro Vs profiles discussed below (refer to Table 4.1).

Vs statistical parameters for the Toro (1995) model include the depth-dependent log-normal standard deviation of Vs (σ_{lnVs}) and the inter-layer correlation parameters (Δ, d_0, b, ρ_0, and ρ_{200}). σ_{lnVs} versus depth was computed for the population of 250 Vs profiles and is shown in Figure 4.3b. Once again, for the calculation of σ_{lnVs}, each Vs profile was weighted by the inverse of its misfit value, resulting in more weight being applied to those profiles whose dispersion data best matches the experimental dispersion data. σ_{lnVs} ranges from 0.04 near the ground surface to 0.22 below approximately 60 m. It is clear that there is significantly more uncertainty involved in estimating the depth/velocity of bedrock from surface wave inversions than in estimating soil velocities. This finding has been noted by others (e.g., Cornou et al. 2009, Garafalo et al. 2016a). A robust determination of site-specific Vs inter-layer correlation parameters (Δ, d_0, b, ρ_0, and ρ_{200}) is beyond the scope of this study. Thus, recommended values were used in both the default and site-specific analyses (see Table 4.1).

Regarding the "default" σ_{lnVs} values, it should be noted that Toro (1995) provides both "generic" σ_{lnVs} based on seismic site class and "site-specific" σ_{lnVs} computed from "clusters" of Vs profiles (not to be confused with the site-specific σ_{lnVs} for Site 4 based

on Vs profiles from surface wave inversion, as discussed in the previous paragraph). Based on the most reliable "clusters" (i.e., those containing more than 10 Vs profiles), a site-specific σ_{lnVs} of 0.15 between 0 and 50 m and 0.22 at greater depths is recommended in Stewart et al. (2014). The "generic" σ_{lnVs} for sites with a V_{S30} ranging from 180 to 360 m/s is 0.31, which is significantly higher than the site-specific values. In practice, the site-specific σ_{lnVs} should be used when a site-specific Vs profile is available and geologic variability across the site is modest (Stewart et al. 2014). For this study, randomized Vs profiles were developed using both the site-specific values recommended in Stewart et al. (2014) and the generic σ_{lnVs} values, however, only the results for the generic σ_{lnVs} are shown here. Although this is not the optimum approach when a site-specific Vs profile is available, we chose to show the results associated with the generic σ_{lnVs} for two reasons. First, the Vs profiles developed using the site-specific σ_{lnVs} from Stewart et al. (2014) yielded results that were fairly similar to those obtained using the site-specific parameters that we developed using the inversion Vs profiles from Site 4. Indeed, the σ_{lnVs} in Stewart et al. (2014) and the σ_{lnVs} computed from the inversion Vs profiles at Site 4 are equal to one another below a depth of 60 m. Moreover, the generic σ_{lnVs} values are programed in STRATA, represent a more extreme case, and are commonly used.

The Toro (1995) model develops the layering for a Vs profile using a non-homogeneous Poisson process where the occurrence rate (λ_t) is a function of depth. The occurrence rate defines the distance between layer boundaries (i.e., thickness) and has units of the inverse of distance. The number of expected layer interfaces over a given depth interval decreases with occurrence rate (i.e., layer thickness generally increases with decreasing occurrence rate). Thus, occurrence rate is generally higher near the ground surface where thinner layers may be resolved, and lower at depth where layers are assumed to be thicker and the ability to resolve thin layers diminishes with most invasive

and non-invasive methods. The Toro model uses three parameters, referred to as a, b and c in STRATA (or c_3, c_1, and $-c_2$ in Toro (1995), respectively), to define the occurrence rate. A site-specific occurrence rate was developed by plotting the inverse of layer thickness versus mid-depth for all layers associated with the 250 Vs profiles in the population. The parameters a, b, and c were varied until a visually-satisfactory fit to the data was achieved. The site specific and default parameters are provided in Table 4.1, and the occurrence rates as a function of depth are plotted in Figure 4.3c. Note that the default occurrence rate is lower than the site-specific relationship near the ground surface, resulting in thicker near-surface layers for the default case. However, the default occurrence rate is higher than the site-specific relationship over most depths, resulting in thinner layers for the default case at depth.

The site-specific and default Toro model parameters were used to develop 50 random site-specific Vs profiles and 50 random default Toro Vs profiles, respectively, as shown in Figure 4.4a and 4.4c. The surficial layers are generally thinner and less variable for the site-specific Toro profiles, which is due to the higher occurrence rate and significantly lower σ_{lnVs} values used to constrain the near-surface velocities (refer to Table 4.1). The default Toro profiles exhibit significantly more variability at all depths, which stems primarily from the relatively high default σ_{lnVs}. The depth to rock in the randomized Vs profiles is quite variable in both cases, stemming from the relatively large standard deviation on the depth to bedrock that was used in the model ($\sigma_{lnZrock} = 0.33$). However, generally speaking, the median Vs profile derived from each set of 50 Toro Vs profiles matches the solution/mean base-case profile relatively well down to a depth of about 56 m, which corresponds to the depth to bedrock. Thus, while the individual Vs profiles developed from randomization can be highly erratic, on average they tend to

recover the base-case profile relatively well, particularly for the site-specific Toro profiles.

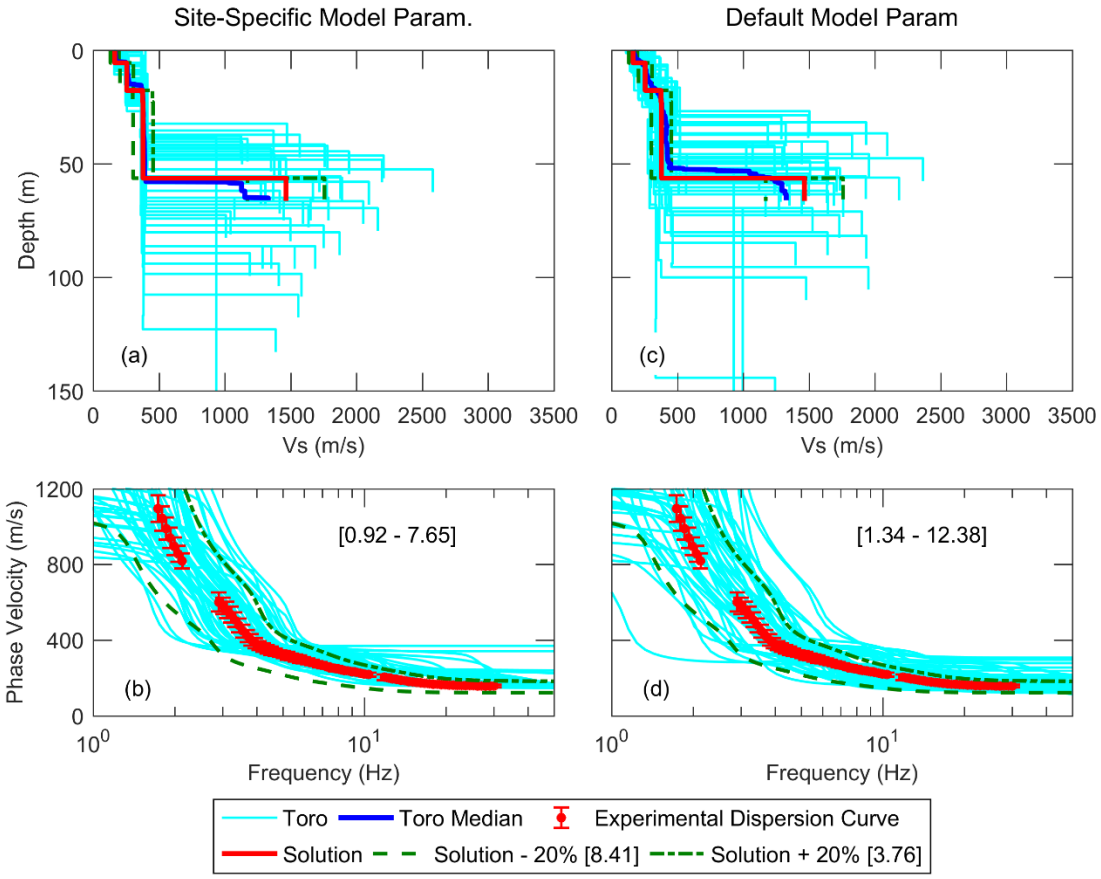

Figure 4.4: Fifty Vs profiles developed using the Toro (1995) randomization model and their corresponding theoretical dispersion curves with: (a, b) site-specific Toro model parameters and (c, d) default/recommended Toro model parameters. Note that the numbers in brackets represent dispersion misfit values. Also shown are the theoretical dispersion curves and the Vs profiles corresponding to the solution profile +/- 20%.

Theoretical dispersion curves were computed for each randomized Vs profile developed using the Toro (1995) model. Again, consistent and reasonable assumptions were made regarding Vp and mass density for these calculations. Theoretical dispersion curves for the site-specific and default Toro profiles are shown in Figures 4.4b and 4.4d,

respectively. Dispersion misfit values are shown in brackets within the figures. These misfits are generally one to two orders of magnitude greater than those associated with the profiles developed using the layering ratio surface wave inversion approach (Figure 4.2), which will be collectively referred to as the "inversion profiles" for the remainder of the paper. Most theoretical dispersion curves associated with both sets of Toro profiles would not be deemed acceptable by even the most permissive of standards, as they lie well above/below the uncertainty bounds of the experimental data. This is especially true for the dispersion curves associated with the default Toro Vs profiles, many of which are well outside the dispersion curves associated with the +/-20% profiles. Since the Toro profiles generally fall well above or below the experimental dispersion data at all frequencies, the poor misfit values cannot be attributed to a single factor such as the depth to bedrock. This poor representation of the experimental dispersion data by both the upper/lower range base-case and randomized Vs profiles is worth careful consideration when attempting to realistically quantify Vs uncertainty for site response. If the experimental dispersion data is demonstrated to be relatively constant across a site, it could be argued that Vs profiles that do not fit the data are over-estimating the aleatory variability. However, if surface wave testing has only been performed over a relatively small footprint, then this poor representation of the experimental dispersion data may be deemed acceptable, but only after careful consideration.

4.4 Linear-Elastic Transfer Functions and the H/V Peak

Similar to the experimental dispersion curve, the experimental horizontal-to-vertical (H/V) spectral ratio curve contains valuable information regarding small-strain wave propagation and site resonance. Numerous studies have demonstrated that if an H/V curve exhibits a well-defined peak, then this peak approximately coincides with the

fundamental shear wave resonant frequency of the site, although the magnitudes are poorly correlated (e.g., Lachez and Bard 1994, Lermo and Chavez-Garcia 1994). Thus, by comparing the theoretical linear-elastic shear wave transfer function for a candidate Vs profile to the experimental H/V curve, it is possible to make judgements regarding which candidate Vs profiles are appropriate for use in seismic site response analyses. While it is possible to perform a joint inversion of surface wave dispersion data and the peak frequency of the H/V curve in Geopsy (Wood et al. 2014, Bonnefoy-Claudet et al. 2006), we were not able to do this at blind-study Site 4 because the H/V data was not initially provided to participants. However, it is valuable to consider how the experimental H/V curve coincidentally compares with the linear elastic transfer functions for the Vs profiles under consideration.

Figures 4.5a though 4.5f show the linear-elastic transfer functions for the Vs profiles obtained using each layering ratio in comparison to the experimental H/V curve for Site 4. In order to calculate the transfer functions, small-strain damping values for each layer were assigned using the Darendeli (2001) modulus reduction and damping curve relationships. It can be seen that the fundamental resonant frequency obtained from the transfer functions coincides with the H/V peak at 1.6 Hz for almost all Vs profiles determined from surface wave inversions, including those from the presumably poorly-parameterized layering ratios of 1.2 and 5.0. While there are a few outliers for a layering ratio of 1.5, the majority of profiles have a resonant frequency between approximately 1.5 and 1.7 Hz. Despite the fact that the resonant frequencies are similar for all inversion profiles, the transfer function amplitudes at this frequency vary considerably, with Fourier amplitude ratios ranging from less than 4 to greater than 10. This variability in amplitude is primarily due to the impedance contrast between bedrock and the overlying soil layers. Profiles with higher impedance contrasts, such as those corresponding to

layering ratios of 3.0 and 5.0 (refer to Figure 4.2), have higher transfer function amplitudes. This underscores the epistemic uncertainty regarding the Vs of bedrock, which can be difficult to determine using surface wave methods (Garofalo et al. 2016).

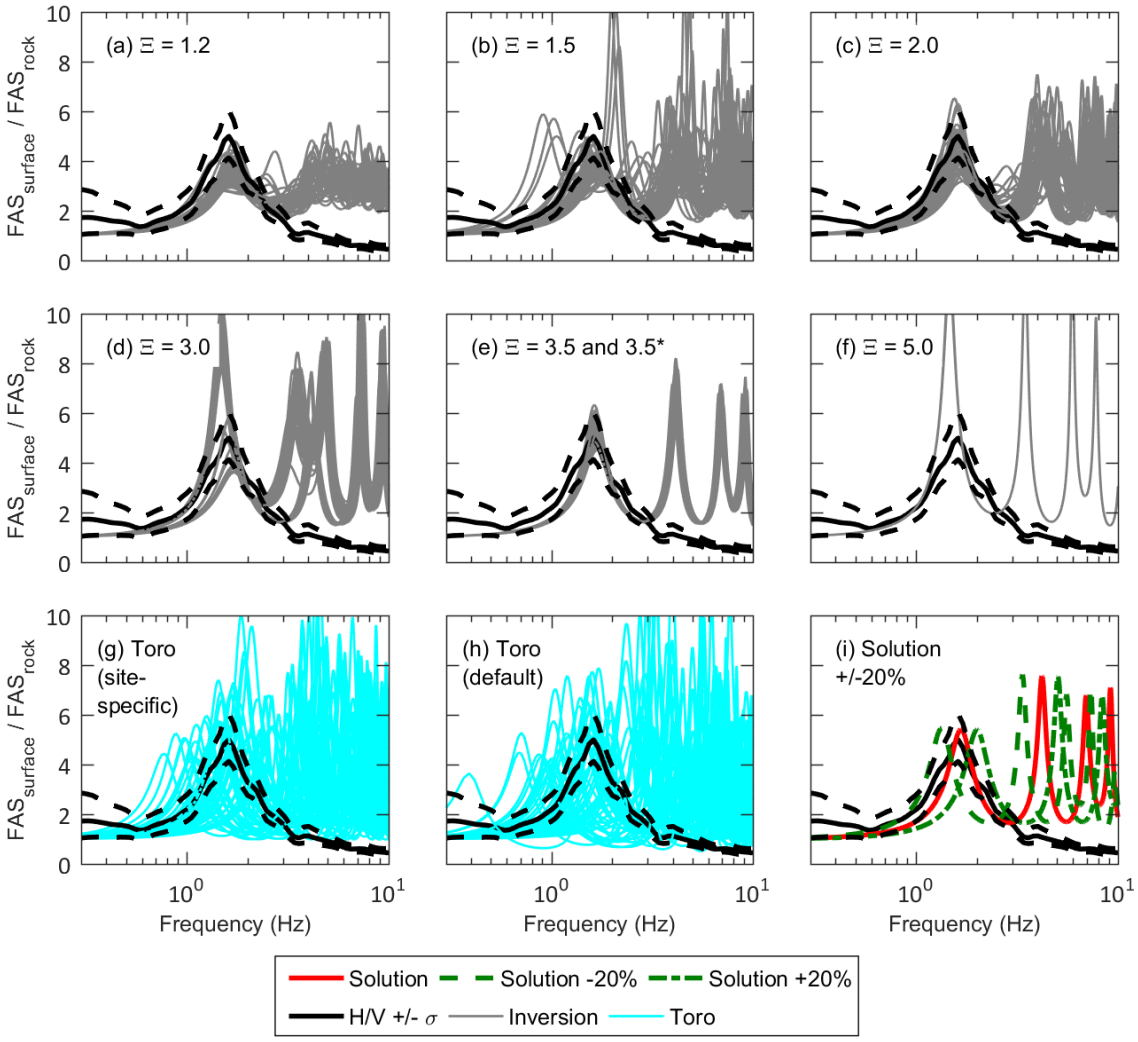

Figure 4.5: Linear-elastic transfer functions corresponding to Vs profiles obtained using surface wave inversion layering ratios of (a) 1.2, (b) 1.5, (c) 2.0, (d) 3.0, (e) 3.5 and 3.5*, and (f) 5.0. Also shown are transfer functions for Vs profiles obtained using (g) the site-specific Toro (1995) randomization model; (h) the default Toro (1995) randomization model; and (i) the solution +/-20%.

The transfer functions for Vs profiles derived from the Toro randomization model exhibit significantly more variability with regards to the resonant frequency (refer to Figures 4.5g and 4.5h). While the resonant frequencies match the H/V peak for a number of the randomized Vs profiles, many do not. Half of the site-specific Toro profiles have a resonant frequency lower than 1.3 or greater than 2.0. Resonant frequencies are generally lower for the default Toro profiles, with half falling below 1.1 or above 1.8. If the fundamental shear wave resonant frequency of the site is expected to exhibit significant variability, then the variability exhibited by the Toro profiles in Figures 4.5g and 4.5h may be deemed to reasonably represent aleatory variability. However, if H/V measurements across the site indicate that the fundamental frequency is relatively constant, then it is worth considering whether the variability seen in Figures 4.5g and 4.5h is excessive. If this is deemed to be the case, then the Toro (1995) randomization can be repeated with a rejection criteria that automatically eliminates Vs profiles whose fundamental frequency is deemed to be too high or too low. It is worth noting that one or more three-component seismometers can quickly be deployed in a grid pattern to obtain H/V measurements over a large footprint. Thus, the H/V technique provides an efficient means of inferring the variability of the fundamental shear wave resonant frequency (assuming that the H/V curve exhibits a well-defined peak). The resonant frequencies for the +/- 20% Vs profiles (refer to Figure 4.5i) are 1.34 and 2.00 Hz, respectively, for the softer and stiffer Vs profiles.

4.5 EQUIVALENT LINEAR SITE RESPONSE ANALYSES

Both low- and high-intensity equivalent-linear site response analyses were performed on the candidate Vs profiles, including: (1) the solution Vs profile, 350 Vs profiles derived from surface wave inversion, (2) the two upper/lower range Vs profiles,

and (3) the 100 Vs profiles statistically derived using the Toro (1995) randomization procedure. The Boore and Atkinson (2008) ground motion prediction equation (GMPE) was used to develop a target spectrum for the selection of reasonably consistent input rock ground motions. The target was computed using the following assumptions: a moment magnitude (M_W) of 7.5, a Joyner-Boore distance (R_{JB}) of 15 km, and an average Vs in the top 30 m (V_{S30}) of 1300 m/s, which is the upper limit for this GMPE. A V_{S30} value of 1300 m/s was chosen for the target spectrum because the majority of the bedrock velocities for the candidate Vs profiles ranged from approximately 1,000 to 2,000 m/s (refer to Figures 4.2 and 4.4). While some profiles approached or exceeded 3,000 m/s, these bedrock velocities were less frequent. After developing a target spectrum, the PEER NGA-West2 database (Ancheta et al. 2015) was used to develop a library of 40 ground motions with MW between 6.2 and 7.6, R_{JB} between 1.8 and 65 km, and V_{S30} between 770 and 2,000 m/s. The SigmaSpectra software (Kottke and Rathje 2008, Kottke and Rathje 2012) was used to select and scale eight ground motions that, on average, matched the shape and amplitude of the target response spectrum. No conditions were imposed upon the variability of the selected ground motions (i.e., the motions were not scaled to match a target standard deviation).

In order to study the influence of earthquake intensity, the input ground motions were subsequently re-scaled to achieve average peak ground accelerations (PGA) of 0.05 and 0.30 g. Analyses performed using these re-scaled GMs are referred to, respectively, as the "low-intensity" and "high-intensity" site response analyses for the remainder of the paper. Note that in practice, different target spectra and input ground motions would be used for the low- and high-intensity site response analyses because spectral amplitudes do not necessarily scale linearly. However, the objective of this study is to assess differences in site response resulting from differences in the input Vs profile.

Thus, the same GMs were used for consistency and simplicity. Also note that no attempts were made to variably-scale the input ground motions in order to account for significant differences in the bedrock impedance ratio for some of the Vs profiles (e.g., Figure 4.2l). Rather, all Vs profiles, regardless of bedrock Vs, were subject to the same suites of low- and high-intensity GMs. While not ideal, all Vs profiles had bedrock Vs consistent with fairly competent rock conditions and it would have been challenging to rescale GMs to account for specific bedrock velocity contrast in so many candidate profiles.

Equivalent-linear site-response analyses were performed using Matlab codes developed at the University of Texas (George Zalachoris, personal communication, 2014). These codes allowed the analyses to run in batch mode, looping through sets of candidate Vs profiles using eight GMs per profile. The Matlab code included auto-discretization of the layered earth model, which subdivided the major layers in the Vs profiles into sub layers so that numerical filtering below 50 Hz would not be problematic. The code has been verified in the past (Griffiths et al. 2016b) by comparing amplification factors and pseudo-acceleration response spectra with those computed using DEEPSOIL v5.1 (Hashash et al. 2012 [43]). The non-linear properties of each soil layer were set using the depth/confining pressure-dependent normalized modulus reduction (G/G_{max}) and damping (D) relationships proposed by Darendeli (2001). For ease and consistency, all layers were assumed to be non-plastic (PI = 0) and normally-consolidated (OCR = 1).

4.5.1 Low-Intensity Input Ground Motions

A median pseudo-acceleration response spectrum (simply referred to as a response spectrum hereafter) was computed for each candidate Vs profile using the eight individual response spectra resulting from the eight input ground motions. The median response spectra for all Vs profiles subjected to the low intensity input ground motions

(0.05 g average PGA) are shown in Figure 4.6. For the inversion Vs profiles (Figures 4.6a through 4.6f), most response spectra are in good agreement with the response spectrum of the true solution profile. Vs profiles associated with a layering ratio of 3.5 and 3.5* not only have the lowest dispersion misfit values (0.026 to 0.135; refer to Figure 4.2), but their response spectra also best match the response spectrum of the solution Vs profile, suggesting that relatively low dispersion misfit values are correlated with accurate site response predictions. However, it is also clear that the relationship between dispersion misfit and accuracy of site response is not perfect. While the Vs profiles associated with a layering ratio of 3.0 have relatively low dispersion misfit values (0.10 to 0.17), the associated response spectra overestimate the spectral acceleration (SA) by as much as 85 percent at a period of 0.35 s. This is due to the large impedance contrast between the bedrock and the overlying soil layers (see Figure 4.2h). On the other hand, the Vs profiles for a layering ratio of 1.2 were found to be under-constrained with relatively high dispersion misfit values (0.28 to 0.46), yet their response spectra better match the solution. Similarly, Vs profiles for a layering ratio of 5.0 were found to be over-constrained with relatively high misfit values (0.25), yet their SAs better match the solution than those for a layering ratio of 3.0. This indicates that while dispersion misfit may be useful for making relative judgements of the quality of Vs profiles resulting from inversion, it should not be used as the only basis for selecting candidate Vs profiles for site response. The shear wave velocity of the bedrock layer should also be carefully considered and constrained, if possible, by geology and/or other information (e.g., borehole Vs measurements).

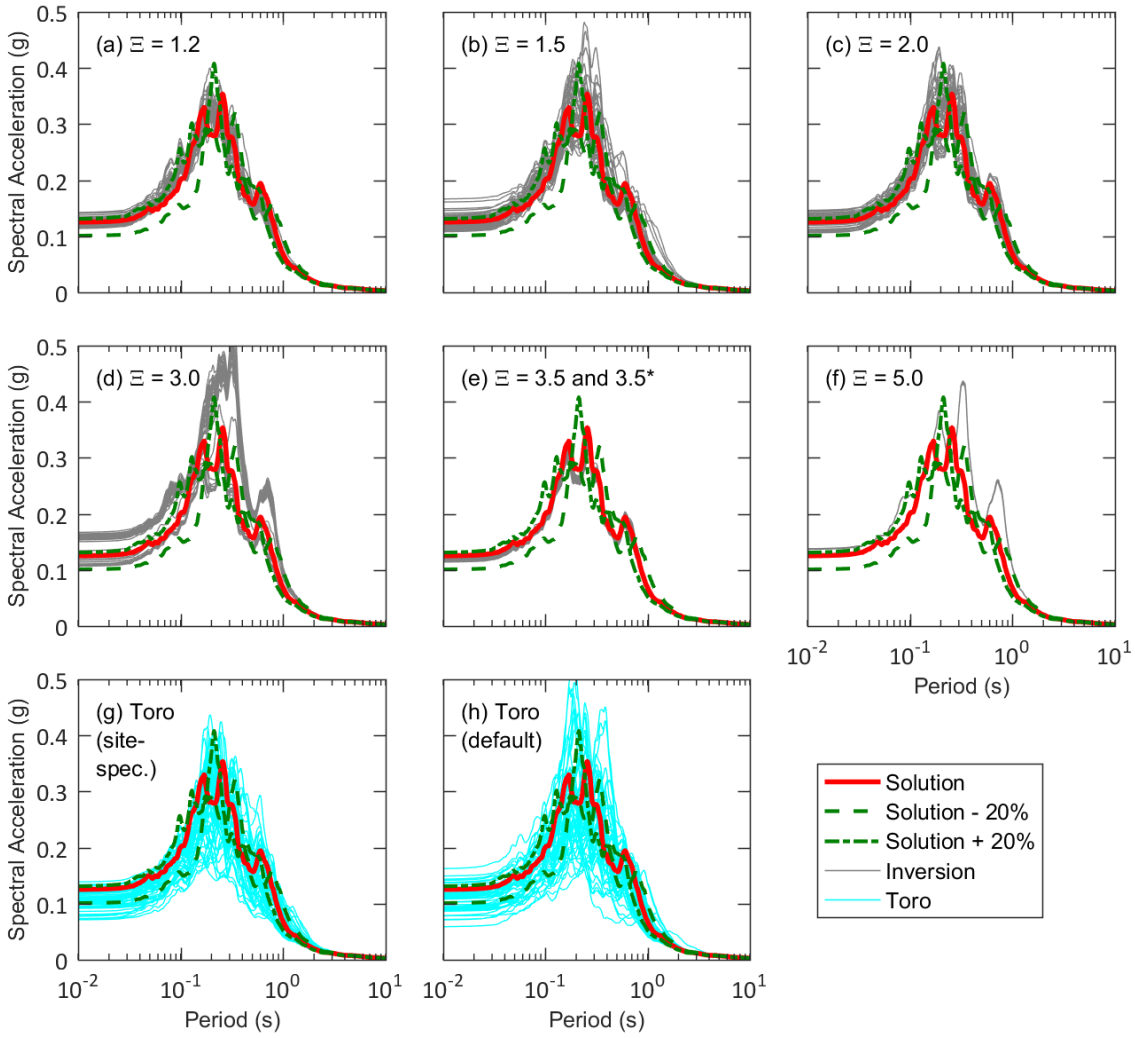

Figure 4.6: Median response spectra obtained from low-intensity equivalent-linear site response analyses using a suite of eight low-intensity input ground motions scaled to an average PGA of 0.05 g and Vs profiles from layering ratios of: (a) 1.2, (b) 1.5, (c) 2.0, (d) 3.0, (e) 3.5 and 3.5*, and (f) 5.0; and those from the Toro (1995) randomization model with: (g) the site-specific parameters, and (h) default parameters. The response spectra for the solution Vs profile and the solution Vs profile +/-20% are shown in all sub-plots for comparison.

The median response spectra for the +20% Vs profile is generally in good agreement with the solution (refer to Figure 4.6), however, it does over-predict SA by about 40% at 0.21 s. The -20% profile under-predicts the SA by about 20 to 40% at periods ranging from 0.01 to 0.17 s, but is in good agreement at longer periods. The fact that the +20% Vs profile is in better agreement with the solution than the -20% profile underscores the influence of soil nonlinearity, even for relatively low-intensity input GMs.

Similar to the linear elastic transfer functions, the response spectra associated with the Toro profiles (Figures 4.6g and 4.6h) exhibit significantly more variability than those associated with the inversion or +/-20% profiles. The response spectra associated with the Toro profiles generally under-estimate SA. While this under-prediction is more pronounced for the default Toro profiles than for the site-specific Toro profiles, it is quite significant in both cases. As stated previously, the theoretical dispersion data for the Toro profiles poorly matches the experimental dispersion data (with misfits ranging from 0.92 to 15) and the fundamental resonant frequencies generally do not match the experimental H/V peak. Thus, while the relationship between dispersion misfit and accuracy in site response prediction is not perfect, these results suggest that high dispersion misfit values are correlated with poor prediction of site response. Accordingly, if a site signature is robustly determined via surface wave surveys and H/V measurements over the area of interest, and if the candidate Vs profiles fail to capture this site signature, it is worth questioning their use for quantifying uncertainty associated with the site response predictions.

4.5.2 High-Intensity Input Ground Motions

The median response spectra for all Vs profiles based on the high-intensity input ground motions (0.30 g average PGA) are shown in Figure 4.7. The response spectra for the inversion Vs profiles are shown in Figures 4.7a through 4.7f. It can be seen that the response spectra for layering ratios of 2.0, 3.0, 3.5, 3.5*, and 5.0 all match the response spectrum from the solution profile relatively well. Again, the response spectra for layering ratios of 3.5 and 3.5*, which have the lowest dispersion misfit values, best match the solution. Interestingly, a good match of the solution response spectrum based on the low-intensity ground motions does not necessarily result in an equally good agreement with the solution response spectrum for the high-intensity GMs. For example, the response spectra for layering ratios of 1.2 and 1.5 over-predict the solution SA for the high-intensity GMs, but reasonably predict the solution SA for the low-intensity GMs. Conversely, the response spectra for a layering ratio of 3.0 is in much better agreement with the solution for the high-intensity GMs. These differences are caused by the non-linear soil behavior induced by the high-intensity GMs. Specifically, the inversion Vs profiles with less significant velocity contrasts layer-to-layer (i.e., layering ratios 1.2 and 1.5) do not generate as high of shear strains at layer interfaces. Thus, more energy gets through to the ground surface and their SAs are, on average, significantly higher than for the solution Vs profile, which contains a significant impedance contrast. The exact opposite is true for all inversion Vs profiles with more significant velocity contrasts (i.e., layering ratios of 2.0, 3.0, 3.5 and 5.0). Meaning, high shear strains and significant soil nonlinearity occur at the layer boundaries where large impedance contrasts exist, limiting the amount of energy that arrives at the ground surface. Regardless, all of the inversion Vs profiles yield significantly less variability in SA than the upper/lower range profiles and the randomized profiles. When comparing the results from Figure 4.6 and Figure 4.7,

it is evident that the under- and over-prediction associated with the +/-20% Vs profiles is much more significant for the high-intensity GMs. The same is also true for the Toro Vs profiles, particularly those developed using the default parameters.

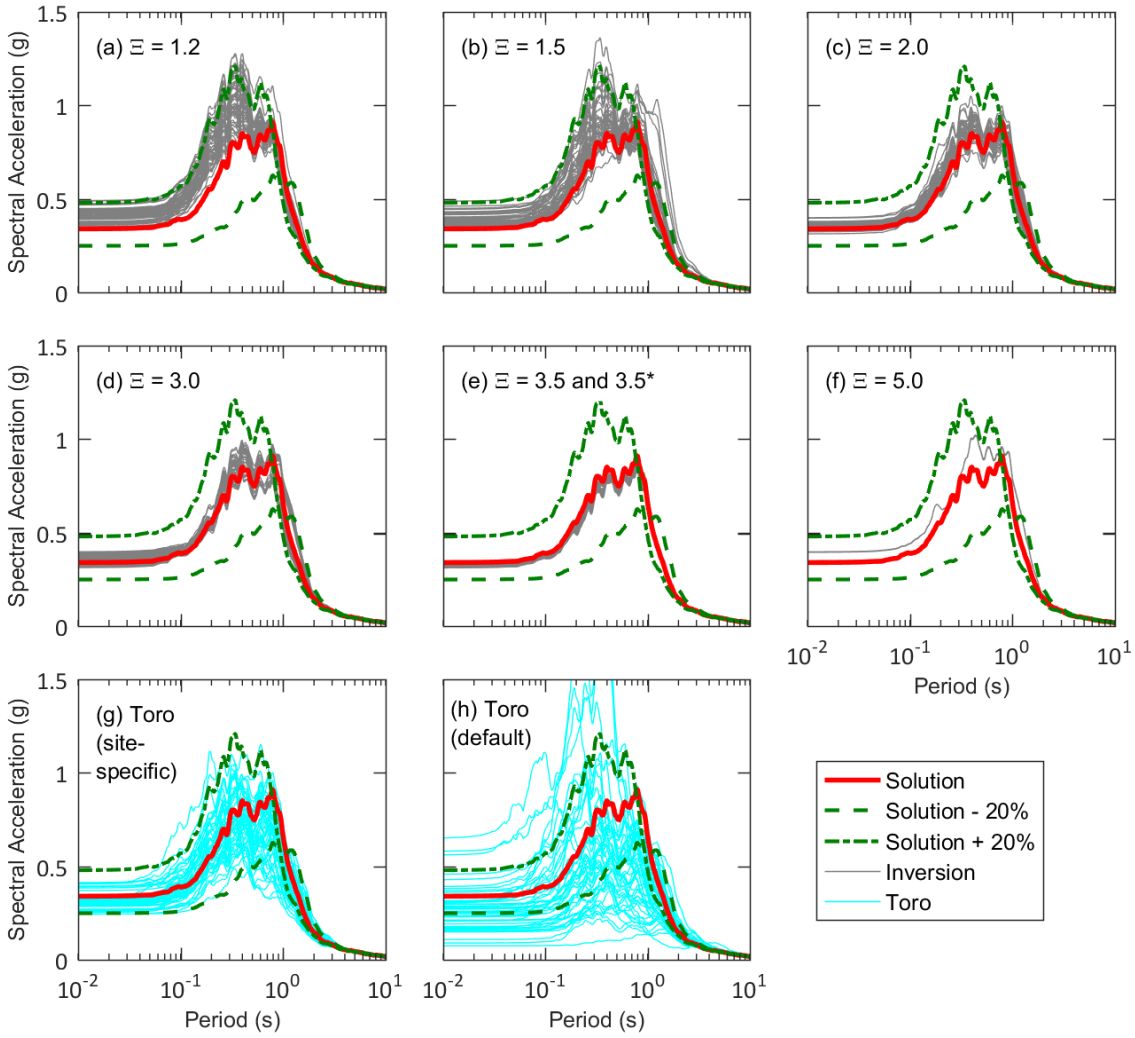

Figure 4.7: Median response spectra obtained from high-intensity equivalent-linear site response analyses using a suite of eight high-intensity input ground motions scaled to an average PGA of 0.3 g and Vs profiles from layering ratios of: (a) 1.2, (b) 1.5, (c) 2.0, (d) 3.0, (e) 3.5 and 3.5*, and (f) 5; and those from the Toro (1995) randomization model with: (g) the site-specific parameters, and (h) default parameters. The response spectra for the solution Vs profile and the solution Vs profile +/-20% are shown in all sub-plots for comparison.

Figure 4.8 shows the median response spectra for each set of 50 inversion Vs profiles and each set of 50 Toro Vs profiles (i.e., the median of medians for each set) along with those for the +/-20% Vs profiles and solution Vs profile subject to high-intensity GMs. It can be seen that response spectra for the +/-20% Vs profiles significantly over/under-predict SA across most periods, with maximum errors up to 60% between periods of 0.2 and 0.3 s. The Toro Vs profiles also result in poor site response estimates for high-intensity GMs, generally under predicting SA at most periods. The default Toro profiles exhibit greater error (20%-50% at periods < 1.0 s) than the site-specific profiles (maximum errors < 30%). As noted earlier, the default Toro profiles were developed using the generic σ_{lnVs} values provided in Toro (1995). Although not shown here, it should be noted that when the site-specific σ_{lnVs} recommended in Stewart et al. (2014) is used, the results are quite similar to those obtained using the randomization parameters that we developed for this particular site using the Vs profiles derived from surface wave inversions (referred to throughout the paper as the "site-specific Toro profiles"). Thus, we further the recommendation of Stewart et al. (2014) that the site-specific σ_{lnVs} values be used in lieu of the generic values when lateral variability is not expected to be significant.

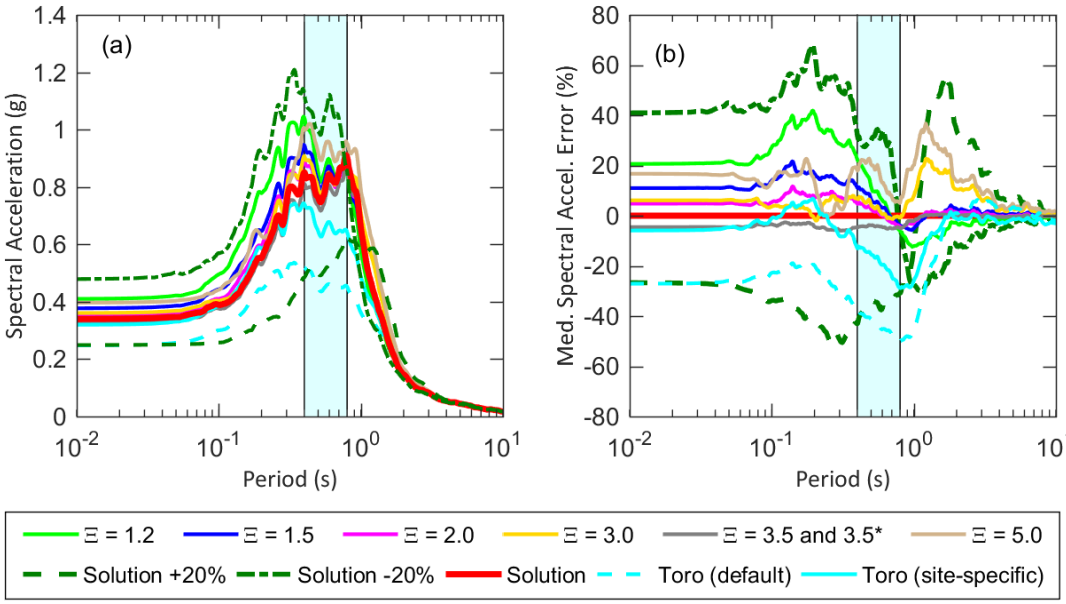

Figure 4.8: (a) Median response spectra for each set of 50 inversion Vs profiles and each set of 50 Toro Vs profiles (i.e., the median of medians for each set) along with those for the +/-20% Vs profiles and solution Vs profile subject to a suite of eight high-intensity input ground motions scaled to a PGA of 0.3g, and (b) Percent spectral acceleration error with respect to the response spectrum for the solution profile. Shaded region indicates the softened predominant period range of the solution Vs profile.

For both suites of Toro profiles the under predictions of SA are greatest at the softened natural period of the site, where site response estimates are critical. It is worth noting that, because the softened natural site period varies considerably for the site-specific and default Toro profiles, the site periods for individual response spectra are essentially smoothed-out and not well represented by the median response spectrum. This suggests that it may be best to consider individual response spectra from each suite rather than a statistical representation (e.g., the median or mean) of the suite. Nonetheless, it is clear from Figures 4.7g and 4.7h that the majority of individual response spectra underestimate the SA associated with the site period. Thus, the under-prediction shown in Figure 4.8 cannot be attributed solely to smoothing/averaging.

Remarkably, the visually-variable Vs profiles determined directly from inversion have SA values, on average, that are very similar to the solution Vs profile. Indeed, if the results from layering ratios of 1.2 and 5.0 are neglected due to poor parameterization (refer to discussion above), the remaining surface wave inversion results rarely deviate by more than 10% from the solution.

4.6 DISCUSSION

Although not perfect, there appears to be a relationship between how well the theoretical dispersion data for a Vs profile matches the experimental data and how well the associated response spectrum matches the response spectrum of the solution profile. In order to further investigate this topic, it is desirable to utilize a single parameter that quantifies how well or how poorly a response spectrum matches the solution response spectrum. A root-mean-square-error (RMSE) was computed for this purpose. The RMSE was computed as shown in Equation 2, where SA_i is the spectral acceleration associated with a given profile at period i, $SA_{solution,i}$ is the spectral acceleration associated with the solution profile at period i, and Np is the number of discrete periods in the response spectra. In this study, all response spectra had 512 periods equally spaced on a logarithmic scale between 0.01 and 10 s. Note that narrower period ranges (e.g. 0.1–10 s and 0.1–1 s) were also considered and found to produce similar results.

$$RMSE = \sqrt{\frac{1}{N_p}\sum_{i=1}^{N_p}\left[\ln(SA_i) - \ln(SA_{solution,i})\right]^2} \qquad (4.2)$$

The RMSE is plotted against the dispersion misfit for the low-intensity and high-intensity input GMs in Figure 4.9. While the trends are not perfect and scatter in the data is significant, it is clear that increases in dispersion misfit are generally accompanied by increases in RMSE for both the low- and high-intensity GMs. However, there are notable

exceptions to this trend. As discussed earlier, the Vs profiles associated with a layering ratio of 3.0 result in relatively low misfit values and relatively high RMSE values for the low-intensity GMs. Conversely, there are a few site-specific Toro profiles whose RMSE values are comparable to the inversion profiles despite the fact that the misfit values are one to two orders of magnitude higher than the inversion profiles. Nonetheless, the dispersion misfit is generally a good indicator of the accuracy of the predicted site response at this particular site.

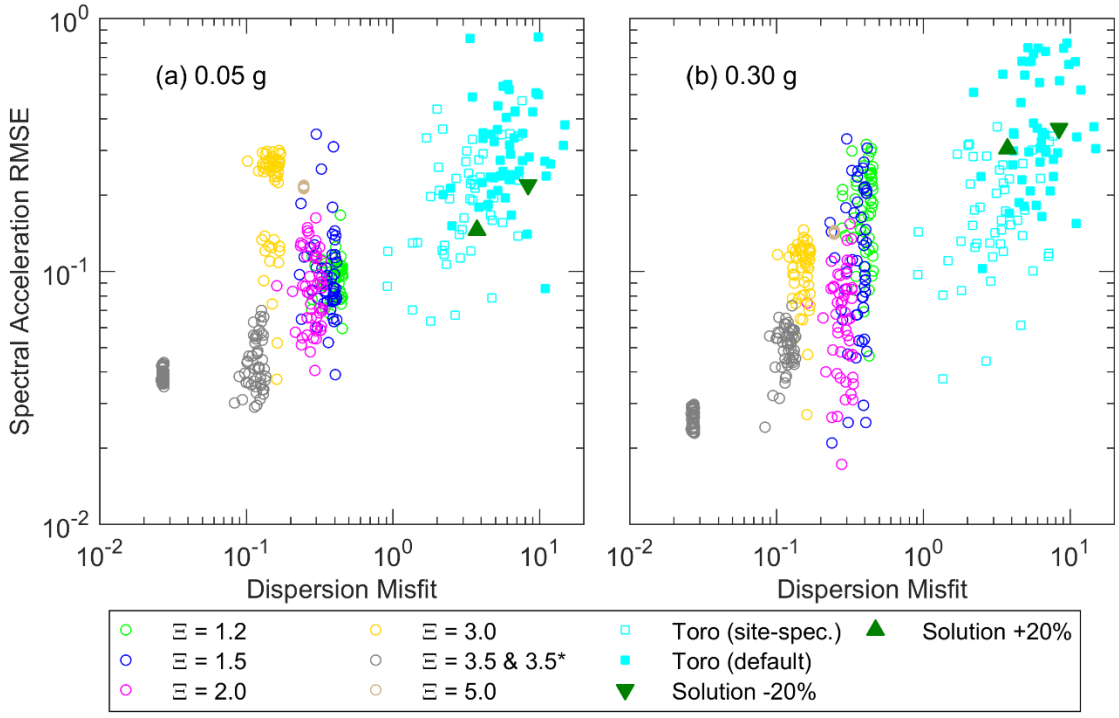

Figure 4.9: Spectral acceleration RMSE versus dispersion misfit for all Vs profiles considered. Response spectra were calculated using input ground motions scaled to an average PGA of (a) 0.05 g (i.e., low-intensity) and (b) 0.30 g (i.e., high-intensity). Note that the response spectrum corresponding to the solution Vs profile was used as a reference in the RMSE calculations.

As discussed previously, the differences between Vs profiles derived from a single inversion parameterization are often much smaller than the differences between Vs profiles derived from different parameterizations (refer to Figure 4.2). Hence, when limited information is known at the site (particularly at significant depths), the non-uniqueness in Vs associated with various inversion parameterizations is a concern. However, the significantly different Vs profiles utilized in this study have been shown to yield similar site response estimates in virtually all cases. In order to further investigate this matter, 250 response spectra associated with layering ratios of 1.5 through 3.5* were used to compute a single, lognormal median response spectrum with associated standard deviation (σ_{lnSA}). Results from layering ratios of 1.2 and 5.0 were excluded from this calculation due to their assumed poor-parameterizations, as discussed above. Similar to what was done for the computation of site-specific Toro parameters, each response spectrum was weighted by the inverse of the dispersion misfit, giving those profiles with a lower misfit more weight in the calculations. The same weighting system was utilized to compute a lognormal median response spectrum and associated standard deviation for the 50 Vs profiles associated with the site-specific Toro parameters and the 50 Vs profiles associated with the default Toro parameters.

The dispersion misfit-weighted lognormal median response spectra with +/- one standard deviation values are provided in Figure 4.10. The weighted response spectra obtained from the inversion Vs profiles are shown in Figure 4.10a and 4.10b for the low- and high-intensity input GMs, respectively. In both cases, the lognormal median response spectrum is almost identical to the response spectrum of the solution Vs profile. This finding is quite remarkable, given the apparent non-uniqueness in the inversion Vs profiles. Moreover, the associated standard deviations are also quite low, particularly for the high-intensity GMs. Thus, while the input profiles may vary considerably, their

associated misfit-weighted response spectra exhibit minimal variability and match that of the solution remarkably well.

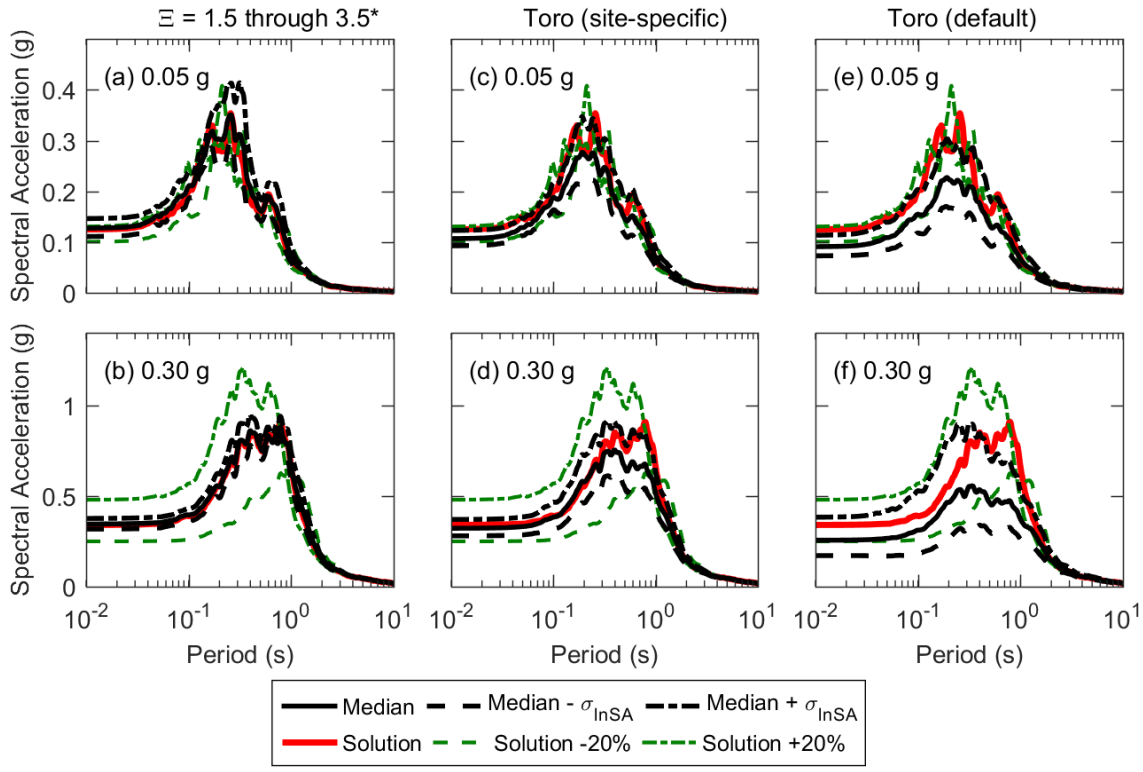

Figure 4.10: Dispersion misfit-weighted lognormal median response spectrum (solid line) with +/- one standard deviation (dashed lines) for: (a,b) the combination of 250 inversion Vs profiles from layering ratios of 1.5, 2.0, 3.0, 3.5, and 3.5*; (c,d) 50 site-specific Toro profiles; and (e,f) 50 default Toro profiles. Response spectra were obtained using both low-intensity (a,c,e) and high-intensity (b,d,f) input ground motions. The response spectra for the solution Vs profile and the +/-20% Vs profiles are shown for reference in all sub-plots.

The results corresponding to the site-specific Toro profiles are shown for the low- and high-intensity GMs in Figure 4.10c and 4.10d, respectively. For the low-intensity GMs (Figure 4.10c), the solution response spectrum generally better matches the plus-one standard deviation curve than the lognormal median. This indicates consistent under-

prediction of the true site-response. For the high-intensity GMs (Figure 4.10d), the lognormal median response spectrum for the site-specific Toro profiles matches the solution until approximately 0.30 s (i.e., the softened site period), above which the plus-one standard deviation curve better matches the solution.

As shown in Figures 4.10e and 4.10f, the lognormal median response spectrum for the default Toro profiles poorly matches the solution and significantly under-predicts SA at all periods for both the low- and high-intensity GMs. Moreover, the high-intensity plus-one standard deviation curve falls below the solution response spectrum at periods longer than 0.4 s (i.e., near the softened site period). This happens in spite of the fact that the standard deviation is quite large. Thus, the default Toro profiles yield significant variability in site response and severely under-estimate the SA in the vicinity of the predominant period. These results show similar trends to those shown in Rathje et al. (2010), who found that the median surface response spectrum decreases as more variability (i.e., increased σ_{lnVs}) is incorporated into the randomization model. Thus, while it may appear conservative to assume higher variability in the Vs randomization, the resulting site response may in fact underestimate the "true" spectral accelerations. Again, the substantial variability and resulting smoothing-out of individual site periods contributes in part to the under-prediction associated with the median response spectrum for the site-specific and default Toro profiles.

Figure 4.11 shows the dispersion misfit-weighted standard deviation of the natural logarithm of SA (σ_{lnSA}) as a function of period for both the low- and high-intensity input GMs. Note that these standard deviations correspond to the response spectra shown in Figure 4.10. The σ_{lnSA} curves associated with the low-intensity input GMs are shown in Figure 4.11a. These curves are similar for the inversion profiles and for the site-specific Toro profiles, although the σ_{lnSA} curve associated with the inversion profiles shows local

minima at periods of 0.13 and 0.53 s. The σ_{lnSA} associated with the default Toro profiles is about 0.05 to 0.1 greater than that associated with the site-specific Toro profiles. In all cases σ_{lnSA} shows similar trends in terms of shape. Specifically, σ_{lnSA} is relatively constant at periods below 0.1 s, reaches a maximum at or near the softened site period (shaded region), and decreases at periods longer than 1 s. The amplitude and shape of the σ_{lnSA} curve for the default Toro Vs profiles are in good agreement with σ_{lnSA} curves developed from weak ground motions at the La Cienga site described in Li and Assimaki (2010). Similar to the default Toro Vs profiles described in this paper, they also used generic parameters to randomize about their base case Vs profile.

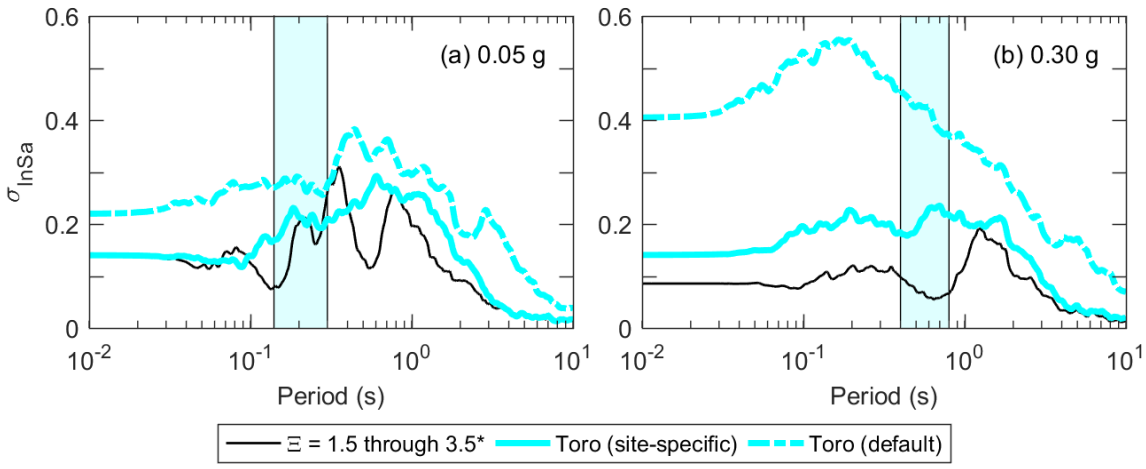

Figure 4.11: Dispersion-misfit weighted standard deviation of the natural logarithm of surface spectral acceleration associated with (a) the low-intensity input ground motions and (b) the high-intensity input ground motions. Note that the standard deviations correspond to the response spectra shown in Figure 4.10. Shaded regions indicate the softened predominant period range of the solution Vs profile.

The σ_{lnSA} curves associated with the high-intensity input GMs are shown in Figure 4.11b. For the inversion and site-specific Toro profiles, the σ_{lnSA} curves associated with the high-intensity GMs are slightly lower than for the low-intensity GMs (Figure 4.11a)

and begin to drop off at longer periods (roughly 1.5-2 s versus 0.8-1s, respectively). This shift may be due in part to the fact that the softened site period is longer for the high intensity GMs. On the other hand, the σ_{lnSA} associated with the default Toro Vs profiles is substantially higher for the high-intensity GMs than for the low-intensity GMs. This demonstrates that the influence of Vs profile uncertainty on the overall site response uncertainty is site and ground motion dependent and may not always follow the same trends.

It is important to note that the reference/baseline profile used to develop all Toro profiles was equal to the solution profile and represents a best case scenario. Thus, if a different, less accurate reference profile had been used then the resulting site response predictions would deviate even more from the "true" site response. Of course, this assumes that a "true" site response exists, whereas at real sites the ground response may vary over the area of interest. The use of site-specific Vs randomization parameters developed directly from a large number of surface wave Vs profiles led to significantly more accurate and less variable site response estimates. Thus, the authors strongly recommend that site-specific Vs randomization parameters be developed whenever possible. High quality surface wave testing with rigorous inversions considering multiple parameterizations can be used for this purpose. When this is not possible, the authors recommend that the site-specific variability recommended in Stewart et al. (2014) be used, unless extreme aleatory variability is expected at the site. The site response results obtained from the +/- 20 Vs profiles are even more variable than those associated with those from Vs randomization for the high-intensity input ground motions. The fact that the upper/lower range and randomized Vs profiles yield significantly different site response than the solution profile and the Vs profiles determined directly from inversion

should not be surprising given how poorly these profiles matched the experimental dispersion and H/V data.

As noted earlier, if the peak of the experimental H/V curve and dispersion data can be demonstrated to represent a consistent signature of the site, then it is worth considering if Vs profiles that fail to capture this site signature are appropriate for use in site response. The results of this paper are not meant to suggest that the Toro (1995) model is not useful for accounting for Vs uncertainty. Rather, the results suggest that analysts should be mindful about the appropriate use of this randomization model. At real sites, experimental dispersion data and H/V curves measured over a large area may vary considerably or they may be extremely consistent. For the former situation, Vs profiles developed using the Toro (1995) model may perform more favorably because the site signature itself exhibits significant variability. In either case, if sufficient measurements are conducted and a site signature can be established, then an analyst may choose to implement certain rejection criteria in the randomization process, whereby Vs profiles whose theoretical dispersion curves or fundamental frequencies deviate substantially from the site signature are rejected.

4.7 CONCLUSIONS

Variability and accuracy of site response predictions performed using shear wave velocity profiles (Vs) derived from non-unique surface wave inversions and other commonly used statistical methods of accounting for epistemic uncertainty and aleatory variability in Vs have been considered. Despite visually-significant differences in the Vs profiles derived from surface wave inversions using different layering parameterizations, so long as their theoretical dispersion data fit the experimental dispersion data well, their dispersion misfit-weighted site response results were quite accurate with minimal

variability. If a site signature can be established, then non-unique Vs profiles derived from surface wave inversion provide a means for accounting for Vs uncertainty in a rational manner, so long as they are obtained properly by systematically exploring various layering parameterizations.

Upper/lower range Vs profiles (e.g., mean +/- 20%) commonly utilized to account for epistemic uncertainty did not fit the experimental dispersion data well and were found to significantly over/under-predict spectral accelerations (SA) for high-intensity input GMs. Many statistically-based, randomly-generated Vs profiles commonly utilized to account for aleatory variability also failed to fit the experimental dispersion data or H/V curve and were found to yield inaccurate and highly-variable SA predictions, although the inclusion of site-specific Vs randomization model parameters derived from the surface wave inversion Vs profiles improved the results. While not perfect, a clear trend between dispersion misfit and error/variability in site response has been demonstrated. When attempting to realistically account for Vs uncertainty in site response, the use of Vs profiles that do not well-fit the experimentally-measured site signature (i.e., experimental dispersion data and H/V curves measured over the area of the site) should be questioned. It should be noted that at many real sites the site signature may exhibit considerable variability and the randomized and upper/lower range Vs profiles may better capture the site signature and yield more reasonable site response estimates than they did for this semi-synthetic example with lesser uncertainty/variability. The results of this paper do not suggest that analysts should not consider upper/lower range or randomized Vs profiles in site response, rather, they suggest using a more thoughtful approach when developing these profiles. If the site signature has been robustly determined, it may be possible to develop rejection criteria, whereby Vs profiles that poorly capture the site signature are not considered in subsequent site response analyses.

Chapter 5: Measured vs. Predicted Site Response at the Garner Valley Downhole Array Considering Shear Wave Velocity Uncertainty from Borehole and Surface Wave Methods

David P. Teague, Brady R. Cox, and Ellen M. Rathje

This chapter contains a journal article that has been submitted to Soil Dynamics and Earthquake Engineering for peer review. The full citation is listed below:

Teague, D. P., Cox, B. R., Rathje, E. M. (2017 submitted). "Measured vs. Predicted Site Response at the Garner Valley Downhole Array Considering Shear Wave Velocity Uncertainty from Borehole and Surface Wave Methods," Soil Dynamics and Earthquake Engineering, in review.

As first author, I was responsible for approximately 75% of the project planning, 50% of the data acquisition, 100% of the data processing, and 50% of the results interpretation.

ABSTRACT

This paper compares measured and predicted site response at the Garner Valley Downhole Array (GVDA) using a wide range of shear wave velocity (Vs) profiles developed from both borehole methods and inversion of surface wave data. Only low amplitude ground motions (GMs), resulting in approximately linear-viscoelastic site response between the downhole accelerometer (reference rock condition) and the surface accelerometers, were considered in this study. Thus, uncertainties associated with the small-strain Vs profiles used for site response predictions play a considerable role in attempting to match the recorded site response and its associated variability. Prior to our study, two borehole Vs profiles extending into rock were available for the site: one derived from seismic downhole testing and one derived from PS logging. These Vs profiles were fairly similar over the top 60 m, but varied considerably in the ultimate depth and stiffness of the underlying rock. As such, their predicted/theoretical transfer functions (TTFs) were quite different and in poor agreement with the measured/empirical transfer functions (ETFs). These differences provided motivation to collect and interpret

an extensive set of active-source and passive-wavefield surface wave measurements in an attempt to develop deep Vs profiles for the site that might be used to more accurately match the measured site response and its associated variability. Vs profiles developed from joint inversion of surface wave dispersion data and horizontal-to-vertical spectral ratio (HVSR) curves visually exhibited considerable differences, yet their predicted TTFs matched the measured ETFs quite-well, particularly at the fundamental and first-higher modes. Furthermore the experimental surface wave dispersion and HVSR data used to develop these Vs profiles is hypothesized to represent a "site signature" that provides a valuable means of assessing whether candidate Vs profiles are appropriate for use in site response analyses.

5.1 INTRODUCTION

Downhole arrays are invaluable tools in our attempts to understand and accurately model seismic site response. Ground motions (GMs) recorded at various depths within these vertical arrays are used to compute how seismic waves are amplified or attenuated as they travel from bedrock to the ground surface. Downhole array sites, such as the Kiban Kyoshin network (KiK-net) in Japan and various geotechnical arrays in the United States (e.g., https://www.strongmotioncenter.org/), are commonly utilized to study several aspects of seismic site response, such as: similarities and differences between equivalent linear and fully nonlinear analyses (e.g., Kaklamanos et al. 2013 and 2015; Zalachoris and Rathje 2015); modeling of soil non-linearity (e.g., Stewart and Kwok 2008; Kim and Hashash 2013; Regnier et al. 2013); attenuation properties of soils (e.g., Afshari and Stewart 2015; Cabas and Rodriguez-Marek 2017; Tau and Rathje 2017); and limitations of one-dimensional (1D) ground response analyses (Thompson et al. 2012; Afshari and Stewart 2015). These studies generally involve performing seismic site

response analyses using the bedrock GMs recorded at the bottom of the array as an input and comparing the predicted surface response results to those recorded at the surface.

Surface ground motions predicted from seismic site response analyses are strongly dependent on the shear wave velocity (Vs) profile used to model the small-strain shearing stiffness of subsurface materials (Bazzuro and Cornell 2004; Rathje et al. 2010; Barani et al. 2013; Griffiths et al. 2016b). Furthermore, uncertainties inherent in the modeled Vs profile lead to uncertainty in the predicted site response. However, downhole array sites are typically characterized by only a single, invasively-measured Vs profile with no estimates of uncertainty. Thus, analysts that use downhole array data are required to accept these Vs profiles as "ground truth" and/or make assumptions regarding Vs uncertainty. Current design codes highlight the importance of considering Vs uncertainty in site response analyses (e.g., ASCE 2010, AASHTO 2011). However, little guidance is provided on exactly how to do this and several approaches ranging from simplistic to complex are used in practice (Matasovic and Hashash 2012). Furthermore, many of these strategies to account for Vs uncertainty have not been robustly validated.

When considering uncertainties associated with the Vs profile and their influence on predicted site response, it is important to note that two types of uncertainty are traditionally accounted for in probabilistic seismic hazard studies. The first type, known as aleatory variability, refers to inherent randomness and is typically deemed to be primarily a function of spatial (horizontal and vertical) variability in Vs across the site. The second type, known as epistemic uncertainty, stems primarily from data uncertainty, or a lack of scientific knowledge that limits our ability to perfectly measure and model the Vs profile. Despite the difficulties that can arise in separating these two types of uncertainty (Griffiths et al. 2016a; Chapter 4), attempts are made to account for them in distinctly different ways when performing site response analyses for critical structures

such as nuclear facilities (EPRI 2012). Epistemic uncertainty is generally accounted for by considering alternative "base-case" Vs profiles. Aleatory variability is typically accounted for via Vs randomization, wherein a statistical model is used to randomly vary the properties of each base-case profile. The Toro (1995) Vs randomization model is generally used for this purpose. It is important to note that these procedures for considering aleatory variability and epistemic uncertainty are independent of the method(s) used to derive the Vs profiles. However, the technique used to obtain the Vs profile influences the uncertainties that are present and thus should be considered.

Vs profiles are generally developed using "direct"/invasive borehole methods and/or "indirect"/non-invasive surface wave methods. Griffiths et al. (2016a) provide a detailed discussion regarding how aleatory variability and epistemic uncertainty influence Vs profiles developed using these two general techniques. To summarize, borehole methods involve the direct measurement of Vs within one or more boreholes. All invasive borehole tests are influenced by epistemic uncertainties stemming from disturbances caused by drilling, challenges associated with picking wave arrival times, and assumptions regarding wave travel path. However, these uncertainties are rarely considered in a rigorous manner or communicated to the end user, despite recent studies showing that these epistemic uncertainties can be quite significant (Garofalo et al. 2016b). Furthermore, borehole methods sample over a relatively small area. Thus, it is not possible to make inferences regarding how Vs varies across a site (i.e., aleatory variability within the EPRI 2012 framework) unless multiple tests are performed across the site footprint. If multiple invasive Vs profiles are developed across a site, then statistics may be computed and used to quantify spatial variability. These statistics can then be used in randomization models. However, at many sites it is rare to have multiple

invasively-measured Vs profiles and default/assumed/recommended parameters are often used in randomization.

In contrast to borehole methods, surface wave methods do not involve the direct measurement of Vs. Rather, surface wave testing is used to indirectly derive Vs profiles using a three-step process. First, actively-generated or passively-monitored seismic signals with strong surface waves (Rayleigh or Love waves) content are measured over a relatively large area (array apertures of 10's to 100's of meters) at the ground surface. Next, these field measurements are used to compute experimental dispersion data, which relates the frequency (or wavelength) of surface waves to phase velocity. Finally, layered earth models whose forward-computed theoretical dispersion curves are consistent with this field experimental dispersion data and its associated uncertainty bounds are sought through an inversion process. The inversion process is non-unique; meaning, that many different layered earth models may result in theoretical dispersion curves that are consistent with the measured field experimental dispersion data within its uncertainty bounds. Layered earth models comprise a system of stacked, linear-elastic layers, each defined by its thickness, Vs, compression wave velocity (Vp) or Poisson's ratio, and mass density. Vs and thickness are extracted from the final layered earth model(s) and used in site response analyses. Given the relatively large area sampled by surface wave testing, the measured field data is influenced by both aleatory variability as well as data and modeling uncertainty (i.e., epistemic uncertainty), which cannot feasibly be separated and tracked through a series of complicated dispersion processing and inversion procedures (Lai et al. 2005; Foti et al. 2014; Griffiths et al. 2016a; and Chapter 4). Nonetheless, even if these two types of uncertainty cannot be perfectly decoupled, this does not mean that Vs uncertainties derived from surface wave testing cannot be considered in a meaningful manner in site response studies.

Uncertainties in Vs profiles derived from surface wave testing arise from the calculation/interpretation of experimental dispersion data and from the inversion of this data. However, two recent blind studies (Cox et al. 2014 and Garofalo et al. 2016a) indicate that the experimental dispersion data can be robustly retrieved by experienced analysts with an inter-analyst coefficient of variation (COV) of only 5% to 10% over broad frequency ranges. In fact, recent studies by Griffiths et al. (2016a and 2016b) and Chapter 4 suggest that the experimental dispersion data and horizontal-to-vertical spectral ratio (HVSR) data from a site can be used to develop a robust "site signature", which may be used not only in surface wave inversion, but also to assess the validity of any candidate Vs profiles used for site response. Thus, although ambiguities in the interpretation of experimental dispersion data can introduce uncertainty in derived Vs profiles (Foti 2000; Boaga et al. 2013; Chapter 2), the majority of Vs uncertainty stems from the inversion process and its associated non-uniqueness (DiGiulio et al. 2012, Cox et al. 2014, Garofalo et al. 2016a and 2016b, Chapters 2 and 3).

Several authors have considered the influence of inversion non-uniqueness on site response predictions (Foti et al. 2009, Boaga et al. 2011, Boaga et al. 2012, Jakka et al. 2014a, Comina and Foti 2014, Jakka et al. 2014b, Socco et al. 2012, Griffiths et al. 2016b). However, as noted in Chapter 4, these studies did not account for Vs uncertainty associated with choice of inversion parameterization (i.e., number of layers and ranges in their respective Vs, Vp, and mass densities), which can be quite significant. The inversion parameterization, particularly the number of layers used, strongly influences the smoothness and/or sharpness of the velocity contrasts and the position of layer boundaries in the resulting Vs profiles (DiGiulio et al. 2012, Chapter 3). Therefore, Chapter 4 studied the influence of variable inversion parameterizations on predicted site response at a synthetic site associated with the InterPacific Project (Garofalo et al. 2016a

and 2016b). They found that while the Vs profiles developed from various inversion parameterizations were extremely different in some cases, the site response predictions for these Vs profiles were quite similar to one another and matched the linear and equivalent-linear site response associated with the true/solution Vs profile quite well, provided that the inverted Vs profiles were consistent with the site signature. Similar to Griffiths et al. (2016a and 2016b), they also considered site response predictions associated with Vs profiles developed via randomization and upper/lower base-case Vs profiles. These Vs profiles did not match the site signature and were found to produce highly variable site response estimates that poorly matched the site response associated with the solution Vs profile.

Chapter 4 suggests that, although the non-uniqueness associated with Vs profiles developed from surface wave inversion may be quite significant, accurate estimates of site response with minimal variability can be obtained if Vs non-uniqueness is considered in a systematic manner. Furthermore, the Chapter 4 and Griffiths et al. (2016a and 2016b) suggest that existing practices of accounting for aleatory variability and epistemic uncertainty in Vs may produce inaccurate site response estimates that exhibit excessive variability. However, accuracy of site response predictions is difficult to assess at most real world sites. Hence, the desire to evaluate measured versus predicted site response at a downhole array site considering Vs uncertainty from both borehole and surface wave methods.

This study considers Vs uncertainty and its impact on seismic site response predictions at the Garner Valley Downhole Array (GVDA) Site in Southern California. First, an overview of the GVDA Site is provided and the calculation of linear-viscoelastic empirical transfer functions (ETFs) from low-amplitude GMs recorded at the site is described. Next, the linear-viscoelastic theoretical transfer functions (TTFs) for two

previously-measured invasive borehole Vs profiles at the site are provided. Randomization is performed on these borehole profiles using the Toro (1995) model and common assumptions regarding spatial variability in Vs. TTFs for each randomized Vs profile are presented. We then consider the TTFs associated with Vs profiles that were developed from inversion of an extensive surface wave dataset collected at the site. The TTFs associated with the borehole, randomized, and inversion Vs profiles are qualitatively and quantitatively compared to the measured ETFs. Finally, recommendations are proposed for utilizing the experimental site signature to help select realistic Vs profiles resulting from randomization.

5.2 GARNER VALLEY SITE DETAILS

The Garner Valley Downhole Array Site is located in a seismically-active region approximately 7 km from the San Jacinto fault and 35 km from the San Andreas fault (Archuleta et al. 1992). The site is in a shallow valley within the Peninsular Ranges Batholith (Bonilla et al. 2002). It is adjacent to Lake Hemet and is the site of extensive deposition of fine materials derived from both crystalline rocks and from dissection of older alluvial deposits (Hill 1981). Existing data indicates that soft soils are present to a depth of 19 to 25 m (Steidl et al. 1996). Beneath these soft soils, weathered granite transitions to more competent bedrock. Prior geophysical studies suggest that the depth of the contact between weathered and competent rock occurs between 65 and 90 m (Gibbs 1989 and Steller 1996). Boreholes drilled in nearby igneous rocks without sediment cover indicate a Vs of 2650 m/s below 50 m (Fletcher et al. 1990), indicating that the deeper granite is quite stiff.

The site is instrumented with downhole accelerometers at depths of 15, 22, 50, and 150 m, the deepest of which is embedded in granite bedrock. The site also has three

surface accelerometers placed in a straight line and equally spaced at approximately 61 m. Figure 5.1 shows the locations and station numbers of the surface accelerometers along with the vertical projection and station number of the 150-m deep accelerometer. For simplicity, surface accelerometers number 00, 08, and 09 will be referred to as the "North", "Central", and "South" accelerometers, respectively. Downhole accelerometer number 05, which is embedded in the competent granite at a depth of 150 m, will simply be referred to as the "rock" accelerometer.

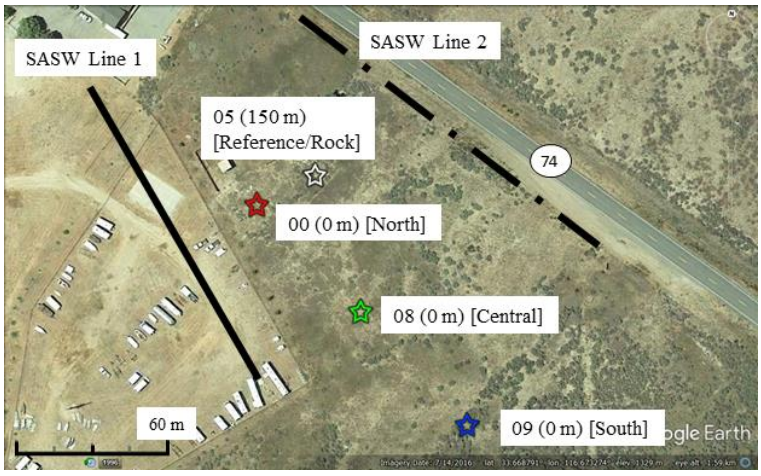

Figure 5.1: Plan view of the North (00), Central (08), and South (09) surface accelerometer locations at the GVDA site. The location of the 150-m deep borehole accelerometer (05), which penetrates granite bedrock is indicated. Also shown are the approximate extents of SASW Lines 1 and 2 from Stokoe et al. (2004).

5.3 EMPIRICAL TRANSFER FUNCTIONS

At present, the accelerometers installed at the GVDA Site have recorded approximately 7000 events with Richter Local Magnitudes (ML) ranging from 1.0 to 7.2 and distances ranging from 0.1 to 720 km (nees.ucsb.edu/data-portal). For each of these events, the "true" site response for a given component (i.e., north-south [NS], east-west

[EW], and vertical [V]) can be determined by computing the transfer function between the GM recorded at the surface and the GM recorded within rock.

At very low-strain levels, the site response is approximately linear-viscoelastic and controlled by the thickness, Vs, and small-strain damping ratio (D_{min}) of the soil layers and bedrock. As strains increase, modeling of nonlinear shear modulus and damping for each soil layer introduces additional uncertainties into site response predictions (Rathje et al. 2010, Li and Assimaki 2010). Because this study is focused on the influence of the input Vs profile, it is ideal to avoid non-linear soil behavior and the challenges associated with modeling it. Thus, low-amplitude GMs resulting in an approximately linear-viscoelastic response were sought.

Tau and Rathje (2017) studied the influence of Dmin on the predicted site response at the GVDA Site. For their study, they chose a suite of 50 GMs that produce an approximately linear soil response and calculated empirical transfer functions (ETFs) at the North accelerometer location using the 150-m deep accelerometer as a reference rock condition. For this study, we used the same GMs to compute the ETFs at the Central and South accelerometers. Note that the surface accelerometer at the South location appears to have been temporarily inactive, therefore, only 42 GMs were used at this location. The Peak Ground Accelerations (PGAs) of these GMs were on the order of 0.001 to 0.01 g, with local magnitude (ML) ranging from 3.0 to 5.1 and distance ranging from 6.6 to 133 km.

Transfer functions between the rock and surface accelerometers were computed using the same procedures documented in Tau and Rathje (2017). First, a 5th order Butterworth filter with a pass band of 1 to 40 Hz was applied to all acceleration time histories. This pass band was chosen to include frequencies where the signal-to-noise ratio (SNR) was acceptably high (i.e., greater than 3 dB). Although frequencies below 1

Hz are of interest for strong GMs, the GMs used in this study are significantly influenced by noise at lower frequencies. After filtering, acceleration time histories were integrated twice to compute displacement time histories. Each displacement time history was baseline-corrected using a 2nd order polynomial correction. The second derivative was then computed on each baseline-corrected displacement time history to retrieve a baseline-corrected acceleration time history. For a given GM and component, the "raw" ETF was computed as the ratio of the Fourier Amplitude Spectra (FAS) of the surface (North, Central, or South) and reference/rock baseline-corrected acceleration time histories. The raw ETF was then smoothed by applying a log-scale rectangular window in the frequency domain.

The median, smoothed ETFs from each surface accelerometer for both the NS and EW components are shown in Figure 5.2a. The median ETFs for all three accelerometers and both components are quite similar, particularly at the first three resonant frequencies. The fundamental ($f_{0,ETF}$), first-higher ($f_{1,ETF}$), and second-higher ($f_{2,ETF}$) modes associated with the median ETFs are approximately 2.0, 3.5, and 6.0 Hz, respectively. The median ETFs at all locations generally decrease rapidly in amplitude above 12-15 Hz. Figure 5.2b shows the individual ETFs from all three accelerometer locations for the both the NS and EW components. Also shown is the lognormal median +/- one standard deviation (σ_{lnETF}) of all individual ETFs. The σ_{lnETF} is approximately 0.30 to 0.40 in the range of 1 to 40 Hz. The median ETF and +/- σ_{lnETF} curves are subsequently used to represent the measured, small-strain site response at the GVDA site. Additionally, the mean fundamental resonant frequency ($f_{0,ETF}$) and its associated standard deviation ($\sigma_{f0,ETF}$) were computed (refer to Figure 5.2b) and are later compared to the observed peaks in the horizontal-to-vertical spectral ratio (HVSR) curves measured at the site during surface wave testing.

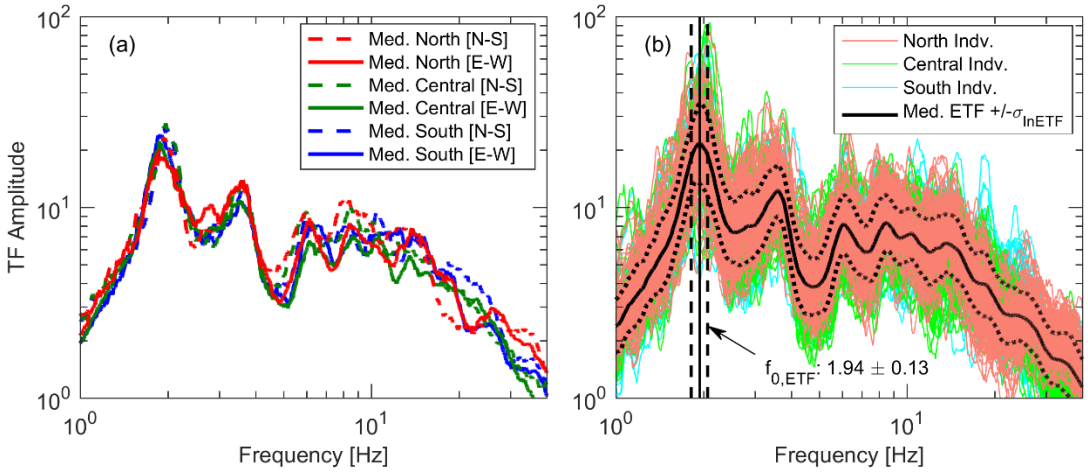

Figure 5.2: (a) Median empirical transfer functions (ETFs) associated with the north-south and east-west components of the North, Central, and South surface accelerometers at the GVDA site. (b) Individual ETFs for all locations and components along with the lognormal median and +/- one standard deviation (σ_{lnETF}) for all locations/components. Also shown in (b) is the mean fundamental resonant frequency ($f_{0,ETF}$) and its associated standard deviation ($\sigma_{f0,ETF}$).

5.4 Previously Developed Vs Profiles

Vs profiles have been previously developed at the GVDA Site using invasive borehole methods and surface wave testing. Prior invasive borehole testing includes seismic downhole (Gibbs 1989) as well as shallow and deep PS suspension logging (Steller 1996). Unfortunately, the exact locations of the downhole and PS logging at the site are not well documented. Surface wave testing was conducted using the Spectral Analysis of Surface Waves (SASW) Method (Stokoe 2004) at two locations, as shown in Figure 5.1. Additionally, passive surface wave testing was performed by Liu et al. (2000). However, they chose not to invert their experimental dispersion data and thus no Vs profile is available. Interestingly, they calculated theoretical dispersion curves for the PS log Vs profile and found that it was in good agreement with their experimental dispersion data, which ranged from approximately 2.5 to 6 Hz.

Previously developed Vs profiles at the GVDA Site are compared in Figure 5.3a. The Vs profiles are in good agreement with one another until a depth of approximately 65 m. The Vs profiles show a transition from soft soil, with a Vs of 180 to 270 m/s, to a stiffer material at depth of 18 to 25 m. This stiffer material corresponds to weathered granite and has a Vs of 500 to 660 m/s. Both the downhole and the deep PS log reach materials with Vs in excess of 1000 m/s. However, the downhole Vs profile reaches this more competent material at a depth of 65 m, while the deep PS log does not show these stiffer materials until a depth of approximately 85 m. Also, it is important to note that neither the downhole nor the PS log resolved velocities that are consistent with the nearby measurements described in Fletcher et al. (1990), which indicate that competent granite in this area may have Vs greater than 2500 m/s.

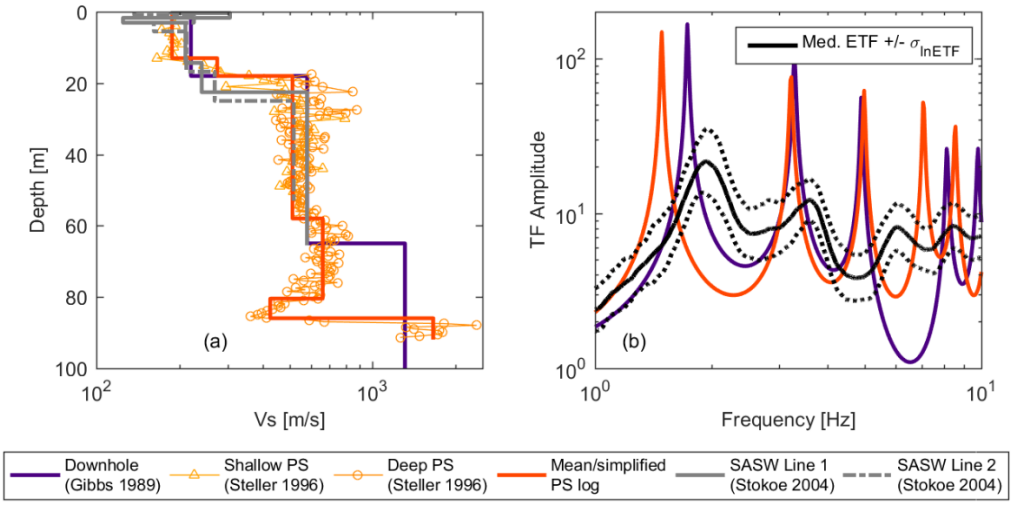

Figure 5.3: (a) Vs profiles previously developed at the GVDA site using seismic downhole testing (Gibbs 1989), shallow and deep PS suspension logging (Stellar 1996), and SASW testing (Stokoe 2004). (b) Theoretical linear viscoelastic shear wave transfer functions (TTFs) between a depth of 150 m and the ground surface were computed for the previously developed Vs profiles that extended into rock (i.e., seismic downhole and simplified PS log) using small-strain damping ratios [D_{min}] that were assigned based on the relationship proposed by Darendeli (2001). Also shown in (b) is the median ETF +/- σ_{lnETF}.

Linear-viscoelastic theoretical transfer functions (TTFs) were computed for the previously-developed borehole Vs profiles that reached bedrock. The borehole TTFs are compared to the median ETF +/- σ_{lnETF} in Figure 5.3b. In order to calculate TTFs, the bottommost layer in the borehole Vs profile was extrapolated to a depth of 150 m (i.e., the depth of the downhole accelerometer at the site). TTFs are not shown for the SASW Vs profiles because they do not reach more competent rock materials and thus do not have a reference rock condition. TTFs were calculated based on the "within" condition because they are compared to ETFs that were computed using borehole measurements. Calculations were performed using personal Matlab codes, which have been verified by comparing the results to the Strata software (Kottke and Rathje 2009). Additionally, for the purpose of computing TTFs, the shallow and deep PS logs were averaged and simplified/smoothed (refer to Figure 5.3a).

TTFs were calculated using the small strain damping values proposed in Darendeli (2001) [D_{min}] This paper is primarily focused on the influence of the input Vs profile. However, the selection of an appropriate small-strain damping ratio is not trivial. Tau and Rathje (2017) recently investigated the choice of small-strain damping ratio at this site. They found that if a single Vs profile is used in a deterministic manner to compute the TTF, then an effective in-situ small-strain damping ratio of $4 \cdot D_{min}$ is appropriate for the GVDA site. This higher small-strain damping ratio is meant to account for site-specific scattering/loss of seismic energy resulting from 3D subsurface variability that cannot be accounted for using D_{min} values measured in the laboratory in conjunction with 1D site response analyses. Alternatively, they found that this scattering could be accounted for by computing the median TTF from a suite of TTFs associated with Vs profiles developed via randomization and the lower, commonly-assumed D_{min}

values. For this paper, we consider suites of Vs profiles from randomization and/or surface wave inversion and thus chose to use the typically-assumed D_{min} values.

It is clear from Figure 5.3b that the amplitudes of the TTFs for both invasive Vs profiles are significantly higher than the median ETF, although they are only slightly higher than the amplitudes of many of the individual ETFs (Figure 5.2b). It is also clear that the locations of the resonant frequencies generally do not well represent the ETF. The fundamental mode of the TTF associated with the downhole Vs profile better matches the fundamental mode of the median ETF than the fundamental mode of the TTF associated with the PS log. Conversely, the first-higher modes are quite similar and within 0.5 Hz of the first higher mode of the median ETF. All other higher modes for both Vs profiles poorly match the higher modes of the median ETF. In a qualitative sense, neither of the TTFs match the ETFs well. Thus, one must consider that the available borehole Vs profiles do not well-represent the small-strain stiffness profile and its variability across the site.

5.5 Existing Practices of Accounting for Vs Uncertainty

Although the invasively-measured Vs profiles do not well represent the measured ETF, an ETF is generally not available at most sites and there is no way of knowing how well/poorly the TTF for a given Vs profile will capture the true site response. Furthermore, each invasively-measured Vs profile represents a single sample from a larger 3D structure and is influenced by epistemic uncertainties. Thus, it is worth investigating if existing practices of accounting for spatial variations in Vs and epistemic uncertainty can be used to develop Vs profiles that yield better site response estimates. In order to investigate existing practices of accounting for aleatory/spatial variability, Vs randomization was performed about two base case Vs profiles: (1) the downhole Vs

profile, and (2) the simplified PS log Vs profile. As noted earlier, if multiple Vs profiles from various locations at a single site are available, then statistics can be computed and used to set the parameters in the randomization model. However, only two borehole Vs profiles that extend into rock are available at the GVDA Site and their locations are not well-documented. Consequently, calculation of robust statistics regarding spatial variation in Vs was not possible. However, default/recommended parameters are often used in the randomization model when robust Vs statistics cannot be computed. These default parameters incorporate higher variability and are often thought to be more conservative.

The use of default/assumed parameters in Vs randomization reflects a lack of knowledge and is arguably more representative of epistemic uncertainty than aleatory variability. Of course, the spatial variation in Vs at a site is also arguably more epistemic in nature because it could be reasonably quantified with an abundance of data. Nonetheless, epistemic uncertainty is typically accounted for separately through the development of alternative upper/lower base-cases, which are generated by increasing/decreasing the Vs of the mean base-case Vs profiles by a depth-independent epistemic uncertainty factor (σ_{μ}ln or COV). We originally developed upper/lower base-cases for each of the borehole Vs profiles based on the recommended σ_{μ}ln value of 0.35 (EPRI 2012). However, similar to Teague and Cox (2016), Griffiths et al. (2016a and 2016b), and Teague et al. (2017a), we found that these upper/lower base-cases based on a constant COV/σ_{μ}ln yielded unrealistic Vs profiles that did not fit the site signature and produced inaccurate site response estimates. Thus, we chose not to show them here for brevity and only applied the Toro (1995) randomization model to each borehole Vs profile.

The Toro (1995) model operates on the following three sets of parameters: (1) "Velocity Model" parameters, which define the Vs of each layer; (2) "Layering Model" parameters, which control the occurrence of layer boundaries; and (3) "Depth to Bedrock Model" parameters, which control the depth to bedrock (Toro 1995, Kottke and Rathje 2009). Recommended Velocity Model parameters for sites with a time averaged shear wave velocity over the top 30 m (V_{S30}) ranging from 180 to 360 m/s were used in this study because the V_{S30} of the GVDA Site falls within this range. The Velocity Model parameters are provided in Table 5.1. The standard deviation of the natural logarithm of Vs (σ_{lnVs}) parameter controls the variation of Vs within each layer. The "site-specific" σ_{lnVs} values recommended in Stewart et al. (2014) were used in this study. These σ_{lnVs} values were developed based on clusters of profiles at various sites and are preferable to the higher, "generic" σ_{lnVs} values provided in Toro (1995) when spatial variations are not expected to be extreme.

Table 5.1: Velocity Model parameters used in the Toro (1995) randomization model to randomize about the downhole and simplified PS log Vs profiles.

Parameter	*Downhole*	*PS Log*
σ_{lnVs} ($z \leq 50$ m)	0.15	0.15
σ_{lnVs} ($z > 50$ m)	0.22	0.22
ρ_0	0.99	0.99
ρ_{200}	0.98	0.98
Δ	3.9	3.9
d_0	0	0
b	0.344	0.344

The Layering Model defines the layer boundaries for a given Vs profile using a non-homogeneous Poisson process with a depth-dependent transition rate (λ_t). The transition rate is set by three parameters (c_1, c_2, and c_3) and has units equal to the inverse of distance (m^{-1}). At any given depth, the expected layer thickness is equal to $1/\lambda_t$. The

recommended/default parameters from Toro (1995) were used in this study and are provided in Table 5.2. These parameters result in expected layer thicknesses ranging from 4.2 m at the ground surface to 39 m at a depth of 120 m.

Table 5.2: Layering model parameters used in the Toro (1995) model to randomize about the downhole and simplified PS log Vs profiles.

Parameter	*Downhole*	*PS Log*
c_1	10.86	10.86
c_2	0.89	0.89
c_3	1.98	1.98

The depth to bedrock (z_{rock}) is modeled separately from the soil layers. Unlike the Velocity and Layering Model parameters, little guidance is provided in Toro (1995) regarding the depth to bedrock model parameters. Toro (1995) utilized a uniform distribution, but did not specify how the minimum and maximum values of this uniform distribution were set. The Strata software (Kottke and Rathje 2009) gives the user the option to model zrock using a uniform, normal, or lognormal distribution. However, the parameters used to model the variation in the depth to rock (minimum/maximum z_{rock}, σ_{Zrock}, or $\sigma_{lnZrock}$ for uniform, normal, and lognormal distributions, respectively) are left to the discretion of the analyst. In this study, we decided to use a uniform distribution because little information was available to develop parameters for a more complicated model. The parameters needed for a uniform distribution are the minimum and maximum zrock for each base-case. With little information to go on, we simply calculated the difference between the zrock values associated with the downhole and PS log Vs profiles. We then subtracted and added half of this distance to the zrock associated with each base-case profile, as reported in Table 5.3.

Table 5.3: Depth to bedrock model parameters used in the Toro (1995) mode to randomize about the downhole and simplified PS log Vs profiles.

Parameter	*Downhole*	*PS Log*
Distribution	Uniform	Uniform
mean z_{rock} [m]	65	86
Min. z_{rock} [m]	54.5	75.5
Min. z_{rock} [m]	75.5	96.5

Randomization was performed about the downhole (Figure 5.4a) and PS log (Figure 5.4b) Vs profiles. A total of 100 realizations were generated for each base-case. The median randomized Vs profile is similar to the base-case in both instances, indicating that, on average, the randomized Vs profiles capture the base-cases. However, many of the individual Vs profiles are largely inconsistent with the invasively-measured Vs profiles. For example, both sets of randomized Vs profiles contain some Vs profiles with very thick and stiff near-surface layers. This is due to the combination of two factors. First, the non-homogeneous Poisson process may result in very thick layers, even if the expected layer thicknesses ($1/\lambda_t$) appear reasonable. Furthermore, the Vs value of each layer is set based on the mid-depth of that layer. Thus, very thick near-surface layers may exhibit velocities that are consistent with much deeper/stiffer layers. For example, many of the thick near-surface layers in Figure 5.4a and 5.4b have Vs values ranging from 500 to 700 m/s. The top depths of these layers occur where soft soil is known to exist; however, the mid-depths of these layers overlap with the stiffer weathered granite. Thus, the Vs of the layer is set to an unrealistically high value. A potential remedy for this issue would be to either impose a depth-dependent maximum layer thickness to avoid excessively thick near-surface layers and/or to impose criteria whereby both the top and bottom depths of a layer are considered when assigning Vs values. (Note that the Strata implementation of the Toro model allows the analyst to set a layer-dependent maximum

Vs, but this does not resolve the issue because the maximum Vs is imposed based on the mid-depth).

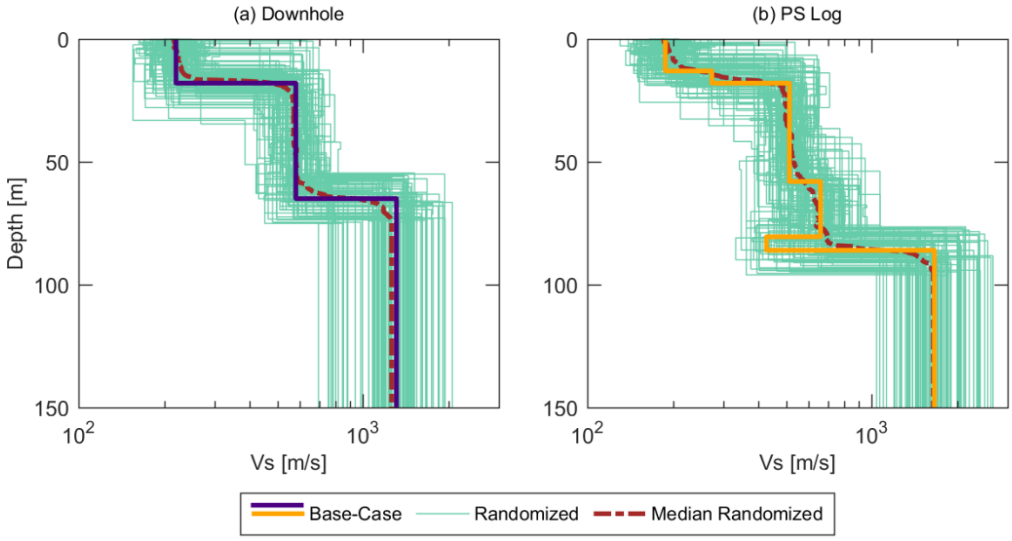

Figure 5.4: Vs profiles developed to account for aleatory variability at the GVDA site. Aleatory variability was considered by randomizing about the (a) downhole Vs profile and the (b) PS suspension log Vs profile. Randomization was performed using the Toro (1995) procedure. A total of 100 realizations were generated during each randomization.

TTFs associated with the downhole- and PS log-randomized Vs profiles are shown along with the median ETF +/- σ_{lnETF} in Figure 5.5. For both base-cases, the variability is extreme, making it difficult to distinguish any overall trends by eye. In general, the randomized Vs profiles associated with both base-cases are inconsistent with the measured site response. Similar to the base-cases, the individual TTFs for each realization have relatively high amplitudes when compared to the median ETF. However, the median TTF for each set of randomized Vs profiles is generally more than one standard deviation away from the median ETF. This is because the locations of the peaks in the individual TTFs are so variable. Consequently, the computation of a median TTF

essentially smooths the individual TTFs and attenuates the response. Thus, the use of either median TTF in design could be quite unconservative.

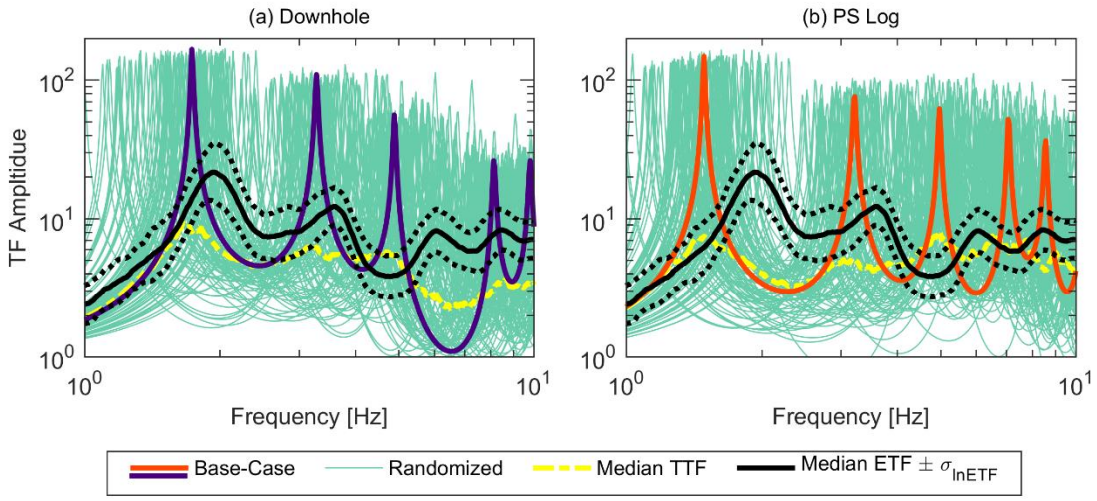

Figure 5.5: Theoretical linear viscoelastic shear wave transfer functions (TTFs) between a depth of 150 m and the ground surface for Vs profiles developed via randomization about the (a) downhole Vs profile and (b) PS suspension log Vs profile. TTFs were computed using small-strain damping ratios proposed in Darendeli (2001) [D_{min}]. Also shown in each panel is the TTF associated with the base-case (i.e., the downhole or PS suspension log Vs profile) and the median ETF +/- σ_{lnETF}.

5.6 Surface Wave Testing at the GVDA Site

In October 2016, a comprehensive surface wave testing program was implemented at the GVDA Site. Surface wave testing was conducted to develop Vs profiles at each of the accelerometer locations and to investigate the validity of the "site signature" concept proposed by Griffiths et al. (2016a and 2016b) and Chapter 4. Specifically, this study was developed to investigate whether experimental dispersion data and HVSR curves may be used to develop Vs profiles that yield accurate predictions of site response and its associated uncertainty at a real field site with recorded ground

motions. This section describes both the development of HVSR curves and experimental dispersion data (i.e., the site signature) and Vs profiles at each accelerometer location.

5.6.1 Field Data Acquisition

Surface wave testing at the GVDA Site involved both active-source Multi-Channel Analysis of Surface Waves (MASW) testing and passive-source Microtremor Array Measurement (MAM) testing. MASW testing involved three linear arrays, which were placed adjacent to the North, Central, and South surface accelerometer locations, as shown in Figure 5.6a. These arrays are designated as NL-47m, CL-34.5m, and SL-47m, respectively. The NL-47m and SL-47m arrays each consisted of 48, 4.5-Hz vertical geophones spaced at 1 m (47-m length), while the CL array consisted of 24, 4.5-Hz geophones spaced at 1.5 m (34.5-m length). The multiple-source offset technique (Cox and Wood 2012, Teague et al. 2017b) was used as a means to estimate data uncertainty and avoid near-field effects for each array, with source-offsets of 5, 10, and 20 m used off both ends. Ten repetitions/shots were performed at each source-offset.

MAM testing was performed using circular arrays generally consisting of 7 recording stations along the perimeter and an additional recording station at the center, as shown in Figure 5.6. Note that the individual markers in Figure 5.6 denote station locations. Each recording station comprised either a three-component Nanometrics 120s broadband seismometer with Taurus digitizer or a three-component Nanometrics 20s broadband seismometer with a Centaur digitizer. Three 50-m diameter circular arrays encircled the North, Central, and South accelerometer locations. These arrays are designated NC-50m, CC-50m, and CS-50m, respectively. Note that the CC-50m and SC-50m arrays were recorded simultaneously. While these arrays recorded data, two additional stations were laid out such that they could be combined with the outer stations

of the CC-50m and SC-50m arrays in order to produce an irregular, 10-station array with an aperture of 110 m (referred to as C-110m). A 150-m diameter circular array (designated C-150m) was laid out in the northern part of the site. Additionally, a smaller 20-m diameter array (designated C-20m) was utilized in the northern part of the site around the borehole containing the rock reference accelerometer.

This dense layout of arrays, shown in Figure 5.6a, allows for a robust determination of the spatial variation in the experimental dispersion data across the site at moderate to high frequencies (or, equivalently, short to moderate wavelengths). However, experimental dispersion data is needed at low frequencies (long wavelengths) to characterize the deep structure at the site. Accordingly, 450-m and 1000-m diameter circular arrays (referred to as C-450m and C-1000m, respectively) were deployed, as shown in Figure 5.6b. Recording times for the MAM arrays ranged from 45 minutes to 6 hours, with the longer recording times generally corresponding to the larger arrays.

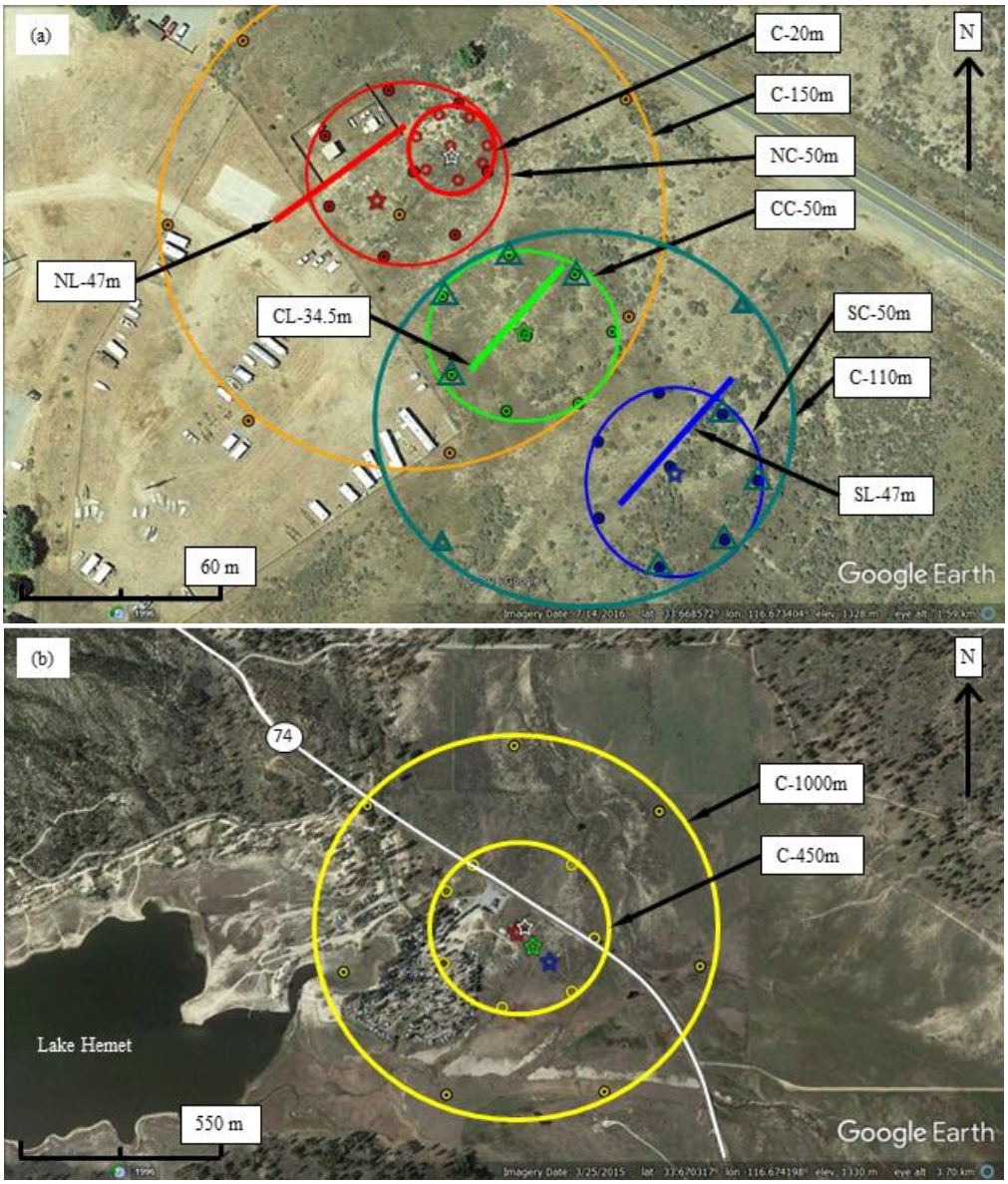

Figure 5.6: (a) Surface wave array locations in the vicinity of the surface and borehole accelerometers (indicated by stars) at the GVDA site. Both active-source (i.e., Multi-Channel Analysis of Surface Waves, MASW) and passive-source (i.e., Microtremor Array Measurements, MAM) testing were performed. Linear MASW arrays ranged from 34.5- to 47-m long. Diameters of the circular MAM arrays ranged from 20 to 1000 m. Individual makers represent seismometer locations in each MAM array. Note that the 110 m aperture array largely consisted of stations that were also used in the Central and South 50-m diameter arrays. (b) Zoomed-out view of the largest 450- and 1000-m diameter circular MAM arrays.

5.6.2 Horizontal to Vertical Spectral Ratios

Each station used in MAM testing (i.e., each marker in Figure 5.6) recorded ambient vibrations in the vertical and two orthogonal horizontal directions (NS and EW). Thus, Horizontal-to-Vertical Spectral Ratios (HVSR) were computed at each location. If the HVSR curve exhibits a sharp, well-defined peak, then the frequency at which this peak occurs ($f_{0,HV}$) may be used to approximate the fundamental shear wave resonant frequency ($f_{0,ETF}$) at that location. If HVSR curves are obtained at various locations across a site, then it is possible to estimate how the fundamental frequency varies across the site. If the fundamental frequency varies significantly, this is a sign of lateral variations in the subsurface Vs structure. Thus, before computing experimental dispersion data, it is useful to consider the HVSR curves.

HVSR curves were computed for all individual stations in accordance with the recommendations in the SESAME D23.12 (2004) report. The SESAME (2004) report provides clarity criteria for inferring $f_{0,HV}$ from HVSR curves. The authors of the SESAME (2004) report do not recommend inferring $f_{0,HV}$ from HVSR curves that fail to meet these criteria. We chose to follow those recommendations here. The HVSR curves for each individual station passing the SESAME (2004) peak clarity criteria are shown for the NC-50m, CC-50m, SC-50m, C-150m, C-450m, and C-1000m arrays in Figure 5.7. Also shown for each array is the lognormal median of the individual station HVSR curves along with the associated standard deviation. The mean $f_{0,HV}$ and associated standard deviation is also listed for each array.

Some individual HVSR curves associated with the CC-50 m (Figure 5.7b) and C-1000 m (Figure 5.7f) arrays increase in amplitude below approximately 1.5 Hz. However, well-defined peaks do not exist at any of the stations below 1.5 Hz. These high amplitudes on a few stations at low frequencies are unstable and do not appear to reflect

resonance features of the site, but are likely attributed to poor receiver coupling. It is useful to first consider the HVSR curves from the 50-m diameter arrays (Figure 5.7a through 5.7c), which were obtained over relatively small areas in the immediate vicinity of the surface accelerometers. All individual HVSR curves have similar shapes and exhibit a well-defined peak ($f_{0,HV}$) near 2 Hz. The $f_{0,HV}$ for the 50-m diameter arrays decreases slightly from a mean of 1.90 Hz in the northwest to 2.05 Hz in the southeast, indicating a slight decrease in the depth to rock from northwest to southeast. Thus, while the GVDA site is located in a valley, the area of interest is reasonably 1D in terms of depth to bedrock. It is also important to note that the $f_{0,HV}$ associated with the 50-m diameter arrays is quite consistent with the mean $f_{0,ETF}$ (1.94 Hz) of the site (refer to Figure 5.2), underscoring the value of HVSR measurements for inferring site resonance and developing a "site signature" at sites without downhole arrays.

The $f_{0,HV}$ values generally increase with increasing array diameter (refer to Figure 5.7d through 5.7f). The $f_{0,HV}$ values for the C-150m array are quite consistent with the 50-m diameter arrays. However, the $f_{0,HV}$ values associated with the C-450m and C-1000m arrays are higher and more variable. This is not surprising because the soil cover is thinner (i.e., $f_{0,HV}$ is higher) closer to the edges of the valley. The variation in $f_{0,HV}$ across these large arrays is an important consideration when computing experimental dispersion data. The surface wave inverse problem assumes a 1D layered earth model, which may be a reasonable assumption over smaller areas. However, as the aperture of an array increases, it incorporates more spatial variability. Unfortunately, larger arrays are necessary to develop low frequency (long wavelength) dispersion data needed for deep profiling, even though many of the stations used in these arrays are outside of the primary area of interest.

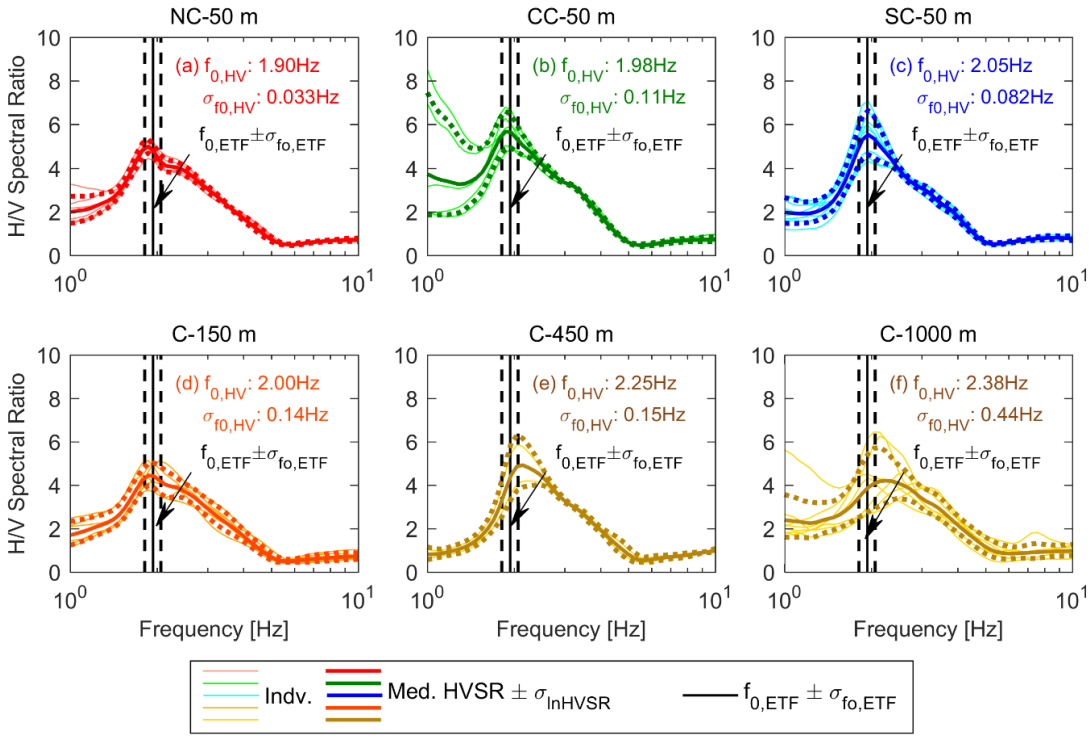

Figure 5.7: Horizontal-to-vertical spectral ratio (HVSR) curves obtained from ambient/noise measurements associated with the North, Central, and South 50-m diameter arrays (a, b, and c, respectively), along with the larger 150-, 450-, and 1000-m diameter arrays (d, e, f), respectively. Colored thin lines represent the median HVSR curves for individual stations, while colored thick solid and dashed lines represent the lognormal median of the individual station medians and +/- one standard deviation, respectively. Note that only those HVSR curves that satisfy the SESAME (2004) peak clarity criteria are shown. The frequency associated with the HVSR peak ($f_{0,HV}$) and the associated standard deviation are provided for each array. The frequency associated with the fundamental mode of the ETF ($f_{0,ETF}$) +/- one standard deviation ($\sigma_{f0,ETF}$) are represented by vertical solid and dashed black lines, respectively.

5.6.3 Experimental Dispersion Data

Experimental dispersion data was computed for all individual arrays. For the MASW arrays, individual records/shots from each source-offset were summed to produce a single, stacked record, which was then processed using the phase-shift transformation

(Park 1998). Dispersion data from each source-offset were then combined and used to compute a mean and standard deviation for each array, as described in Teague et al. (2017b). MAM arrays were processed using both the High Resolution Frequency-Wavenumber Transformation (HRFK) method (Capon 1969) and the Modified Spatial Autocorrelation (MSPAC) method (Bettig et al. 2001) using similar procedures as those described in Chapter 2. Ultimately, the HRFK dispersion data were deemed to be of higher quality based on several considerations, including noise directionality and bias towards lower/higher velocities.

In order to assess spatial variability in Vs using surface wave methods, it is necessary to develop representative experimental dispersion curves for various locations at the site and then invert each of these curves. Thus, experimental dispersion curves that are representative of the North, Central, and South accelerometer locations were developed by averaging the dispersion estimates from individual arrays at these locations, as shown in Figure 5.8. For the North location, dispersion data from the NL-46m, C-20m, NC-50m, and C-150m arrays were used to compute a mean and standard deviation dispersion curve. For the Central location, dispersion data from the CL-34.5m, CC-50m, C-150m, and C-110m arrays were utilized. For the South location, dispersion data from the SL-46m, SC-50m, and C-110m arrays were used. It is clear from Figure 5.8c that phase velocities above 10 Hz are highest (i.e., near-surface materials are stiffest) in the North and lowest in the South. Below 10 Hz, the experimental dispersion data is quite consistent.

The C-450m and C-1000m arrays encircled the North, Central, and South locations. Thus, dispersion data computed from these arrays was used in the inversion for all three locations. However, it was only possible to extract reliable experimental dispersion data from these arrays at frequencies below 1 Hz because the dispersion data

at higher frequencies was quite scattered due spatial averaging of the variable depth to bedrock across the extent of the arrays. Nonetheless, at very low frequencies the dispersion data primarily represents the velocity of the deep bedrock beneath the entire site and can be used to constrain the velocity of the granite, which is apparently quite stiff (greater than 3000 m/s).

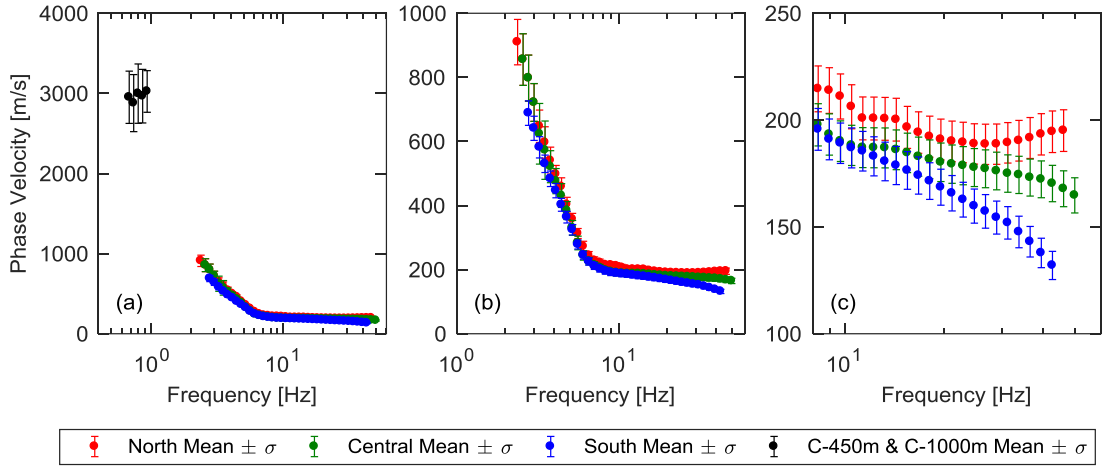

Figure 5.8: (a, b, c) Mean experimental dispersion estimates and associated standard deviations for the North, Central, and South accelerometer locations at the GVDA site, shown at various scales. Note that the low-frequency experimental dispersion data used in the inversion was the same for the North, Central, and South accelerometers and was obtained from the C-450 m and C-1000 m arrays.

At frequencies where the coefficient of variation (COV) in the dispersion estimates was lower than 5%, the standard deviations were increased to achieve a COV of 5%. This was done for two reasons. First, it facilitates the inversion. The inversion optimization algorithm (discussed later) can be quite sensitive to very low standard deviations associated with a few dispersion data points. Essentially, the inversion can get "stuck" trying to perfectly fit these few data points, with less emphasis placed on fitting

other points with higher/more realistic COVs. Secondly, recent studies by Cox et al. (2014) and Garofalo et al. (2016a) suggest that the experimental dispersion data can be retrieved with an inter-analyst variability of 5-10%. Thus, COV values below 5% do not necessarily reflect the dispersion uncertainty that would be computed if multiple analysts had analyzed this same dataset.

5.6.4 Inversion Vs Profiles

Inversions were performed using the dispersion curves from the North, Central, and South accelerometer locations (refer to Figure 5.8). As discussed earlier, the inversion is signficantly influenced by the parameterization (i.e., trial number of layers and ranges in their respective thicknesses, Vs, Vp, and mass densities). Specifically, the number and thickness of trial layers is critical (DiGiulio et al. 2012, Cox and Teague 2016). Thus, various possibilities must be considered if the number of layers is not known a-priori. At the GVDA site, the deep structure is uncertain and thus the total number and thickness of layers cannot be determined with certainty. Cox and Teague (2016) outlined a procedure to systematically perform multiple inversions, each with a different number of layers defined by a unique layering ratio (Ξ). In this approach, the number of layers decreases and each individual layer generally becomes thicker with increasing Ξ. The layering ratio approach was used here, with Ξ of 1.5, 2.0, 3.0, 3.5, 5.0, and 7.0 considered at each location. This results in six different paramterizations with the number of trial layers ranging from 5 to 12. The bottommost layer in each parameterization was not perimitted to be deeper than 300 m because bedrock was anticipated to be much shallower at this site.

The inversions were performed using the Geopsy software (www.geopsy.org). Theoretical dispersion forward computations for each trial earth model are based on the

transfer matrix approach originally developed by Thomson (1950) and Haskell (1953) and later modified by Dunkin (1965) and Knopoff (1964). Multi-mode inversions were initially performed. However, the experimental dispersion data from the site was ultimately deemed to represent the fundamental Raleigh wave mode. For each trial model, a dispersion misfit value (m_d) was computed between the experimental data and the theoretical curve, as described in Wathelet (2004). The software uses the Neighborhood Algorithm (Sambridge 1999, Wathelet et al. 2004) to search for layered earth models within the user-defined parameterization with the lowest possible misfit values. A misfit value below 1.0 indicates that, on average, the theoretical dispersion curve for a given ground model falls within one standard deviation of the experimental dispersion data. In addition to consideration of dispersion misfit, the HVSR curves were also used to constrain the inversion results by comparing the fundamental resonant frequency values associated with the TTFs for all inversion Vs profiles ($f_{0,TTF}$) with the experimentally-measured mean $f_{0,HV}$ at that location (refer to Figure 5.7). Vs profiles whose theoretical $f_{0,TTF}$ deviated by more than approximately three standard deviations from the mean $f_{0,HV}$ for that location were rejected. (Note that the $f_{0,ETF}$ was not used to constrain the inversion because it is generally not known at most sites).

A total of 200 thousand to 1 million trial models were searched during each inversion, with more trial models being used for lower layering ratios, which include more layers and thus have more unknowns to solve for. For each combination of location and layering ratio, two separate inversions were performed. The first inversion was intended to search for the ground models with the lowest possible misfit values. This approach is useful for finding the "best" ground models, but oftentimes the final ensemble of ground models from inversion fails to capture other acceptable models with slightly higher misfit values. Thus, the second inversion was used to search for any

ground models with a misfit below 1.0 (i.e., whose theoretical dispersion curves fall within one standard deviation of the experimental dispersion data). This type of inversion yields a more diverse ensemble of realistic ground models, but oftentimes cannot find the best possible answer (i.e., the lowest possible misfit). Thus, by combining the results from these two inversions, it is possible to create an ensemble of ground models that contains the best possible answer for a given parameterization, but also includes other models that are still considered possible. The results from these two types of inversions were combined to develop an ensemble of 33 Vs profiles for each combination of layering ratio parameterization and location. The Vs profiles from all locations were then combined for a given layering ratio, yielding 99 Vs profiles per layering ratio. This number was chosen to be consistent with the number of Vs profiles obtained from randomization about each borehole profile, which considered 100 realizations per base-case. By developing Vs profiles from three separate locations (North, Central, and South), aleatory variability is implicitly considered. Furthermore, epistemic uncertainty is also accounted for by considering six different layering ratios.

The 99 theoretical dispersion curves for each location and layering ratio are shown relative to the experimental data in Figure 5.9. The Vs profiles associated with these theoretical dispersion curves are shown in Figure 5.10. Values of md for the 99 Vs profiles associated with each layering ratio and location are shown in Table 5.4. It is clear from Figure 5.9 that, for a given location, all layering ratios yield similar fits of the experimental dispersion data despite the fact that different numbers of layers were used. This is underscored by the similar ranges in md shown in Table 5.4. However, Figure 5.10 demonstrates that the Vs profiles associated with these similar theoretical dispersion curves are quite different. This highlights the non-unique nature of the inverse problem. Furthermore, as discussed above, the experimental dispersion data contains a gap

between 1-2 Hz, which further exacerbates the non-unique nature of the inversion for this dataset. Note that Vs profiles are only shown to a depth of 150 m because their associated TTFs (discussed later) were computed between the ground surface and this depth.

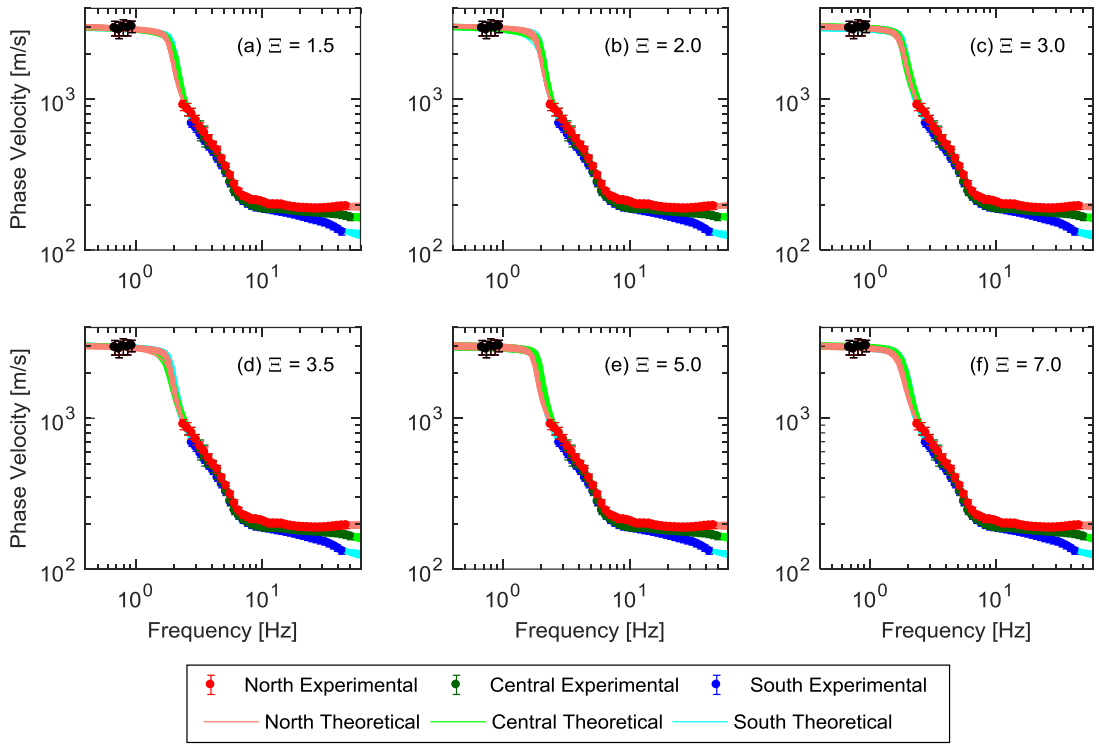

Figure 5.9: Fundamental mode theoretical dispersion curves associated with the 99 ground models obtained from surface wave inversion at the North, Central, and South accelerometer locations at the GVDA site developed using layering ratios (Ξ) of (a) 1.5, (b) 2.0, (c) 3.0, (d) 3.5, (e) 5.0, and (f) 7.0. Also shown are the experimental dispersion data for the North, Central, and South accelerometer locations (refer to Figure 5.8). Note that the low frequency data below 1 Hz (shown in black) is the same for all locations.

Table 5.4: Range of dispersion misfit values associated with the 1000 lowest misfit Vs profiles obtained from surface wave inversion at the North, Central, and South accelerometer locations at the GVDA site for each layering ratio (Ξ).

Layering Ratio (Ξ)	m_d		
	North	Central	South
1.5	0.25 - 0.54	0.22 - 0.56	0.21 - 0.60
2.0	0.25 - 0.57	0.21 - 0.54	0.21 - 0.62
3.0	0.20 - 0.57	0.23 - 0.55	0.18 - 0.58
3.5	0.23 - 0.59	0.23 - 0.65	0.18 - 0.59
5.0	0.20 - 0.59	0.20 - 0.63	0.15 - 0.59
7.0	0.34 - 0.57	0.14 - 0.61	0.30 - 0.58

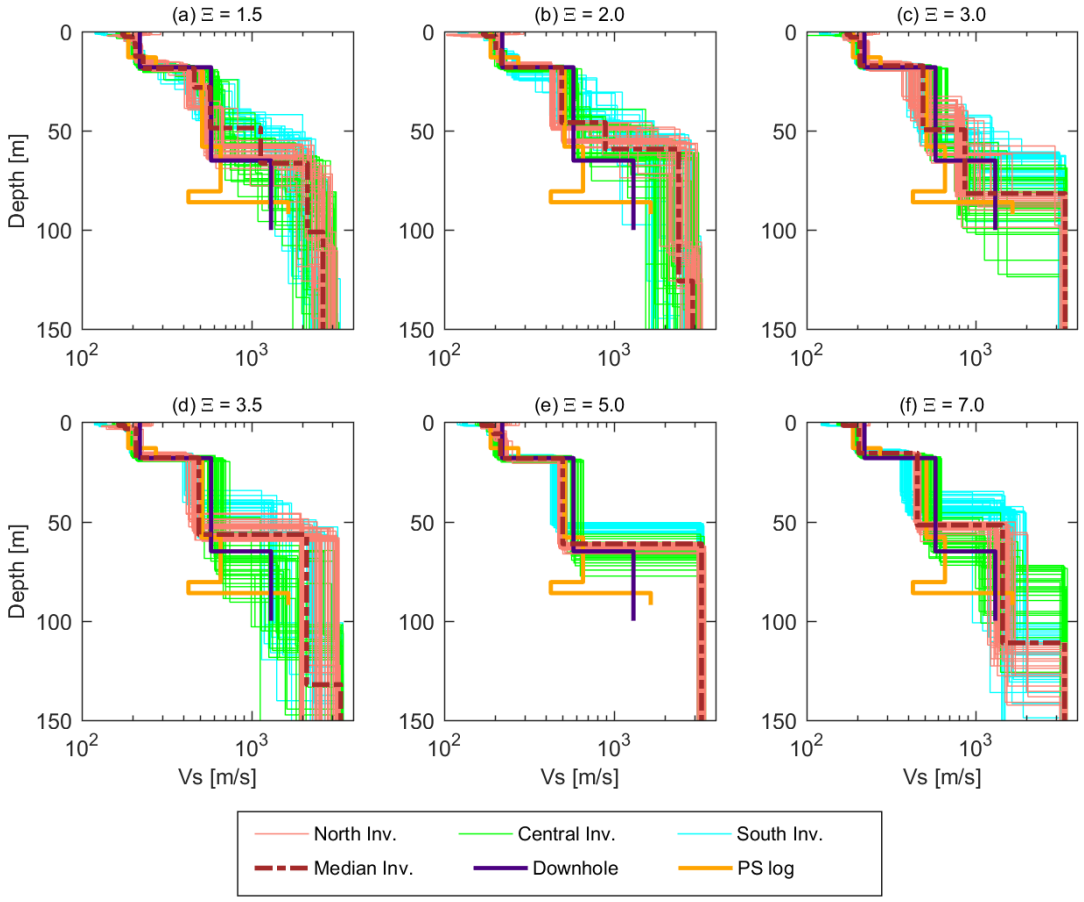

Figure 5.10: Inversion Vs profiles associated with the 99 ground models from the North, Central, and South accelerometer locations at the GVDA site developed using layering ratios (Ξ) of (a) 1.5, (b) 2.0, (c) 3.0, (d) 3.5, (e) 5.0, and (f) 7.0. The median inversion Vs profile is indicated for each layering ratio. Also shown are the Vs profiles previously developed from PS suspension logging (Steller 1996) and seismic downhole testing (Gibbs 1989).

The variability among the Vs profiles obtained from a single location and Ξ generally increases below approximately 40 m. Furthermore, the variability between the different locations and Ξ increases with depth. This variability is due to both the gap in the experimental dispersion data between 1-2 Hz and the fact that Vs profiles obtained from inversion (referred to herein as the "inversion Vs profiles") are generally better-constrained at shallower depths. The median Vs profile, computed using the 99 Vs profiles from all locations, is shown for each Ξ along with the downhole and PS log Vs profiles in Figure 5.10. The inversion Vs profiles tend to be in better agreement with the downhole Vs profile, with many inversion Vs profiles showing a strong impedance contrast between 50-70 m. However, many Vs profiles associated with a Ξ of 3.0 show a strong velocity contrast at 85 m, which is the same depth that the PS log shows bedrock (albeit at a much lower velocity). Overall, the bottommost layer of most inversion Vs profiles above a depth of 150-m generally has a much higher Vs than indicated by either of the invasive borehole Vs profiles.

The theoretical transfer functions associated with the inversion Vs profiles are shown for in Figure 5.11. Despite major visual differences in the Vs profiles from various locations and Ξ, the fundamental and first-higher resonant frequencies of the TTFs are quite consistent with the median ETF. Moreover, many TTFs have second- and third-higher modes whose locations are consistent with the median ETF. The good agreement between the resonant frequencies of the TTFs determined from inversion Vs profiles and the ETF is in stark contrast to the TTFs associated with the measured borehole and randomized Vs profiles (refer to Figure 5.5). The median TTF calculated from the 99 TTFs for each Ξ is shown in Figure 5.11 These median TTFs are generally in excellent agreement with the median ETF. Thus, even though inversion non-uniqueness is significant (Figure 5.10) and a single "true" Vs profile cannot be determined with

certainty, the results from surface wave testing can produce very accurate site response estimates when Vs uncertainty is considered in a meaningful way. It is also worth noting that the invasively-measured Vs profiles, which are often deemed to represent "ground truth", do not yield accurate site response estimates at this site. This is an important point to consider, as many downhole array sites are characterized by a single, invasively-measured Vs profile.

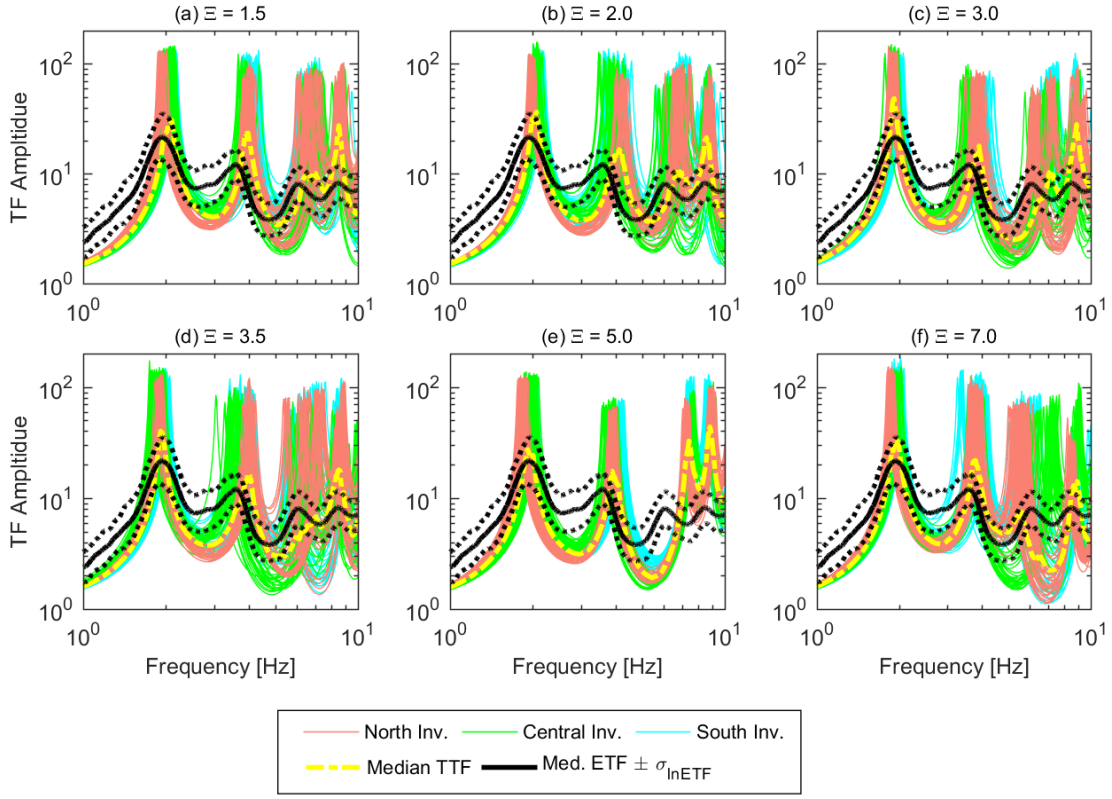

Figure 5.11: Theoretical linear viscoelastic shear wave transfer functions (TTFs) between the ground surface and a depth of 150 m computed using the inversion Vs profiles and small-strain damping ratios proposed in Darendeli (2001) [D_{min}] for the 99 ground models from the North, Central, and South accelerometer locations at the GVDA site developed using layering ratios (Ξ) of (a) 1.5, (b) 2.0, (c) 3.0, (d) 3.5, (e) 5.0, and (f) 7.0. The median transfer function, computed using 99 TTFs (33 from each accelerometer location), is indicated for each layering ratio. Also shown is the median ETF +/- σ_{lnETF}.

5.7 QUALITATIVE AND QUANTITATIVE COMPARISON OF TTFS

It is clear, by comparison of Figure 5.11 to Figure 5.5, that the TTFs associated with the inversion Vs profiles better match the measured ETF than those associated with the borehole profiles and Vs randomization. Although the non-unique nature of the inversion Vs profiles is visually considerable (refer to Figure 5.10), these very different interpretations of the subsurface all fit the experimentally-measured site signature (i.e., dispersion data and HVSR fundamental frequency) and result in very similar site response estimates that are relatively consistent with the observed site response. Furthermore, the inversion Vs profiles implicitly account for the spatial variations in Vs in a more meaningful way than assumed Vs randomization parameters. Meaning, the variability in the inversion Vs profiles is due in part to the variations in the measured dispersion of surface waves across the site, rather than on assumptions about the variation in Vs that are not validated by in-situ measurements.

In order to further assess the suites of Vs profiles derived from both randomization and from inversion, it is useful to compare the median TTFs to the median ETF +/- σ_{lnETF}, as shown in Figure 5.12. (Note that the median TTFs shown in Figure 5.12a are the same as those shown in Figure 5.11). As discussed earlier, the median TTFs from all Ξ are remarkably similar and match the median ETF quite well, particularly at the fundamental and first-higher modes. Nonetheless, the median TTF associated with Ξ of 5.0 does not well-capture the second- and third-higher modes of the ETF and the median TTF for a Ξ of 7.0 does not well-capture the median ETF at the second -higher mode. A median TTF was computed using the individual TTFs from all Ξ, as shown in Figure 5.12b. This TTF is compared to the median TTFs associated with the downhole-randomized and PS log-randomized Vs profiles. (Note that the median TTFs associated with the randomized Vs profiles are the same as those shown in Figure 5.5).

Qualitatively, it is clear that the median TTF associated with all inversion Ξ better matches the median ETF, particularly at the resonant frequencies.

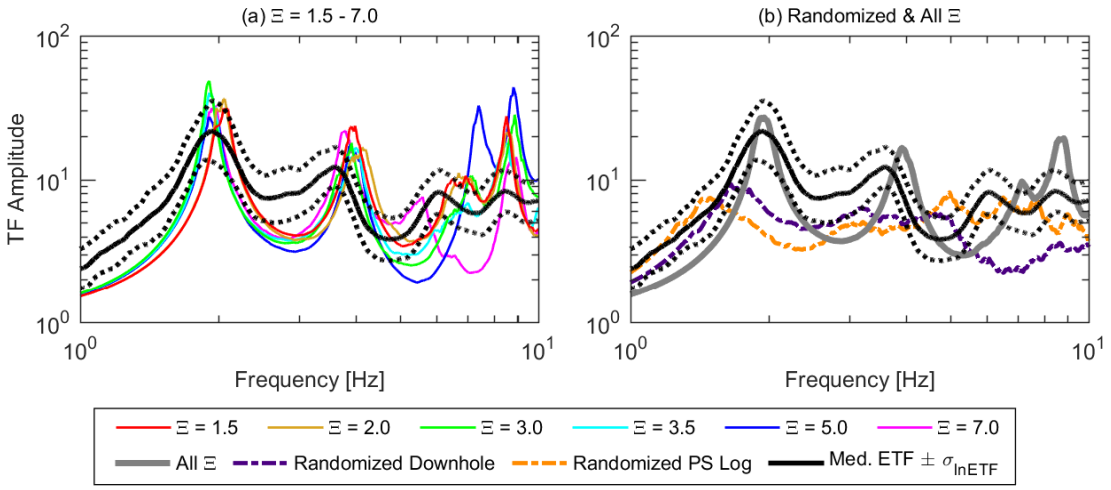

Figure 5.12: Median theoretical linear viscoelastic shear wave transfer functions (TTFs) between a depth of 150 m and the ground surface for (a) inversion layering ratios (Ξ) of 1.5, 2.0, and 3.0, 3.5, 5.0, and 7.0 and (b) median TTFs calculated from all inversion Ξ and the randomized Vs profiles associated with the downhole and simplified PS log. TTFs were computed using the small-strain damping ratio values proposed in Darendeli (2001) [D_{min}]. Also shown are the median ETF +/- σ_{lnETF}.

In addition to a qualitative assessment of the various TTFs, it is also helpful to have a quantitative measure of how well/poorly the median TTFs match the the median ETF. This study utilizes two parameters for quantitative assessment. These parameters assess both how well the spectral shapes match as well as the residuals between the two curves. For the former, we use a similar approach to Afshari and Stewart (2015). Namely, we calculated the Pearson correlation coefficient, *r*, between the median ETF and the median TTF (simply labeled the "ETF" and "TTF" in Eq. (1) and (2), respectively) for each Ξ and randomization. A higher *r* (i.e., closer to 1.0) indicates that the resonant

frequencies in the median TTF are better aligned with the resonant frequencies in the median ETF. Values of *r* were computed as follows:

$$r = \frac{\sum_{i=1}^{n_f}(ETF_i(f)-\mu_{ETF})(TTF_i(f)-\mu_{TTF})}{\sqrt{\sum_{i=1}^{n_f}(ETF_i(f)-\mu_{ETF})^2}\sqrt{\sum_{i=1}^{n_f}(TTF_i(f)-\mu_{TTF})^2}} \quad (5.1)$$

where μ_{ETF} and μ_{TTF} represent the mean values of the ETF and TTF across the frequency range considered. The summations were performed over n_f = 256 frequencies between 1 and 10 Hz. As noted earlier, the ETF could not be reliably computed below 1 Hz due to low signal-to-noise ratios. Above 12-15 Hz, the ETF rapidly attenuates. Thus, *r* was simply computed over a single log cycle from 1 to 10 Hz using 256 logarithmically-spaced points.

In order to quantify the residuals between the ETF and the TTF, a transfer function misfit, m_{TF}, was calculated, as shown in Eq. (2). Similar to *r*, m_{TF} was computed over a limited frequency range from 1 to 10 Hz with 256 logarithmically-spaced points. As with m_d, an m_{TF} value greater than ε indicates that, on average, the median TTF for a given Ξ or randomization deviates by more than ε standard deviations from the median ETF.

$$m_{TF} = \sqrt{\frac{1}{n_f}\sum_{i=1}^{n_f}\frac{[\ln(TTF_i)-\ln(ETF_i)]^2}{\sigma_{lnETFi}^2}} \quad (5.2)$$

The *r* and m_{TF} values for the median TTFs associated with randomization and inversion are shown in Figure 5.13. The *r* value associated with the median TTF of the PS log-randomized Vs profiles is quite poor (i.e., less than 0). One the other hand, the *r* values associated with the inversion and downhole-randomized Vs profiles are generally greater than 0.5. The *r* values associated with the inversion Vs profiles are marginally higher than the *r* values associated with the downhole-randomized Vs profiles. The only exception to this is the *r* value for a Ξ of 5.0. Since it is difficult to tell which inversion layering ratio Vs profiles are the best without additional subsurface

information (recalling that all layering ratio parameterizations yielded similar dispersion misfit values; refer to Table 5.4), it is wise to use a median TTF computed from all Ξ. Indeed, the *r* value associated with the median TTF computed from all Ξ is quite high and just slightly less than some of the *r* values calculated from individual layering ratio parameterizations.

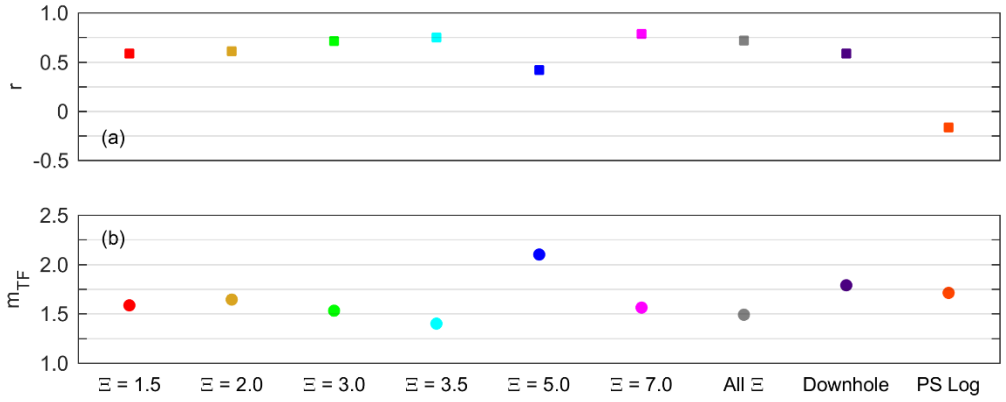

Figure 5.13: (a) Pearson correlation coefficient, *r*, and (b) transfer function misfit, m_{TF}, values associated with the median TTFs calculated from all inversion layering ratios (Ξ) and the randomized Vs profiles associated with the downhole data and simplified PS log.

Values of m_{TF} are shown in Figure 5.13b. The m_{TF} values are generally lowest for the median TTFs associated with the inversion Vs profiles, indicating that they best-capture the median ETF. The only exception to this is the median TTF associated with a Ξ of 5.0. Interestingly, the dispersion misfit values associated with this Ξ were some of the lowest achieved during inversion (see Table 5.4). This underscores the importance of considering multiple parameterizations during surface wave inversion in order to develop Vs profiles for site response. Indeed, the m_{TF} value calculated from the median TTF associated with all Ξ inversions is among the very best/lowest values. It is also interesting to note that the m_{TF} values for the median TTFs associated with the downhole-

randomized and PS log-randomized Vs profiles are only marginally higher than those associated with the inversion Vs profiles, yet, their TTFs qualitatively fit the median ETF much more poorly than the median TTFs associated with inversion. This is due to the relatively flat nature of the median TTFs for the randomized borehole Vs profiles and the fact that the inversion TTFs tend to underestimate the median ETF at the local minima (refer to Figure 5.12b). It is worth noting that other qualitative parameters, such as the variance reduction parameter described in Thompson (2009), were used to assess the quality of fit between the median TTFs and median ETF. Each qualitative parameter has its strengths and weaknesses, but the trends indicated by the r and m_{TF} values shown in Figure 5.13 remained the same. In our opinion, the median TTF computed from all Ξ inversions (refer to Figure 5.12b) provides a far superior fit to the median ETF at this site than the median TTFs calculated from randomized suites of Vs profiles based on the downhole and PS log profiles. While the quantitative parameters support this assessment, the values are not drastically different. This highlights the difficulty of assessing the overall agreement of ETFs and TTFs using a single quantitative value and underscores the need for more robust methods of comparing TTFs to a measured ETF.

5.8 Improved Realizations from the Toro (1995) Model

It is clear from this study, as well as prior studies (e.g., Griffiths et al. 2016b, Chapter 4), that the Toro (1995) model may produce many Vs realizations that do not fit the experimental site signature and whose calculated site response is inconsistent with the true/measured site response. Nonetheless, it is important to note that the site response estimates associated with some realizations are consistent with both the site signature and the true site response. Thus, it is worth investigating strategies that may be used to reduce the number of realizations that produce unrealistic site response estimates in order to

develop a more appropriate set of Vs profiles for use in site response analyses. This section investigates two strategies that are aimed at this goal. Specifically, (1) the use of a more accurate base-case in combination with site-specific parameters is considered, and (2) the implementation of a rejection criteria based on the site signature (i.e., experimental dispersion and HVSR data) is investigated.

5.8.1 Site-Specific Randomization Parameters

The randomization discussed earlier was performed using default/assumed parameters applied to each base-case Vs profile (i.e., the downhole and PS log Vs profiles). However, the base-case profiles themselves did not yield TTFs that satisfactorily matched the empirically measured transfer functions. Thus, it is useful to consider whether more satisfactory results can be obtained by performing randomization using site-specific parameters in conjunction with a base-case Vs profile whose TTF well-captures the ETF. Accordingly, we chose to develop randomized profiles about the median Vs profile obtained from a Ξ of 3.0 (Figure 5.10c). We chose this Vs profile because, as shown in Figure 5.14c, the resonant frequencies of its TTF are in excellent agreement with the median ETF. In order to develop site-specific randomization parameters for this base-case, statistics were computed using the 99 inversion Vs profiles that were used to compute the median Vs profile. The σ_{lnVs} parameter used in this randomization was layer-specific and ranged from 0.05 to 0.27 as a function of depth. Inter-layer correlation was investigated using procedures similar to those described in Rathje et al. (2015). Specifically, the normalized residual of the natural logarithm of Vs (ε) was calculated for each layer and layer-to-layer correlation was assessed at various depths and thicknesses. Overall, there was no strong positive layer-to-layer correlation. In fact, many layers showed weak negative correlation. Thus, the inter-layer correlation was

set to zero ($\rho_{200} = \rho_0 = 0$). It is worth noting that a randomization was performed using the default correlation parameters and was found to produce worse results. The layering model parameters were determined as described in Griffiths et al. (2016a) and Teague and Cox (2016) and found to be: $c_1 = 1.5$, $c_2 = 0.82$, and $c_3 = 8.0$. These parameters result in expected layer thicknesses of 1.7 m at the ground surface and 55 m at a depth of 100 m. The depth to bedrock was found to be most accurately modelled with a lognormal distribution with a median depth to rock of 82 m and a $\sigma_{lnZrock}$ of 0.15.

The Vs profiles from randomization about the median Vs profile from a Ξ of 3.0 are shown in Figure 5.14a. The variability exhibited by these Vs profiles below 40 to 50 m appears reasonable when compared to the inversion Vs profiles that were used to develop the base-case profile and randomization parameters (refer to Figure 5.10c). Nonetheless, similar to Figure 5.4, many near-surface layers are excessively thick and stiff, although the site-specific layering parameters (c_1, c_2, and c_3) slightly alleviate this issue. Fundamental mode, theoretical Rayleigh wave dispersion curves were computed for these randomized Vs profiles, as shown in Figure 5.14b. (In order to perform these calculations, assumptions regarding Vp and mass density were made, as described in Griffiths et al. 2016a). Interestingly, in contrast to the dispersion curves for the inversion Vs profiles (refer to Figure 5.9c), the theoretical dispersion curves computed for these randomized Vs profiles do not well-fit the experimental dispersion data above 1 Hz, which indicates that they are not well-capturing the site signature. The individual TTFs for these randomized Vs profiles are shown in Figure 5.14c. The median randomized TTF now has peaks that correspond very well to the peak frequencies in the ETF at all modes. However, similar to Figure 5.4, the median TTF from randomized Vs profiles significantly under-predicts the median ETF at the fundamental and first-higher modes. Nonetheless, the median TTF matches the median ETF quite well at the second- and

third-higher modes, indicating that there is benefit to using site-specific parameters in the randomization.

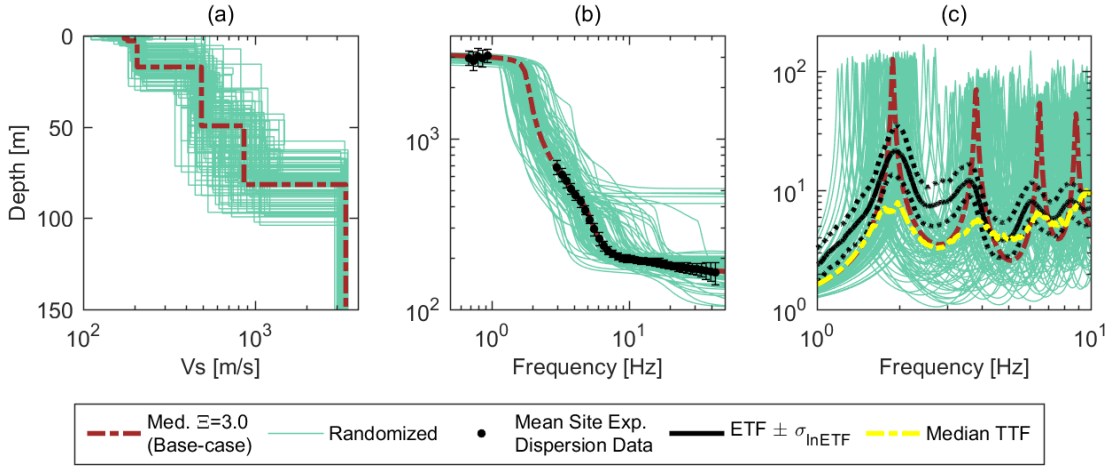

Figure 5.14: (a) Vs profiles developed via randomization about the median Vs profile derived from a layering ratio (Ξ) inversion of 3.0. Site-specific parameters, based on statistics for the suite of Vs profiles from a Ξ of 3.0, were used in the randomization. Also shown are (b) the corresponding theoretical dispersion curves along with the mean experimental dispersion data for the GVDA site and (c) the corresponding TTFs along with their associated median and the median ETF +/- σ_{lnETF}.

5.8.2 Screening Randomized Vs Profiles Using the Site Signature

Given that the site response estimates associated with the inversion Vs profiles generally well-capture the observed site response, it is useful to consider whether the site signature that was used to develop these inversion Vs profiles can be used for screening the randomized Vs profiles. Here, we consider the original randomized Vs profiles, which were developed by randomizing about the downhole and PS log Vs profiles. In order to screen the randomized Vs profiles, we averaged all of the experimental dispersion and HVSR data from the area of interest (i.e., the area enclosed by the C-150 m and C-110 m arrays shown in Figure 5.6). We then calculated theoretical fundamental mode Rayleigh wave dispersion curves for each randomized Vs profile and computed an

md value between the theoretical curve and the experimental dispersion data from the entire site. We did not include the experimental dispersion data from the C-450 m and C-1000 m arrays when calculating dispersion misfit values because the Vs associated with the deepest layer in all randomized Vs profiles is less than 2500 m/s. Consequently, no theoretical dispersion curves would fit the low-frequency data obtained from these larger arrays. The $f_{0,TTF}$ for each randomized Vs profile was also identified and compared to the mean $f_{0,HV}$ (1.98 Hz) for the entire site and its associated standard deviation (0.10 Hz). Those randomized Vs profiles with md values greater 3.0 (i.e., whose theoretical dispersion curves, on average, are more than 3.0 standard deviations outside of the experimental dispersion data) and/or whose $f_{0,TTF}$ was more than 3.0 standard deviations above or below the mean $f_{0,HV}$ for the entire site were rejected.

The original set of randomized Vs profiles are shown along with the smaller subset of screened-randomized Vs profiles in Figure 5.15a and 5.15b for the downhole and PS log Vs base cases, respectively. As noted previously, many of the near-surface layers associated with the full set of randomized Vs profiles are excessively thick and/or stiff. However, the near-surface layers associated with the subset of screened Vs profiles are not excessively thick and/or stiff. This is due to the fact that excessively stiff and thick near-surface layers result in a poor fit of the experimental dispersion data, as illustrated in Figure 5.15c and 5.15d.

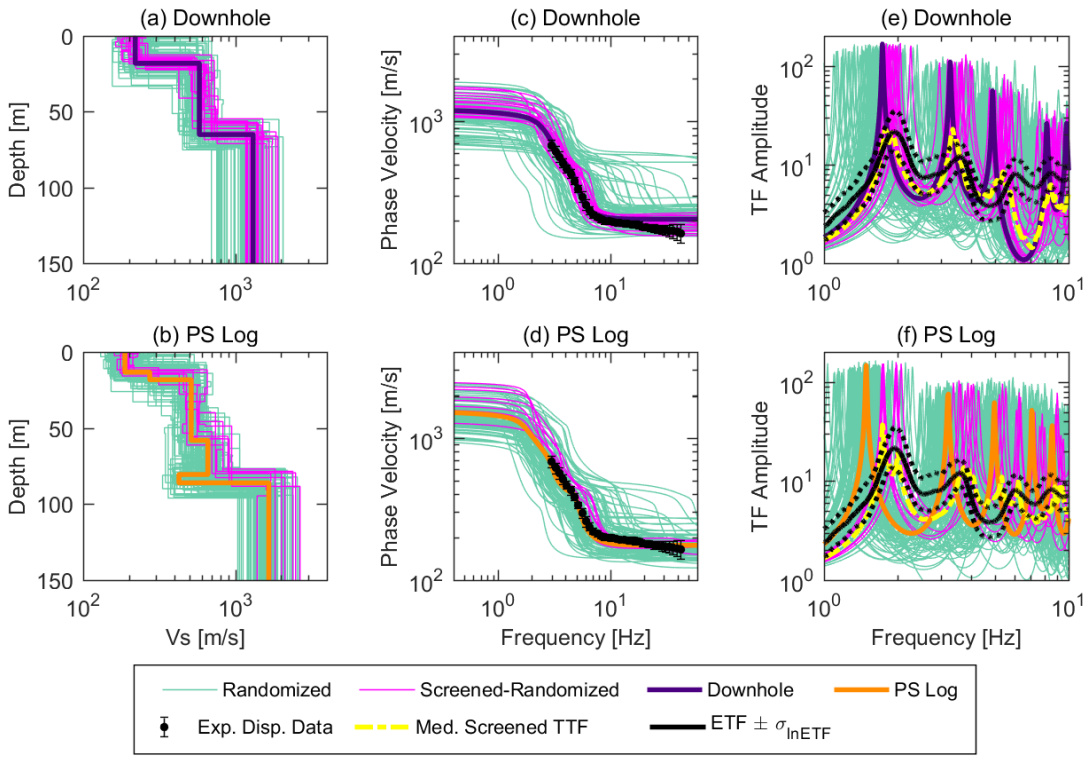

Figure 5.15: (a, b) Vs profiles, (c, d) theoretical fundamental mode Rayleigh wave dispersion curves, and (e, f) TTFs associated with the randomized and screened-randomized Vs profiles developed at the GVDA site. Randomized and screened-randomized profiles were developed using the downhole (a, c, e) and PS log (b, d, f) Vs profiles as base cases. Note that the screened-randomized Vs profiles were developed by applying a rejection criteria to the randomized Vs profiles based on the experimental site signature. Shown in (c) and (d) is the mean experimental dispersion data from the GVDA site. Shown in (e) and (f) are the median ETF and its associated standard deviation.

It is clear from Figure 5.15e and 5.15f that the TTFs associated with the subset of screened Vs profiles better match the observed ETF. This is underscored by observing the median TTF for each set of screened Vs profiles, which well-captures the median ETF at the fundamental and first-higher modes. The median screened TTFs associated with the downhole and PS log have r values of 0.78 and 0.66 and mTF values are 1.60 and 1.22,

respectively. These values are considerably better than those associated with the original sets of randomized Vs profiles (refer to Figure 5.13).

It is important to note that the $f_{0,TTF}$ values associated with the base-case Vs profiles (1.73 and 1.49 Hz for the downhole and PS log Vs profiles, respectively) do not well-match the measured $f_{0,HV}$ (1.98) or $f_{0,ETF}$ (1.94), although their associated theoretical dispersion curves are in good agreement with the experimental dispersion data above 1 Hz. Thus, even though the base-cases used in randomization did not well-represent the site signature or the ETF, a suite of Vs profiles whose theoretical TTFs acceptably match the ETF were obtained through randomization about these Vs profiles with a screening criteria. Thus, the Toro (1995) randomization model can be quite useful for developing realistic Vs profiles for site response provided it is carefully applied with a logical criteria for rejecting unrealistic Vs profiles using the experimental site signature. Conversely, the blind application of the Toro (1995) model yielded very poor site response estimates. The improved match of the median ETF is largely due to the HVSR fundamental frequency rejection criteria. The HVSR gives a good approximation of the fundamental mode resonant frequency at the site, allowing for a rejection of Vs profiles whose TTFs are inconsistent with this frequency. Thus, even if robust dispersion data cannot be developed for a site, simple single-station HVSR curves can provide valuable information that could aid in selecting reasonable randomized Vs profiles for realistically quantifying Vs uncertainty in site response. This underscores the value of performing HVSR measurements across the footprint of the site of interest. It is important to note that HVSR measurements are very quick to obtain and can be done rapidly by re-positioning a single seismometer at numerous points across the footprint of the site.

Even without dispersion or HVSR data, randomized Vs profiles could be potentially eliminated by calculating the time averaged shear wave velocity over the top

30 m (V_{S30}) and ensuring that it is reasonably consistent with the original base-case Vs profile. Figure 5.16 shows the V_{S30} values associated with the inversion, base-case, randomized, and screened-randomized Vs profiles. Many of the V_{S30} values associated with the original set of randomized Vs profiles are extremely inconsistent with the inversion and base-case Vs profiles. In fact, many of the randomized Vs profiles would receive a higher/lower NEHRP site classification. On the other hand, the V_{S30} values for the screened-randomized Vs profiles are much more reasonable. As noted in previous studies (e.g., Cox et al. 2014; Garofalo et al. 2016b), V_{S30} can be robustly determined with minimal variability. Thus, those realizations yielding excessively high/low V_{S30} values should be questioned even if a more robust screening process based on the site signature cannot be implemented.

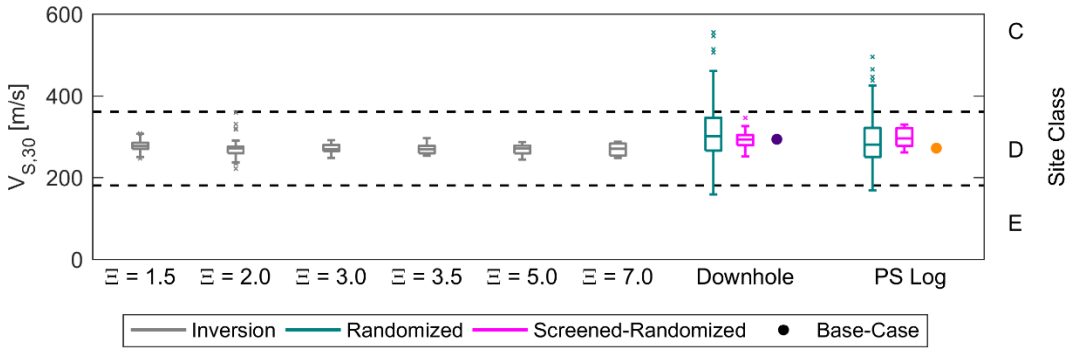

Figure 5.16: V_{S30} values associated with the layering ration (Ξ) inversion, base-case (i.e., downhole and PS log), randomized, and screened-randomized Vs profiles. Dashed lines represent the boundaries of the Natural Earthquake Hazard Reduction Program (NEHRP) Site Classes C, D, and E.

5.9 CONCLUSIONS

This study compared the observed/empirical linear-viscoelastic transfer functions (ETFs) from the GVDA site to the theoretical linear-viscoelastic transfer functions (TTFs) calculated from various Vs profiles. These Vs profiles were developed from:

invasive borehole measurements, randomization about the invasive Vs profiles, and surface wave testing. Although Vs profiles derived from borehole measurements are often deemed to represent "ground truth," the TTFs associated with the invasively-measured Vs profiles were inconsistent with the observed ETF. This is an important consideration because many downhole array sites used to study site effects are characterized by a single invasively-measured borehole. In an effort to account for Vs uncertainty and achieve a better match of the ETF, Vs randomization was performed about the borehole Vs profiles using the Toro (1995) model along with common assumptions regarding spatial variations in Vs. However, randomization in this "blind" manner (i.e., with no criteria for rejecting unrealistic realizations) yielded poor site response estimates.

Surface wave testing was performed in an effort to obtain Vs profiles whose theoretical TTFs better match the ETF than those associated with the invasive and randomized Vs profiles. Although the Vs profiles derived from surface wave inversion exhibited considerable differences, their TTFs were generally quite similar and matched the ETF quite well, particularly at the fundamental and first-higher mode. Thus, although surface wave inversion non-uniqueness is an important consideration and a source of considerable uncertainty, accurate site response estimates can be obtained if this non-uniqueness is accounted for in a rigorous manner. Furthermore, the experimental dispersion and HVSR data (i.e., the site signature) that were used to perform the inversion can be quite useful for assessing candidate Vs profiles.

The site signature was used to screen the original set of Vs profiles developed from blind randomizations. In contrast to the original set of randomized Vs profiles, the TTFs associated with the screened Vs profiles were in excellent agreement with the ETF. This suggests that randomization can be quite useful if a rational criteria for rejecting

unrealistic Vs profiles is implemented. If dispersion data and/or HVSR data are not available, this rejection criteria could simply amount to rejecting Vs profiles with excessively high/low V_{S30} values. In any case, this study and previous studies indicate that poor site response estimates may be obtained if Vs randomization is performed in a blind manner.

Chapter 6: Conclusions and Recommendations for Future Work

6.1 CONCLUSIONS

Surface wave inversion non-uniqueness is well-established. This non-uniqueness is exacerbated by potential ambiguities in the interpretation of surface wave modes and/or the subjectivity of defining the inversion parameterization. In many cases, multiple mode interpretations must be considered, which increases the computational cost. However, even when the surface wave modes can be readily determined, the choice of parameterization is significant.

The Vs profiles obtained from surface wave inversion are highly dependent on the inversion parameterization (i.e., trial number of layers and ranges in their respective Vs, Vp, and mass densities). In particular, the number of layers and presence or absence of potential velocity reversals strongly influences the Vs profiles attained from an inversion. In complex geologic conditions such as those at the 14 sites in Christchurch discussed in Chapter 2, it may be possible to develop unrealistic, overly-simplistic Vs profiles that result in a satisfactory fit of the experimental dispersion data. In such cases, a-priori information should be sought and used to aid in the inversion. This information not only helps to develop a realistic inversion parameterization, but it also can aid in the interpretation of surface wave modes.

In many cases, a-priori information is not available and a "blind" inversion must be performed. In such cases, the full non-uniqueness cannot be captured unless multiple parameterizations are considered. In particular, it is important to consider the influence of the number of trial layers. If too many layers are included in the parameterization, then the experimental dispersion data may be insufficient to constrain all of the unknowns. Consequently, the resulting Vs profiles may be overly smooth and may fail to capture major velocity contrasts. Conversely, if too few layers are included in the

parameterization, then it may excessively restrict the inversion and prevent it from finding the "best" possible solution. In such cases, the resulting Vs profiles may place large velocity contrasts at incorrect depths. In general, it can be difficult to know if there are too many or too few layers in the parameterization. The best way to make this determination is to compare Vs profiles developed from inversion of the same surface wave data, but with different parameterizations. The "layering ratio" procedure outlined in Chapter 3 may be used for this purpose. Nonetheless, in many situations it may still be difficult to conclude that one parameterization is best and to definitively rule out the Vs profiles obtained from other parameterizations. This introduces Vs uncertainty and the implications of this uncertainty on the seismic site response are of interest.

The layering ratio approach was applied to a synthetic site (Chapter 4) and the Garner Valley Downhole Array Site (Chapter 5). Site response analyses were then performed on all non-unique Vs profiles obtained from inversion. Interestingly, despite major differences in the Vs profiles obtained from different parameterizations, the site response estimates were extremely similar and matched the true site response quite well at both sites. Moreover, Vs profiles obtained from inversion yielded much more accurate site response estimates than those obtained from invasive borehole testing at the GVDA Site. This suggests that if surface wave inversion is performed in a rigorous manner, then accurate site response estimates may be obtained.

These site response estimates associated with Vs profiles from non-unique surface wave inversions were found to be much more accurate and much less variable than the site response associated with Vs profiles obtained from randomization and/or by applying an epistemic uncertainty factor to develop upper/lower base-cases. Moreover, this research suggests that a robust "site signature", consisting of the experimental dispersion data and the horizontal-to-vertical spectral ratio data, may be used to screen Vs profiles

obtained from randomization. In contrast to the original sets of randomized Vs profiles, the site response associated with the screened Vs profiles were in excellent agreement with the measured site response at the Garner Valley Downhole Array Site. This suggests that randomization can be quite useful if a rational criteria for rejecting unrealistic Vs profiles is implemented. If dispersion data and/or HVSR data are not available, this rejection criteria could simply amount to rejecting Vs profiles with excessively high/low V_{S30} values. In any case, this study and previous studies indicate that poor site response estimates may be obtained if Vs randomization is performed in a blind manner.

6.2 Recommendations for Future Research

While this dissertation considers many important topics, more research is needed in regards to the influence of Vs uncertainty on the seismic site response. Proposed topics for future study are as follows:

1) A systematic investigation of the influence of mode interpretations on the predicted site response is needed. When the experimental dispersion data is ambiguous and multiple mode interpretations are feasible, each interpretation should be used to develop Vs profiles. These Vs profiles can vary considerably and thus their associated site response may also vary significantly.

2) While the layering ratio approach outlined here has been demonstrated to be very effective in developing an ensemble of realistic Vs profiles, it is time consuming to perform. In the future, it is desirable to have more efficient procedures. This can include software that streamlines this process and/or alternative, trans-dimensional inversion strategies.

3) The results in Chapters 4 and 5 demonstrate that existing practices of accounting for Vs uncertainty, both aleatory and epistemic, may result in inaccurate site

response estimates that exhibit excessive variability. In the near future, improvements must be proposed to these procedures. In particular, the Toro (1995) model should be modified to avoid excessively-thick near-surface layers with unrealistically high Vs values. Furthermore, the simple application of a depth-independent epistemic uncertainty factor is not a thoughtful means of considering Vs uncertainty and more sophisticated procedures are needed. As discussed previously, the uncertainties inherent in the final Vs profile(s) are controlled by the technique that was used to obtain the Vs profile(s). Thus, strategies of accounting for Vs uncertainty should ultimately take into account the method that was used to obtain the final Vs profile(s). This requires a different approach from current practice.

4) While the results in Chapter 5 illustrate that one-dimensional site characterization coupled with 1D site response analyses can produce satisfactory estimates of the true seismic site response at real-world sites, all sites are truly three-dimensional in nature. Ultimately, the three-dimensionality of real-world sites and the corresponding influence on the seismic site response must be considered. This will inevitably involve modifications to the manner in which site characterization is performed and the way in which seismic site response analyses are executed.

References

American Association of State Highway and Transportation Officials (AASHTO). Guide Specifications for LRFD Seismic Bridge Design 2011. 2nd ed., AASHTO Washington, D.C.

American Society of Civil Engineers (ASCE). Minimum design loads for buildings and other structures, ASCE Standard ASCE/SEI 7-10, published by ASCE, Reston, Virginia.

Afshari, K. and Stewart, J.P. (2015). "Effectiveness of 1D ground response analyses at predicting site response at California vertical array sites." Proc. SMIP2015 Seminar on Utilization of Strong Motion Data, California Strong Motion Instrumentation Program, Sacramento, CA.

Ancheta, T., Darragh, R., Stewart, J., Seyhan, E., Silva, W., Chiou, B., Wooddell, K., Graves, R., Kottke, A., Boore, D., Kishida, T., and Donahue, J. (2014). "NGA-West2 database," Earthquake Spectra, Vol. 30, pp. 989-1005.

Archuleta, R. J., Seale, S. H., Sangas, P. V., Baker, L. M., & Swain, S. T. (1992). Garner Valley downhole array of accelerometers: instrumentation and preliminary data analysis. Bulletin of the Seismological Society of America, Vol. 82(4), pp. 1592-1621.

Barani, S., Ferrari, R.D., and Ferretti, G. (2013) "Influence of Soil Modeling Uncertainties on Site Response." Earthquake Spectra, Vol. 29(3), pp. 705-732.

Bazzuro,P., and Cornell, C. (2004). "Ground Motion Amplification in Nonlinear Soil Sites with Uncertain Properties". Bulletin of the Seismological Society of America, Vol. 94(6), pp. 2090 2109.

Bettig, B., Bard, P.Y., Scherbaum, F., Riepl, J., Cotton, F., Cornou, C., and Hatzfeild, D. (2001). "Analysis of dense array noise measurements using the modified spatial auto correlation method (SPAC): application to the Grenoble area." Bollettino de Geofisica Teoria e Applicata, Vol. 42(3-4), pp. 281-304.

Boaga, J., Vignoli, G., and Cassiani, G. (2011). "Shear wave profiles from surface wave inversion: the impact of uncertainty on seismic site response analysis," Journal of Geophysics and Engineering, Vol. 8, pp. 162-174.

Boaga, J., Vignoli, G., and Cassiani, G. (2012). "Reply to comment on 'Shear wave profiles from surface inversion: the impact of uncertainty on seismic site response analysis'," Journal of Geophysics and Engineering, Vol. 9, pp. 244-246.

Boaga, J., Cassiani, G., Strobbia, C. L., & Vignoli, G. (2013). “Mode misidentification in Rayleigh waves: Ellipticity as a cause and a cure.” Geophysics, Vol. 78(4), pp. EN17-EN28.

Bonnefoy-Claudet, S, Cornou, C., Bard, P.Y., Cotton, F., Moczo, P., Kristek, J., and Fah, D. (2006). "H/V ratio: a tool for site effects evaluation. Results from 1-D noise simulations," Geophysical Journal International, Vol. 167, pp. 827-837.

Bonilla, L. F., Steidl, J. H., Gariel, J. C., and Archuleta, R.J. (2002). “Borehole Response Studies at the Garner Valley Downhole Array, Southern California.” Bulletin of the Seismological Society of America, Vol. 92(8), pp. 3165–3179.

Boore, D.M. and Atkinson G.M. (2008). "Ground-motion Prediction Equations for the Average Horizontal Component of PGA, PGV, and the 5%-damped PSA at spectral periods between 0.01 s and 10.0 s," Earthquake Spectra, Vol. 24, pp. 99-138, 2008.

Cabas, C. and Rodriguez-Marek, A. R., (2017). “What Can We Learn from Kappa (κ) to Achieve a Better Characterization of Damping in Geotechnical Site Response Models?” In Geotechnical Frontiers 2017: Seismic Performance and Liquefaction, pp. 1–9.

Campbell, K. W. (2009). Estimates of shear-wave Q and κ0 for unconsolidated and semiconsolidated sediments in eastern North America. Bulletin of the Seismological Society of America, Vol. 99(4), pp. 2365-2392.

Capon, J. (1969). “High Resolution Frequency-Wavenumber Spectrum Analysis.” Proceedings of the IEEE, Vol. 57(8), pp. 1408–1418.

Comina, C., and Foti, S.. (2014). "Discussion on 'Implications of Surface Save Data Measurement Uncertainty on Seismic Ground Response Analysis' by Jakka et al.," Soil Dynamics and Earthquake Engineering.

Cornou, C., Ohrnberger, M., Boore, D.M., Kudo, K., and Bard, P. Y. (2009). "Derivation of structural models from ambient vibration array recordings: results from an international blind test," in 3rd International symposium on the effects of surface geology on seismic motion, Grenoble, Vol. 2, pp. 1127-1219.

Cox, B. R., & Wood, C. M. (2011). “Surface wave benchmarking exercise: methodologies, results, and uncertainties.” In Geo-Risk 2011: Risk Assessment and Management, pp. 845-852.

Cox, B.R., Wood, C.M. and Teague, D.P. (2014) “Synthesis of the UTexas1 Surface Wave Dataset Blind-Analysis Study: Inter-Analyst Dispersion and Shear Wave

Velocity Uncertainty" Proceedings of the 2014 Geo Congress Technical Papers, pp. 850-859.

Cox, B.R. and Teague, D.P. (2016). "Layering ratios: a systematic approach to the inversion of surface wave data in the absence of a priori information." Geophysical Journal International, Vol. 207(1), pp. 422-438.

Darendeli, M.B. (2001). "Development of A New Family of Normalized Modulus Reduction and Material Damping Curves." Ph.D. Dissertation, School of Civil, Architectural and Environmental Engineering, The University of Texas at Austin, Austin, TX.

DiGiulio, G., Savvaidis, A., Ohrnberger, M., Wathelet, M., Cornou, C., Knapmeyer-Endrun, B., Renalier, F., Theodoulidis, N., and Bard, P.Y. (2012). "Exploring the model space and ranking a best class of models in surface-wave dispersion inversion: Application at European strong-motion sites." Geophysics, Vol. 77(3), pp. B147–B166.

Dunkin J.W. (1965). "Computation of modal solutions in layered, elastic media at high frequencies." Bulletin of the Seismological Society of America, Vol. 55, pp. 335–358.

Dou, S. & Ajo-Franklin, J.B., 2014. "Full-waveform inversion of surface waves for mapping embedded low-velocity zones in permafrost." Geophysics, Vol. 79, pp. EN107–EN124.

Electric Power Research Institute (EPRI) "Seismic Evaluation Guidance: Screening, Prioritization and Implementation Details (SPID) for the Resolution of Fukushima Near-Term Task Force Recommendation 2.1: Seismic" Eletric Power Research Institute, Palo Alto, CA: 2012, Report 1025287, pp. B1–B45.

Fathi, A., Poursartip, B., Stokoe II, K. H., & Kallivokas, L. F. (2016). "Three-dimensional P-and S-wave velocity profiling of geotechnical sites using full-waveform inversion driven by field data." Soil Dynamics and Earthquake Engineering, Vol. 87, pp. 63-81.

Fletcher, J. B., Fumal, T., Liu, H. P., & Carroll, L. C. (1990). Near-surface velocities and attenuation at two boreholes near Anza, California, from logging data. Bulletin of the Seismological Society of America, Vol. 80(4), pp. 807-831.

Foti, S. (2000). "Multistation methods for geotechnical characterization using surface waves." Doctoral Dissertation, Politecnico di Torino.

Foti, S., Comina,C., Boiero, D., and Socco, L.V. (2009). “Non-uniqueness in surface-wave inversion and consequences on seismic site response analyses.” Soil Dynamics and Earthquake Engineering, Vol. 29, pp. 982–993.

Foti, S., Lai, C. G., Rix, G. J., & Strobbia, C. (2014). Surface wave methods for near-surface site characterization. CRC Press.

Garofalo, F., Foti, S., Hollender, F., Bard, P. Y., Cornou, C., Cox, B. R., Ohrnberger, M., Sicilia, D., Asten, M., Di Giulio, G. and Forbriger, T. (2016). “InterPACIFIC project: Comparison of invasive and non-invasive methods for seismic site characterization. Part I: Intra-comparison of surface wave methods.” Soil Dynamics and Earthquake Engineering, Vol. 82, pp. 222-240.

Garofalo, F., Foti, S., Hollender, F., Bard, P. Y., Cornou, C., Cox, B. R., Dechamp, A., Ohrnberger, M., Perron, V., Sicilia, D. and Teague, D. (2016). InterPACIFIC project: Comparison of invasive and non-invasive methods for seismic site characterization. Part II: Inter-comparison between surface-wave and borehole methods. Soil Dynamics and Earthquake Engineering, Vol. 82, pp. 241-254.

Gibbs, J. F. (1989). Near-surface P- and S-wave velocities from borehole measurements near Lake Hemet, California, U.S. Geological Survey Open File Report, pp. 89–630.

Griffiths, S.C., Cox, B.R., Rathje, E.M., Teague, D. (2016). “A Surface Wave Dispersion Approach for Evaluating Statistical Models that Account for Shear Wave Velocity Uncertainty,” Journal of Geotechnical and Geoenvironmental Engineering, Vol. 142(11), DOI: 10.1061/(ASCE)GT.1943-5606.0001552.

Griffiths, S.C., Cox, B.R., Rathje, E.M., Teague, D. (2016). “Mapping Dispersion Misfit and Uncertainty in Vs Profiles to Variability in Site Response Estimates,” Journal of Geotechnical and Geoenvironmental Engineering, Vol. 142(11), DOI: 10.1061/(ASCE)GT.1943-5606.0001553.

Hashash, Y.M., Groholski, D.R., Phillips, C.A., Park, D., and Musgrove, M. (2012). "DEEPSOIL 5.1, User Manual and Tutorial".

Haskell, N. A. (1953). “The dispersion of surface waves on multilayered media.” Bulletin of Seismological Society of America, Vol. 43, pp. 17–34.

Hill, R.I. (1981). Geology of Garner Valley and vicinity, in Geology of the San Jacinto Mountains, Annual Field Trip Guidebook No. 9, A. R. Brown and R. W. Ruff, (Editors), South Coast Geological Society, Santa Ana, California, pp. 90–99.

Jakka, R.S., Roy, N., and Wason, H.R. (2014a). "Implications of Surface Save Data Measurement Uncertainty on Seismic Ground Response Analysis," Soil Dynamics and Earthquake Engineering, Vols. 61-62, pp. 239-245.

Jakka, R.S., Roy, N., and Wason, H.R. (2014b). "Reply on 'Implications of Surface Save Data Measurement Uncertainty on Seismic Ground Response Analysis'," Soil Dynamics and Earthquake Engineering.

Kaklamanos, J., Bradley, B. A., Thompson, E. M., & Baise, L. G. (2013). Critical parameters affecting bias and variability in site-response analyses using KiK-net downhole array data. Bulletin of the Seismological Society of America, Vol. 103(3), 1733-1749.

Kaklamanos, J., Baise, L. G., Thompson, E. M., & Dorfmann, L. (2015). Comparison of 1D linear, equivalent-linear, and nonlinear site response models at six KiK-net validation sites. Soil Dynamics and Earthquake Engineering, Vol. 69, 207-219.

Kim, B., & Hashash, Y. M. (2013). Site response analysis using downhole array recordings during the March 2011 Tohoku-Oki earthquake and the effect of long-duration ground motions. Earthquake Spectra, Vol. 29(s1), S37-S54.

Knopoff L. (1964). “A matrix method for elastic wave problems.” Bulletin of the Seismological Society of America, Vol. 54, pp. 431–438.

Kottke, A.R. and Rathje, E.M. (2008). "A Semi-Automated Procedure for Selection and Scaling of Recorded Earthquake Motions for Dynamic Analysis," Earthquake Spectra, Vol. 24(4), pp. 911-932.

Kottke, A.R. and Rathje, E.M. (2009). “Technical Manual for Strata.” Report No. 2008/10, Pacific Earthquake Engineering Research Center, Berkeley, California.

Kottke, A. R. and Rathje, E.M. (2012). "Technical Manual for SigmaSpectra".

Lachet, C. and Bard, P.-Y. (1994). “Numerical and theoretical investigations on the possibilities and limitations of Nakamura’s technique.” Journal of Physics of the Earth, Vol. 42, pp. 377–397.

Lai, C.G., Foti, S., and Rix, G. (2005). “Propagation of Data Uncertainty in Surface Wave Inversion.” Journal of Environmental and Engineering Geophysics, Vol. 10(2), pp. 219-228.

Lermo, J. and Chavez-Garcia, F.J., (1993). “Site effects evaluation using spectral ratios with only one station.” Bulletin of the Seismological Society of America, Vol. 83, pp. 1574–1594.

Li, W. and Assimaki, D. (2010). "Site- and Motion-Dependent Parametric Uncertainty of Site-Response Analyses in Earthquake Simulations," Bulletin of the Seismological Society of America, Vol. 100(3), p. 954–968.

Lin, Y., Joh. S., & Stokoe, K. (2014). “Analyst J: Analysis of the UTexas 1 Surface Wave Dataset Using the SASW Methodology,” Geo-Congress 2014 Technical Papers, Atlanta, GA, pp. 830-839.

Liu, H. P., Boore, D. M., Joyner, W. B., Oppenheimer, D. H., Warrick, R. E., Zhang, W., Hamilton, J. C., and Brown, L. T. (2000). “Comparison of Phase Velocities from Array Measurements of Rayleigh Waves Associated with Microtremor and Results Calculated from Borehole Shear-Wave Velocity Profiles.” Bulletin of the Seismological Society of America, Vol. 90, pp. 666-678.

Matasovic, N., and Hashash, Y. (2012) “NCHRP Synthesis 428: Practices and Procedures for Site Specific Evaluations of Earthquake Ground Motions, A Synthesis of Highway Practice.” National Cooperative Highway Research Program of the Transportation Research Board, Washington, D.C.

McMechan, G. A., & Yedlin, M. J. (1981). “Analysis of dispersive waves by wave field transformation.” Geophysics, Vol. 46(6), pp. 869-874.

Nolet, G., & Panza, G. F. (1976). “Array analysis of seismic surface waves: Limits and possibilities.” Pure and Applied geophysics, Vol. 114(5), pp. 775-790.

O'Neill, A. (2004). “Shear velocity model appraisal in shallow surface wave inversion.” In Symposium on the Application of Geophysics to Engineering and Environmental Problems 2004, Society of Exploration Geophysicists, pp. 1544-1555.

Park, C. B., Miller, R. D., & Xia, J. (1998). “Imaging dispersion curves of surface waves on multi-channel record.” In SEG Technical Program Expanded Abstracts 1998, Society of Exploration Geophysicists, pp. 1377-1380.

Rathje, E.M., Kottke, A.R., and Trent, W.L. (2010). “Influence of Input Motion and Site Property Variabilities on Seismic Site Response Analysis.” Journal of Geotechnical and Geoenvironmental Engineering, Vol. 136(4), pp. 607-619.

Rathje, E. M., Pehlivan, M., Gilbert, R., and Rodriguez-Marek, A., (2015). “Incorporating site response into seismic hazard assessments for critical facilities: A

probabilistic approach." In Perspectives on Earthquake Geotechnical Engineering. Springer International Publishing, pp. 93–111.

Régnier, J., Cadet, H., Bonilla, L. F., Bertrand, E., & Semblat, J. F. (2013). Assessing Nonlinear Behavior of Soils in Seismic Site Response: Statistical Analysis on KiK-net Strong-Motion Data. Bulletin of the Seismological Society of America, Vol. 103(3), pp. 1750-1770.

Sambridge, M. (1999). "Geophysical inversion with a neighbourhood algorithm –I. Searching a parameter space." Geophysical Journal International, Vol. 134, pp. 479–494.

SESAME European project, (2004). Guidelines for the Implementation of the H/V Spectral Ratio Technique on Ambient Vibrations: Measurements, Processing and Interpretation. Deliverable D23.12.

Socco, L.V., Foti, S., & Boiero, D. (2010). "Surface-wave analysis for building near-surface velocity models – Established approaches and new perspectives." Geophysics, Vol. 75, pp. 75A83–75A102.

Socco, L.V., Foti, S., and Comina, C. (2012). "Comment on 'Shear wave profiles from surface inversion: the impact of uncertainty on seismic site response analysis'," Journal of Geophysics and Engineering, Vol. 9, pp. 241-243.

Steidl, J. H., Tumarkin, A. G., & Archuleta, R. J. (1996). "What is a reference site?" Bulletin of the Seismological Society of America, Vol. 86(6), pp. 1733-1748.

Steller, R. (1996). New borehole geophysical results at GVDA, UCSB Internal report, http://nees.ucsb.edu/sites/eot-dev.nees.ucsb.edu/files/facilities/docs/GVDA-Geotech-Stellar1996.pdf.

Stewart, J. P., & Kwok, A. O. (2008). "Nonlinear seismic ground response analysis: Code usage protocols and verification against vertical array data." In Geotechnical earthquake engineering and soil dynamics IV, pp. 1-24.

Stewart, J., Afshari, K, Hashash, Y. (2014). Guidelines for performing hazard-consistent one-dimensional ground response analysis for ground motion prediction. Berkely, California: Pacific Earthquake Engineering Research Center.

Stokoe, K. H., Kutulus, A., and Menq, F.-Y. (2004). SASW measurements at the NEES Garner Valley test site, California, University of Texas at Austin, College of Engineering Data Report.

Strobbia, C., & Foti, S. (2006). “Multi-offset phase analysis of surface wave data (MOPA).” Journal of Applied Geophysics, Vol. 59(4), pp. 300-313.

Tau, Y. and Rathje, E. (2017). “Insights Into Small-strain Damping from Downhole Array Recordings.” Presented at the 2017 Annual Meeting of the Seismological Society of America.

Teague, D., Cox, B., Bradley, B., and Wotherspoon, L.M. (2015). “Development of Realistic Vs Profiles in Christchurch, New Zealand via Active and Ambient Surface Wave Data: Methodologies for Inversion in Complex Interbedded Geology.” Proc. of the 6th International Conference on Earthquake Geotechnical Engineering, Christchurch, NZ, 1–4 November 2015.

Teague, D. and Cox, B.R. (2016). “Site Response Implications Associated with using Non-Unique Vs Profiles from Surface Wave Inversion in Comparison with Other Commonly Used Methods of Accounting for Vs Uncertainty.” Soil Dynamics and Earthquake Engineering, Vol. 91, pp. 87–103, http://dx.doi.org/10.1016/j.soildyn.2016.07.028i.

Teague, D., Cox, B., and El-Afifi, T. (2017a). “Site Response Implications of Using Vs profiles Derived from ‘Blind’ and Geologically-Guided Surface Wave Inversions.” 16th World Conference on Earthquake Engineering, Santiago, Chile, 9–13 January 2017.

Teague. D. P., Cox, B. R., and Wood, C. M. (2017b). “A Methodical Procedure for the Consideration of MASW Uncertainties and the Development of Robust Dispersion Estimates.” Geophysical Journal International (plan to submit).

Thompson, E., Baise, L., Tanaka, Y., and Kayen, R. (2012). "A taxonomy of site response complexity," Soil Dynamics and Earthquake Engineering, Vol. 41, pp. 32-43.

Thomson, W. T. (1950). “Transmission of elastic waves through a stratified solid medium.” Journal of Applied Physics, Vol. 21, pp. 89–93.

Tokimatsu, K. (1995). “Geotechnical site characterization using surface waves.” Proceedings of the 1st International Conference on Earthquake Geotechnical Engineering IS-Tokyo ’95, Balkema, Rotterdam, The Netherlands, pp. 1333–1368.

Toro, G. (1995) “Probabilistic models of the site velocity profiles for generic and site specific ground motion amplification studies.” Technical Report No. 779574, Brookhaven National Laboratory, Upton, N.Y. pp. 147.

Wathelet, M., Jongmans, D., and Ohrnberger, M. (2004). “Surface-wave inversion using a direct search algorithm and ts application to ambient vibration measurements.” Near Surface Geophysics, Vol. 2(4), pp. 211–221.

Wood, C. M., & Cox, B. R. (2012). “A comparison of MASW dispersion uncertainty and bias for impact and harmonic sources.” In GeoCongress 2012: State of the Art and Practice in Geotechnical Engineering, pp. 2756-2765.

Wood, C.M., Ellis, T., Teague, D.P., and Cox, B.R., "Analyst I: Comprehensive Analysis of the UTexas1 Surface Wave Dataset," in Geo-Congress 2014 Technical Papers, Atlanta, GA, pp. 820-829, 2014.

Xia, J., Miller, R. D., Park, C. B., & Ivanov, J. (2000). “Construction of 2-D vertical shear-wave velocity field by the multichannel analysis of surface wave technique.” In Symposium on the Application of Geophysics to Engineering and Environmental Problems 2000, Society of Exploration Geophysicists, pp. 1197-1206.

Xia, J., Chen, C., Li, P. H., & Lewis, M. J. (2004). “Delineation of a collapse feature in a noisy environment using a multichannel surface wave technique.” Geotechnique, Vol. 54(1), pp. 17-28.

Yamanaka, H. & H. Ishida, 1996. “Application of generic algorithms to an inversion of surface-wave dispersion data.” Bull. Earthq. Eng., 86, 436–444.

Yoon, S., & Rix, G. J. (2009). “Near-field effects on array-based surface wave methods with active sources.” Journal of Geotechnical and Geoenvironmental Engineering, Vol. 135(3), pp. 399-406.

Zalachoris, G., & Rathje, E. M. (2015). Evaluation of one-dimensional site response techniques using borehole arrays. Journal of Geotechnical and Geoenvironmental Engineering, Vol. 141(12), 04015053.

Zywicki, D.J. (1999). “Advanced signal processing methods applied to engineering analysis of seismic surface waves.” Ph.D. Dissertation, School of Civil and Environmental Engineering, Georgia Institute of Technology, Atlanta, GA.

Zywicki, D. J., & Rix, G. J. (2005). “Mitigation of near-field effects for seismic surface wave velocity estimation with cylindrical beamformers.” Journal of Geotechnical and Geoenvironmental Engineering, Vol. 131(8), pp. 970-977.